GIS-Supported Simulation of the Spatial Behaviour of Wildland Fire, Cass Basin, New Zealand.

A thesis

submitted in fulfilment

of the requirements for the degree of

Master of Science in Geography

by thesis alone

in the

University of Canterbury

by

George. L.W. Perry

University of Canterbury

1996

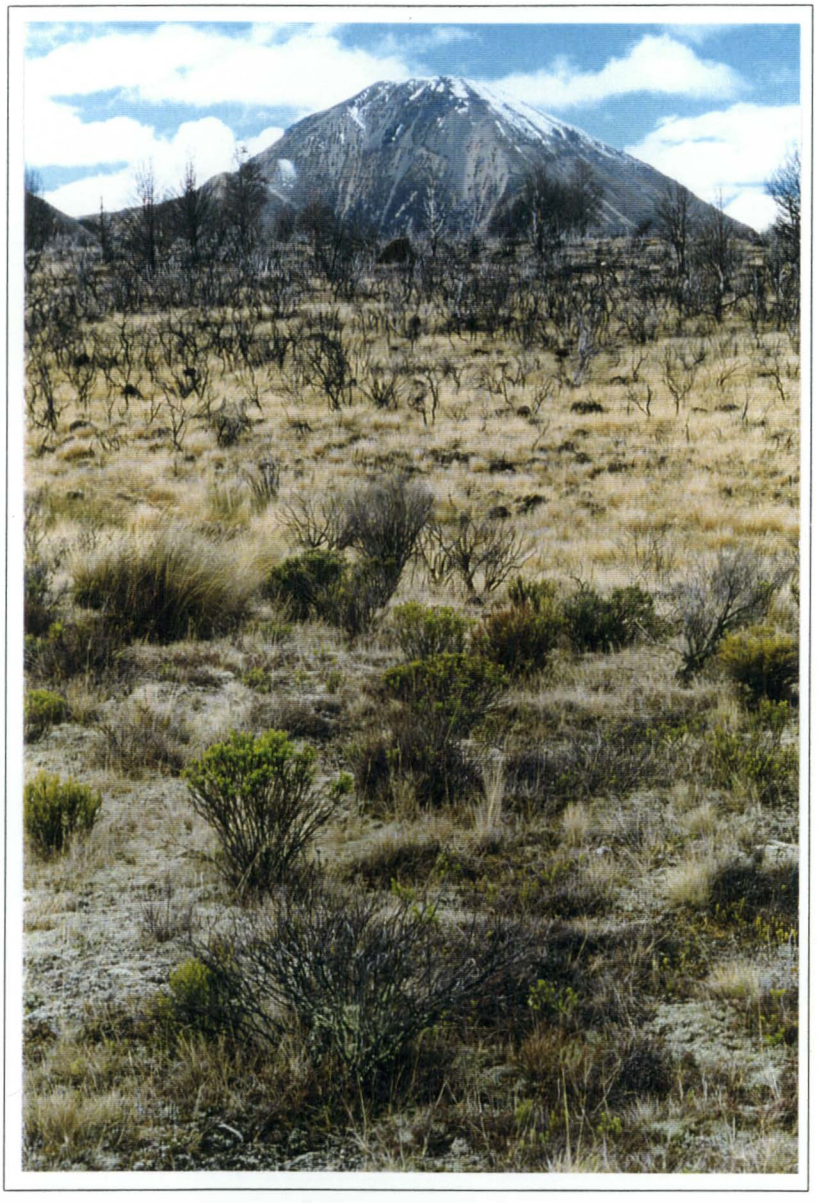

Frontispiece - High intensity fire has moved rapidly through this shrubland on the flanks of Corner Knob, leaving a mosiac of burnt and unburnt patches. Sugarloaf forms the backdrop.

"This world was ever, is now, and ever shall be an ever-living fire with measures of it kindling, and measures going out."
Heracleitus "*The Cosmic Fragments*"

Acknowledgements

This thesis owes a great deal to a number of people. Firstly, many thanks are due to my two supervisors Ian Owens and Ashley Sparrow. Without their continual help and critical insights this research would not have been as fulfilling as it has proved to be. The technical assistance of Andy Kliskey, James Guard and John Thyne is also gratefully acknowledged. The support of the Department of Plant and Microbial Sciences who provided access to their field station is much appreciated. Thank you also to Pip Forer and Graeme Glen at the Department of Geography, University of Auckland who allowed me access to their computer equipment. The financial support provided by the Sir Neil Isaac Scholarship is also most gratefully acknowledged.

On the flip-side of the coin are the crew on the second floor. To Karl, Pete, Oliphana, Nic, Janan, Susan, the deranged honours year, and, of course, my ever-distracting (and distractable) room-mate Jamie, thanks for putting up with me and showing me that 'normality' is very much a relative concept.

Thanks to Matt and Charlotte for all their help and for reminding me that there is a world outside the sixth floor.

Finally, thanks to my family for the support they have given me over my five years at Canterbury. This thesis owes as much to them as it does to me.

This thesis is dedicated to the memory of my grandfather, George Whitefield Armitage.

Abstract

This thesis describes the conceptualisation and development of the PYROCART model. This model simulates the spatial behaviour of fire in spatially heterogeneous environments. The principle aims of the research were to test the applicability of overseas fire spread models to New Zealand fuels, to investigate the environmental controls influencing wildland fire behaviour and to assess the applicability of Geographic Information Systems (GIS) to fire spread prediction.

The PYROCART model integrates a Geographic Information System (Arc/Info) and the fire spread model of Rothermel (1972). The Rothermel model consists of a series of flux equations which describe the physical and chemical processes of combustion. Rate of spread is estimated to be the difference between these fluxes. A problematic limitation of this model is that it is assumed that the landscape in which the fire is being modelled is homogenous with respect to environmental descriptors such as fuel type, slope, wind speed and wind direction. The use of a cellular data model within a Geographic Information System overcomes some of the spatial limitations of the Rothermel model associated with the assumption of environmental homogeneity.

The model is validated using a large wildfire which occurred on 27-28 May, 1995 on the west bank of the Cass River in the Cass Basin. This fire burnt 580 hectares across a complex vegetation mosaic comprising shrubland, stands of *Nothofagus solandri* var *cliffortioides*, bog and tussockland. The pre-fire vegetation was mapped and fuel models were built for nine vegetation types. The topography and variation in the wind field of the fire scar were also surveyed.

The overall prediction of the model is estimated to have an accuracy of 80%. Prediction accuracies within different fuel types, slopes and wind conditions are also presented and it is shown that fuel type and slope appear to be the dominant influence on fire spread. No trends in prediction accuracy by wind speed and wind direction are apparent. The predicted burned area and the real burned area have a similar overall shape. However, problems of over-prediction of backing and flanking rates of spread at high wind speeds are identified.

The PYROCART model shows potential as a management tool, especially for the testing of hypotheses concerning alternative land management strategies. However, due to the complex input data and parameterisation techniques required to operate the model it is not suitable for *in situ* fire management.

Table of Contents

Chapter Four - Analysis of the Rothermel Fire Spread Model

Chapter Five - The PYROCART Simulation Model

Chapter Six - Model Validation

Chapter Seven - Conclusions

List of Figures

List of Tables

List of Plates

Chapter One

Introduction

1.1 The Ecological Significance of Fire

Modification of the earth's surface for urban development and agricultural activity aside, natural and anthropic fire is the most widespread of all terrestrial disturbance forces (Bond and Van Wilgen, 1995). Evidence from a variety of sources suggests that wildfire has been an important feature of the natural environment for at least 350 million years (e.g. Kemp, 1981; Cope and Chaloner, 1985), although reliable evidence on the phylogenetic and climatic role of fire during the past several hundred million years is scarce (Clark and Robinson, 1992). Furthermore, debates continue over issues such as the impacts of global wildland fires on climate change and species extinction at the Cretaceous/Tertiary boundary ca. 65 million years ago (Anders *et al.*, 1991; McLean, 1991). Without doubt, however, fire has influenced terrestrial ecosystems over evolutionary time.

Brain and Sillen (1988) suggest that the earliest evidence of the use of fire by hominids is approximately 1.5 million years BP. Since then, natural fire regimes have been successively altered by humans. As human populations and culture have grown and spread across the globe, anthropogenic fires have, in many places, begun to merge with natural fires and their impacts to create new fire regimes. Large areas of forest (e.g. the Australian eucalpyt forests and the seasonal tropical rainforests), as well as the majority of tropical savannas) have been created and their presence has been sustained by anthropogenic fire. In the words of Stephen Pyne (1992, p. 246) "we are uniquely fire creatures bonded to a uniquely fire planet".

Traditionally, fire has been attributed little importance in pre-human ecosystems in New Zealand. However, this view neglects the fact that at various times in the past New Zealand was dominated by grassland ecosystems and a more continental climate (Markgraf *et al.*, 1995). Lightning is likely to have been the main source of fire (Komarek, 1964; McGlone, 1989), although Daubenmire (1969) notes that other non-anthropic sources of fire have been documented (e.g. volcanic eruptions, spontaneous combustion (Viosca, 1931) and sparks from boulders rolling down hillsides). However, following human colonisation, fire has become an increasingly important force in New Zealand's landscapes. A dramatic rise in charcoal occurrence about 1000 years ago,

coincident with Polynesian colonisation, indicates a time of widespread deforestation that reduced the area of forest cover in New Zealand by 40% (McGlone, 1989). With European settlement a further 20 to 30% of the original forest, and much regenerating land, was cleared, burnt and developed into farmland. Fire has been a major tool in the development and management of rural New Zealand (Basher *et al.,* 1990). Its use began in an *ad hoc* manner with controls and regulations slowly increasing. Fire continues to be used as a cheap and effective tool in tussock grassland management and scrub.

The dramatic increase in fire frequency in post-settlement New Zealand has had a number of impacts, both biological and physical (Wardle, 1984; McGlone, 1989). These include shifts in species distribution, such as the increased dominance of early successional species in the landscape, altered rates of erosion in the Southern Alps and changes in hydrologic and micro-climatic conditions (Sewell, 1969). However, fire affects many ecosystem processes and as a result the impacts of fire on soils, plant growth and the long-term stability of ecosystems are complex and open to a range of interpretations. Furthermore, these are complicated by the effect of other disturbance factors such as grazing and climatic fluctuations.

1.2 Research Rationale

Despite the increased importance of fire in the environments of New Zealand, little research has specifically considered its role in indigenous ecosystems. What literature has been published is primarily concerned with historical fire regimes (e.g. Molloy, 1977; McGlone, 1981) and fire-vegetation interactions, especially in montane and sub-alpine tussock fields (e.g. Payton and Brasch, 1978; McKendry and O'Connor, 1990; Gitay *et al.* 1991; Ellis, 1994), with sporadic papers and reports published on the recovery of other ecosystems after fire (e.g. Merton, 1986; Ledgard *et al.*, 1987; Calder *et al.*, 1992; Timmins, 1992). Little research in New Zealand has addressed the mechanics of fire and its behaviour, nor is there a national fire danger rating system of either the type or active application found in countries such as the United States, Canada and Australia. This lack of literature is in marked contrast to the vast body of research concerning fire published in areas such as North America and Australia, and is a reflection of the perceived relative importance of fire in the environments of such countries in comparison to New Zealand. Thus, a major problem associated with fire management in New Zealand is this lack of knowledge regarding fire in natural systems. Historically, management of fire in New Zealand has relied on 'fire containment'; an ability to predict fire behaviour *a priori* may allow a move from fire containment to fire prevention.

Much contemporary fire spread modelling rests upon the model of Rothermel (1972). This model uses a series of flux equations to describe the basic physical and chemical processes of combustion. Fire spread is assessed by measurement of the differences between the various fluxes (Clarke and Olsen, 1996). The foundations of fire geometry upon which most subsequent fire modelling has been based were developed by Anderson (1983). Anderson (1983) produced a series of expressions which describe the geometry of a wind-driven fire as a 'double-ellipse', and enable the calculation of fire area and total perimeter, as well as maximum width. These relationships are based upon the work of McArthur (1966) who showed that the length-to-breadth ratio of a fire is a function of wind speed.

Over the last decade Geographic Information Systems (GIS) have been increasingly used to provide information for wildland fire planning. Most of this effort has been aimed at mapping the spatial distribution of fire hazards (e.g. Hamilton *et al.*, 1989; Chuvieco and Salas, 1996) and providing information for other fire management activities (e.g. Salazar and Bradshaw, 1986; Salazar and Power, 1988). Comparatively few studies have been concerned with simulating the actual spatial behaviour of fire events. However, because most fire models tacitly assume spatial homogeneity in the landscapes in which they are used, GIS, in conjunction with cellular automata models, offers benefits to those modelling fire behaviour in complex, spatially heterogeneous landscapes. Examples of the use of GIS to model the spatial behaviour of fire include the FIREMAP system of Vasconcelos (1988), Vasconcelos and Guertin (1992) and Vasconcelos *et al.* (1994) and the cellular automata model of Clarke *et al.* (1994) and Clarke and Olsen (1996). The FIREMAP model integrates the fire spread model of Rothermel (1972) and a raster-based GIS (MAP) to simulate the spatial dynamics of fire spread. The use of internally homogenous 'cellular worlds' allows the assumption of spatial homogeneity, implicit in the Rothermel model, to be circumvented. Furthermore, GIS provides options for the flexible storage and display of data.

One area in New Zealand where fire has had a particularly dramatic effect is the Canterbury high country. The changes fire has wrought in this environment have long been known, and the role(s) fire should play there, especially with regard to issues such as pasture maintenance, much debated (e.g. Cumberland, 1945; O'Connor, 1982, 1984, 1993; Whitehouse and McSaveney, 1989). The Cass district is an example of a high country area greatly affected by repeated fire over the last 500-800 years (Kelly, 1995) and notably following Polynesian settlement of the district (Molloy, 1977). The most recent large fire there occurred on 27-28 May 1995. It burnt an area of approximately 580 hectares comprising a mosaic of *Nothofagus solandri* var. *cliffortioides* (mountain beech), *Leptospermum scoparium* (manuka), *Cassinia leptophylla* (tauhinu), *Discaria*

toumatou (matagouri), *Coprosma propinqua*, *Coprosma* aff. *parviflora* ('sp. T'), *Dracophyllum longifolium, Poa cita* and *Festuca novae-zelandiae* (Kelly, 1995). It is the spatial behaviour of this fire which is the focus of this thesis.

1.3 Research Objectives

This thesis has the three major objectives of :

- *testing the applicability of fire spread models developed overseas to New Zealand ecosystems,*
- *investigating the controls on fire behaviour by use of a case-study,*
- *assessing the application of a geographic information system (GIS) for predicting the spatial behaviour of fire.*

These objectives are to be achieved through the development of a GIS-supported model which simulates the spatial behaviour of fire, based on the mathematical fire spread model of Rothermel (1972). The model is validated against the large fire which occurred in the Cass Basin in late-May, 1995.

1.4 Thesis Structure

Apart from this introductory chapter and a concluding chapter (Chapter Seven), five other chapters make up the main body of this thesis. This section briefly describes the format of the thesis and provides an overview of the concepts considered in each of the following chapters.

Chapter Two is concerned with the theory of fire dynamics; initially the fundamental concepts of ignition, heat exchange and combustion are reviewed and the roles of fuel, topography and weather in influencing fire spread are discussed. The chapter concludes with a brief overview of the evolutionary ecology of fire and an analysis of the problems involved in quantifying fire behaviour .

Chapter Three reviews the theory and development of fire spread modelling. The relative merits of physical, semi-physical and empirical models are discussed, as are the fundamental concepts of fire shape simulation modelling. The roles of spatial information technologies such as GIS and remote sensing in predictive fire modelling are reviewed. The chapter concludes with a case study of fire modelling (the Yellowstone Park Fires of 1988) and a description of the issues on which contemporary fire behaviour research is focussed.

Chapter Four provides an analysis of the fire spread model of Rothermel (1972); this model forms the basis of the simulation model. The chapter comprises three main sections. Firstly, the mechanics, assumptions and limitations of the model are discussed; secondly, a sensitivity analysis of the model is provided; and, thirdly the use of the model in a range of ecosystems is reviewed. Problems with the use of the Rothermel model in ecosystems and laboratory tests outside that in which it was validated and field-tested are also described.

Chapter Five introduces the PYROCART simulation model. This model (designed and programmed by the author) simulates the spread of fire in both homogenous and complex heterogeneous environments. The modelling structure and the spread algorithms are described and then model outputs from a range of environmental conditions are presented and discussed.

Chapter Six is concerned with the validation of the PYROCART simulation model using the Cass fire of May 1995. The methodology required to parameterise the model is presented along with a description of the study site before the fire shapes predicted by PYROCART are presented. Disparities between the predicted and real fire shape are discussed and areas where the model could be improved are considered.

Chapter Two

The Fire Phenomenon

2.1 Introduction

This chapter examines the mechanisms which drive wildland fire. Many of the concepts considered are incorporated into Rothermel's (1972) semi-physical fire model which forms the basis for much of the rest of the thesis. The physical and chemical reactions of combustion determine the potential characteristics of a fire in that they govern whether it ignites, and how it subsequently burns and behaves. Variations in fire parameters such as intensity and rate of spread are often determined to some degree by factors such as fuel which influence these basic reactions (Chandler *et al.*, 1983; Pyne, 1984; Luke and McArthur, 1986). Environmental variables such as fuel, topography, fire history and weather may act together to modify the potential fire characteristics (Whelan, 1995). These interactions are also examined here, as is the debate surrounding their relative importance. There will be six sections examining different aspects of fire dynamics: (i) the phenomenology of fire; (ii) the ignition process; (iii) the physical-chemical basis of combustion; (iv) fire behaviour and the factors influencing it; (v) the quantification of wildland fire ; and (vi) a review of the debate over whether it is fuel characteristics or weather which control wildland fires.

2.2 The Phenomenology of Fire

Albini (1993, p. 39) states that:

> "as in other specialized endeavours, those who deal regularly with fires in vegetation fuels use a special vocabulary to communicate concisely to other fire specialists a set of attributes associated with a fire and to characterise fires generally."

For the purpose of this chapter, and the thesis as a whole, this section will briefly introduce some of the terminology used to describe wildland fires. The terminology below broadly follows that of Pyne (1984) and Albini (1993). Other terms are introduced and defined in the text as required.

Fires in naturally occurring vegetative fuels are usually unconfined, or *free-burning*. A free-burning fire increases in size by spreading its boundaries through the ignition of

unburnt fuels along its outer edge (Pyne, 1984). It may also grow by *spotting*, that is the ignition of fuel distant from its edge by burning embers and sparks transported by winds and the convection column caused by the fire. The new ignition points are termed *spot fires* (Fuller, 1991).

A fire that spreads by flaming combustion of vegetation contiguous to the land surface, is termed a *surface fire*. Its fuels may be either alive or dead, and may include fallen dead vegetation components, standing dead fuels or vegetation debris from harvesting or land clearing (Agee, 1993). A fire that spreads through the canopy layer of a stand of trees is called a *crown fire*. Most forest fires are surface fires with only incidental burning of the forest crown (Albini, 1993). Crown fires occur most frequently in temperate and boreal conifer forests and Australian eucalyptus, but rarely in temperate or tropical deciduous trees. They are often dependent upon, and are invariably ignited by, surface fires (Van Wagner, 1977a; Pyne, 1984; Albini, 1993).

Ground fires are those fires which burn in sub-surface organic fuels such as humus layers under forest stands an Arctic taiga, and in the organic soils of swamps or bogs (pakihi mires provide a New Zealand example; Merton, 1986). Such fires propagate and burn underneath the surface by smouldering combustion, but, at the surface they may exhibit flaming (Marsden-Smedley, 1993). Flaming usually occurs at the advancing edge of the fire and may be associated with the collapse of upper layers which have been undermined and dried out by the passage of the sub-surface fire edge. Ground fires are usually ignited by surface fires (Albini, 1993).

Typically free-burning fires go through three distinct stages: (i) *ignition*; (ii) *acceleration*; and (iii) a *quasi-steady state rate of spread.* The length of the accelerative phase is dependent upon environmental factors such as fuel type, weather conditions and fire size, and is typically shorter in open non-forest vegetation than in closed forest vegetation (Marsden-Smedley, 1993). A quasi-steady state rate of spread is reached when fire behaviour is essentially stable with a relatively constant rate of spread and intensity. It should be noted that multiple-acceleration phases are possible in response to changing environmental conditions (Pyne, 1984). Albini (1993) extends this concept to include a fourth stage which is a period of decreasing flame production as the fuel elements are converted to char, collapse, and contribute to a glowing ember bed. However, it is questionable as to whether this fourth stage should be included in the classification. For whereas the first three stages describe the state of the fire front, the fourth describes the state at a particular location after the passage of the front.

A precise terminology exists to describe the constituent parts of a fire (Figure 2.1). The

point of fire initiation is the *origin* and the perimeter portions inscribed by the heading, flanking and backing fires are termed the *head* or *fire front*, the *flank*, and the *back* or *tail* respectively. The head is the fastest spreading part of any fire, followed by the flank with the back being the slowest moving edge (Albini, 1993). Small extensions of the perimeter radiating out from the main area are called *fingers*, and the unburnt areas between the main fire and the fingers, *pockets*. If pockets become totally isolated in the fire, they become *islands* or *refugia* (Pyne, 1984).

The description of fuels has also led to the development of a specialised terminology. Fuel characteristics can be described as a hierarchy of levels of increasing structural complexity. The terminology outlined below follows that of Pyne (1984) and McCaw (1988). At the lowest level of the hierarchy are individual *fuel particles* that have specific characteristics of size, shape and density. These characteristics exert a direct influence on heat transfer and combustion as well as on fuel moisture levels. *Fuel beds* consist of particles arranged in defined proportions and structural configurations. Fuel beds are generally associated with specific types of fire behaviour (e.g. ground fuels are deep beds of combustible organic matter which commonly burn by smouldering, as opposed to flaming, combustion). Several fuel beds occurring together with a characteristic vertical configuration comprise a *fuel complex* that will often be associated with a recognised structural vegetation form (e.g. dry sclerophyll forest). The mosaic of fuel complexes across a landscape reflects variation in a number of factors including soil moisture and fertility, altitude, aspect and past fire history.

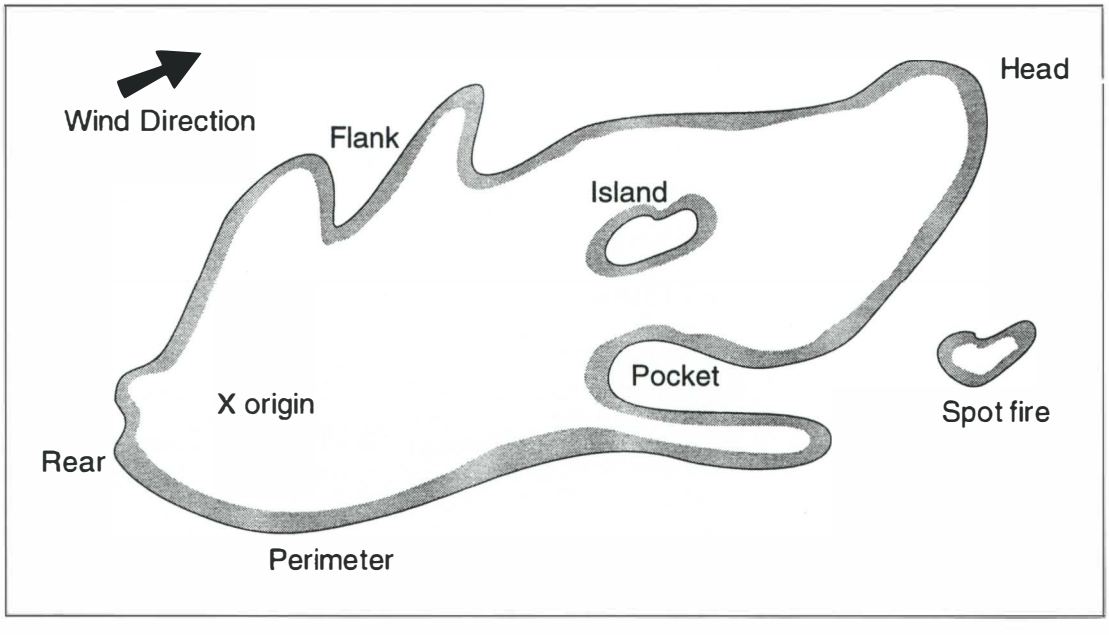

Figure 2.1 The constituent parts of a wildland fire. (Pyne, 1984).

2.3 Ignition

Ignition is a process fundamental to any fire. This section is divided into two sub-sections: the first considers the sources of ignition, and the second the mechanics of ignition itself.

2.3.1 Ignition Sources

Fire will only occur if some source of ignition is present. An important source of ignition for many wildland fires is undoubtedly human activity. Statistics from those parts of the world with a high wildland fire frequency point to anthropogenic fire (either deliberate or accidental) as being the most common source of such fires (Komarek, 1969; Gill, 1981; Kruger and Bigalke, 1984; Luke and McArthur, 1986; Whelan, 1995).

Fire associated with human activity has a long and widespread history. There are numerous reports by early colonial explorers and settlers of the use of fire by the indigenous peoples of New Zealand, Australia, North and South America, Africa and New Guinea, and much anthropological research suggests fire was widely used by these peoples for hunting and land clearing (Mitchell, 1848; Pyne, 1991, 1993; Flannery, 1994). Fire has also been a part of Mediterranean landscapes for a long period of time, with its use reaching a peak in recent centuries when population densities were high relative to those of the New World (Le Houerou, 1974; Travaud *et al.* 1993).

Natural sources of fire include volcanic activity (McGlone, 1981; Bond and Van Wilgen, 1996), sparks from rocks in landslides (Hennicker-Gotley, 1936; Kruger and Bigalke, 1984), spontaneous combustion (Viosca, 1931) and lightning (Komarek, 1969; McGlone, 1989; Pyne, 1984, 1991). However, lightning is by far the most general and widespread non-human cause of wildland fire ignition, with the others important only in localised situations (Cope and Chaloner, 1985). An example of the efficiency of lightning in igniting severe fires is provided by the 1974-75 fire season in Australia. During this period a series of wildfires were ignited by lightning; these fires eventually burnt 117 million hectares of land, an area comprising 15% of the Australian landmass (Luke and McArthur, 1986).

2.3.2 The Ignition Process

Ignition marks the onset of combustion. Combustion is not a single process, but rather a continuum of processes which occur as individual particles within the fuel complex become separately involved (Pyne, 1984). For fire to spread, discrete new ignitions

occurring in unceasing succession are necessary. Thus, the ignition process is fundamental to the overall rate of combustion, and the delay time fundamental to the rate of ignition (Albini, 1993).

Initially ignition is a kinetically controlled process that may terminate before a sufficient, self-sustaining fire starts (Williams, 1977a). The speed and success of subsequent ignition depends upon the properties of the fuel particle and the character of the heat source applied to it. The physical and chemical properties of the fuel particle influence its susceptibility to heating (Chandler *et al.*, 1983). For example, a large flat leaf with a high surface-area-to-volume ratio and high diameter will heat more quickly than a particle with a large diameter; a particle rich in easily volatised extractives will show a lower ignition temperature than one that is not (Vines, 1981). Thus, ignition will vary with the properties of the heat transferred and the duration of heating. The heat source may or may not be associated with flame. Fuel heating in the absence of flame leads to *spontaneous ignition*; fuel heating in the presence of a flame is termed *pilot ignition*. Within the primary reaction zone, the normal mode of combustion is flame; outside that zone, glowing combustion is common (Pyne, 1984; Fuller, 1991).

The various types of ignition can be considered by looking at those that may result from a radiant heat source. The irradiated particle may respond according to one of three states: (i) *non-ignition*; (ii) *transient ignition*; and (iii) *persistent ignition* (Luke and McArthur, 1986). Non-ignition occurs where the duration of heating is too short or its intensity too low to bring the fuel element to its ignition temperature. In the case of transient ignition combustion occurs, but continues only so long as a certain heat intensity persists; if the irradiating heat is withdrawn, combustion will cease. This is because for every fuel particle there exists a threshold of heat intensity below which ignition will fail to occur. This threshold is termed the *critical irradiance* (Pyne, 1984). Wildland fires commonly exhibit transient ignition. It is often found in association with the flaming front whose extreme temperatures partially burn fuels without leading to sustained combustion after the front has passed by. Similarly the disintegration of a fuel complex (each particle of which irradiates the others) often results in the extinction of a fire (Albini, 1993). Lastly, there is the case of sustained ignition in which the range of heat intensities is adequate for combustion to begin and endure (Anderson, 1970).

The factors that permit ignition will also influence fire behaviour. For example well-aerated, fine fuels will burn more intensely and a fire in them will spread more rapidly as well as being initially more susceptible to ignition (Whelan, 1995).

2.4 Combustion: The Physico-Chemical Reaction

A spreading forest fire is a complex combustion in which the flaming front is heating and then igniting unburnt woody and herbaceous fuels. In this heating process the moisture in the fuel is initially evaporated (fuel temperature > 100°C), then the cellulose is thermally degraded and its breakdown products volatised (temperature > 200°C), and finally volatiles are ignited to form a visible flame (300-400°C) (Shafizadeh, 1968). This process is outlined in more detail below.

The basis of any fire is the combustion process. Energy stored in biomass is released as heat when the fuel combines with oxygen to create carbon dioxide, water vapour and small amounts of other substances. Trollope (1984) shows how this process is comparable to the reverse of photo-synthesis:

$CO_2 + H_2O + \text{Solar Energy} \longrightarrow (C_6H_{10}O_5)n + O_2$ *Photosynthesis*

$(C_6H_{10}O_5)n + O_2 + \text{Kindling T°} \longrightarrow CO_2 + H_2O + \text{Heat}$ *Combustion*

Whelan (1995) notes that the chemical equations for combustion can be illustrated in the complete combustion of a simple sugar (eg. d-glucose):

$$C_6H_{12}O_6 + 6O_2 \longrightarrow 6CO_2 + 6H_2O + 1.28x10^6\ kJ$$

Thus, combustion can be seen to be a process of rapid oxidation dependent upon the availability of fuel, heat and oxygen (Albini, 1993).

The fuels burnt in wildland fires are much more complex than the simple glucose illustrated in the equation above. Vegetative material is basically made up of cellulose, hemicelluloses (together 50-75% of most dry plant matter), lignin (15-25%), proteins, nucleic acids, amino acids and volatile extractives (Lobert and Warnatz, 1993). Furthermore, the different components of the fuel (e.g. dead leaf litter, dead wood and live foliage) contain energy stores in a variety of forms (Rothermel, 1972; Chandler *et al.*, 1983). However, in a wildfire combustion is never complete, and therefore the actual heat yield is but a fraction of the potential heat yield (Pyne, 1984).

The term *kindling temperature* in Trollope's (1984) combustion equation indicates that the combustion process is neither a simple nor spontaneous one. It requires the activation energy of an external energy source. The fuel is initially set on fire when enough heat is applied to it for pyrolysis to occur (Albini, 1993; Whelan, 1995). Pyrolysis can be summarised as the chemical degradation of fuel through thermal decomposition and results in the release of water vapour, carbon dioxide and other gases such as methane, methanol and hydrogen (Lobert and Warnatz, 1993). During

this process the combustion reaction changes from being exothermic to endothermic (Pyne, 1984).

Many authors (e.g. Chandler *et al.*, 1983; Pyne, 1984; Albini, 1993; Whelan, 1995) consider the combustion process to occur in three distinct stages: (i) *preheating* - during which the fuel ahead of the fire front is heated, dried and partially pyrolysed; (ii) *flaming combustion* - the result of ignition of flammable carbohydrate gases; and (iii) *glowing combustion* - any remaining charcoal burns as a solid, with oxidation taking place on the surface leaving a small amount of residual ash. Some authors (e.g. Byram, 1959; Agee, 1993) expand the combustion process to include a fourth stage, *cooling* or *extinction.* The various stages of combustion are illustrated in Figure 2.2.

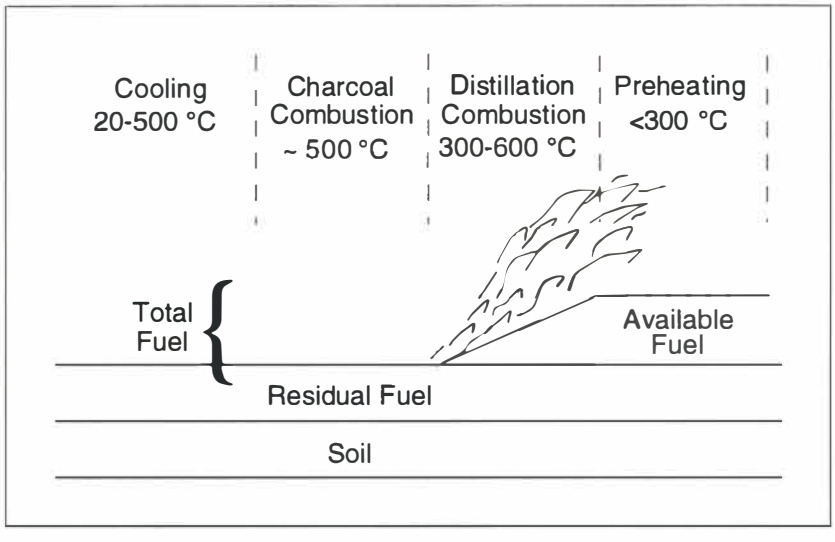

Figure 2.2 The combustion process. (Agee, 1993).

A consideration of the processes of pyrolysis and ignition shows that a fire can, to some degree, be considered as self-sustaining (Whelan, 1995). The initial ignition source provides the activation energy that allows ignition and the subsequent continuation of a fire. Flaming combustion at the fire front then provides both pre-heating of adjacent fuels and the pilot flames to cause its ignition. This process is shown in Figure 2.3.

The amount of energy released by combustion (the *reaction intensity*; see Section 2.7.2) is of great significance because it is closely related to the fire intensity, one of the most significant parameters of any wildland fire. In order of importance the factors influencing heat release are fuel moisture, fuel chemistry and the surface-area to volume ratio of the fuel particle (Chandler *et al.*, 1983).

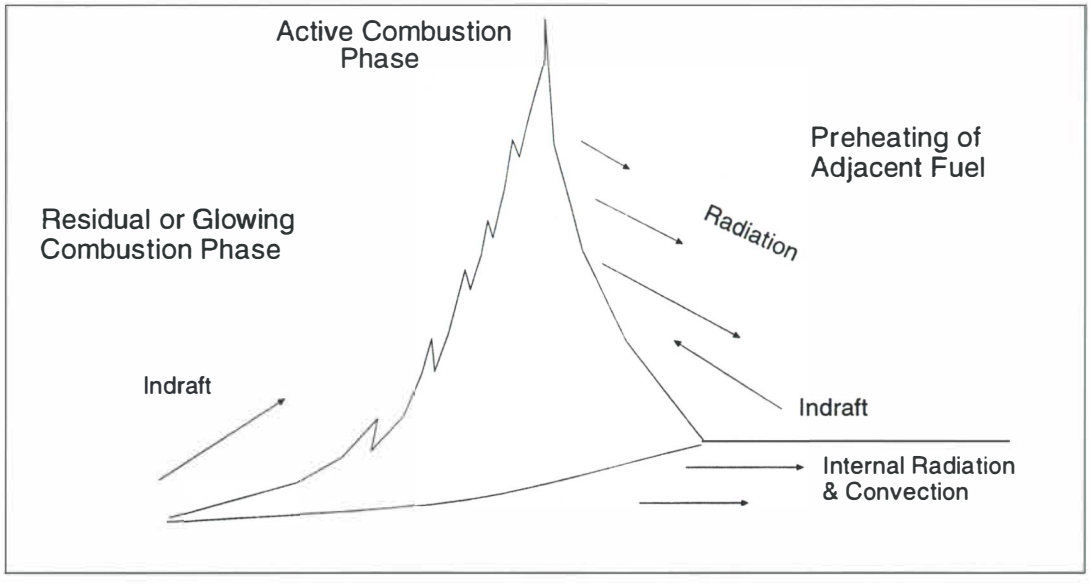

Figure 2.3 The self-sustaining nature of combustion. (Whelan,1995).

The single most crucial element influencing the heat yield is fuel moisture, the most variable component of a fuel's chemistry (Luke and McArthur, 1986; Lobert and Warnatz, 1993; Whelan, 1995). Fuel moisture determines whether a plant is set on fire and how well it will subsequently burn. Fuel moisture differs between live and dead fuels (Pyne, 1984) and ranges between 2.5% (dead savanna grass in the dry season) and 200% (fresh needles or leaves) of the vegetation's dry weight. High fuel moisture contents have the capacity to either completely stop a fire, or to slow down the process to a slow, intense smouldering (Lobert and Warnatz, 1993). Heat is used to: (i) raise fuel water temperatures to 100°C; (ii) separate bound water from the fuel; (iii) vaporise the water in the fuel; and (iv) heat the water vapour to flame temperature (Whelan, 1995). To illustrate the importance of fuel moisture, it is known that in eucalypt fuels the combustion rate is four times greater at a moisture level of 3% than at 10% (Luke and McArthur, 1986). The role of fuel moisture in wildland fire behaviour is considered in more detail in Section 2.5.1.

Secondly, the total heat of combustion is strongly influenced by the presence of volatile resins and oils, and inorganic minerals in the fuel (Mutch, 1970; Bond and Van Wilgen, 1996; Figure 2.4). Crude fats are volatile and make plants more flammable, as they are driven out of plants at relatively low temperatures, and subsequently burn as gases (Bond and Van Wilgen, 1996). Vines and Pompe (1966) found that eucalypt leaves oven-dried at 110°C burnt with a lower heat energy yield than undried leaves. This was attributed to the loss of volatile oils during the drying process. However, Vines (1981) noted that volatiles which have a high-heat content and which flame rapidly are usually present in quantities too small to cause a significant increase in the heat output. A

related factor is the presence of inorganic minerals in the fuel. Some of these compounds affect the pyrolysis pathway and promote char formation (King and Vines, 1969; Pyne, 1984). Many forest and grassland species with high inorganic mineral contents have low flammability levels and burn relatively slowly, and may therefore act to 'damp' the fire (Rothermel, 1972; Vines, 1981).

The third most important characteristic of a fuel particle with respect to its combustion rate is its surface-area to volume ratio which, for a given particle density, is directly correlated with particle thickness. The combustible volatiles can only mix with oxygen after diffusing across the fuel surface boundary layer (Albini, 1980). For a fuel of a specific density, chemical composition and moisture content, the *residence time* (length of time a particle will support flaming) is directly proportional to its thickness. For woody fuels with a moisture content in the range 4-10%, the residence time in seconds is approximately 3-times the fuel thickness in centimetres (Chandler *et al.*, 1983; Lobert and Warnatz, 1993).

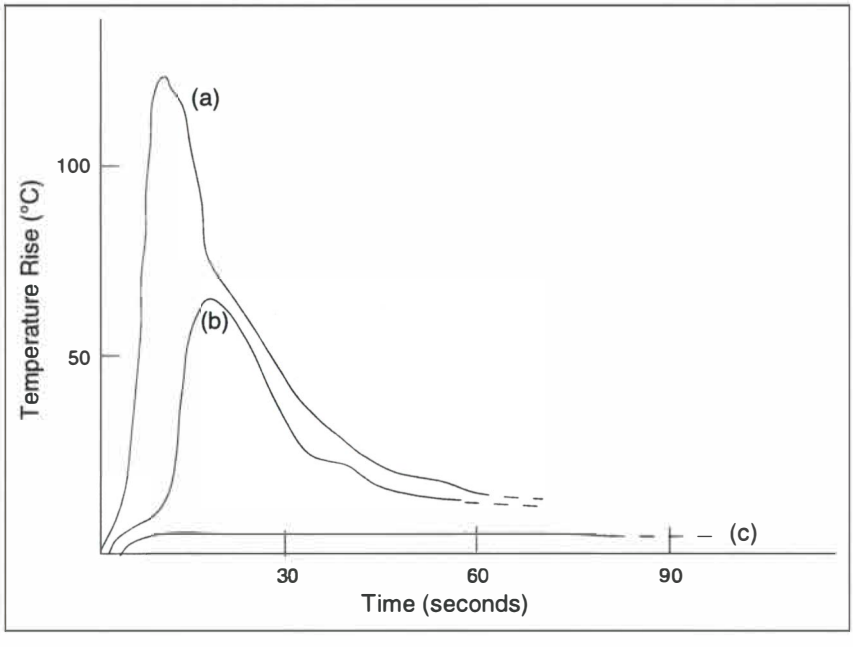

Figure 2.4 Temperature traces obtained by burning leaf samples: (a) 20g sample of oven-dried eucalypt leaves which burnt rapidly; (b) 20g sample of oven-dried leaves of *Phytolacca octandra* - the leaves smouldered only ; (c) 20g samples of *P. octandra* containing 3% absorbed essential oils leaves - flaming was pronounced although the leaves were only partially consumed. (Vines, 1981).

As briefly described earlier, incomplete fuel combustion will reduce the energy output to below the potential maximum. Incomplete combustion describes two possible processes. Firstly, all components of the burning fuel may not be converted to released energy, but are either being given off as particulate carbon compounds in the smoke pall, or remain as charred plant material at the site. Secondly, not all the biomass at the site may ignite in the first place (Whelan, 1995). Ward and Radeke (1993) provide an

equation for measuring combustion efficiency (η) defined as the percent of carbon released as CO_2:

$$\eta = \frac{[CO_2a]}{[CO_2t]} \qquad (2.1)$$

where: CO_2a = actual concentration of CO_2 released by the fire

CO_2t = the theoretical limit of concentration or mass of CO_2 if all carbon is converted to CO_2

2.5 Fire Behaviour

Once a fire has reached a quasi-stable spread state, its behaviour is influenced by a series of complex environmental interactions, primarily between fuels, topography and weather (especially wind). As a fire encounters local differences in fuels, topography and weather, localised changes in rate of spread and deformations to the shape of the fire perimeter will occur (Fujioka, 1985; Chevrou, 1992). The influences of these factors are briefly outlined in Table 2.1 below. When considered in isolation, these three factors may induce certain predictable behaviours. However, in wildfires one variable is rarely dominant; usually all three are present and interact in complex ways (Pyne, 1984). They may act to cause the fire to accelerate; they may 'compete' with each other; yet always they influence fire growth. Within the range of steady-state fires, different variables affect the fire in different ways and at different times, and the variables themselves may change as the fire continues to spread (Luke and McArthur, 1986). It is important to note that these variables usually affect fire spread through their influence on fire intensity (Whelan, 1995). This section specifically examines the roles of fuel, topography and weather in fire spread.

2.5.1 Fuels and Fire Behaviour

> "A fire begins and ends with its fuels. The presence of fuels is mandatory for the smallest of flames, and its absence can shut down the largest of conflagrations." (Pyne, 1984, p. 89).

Both the morphological and chemical properties of individual species and the arrangement of many species and communities in space influence their susceptibility to fire. This section briefly explores the relationships between fuels and fire behaviour.

Fuel Moisture Content (FMC)

Fuel moisture is the single most important fuel factor influencing fire behaviour; it is overwhelmingly crucial to the behaviour of fire across all fuel types (Cheney *et al.*,

1993). Fuel moisture relationships are complex and the numerous attempts to accurately predict the moisture contents of forest fuels have been unsuccessful (Chandler *et al.* 1983; Hartford and Rothermel, 1991). The reason FMC relationships are so complex is that they are driven by processes occurring at the interface of the two most variable components of the fire environment, fuels and weather (Pyne, 1984).

Table 2.1 Summary of the physical and biotic factors affecting fire behaviour (Whelan, 1995).

Factor	Effect
Fuel load	Determines maximum energy available to a fire; Arrangement of fuel can affect aeration (tightly packed fuels), vertical spread (i.e. into canopy) and horizontal spread (patchy ground fuel); Size distribution of fuel can affect likelihood of initial ignition; Chemistry of fuel can increase flammability (i.e. resins & oils), or decrease it (i.e. mineral content).
Overall climate	Determines vegetation productivity and therefore rate of fuel accumulation.
Rainfall & humidity	Increased fuel moisture, combined with high relative humidity decreases likelihood of ignition, rate of combustion & rate of spread.
Wind	Causes drying of fuel; Increases oxygen available for combustion; Pre-heats and ignites fuel in advance of the front, can produce ignition far ahead of the front; Wind direction changes can increase fire front.
Topography	Provides variation in local climate (i.e. fuel moisture, relative humidity, interaction with wind); Permits pre-heating & ignition for fires burning uphill; Can provide natural firebreaks; Partially determines distribution of plant communities of different flammabilities.

Fuels may be either alive or dead and the processes, and resultant amounts, of moisture exchange will differ accordingly. With live fuels, physiological processes can actively work to either accelerate or slow the exchange of moisture between a particle and its environment, but with dead fuels the response is passive. Live fuels have higher FMC levels, resist moisture deficiency better, and exhibit seasonal changes in moisture in accordance with physiological processes such as spring flushing and autumn curing (Pyne, 1984). In short, the moisture content of leaves and small twigs in living fuels (the most important living plant parts in fire behaviour) is governed by physiological processes (Chandler *et al.,* 1983). Live leaves will burn more easily if their moisture content is low as water needs to be driven out of them prior to ignition. Thus leaves well defended against herbivores, with high fibre contents and high leaf specific

weights (Coley, 1988; Reich *et al.*, 1991) will burn more easily due to their lower FMC (Bond and Van Wilgen, 1996). Little other research has focussed on the way in which live fuels burn, but it is known that the proportion of dead fuels within a fuel complex influences how much living fuel will burn (Rothermel, 1972).

Dead fuels are chemically and physiologically simpler than live cells, although the cellular structure inherited from the live state renders moisture exchange more complex than a simple diffusion gradient (Pyne, 1984). Dead fuels are hygroscopic; that is they gain or lose moisture from the surrounding atmosphere until the amount of moisture in the fuel is in balance with that in the atmosphere. The moisture content at this point is termed the *equilibrium moisture content.* It is controlled by atmospheric relative humidity, temperature and certain internal properties of the fuel (Chandler *et al.*, 1983). The moisture content of dead fuels is usually low with most plant fuels having a fibre saturation level of around 30% to 35% of total dry weight (Rothermel, 1972; Cheney, 1981). At this point fibre can absorb no more water and free moisture condenses in the cell (Cheney, 1981; Chandler *et al.*, 1983). A living fuel, moreover, may contain extractives that increase the total flammability of the particle (Section 2.4); these substances are often leached away or volatised in dead materials.

In terms of gross fire phenomenology the lower end of the FMC scale is the crucial one. In eucalypt fuel beds for example a dangerously low level is reached when FMC falls below 7%. Below this point fire spread by spotting becomes increasingly common under the influences of a strong convective circulation and is accompanied by higher combustion rates (Chandler *et al.*, 1983). If FMC is below 7%, a further lowering by 2% will approximately double the rate of spread at a given wind velocity. A reduction of FMC from 7% to 5% is thus equivalent to a drop of around 15-20% in relative humidity if air temperature is held constant (Luke and McArthur, 1986).

The effect of FMC is much more significant in relatively fine fuels in the open. Conversely the influence of wind is much greater on grass fires than on forest fires. Provided a strong wind is blowing, rapid rates of spread are possible in grasslands at very high humidities and at very low temperatures. As a result grass fires may continue to burn vigorously throughout night-time hours whereas forest fires tend to self-extinguish when FMC exceeds 20% (Luke and McArthur, 1986).

Fuel bed Parameters

The ultimate determinant of fire intensity and rate of spread is the amount of energy stored in the fuel. *Fuel load* (the total dry weight of fuel per unit of surface area) is

often used as a quantitative measure of this (Albini, 1993). Walker (1991) notes that fuel load is largely dependent on the balance between the accumulation and breakdown of combustible organic matter. Total fuel loads are very variable and may vary from 0.4 to 2 tonnes per acre for some grasses to 40 to 150 tonnes per acre for heavy slash created by timber harvesting (Fuller, 1991). Alpine tall tussock grasslands in New Zealand have a total above ground biomass of 16 to 55 tonnes per hectare (Williams, 1977b; Meurk, 1978). However, only half of this is combustible since much of the biomass is found in tightly packed dead material at the base of the tussock which does not readily burn (Basher *et al.*, 1990). Luke and McArthur (1986) note that in almost all fuel types the rate of spread of a fire increases in direct proportion to the quantity of available fine fuels. As described in Section 2.4 complete combustion is an extremely rare occurrence in wildland fires and so fuel load provides only a measure of the amount of fuel which may potentially burn (Whelan, 1995). For this reason a measurement termed *available fuel*, which takes particle size and arrangement into account, is often employed (Albini, 1993). Another problem with fuel load is precisely defining what constitutes fuel. The standard forestry definition of a fuel is any substance or composite mixture susceptible to ignition and combustion (Ford-Robertson, 1971). Thus, total fuel load is similar to phytomass, the amount of dead and living plant material found above the mineral soil. This differs from the ecological definition of biomass in that roots and animal matter are not considered, whereas dead matter is (Chandler *et al.*, 1983).

The spacing, or compactness, of the fuel particle arrangement, influences the rate of spread of a fire because it determines how much air may circulate within the fuel and whether the particles are contiguous enough to ignite one another readily (Albini, 1993). If the air can not easily circulate around it, a fuel will burn with greatly reduced vigour (Fuller, 1991). High density fuels like stemwood are more difficult to ignite than low-density, loosely structured grasses, since higher density ensures that any heat produced will dissipate into the fuel rather than stay on the surface. Fire propagation is thus much slower on a piece of wood because more material is available and has to be converted per unit volume; therefore oxygen supply is a more significant variable on wood surfaces than on blades of grass (Lobert and Warnatz, 1993). Rothermel and Anderson (1966), working in uniformly sized fuel beds, found that the rate of spread through the bed is directly related to the product of the surface-area to volume ratio and the porosity (Equation 2.2) of fuel in the fuel bed:

$$\text{fuel bed porosity} = \frac{\text{void volume of the fuel bed}}{\text{total surface - area of the fuel bed}} \qquad (2.2)$$

Fuel continuity is a crucial factor in the early stages of wildland fire development. Any

breaks in fuels tend to slow or stop a fire (Fuller, 1991). Gaps in the vertical continuity of the fuel bed greater than 1.5 times the flame height virtually preclude the fire from burning into the upper stratum (Chandler *et al.*, 1983). The tendency of forest fuels to develop vertically stratified layers is so widespread that fires are often classified by the fuel strata in which they burn (Pyne, 1984; Section 2.2). Horizontal continuity of fuel is also an important determinant of forest fire behaviour. For example, a horizontal break of approximately 100 metres will bring a crown fire to the ground where it must re-establish itself after crossing the opening as a surface fire. Even though a fire may burn around barriers such as low flammability fuel beds or patches of bare soil, the rate of spread will fall, and the fire must return to an accelerative phase (Chandler *et al.*, 1983).

Fuel particle size is another parameter which plays an important role in fire behaviour. In general terms, the finer the fuel particle the more rapid the rate of spread given that there is sufficient continuity of fuel to maintain combustion (Luke and McArthur, 1986). Dead fuels with diameters in excess of 1-2 cm have little influence on rate of spread, although they still contribute to both the convective and reaction intensities. Live fuels with diameters of greater than 2-5 cm do not usually burn; instead they act as heat sinks trapping energy that may otherwise be used to increase the rate of spread (Chandler *et al.*, 1983). Fuel particle size is as important to the ignition process as it is to other fire behaviour processes. Fires will generally start very easily in very fine fuels such as well-aerated grassland. In coarser and heavier forest fuels, fuel moisture content becomes the most significant variable influencing fire behaviour, with wind velocity being of less importance. In fine-textured grass fuels fully exposed to solar radiation and wind, wind speed becomes more important than fine fuel moisture content (Luke and McArthur, 1986).

Although fuels are usually regarded as one of the stable factors influencing fire behaviour, they show significant variations at a range of temporal scales. Fuel moisture changes hourly, but most other fuel parameters change over more extended temporal scales. The time since the last fire is often significant, especially in fire-prone ecosystems, as it influences the amount of available fuel (Luke and McArthur, 1986; Clark, 1988; Marsden-Smedley, 1993; Whelan, 1995). After fire the rate of litter accumulation initially exceeds the decomposition rate. These two variables eventually reach equivalence some time after the fire, producing an equilibrium fuel load of litter that is specific to the plant community and climatic region (Heinselman, 1973; Whelan, 1995). It may take 20 to 50 years for a woodland or shrubland system to return to a steady-state litter mass after fire, but only 3 to 4 years for a tropical grassland or 5 years in a closed tropical forest (Walker, 1981). In this regard the tall tussock grasslands of New Zealand are closer to wooded communities as they take over 15 years to regain

pre-burn biomass (Moore, 1955; Payton and Mark, 1979). Furthermore the percentage of dead vegetative material in an ecosystem varies with stand age (Christensen, 1993). This dead material greatly influences fire rate of spread as it usually contains far less moisture than live fuel (Lobert and Warnatz, 1993). After 20 years much dead material has collected in chaparral ecosystems, but forest ecosystems often do not accumulate significant amounts of dead material until they are 100-300 years old, the exact amount and time varying with factors such as species, growth rates and climate (Fuller, 1991).

The belief that fire behaviour is an attribute of the plant community can be traced to Mutch (1970) and as come to be known as the 'Mutch Hypothesis'. Mutch (1970) hypothesised that as plant communities change due to the growth of individuals, senescence and disturbance, so fire behaviour alters concurrently. The main argument against the Mutch Hypothesis has been that it lacks a mechanism by which community change could affect fire. Fire behaviour relies on only certain structural components that change over time, not on all fuels and all structural changes (Bessie and Johnson, 1995). The Mutch Hypothesis is considered more fully in Section 2.6.

2.5.2 The Wind Field

In the early stages of a fire, rate of spread is largely controlled by wind, air temperature and humidity. Convective influences then become more significant, and finally, as the burning front widens, the direction and speed of the wind again become dominant (Daubenmire, 1968; Vogl, 1974).

Except at very high or very low wind speeds, the forward rate of spread varies as a power function of the wind speed. Thus rate of spread increases rapidly with increasing wind velocity as is shown in Figure 2.5. Above wind speeds of 60 $km.hr^{-1}$ further increases in wind speed do not stimulate additional increases in rate of spread or fireline intensity. Furthermore, fires with very low combustion rates (e.g. initiating fires) do not exhibit changes in forward rate of spread proportional to wind speed.

Wind speed increases rate of spread so rapidly because it changes the angle of the flame such that flames are driven into unburnt fuels and provide increased pre-heating through radiation. This fundamental process is illustrated in Figure 2.6. However, the influences of ambient winds go beyond an increase in rate of spread. They also amplify fireline and reaction intensity and improve the likelihood of spotting by windborne firebrands. (Pyne, 1984; Luke and McArthur, 1986). Such windborne embers may create spot fires 25-30 km ahead of the fire front (Foster, 1976; Vines, 1981). Winds may also play a significant role in fuel drying by providing the means for carrying off

evaporated moisture (Chandler *et al.*, 1983).

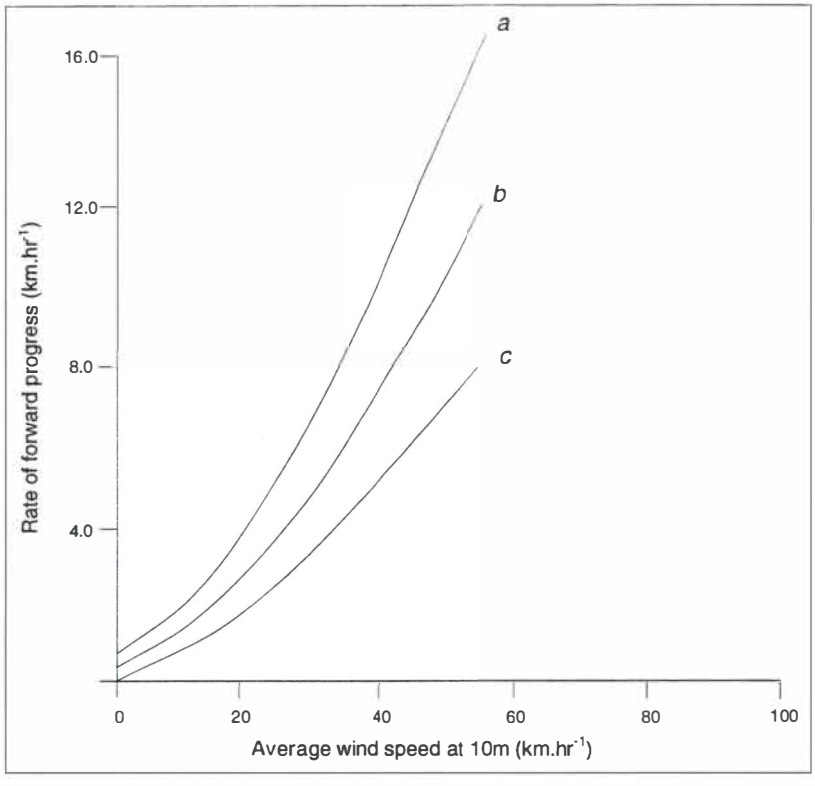

Figure 2.5 The relationship between rate of forward progress of grass fires and wind speed in various pasture growths: (a) heavy continuous pasture (6 t.ha^{-1}); (b) moderate density pasture (3.5 t.ha^{-1}) and (c) sparse pastures (1-2 t.ha^{-1}). (Luke and McArthur, 1986).

Another significant impact of increased wind speed is an elevated supply of oxygen to the flaming fire front. Although this process may increase the combustion rate, its influence is modified by the nature of the fuel being burnt. As discussed in Section 2.5.1, air circulation is reduced in densely packed fuels and so, for such fuels, an increase in oxygen supply is likely to have little impact. Byram (1958) argues that this increased oxygen supply enables backfires to move more rapidly into strong winds than into light winds. However, Luke and McArthur (1986) dispute this, noting that the rate of spread of a fire backing into the wind is relatively constant and is not affected by wind speed in either grassland or forest. Pyne (1984) disagrees with the arguments of both Byram (1958) and Luke and McArthur (1986). Pyne (1984) considers the effect of wind speed on backing fires to be opposite to its effect on heading fires in that it will cool new fuels, separate the convective heat flux from the propagating flux, and take flames away from the fuels, diminishing the effect of heat transfer. The effects of wind speed on flanking fires are mixed, with the flanking front tending to show more forward than lateral spread.

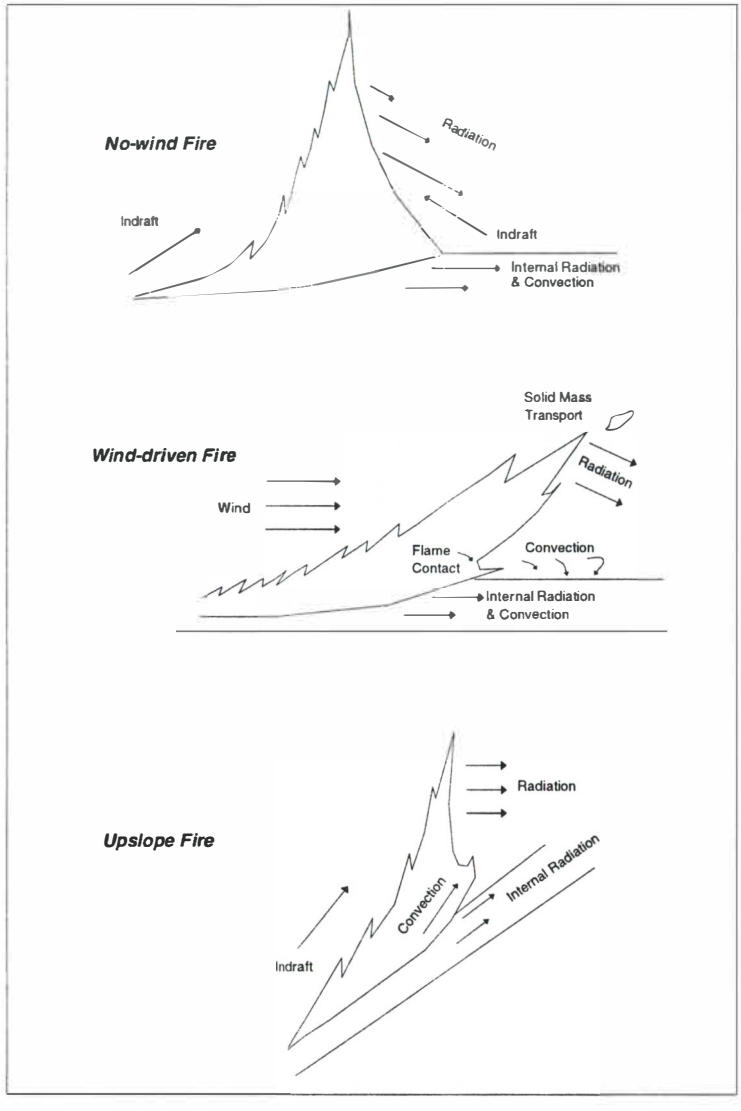

Figure 2.6 The similar influences of wind and topography on fire behaviour are shown in these fire profiles. Both slope and wind bring the flames nearer the adjacent, unburnt fuel, so enhancing the pre-heating and increasing the rate of spread (Rothermel, 1972).

There is some evidence that fires in sparse grasslands have been blown out by very strong winds (Basher *et al.*, 1990). Luke and McArthur (1986) note that large decreases in the forward rate of spread in grassland fires have occurred at wind speeds in excess of 60 $km.hr^{-1}$. Daubenmire (1968) considers that extreme wind speeds may act to cool fires, but notes that this cooling effect is more than compensated for by the increased oxygen circulation created by high wind speeds.

Fuel parameters such as FMC, fuel particle size and fuel distribution have strong inter-relationships with rate of spread and wind speed (Luke and McArthur, 1986; Whelan, 1995). For example, the wind velocity required to carry a fire at a given rate rate of spread increases with the moisture content of the fuel (Daubenmire, 1968).

Plate 2.1 Fire spread has been halted by the combined influences of topography and the nature of the fuel bed. Note how fire has largely failed to spread into the patch of *Nothofagus solandri* var *cliffortioides* in the background.

Plate 2.2 The spread of fire leaves a mosaic of burnt and unburnt patches at a range of spatial scales. In this case, a patch of *Hebe odorata* has remained unburnt while fire has spread through the surrounding shrubland.

The discussion of the influences of wind on fire behaviour has so far been confined to the effects of local winds. However, wind dynamics at larger temporal and spatial scales are also significant in influencing fire behaviour. The effects of sudden wind changes, especially those associated with cold fronts, are widely mentioned in the Australian literature (e.g. Luke and McArthur, 1986; Pyne, 1991). A number of North American authors (e.g. Fuller, 1991; Agee, 1993) discuss the importance of blocking high pressure masses in large-scale fire behaviour; such synoptic-scale events were particularly significant in inducing drought conditions and extending the fire season during the Yellowstone National Park fires of 1988 (Rothermel, 1991a). Meso- to synoptic scale changes in wind direction are significant because when a flank fire moves away on a broad front in a new direction as a head fire, rate of spread and other fire parameters almost invariably increase disproportionately to the wind velocity and meteorological conditions (Luke and McArthur, 1986). Cheney (1981) considers such increases in rate of spread to be a result of the increasingly broad fire front. As the width of the front increases the fire becomes less affected by minor fuel discontinuities and the fire spread mechanism is more efficient. Fire behaviour is also influenced by vertical motions within the atmosphere. The heat of the fire itself generates upward motion and the convective circulation thus established is affected directly by the stability of the air (Browne, 1977). Other significant types of wind direction changes are induced by the land/sea interface, upslope and downslope winds in irregular topography, and the wind speed and direction changes associated with thunderstorm downdraughts (Pyne, 1984; Baines, 1988; Fuller, 1991).

2.5.3. Topography

Slope, elevation, aspect and physiography all influence fire behaviour. The topographic variable which exerts the greatest influence on fire behaviour is slope and this is considered in a separate sub-section. The effect of the other topographic variables on fire behaviour depends largely on how they alter micro- and meso-scale meteorological variables, and how these subsequently influence fuel moisture content and wind speed near the ground (Cheney, 1981).

The Influences of Slope

The effect of slope on fire spread is similar to that of wind (Figure 2.6) in that the flames have closer contact with the fuel bed as slope increases. This results in increased pre-heating by radiation and more efficient ignition by point contact (Van Wagner, 1977b). The combined effect of wind and slope is to change the flames to a very acute angle such that once slopes exceed 15-20° the flaming front is virtually moving as a

sheet parallel to the slope. In such cases heat propagation is one of continuous flame contact (Luke and McArthur, 1986).

Many authors (e.g. McArthur, 1962; Rothermel, 1972; Van Wagner, 1977b) have established an exponential relationship between slope and rate of spread. For example, the relationship used in Australia to estimate upslope rate of spread is given by Cheney (1981):

$$R = R_0 e^{b\theta} \qquad (2.3)$$

where: R = slope correction factor, $b \approx 0.0693$, R_0 = rate of spread on level ground and θ = the angle of the slope in degrees.

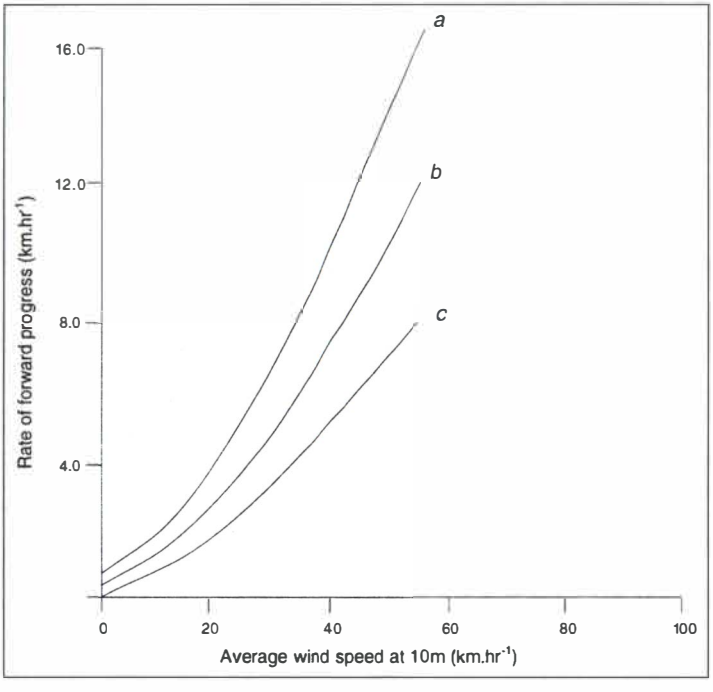

Figure 2.7 The effect of slope on the headfire rate of spread (Luke and McArthur, 1986).

Figure 2.7 and Equation 2.3 show that the forward rate of spread of the fire front on level ground doubles on a 10° slope and increases almost four-fold travelling up a 20° slope (Luke and McArthur, 1986). However, the relationship may not hold for slopes above 30° as, on such steep faces, fuel discontinuities become likely. Such steep faces are unlikely to impede very high-intensity fires as they may cross such topography through spotting (Cheney, 1981).

Little research other than that of Van Wagner (1988) has considered downslope fire progress. The literature which does consider downslope fire spread is largely qualitative and contradictory. Van Wagner (1988) found that the relationship between downslope angle and rate of spread is not the simple negative relationship it has been widely assumed to be. Rate of spread decreases to a minimum on downslopes of around 22°

and then increases so that on downslopes of 45° rate of spread is similar to that on level ground. Van Wagner (1988) attributes the initial decrease in rate of spread to diminished heat radiation as the flame is tilted away from the fuels. Fires backing into a wind are therefore analogous to those spreading down a gentle slope. The reason for increased rate of spread on downslopes in excess of 22° is unclear. Van Wagner (1988) attributes it to the minute downward movement of burning fuels within the flame zone and an increased effective flame thickness on steep downslope thereby increasing effective preheating. Van Wagner (1988) formulated the following relationship for the prediction of downslope rates of fire spread:

$$SF = 1 - 0.0330A + 0.000749A^2 \qquad (2.4)$$

where: SF = downhill spread-rate correction factor, A = slope angle (degrees).

Equations 2.3 and 2.4 produce significantly different results for downslope spread. On downslopes of 22° Equation 2.3 provides a correction factor of only 0.25, by comparison, on the same slopes Equation 2.4 predicts a correction factor of 0.64. No research has considered rate of spread down slopes in excess of 45°. Van Wagner (1988) considers that spread on such slopes may become erratic as fragments of burning matter slide downhill and the intervening slope burns out uphill.

Steepness is not the only slope variable influencing fire behaviour. Position on the slope is another important factor (Vasconcelos *et al.*, 1994). Ridges and summits are more exposed to the effects of jetstreams and to the development of upslope winds to the lee side of the edge (Pyne, 1984). Furthermore, such areas are more susceptible to lightning strikes (McRae, 1992). On the upper third of a slope the fuel drying and fire intensification effects of wind and solar radiation are strongest (Barney *et al.*, 1984). The middle third of a slope can experience anabatic and katabatic flow due to differential night-time and daytime cooling; erratic and highly unpredictable fire may occur during the reversal periods (Baines, 1988). The lower third of a slope usually receives less wind and less solar radiation and is often characterised by vegetation which is not conducive to severe fire behaviour (Barney *et al.*, 1984). Agee (1993) notes that fires starting at the top of a slope are likely to be dominated by flanking and backing fire behaviour, while those starting at the bottom of a slope are more likely to be dominated by heading fire.

The Influences of Other Topographic Variables

Fires are known to decrease in severity with increasing elevation (Cheney, 1981; Basher *et al.*, 1990). Changes in fire behaviour due to increased elevation are partially attributable to changes in wind exposure and changes in FMC due to higher

precipitation levels and slower rates of drying (Cheney, 1981). Lower temperatures will affect the length of the fire season, particularly at high elevations where the snowpack will limit both the growing season and the fire season (Agee, 1993). Furthermore, decreases in atmospheric pressure reduce the emissivity of flames such that they radiate less energy at higher altitudes (McArthur and Packham, 1971). Basher *et al.* (1990) note that field experiments showed that *Chionochloa rigida* was almost impossible to ignite at 1800m, but no such difficulty was encountered at altitudes of 1450m. They attribute this difference to the pressure effect described by McArthur and Packham (1971).

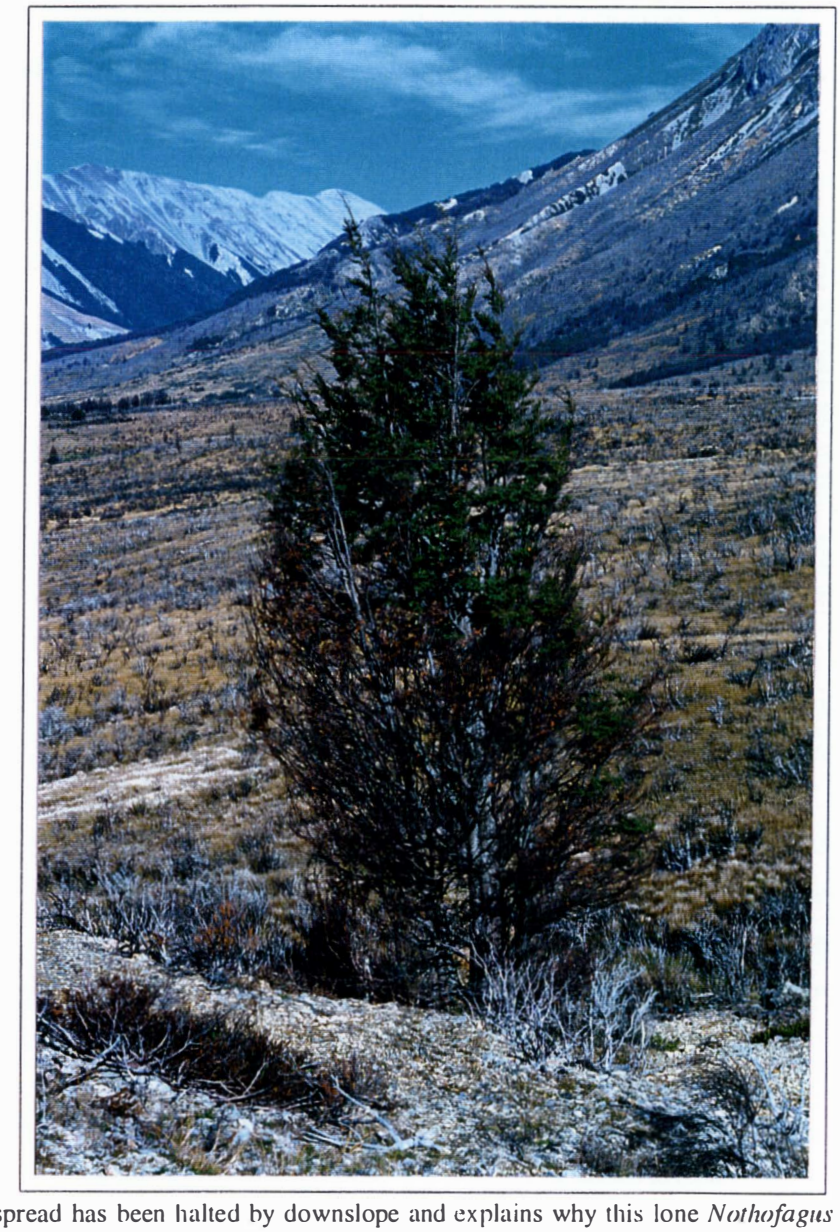

Plate 2.3 Fire spread has been halted by downslope and explains why this lone *Nothofagus solandri* var *cliffortioides* remains partially unburnt.

Under mild burning conditions, or following precipitation, fuels will dry differentially depending upon the aspect of the slope and its orientation in relation to the prevailing

wind (Cheney, 1981). However, under drier conditions the differences in drying, and therefore FMC, lessen and so fire behaviour becomes more uniform as the fuel bed responds increasingly to diurnal changes in temperature and relative humidity. Under these conditions fuels on faces of different aspects may behave differently due to differences in surface instability (as a result of solar heating), or differences in wind speed (due to the relative exposure to the prevailing wind). A further significant feature of the interaction of the wind and topography is the formation of fire whirls on the lee side of ridge crests (Cheney, 1981; Pyne, 1984). A good example of how topography and wind interact to increase fire spread is provided by canyons. In such features, one side may ignite the other through radiant heating and firebrands, thus creating a virtual chimney (Pyne, 1984; Agee, 1993). Where two canyons meet, eddies are formed and fire behaviour often becomes erratic and unpredictable (Fuller, 1991).

Whelan (1995) notes that topographic features can create firebreaks and thereby influence the distribution of fire. Natural barriers to fire, such as waterways, ridges, cliffs and rocky outcrops are all strongly related to topography and increase the spatial heterogeneity of the fire environment (Barney *et al.*, 1984; Fuller, 1991; Albini, 1993). For example Malanson and Butler (1984) consider the significance of avalanche paths as fuel breaks and the implications of such fuel breaks for fire management. Microclimates are created which support distinct fuel types, whose loads and moisture levels are also variable (Pyne, 1984). A fire burning upslope may be expected to burn rapidly and intensely, all other factors being constant. However this is seldom the case, as a large number of additional factors influence fire spread. For example, vegetation found in gullies is likely to differ from hilltop vegetation. It may be more mesophytic, denser and thus less flammable. On a smaller scale the litter below some tree species is likely to vary in flammability, aeration and moisture content, producing local variations in fire intensity (Whelan, 1995). Thus, topography will strongly influence the nature of the fuel present at a given location, and, thereby alter the character of the fire (Section 2.5.1).

2.6. Fuels vs. Weather: Which Drives Wildland Fire Behaviour ?

One of the great unsolved issues in fire ecology is the question of whether fuel characteristics or weather patterns control fire histories at extended temporal scales (eg centuries and millennia). It has been argued that fuel accumulation (Heinselman, 1973), fuel chemistry (Mutch, 1970), crown/understorey fuel structure (Despain and Sellers, 1977) and community structure (Habeck and Mutch, 1973; Clark, 1988; Despain, 1990) are central in driving fire behaviour. On the other hand weather variation has also been regarded as the key factor in dictating fire behaviour (e.g.

Swetnam and Betancourt, 1990; Johnson and Larsen, 1991; Swetnam, 1993). Christensen (1993) suggests that fuel factors and climatic variables show strong inter-relationships. For example fires tend to be most frequent under dry, mesic conditions that favour fuel accumulation and occasional drying of fuels. Although fuel production may increase with the moisture gradient, high FMCs limit fire occurrence. This section will briefly review the debate through a review of the Mutch Hypothesis and a number of other key papers and consider the findings of Bessie and Johnson (1995) who attempt to provide some quantitative solutions to this question.

Mutch (1970, p. 1046) provided a hypothesis on the interaction between fire and the ecosystem that has since come to be known as the 'Mutch Hypothesis'. It argues that though ignition may occur:

> " . . . accidentally or randomly, the character of burning is not random . . . Fire-dependent plant communities burn more readily than non-fire-dependent communities because natural selection has favoured development of characteristics that make them more flammable."

The Mutch Hypothesis seems to provide an evolutionary rationale for the differences between fire-dependent and non-fire-dependent communities (Bond and Midgley, 1995; Possingham *et al.*, 1995). For example, many North American pine species can tolerate regular fires. In the south-eastern USA, pine stands are often subjected to invasion by a suite of fire-intolerant, hardwood species (Monk, 1968; Veno, 1976). The continuity of fuel under pine trees and the high fuel temperatures generated by pine needles appear to eliminate hardwoods without damaging the individual pine trees (Williamson and Black, 1981). An individual pine tree that produces a less-flammable fuel would provide a cool spot in a fire, giving hardwoods more chance of establishment and long-term occupancy of the site than its own offspring. Furthermore, Williamson and Black (1981) note that it is generally early seral species, which are often poor competitors, that exhibit fire-facilitating characteristics while competitively-superior late seral species tend to be fire-retardant. Whelan (1995) suggests that flammability may be favoured as a result of the second-order interaction involving competition and fire. However, a number of other authors (eg Snyder, 1984; Christensen, 1985; Troumbis and Trabaud, 1989) consider the Mutch Hypothesis to be fundamentally flawed. Although communities that burn more readily may be more flammable than those that do not, it is difficult to attribute these differences solely to selection by fire. Snyder (1984) and Troumbis and Trabaud (1989) consider that alternative selection pressures such as drought tolerance, herbivory or nutrient retention may be equally plausible selective paths to high flammability. For example, plants

containing high levels of phenolics, as a defence against herbivory, are often associated with high accumulations of dead fuel as the phenolics prevent the rapid decomposition of dead matter. Malanson (1987) suggests that selection pressures which lead to traits for drought tolerance and nutrient-retention are likely to be important in most fire-prone ecosystems, and that such ecosystems are likely to be inherently flammable. In this case it seems that the selection pressure may be towards increased flammability as opposed to the creation of flammability. In short, flammability, in terms of both the physiognomy of the vegetation and its combustability, may be dependant in part upon the same environmental variables that determine productivity: precipitation, temperature and nutrient-availability (Malanson, 1987).

Snyder (1984) is critical of the Mutch Hypothesis on the grounds that it is group selectionist, noting that while Mutch's hypothesis is presented in terms of community evolution, Mutch (1970) is more concerned with the evolution of flammability by individual species. Most fire-dependent communities are comprised of one or a few species responsible for the elevated flammability as well as many other species well adapted to the fire regime but of low fuel value. Species with low biomass (low fuel value) are likely to be of little competitive threat to dominant species in the ecosystem, and, as such, are likely to be fire tolerators rather than fire promoters. It is difficult to see how an individual, high-flammability plant in a low-flammability population would be favoured, when fire occurs at a community level (Christensen, 1985); as an example Whelan (1995) cites the case of rainforest species that while individually flammable do not cause the rain forest as a whole to be so. Despite the intense debate over the Mutch Hypothesis in the ecological literature it is very difficult to evaluate critically, for while potential fire -retarding and facilitating traits of plant foliage have been measured (e.g. Jackson, 1968; Mutch, 1970), their effects on survival and reproduction have never been demonstrated in the field (Williamson and Black, 1981). Coley *et al.* (1985) and Grubb (1992) consider that an unequivocal demonstration that a flammability-enhancing trait evolved under selection by fire to be as problematic as understanding the importance of herbivores as compared to other selective forces in the evolution of plant defences.

Another argument often used in favour of fuel dynamics driving wildland fire is that of fuel succession and accumulation driving wildland fires. This concept has been advanced by Heinselman (1973), Habeck and Mutch (1973), Romme and Knight (1981) and Clark (1988). The basis of the fuel accumulation argument is that over successional time dead fuel inevitably increases, thus providing increased likelihood of a major fire event. Evidence of such a process is provided by Romme and Knight (1981) who found that major fire events in the Medicine Bow Mountains, Wyoming,

had an average return frequency of 300 years. Furthermore, fires burning intensely in late-successional stands (350+ YA) failed to move into younger stands' (up to 100 YA); Romme and Knight (1981) take this as clear evidence that in the younger stands' fuel loads were so low that fire spread was prevented. However, the importance of fuel accumulation is also recognised by those authors who consider weather to drive wildland fire histories. For example Swetnam (1993) considers that in periods of high fire frequency, fuel will be maintained at low loads, resulting in a patchy pattern of smaller fires and perpetuating a fine-grained spatial pattern. During periods of low frequency, more fuels accumulated and the resulting fires were more widespread and intense, producing a coarse-grained spatial pattern. The fundamental difference between the arguments of Romme and Knight (1981) and Swetnam (1993) is that Romme and Knight (1981) argue that the interval between fire events is a result of fuel succession while Swetnam (1993) considers it to be driven by climatic fluctuations. Grouping the arguments of Romme and Knight (1981) and Clark (1988) with those of Mutch (1970) is too simplistic, for while Clark (1988) argues that aging causes biomass accumulation which subsequently determines the *potential* for fire, Mutch (1970) is arguing that the biomass *modifies this potential* through such factors as highly flammable or flame-retardant chemicals.

The essence of the weather side of the fuels vs. weather debate is that long-term climatic trends drive site-specific fire histories. Examples of this phenomenon are provided by: (i) Flannigan and Harrington (1988) in their analysis of how climatic variables correlate with areas burned by wildfires in Canada; (ii) Fryer and Johnson (1988), in their reconstruction of the 1936 Galatea fire in the Canadian Rockies; (iii) Swetnam and Betancourt (1990) who consider relations between fire and the El-Niño Southern Oscillation (ENSO) relations in the southwestern United States; (iv) Johnson and Larsen (1991) who studied climatically induced changes in fire frequency in the southern Canadian Rockies and (v) Swetnam (1993) who discussed fire history and climate change in *Sequoiadendron giganteum* (giant sequoia) groves. Although the influence of daily weather on fire behaviour is reasonably well understood (e.g. Rothermel, 1983), the influence of seasonal and longer-term climatic patterns is not (Swetnam and Betancourt, 1990). A close linkage between climate and fire history would have important ecological implications. Local processes such as competition, predation and stochastic fluctuations in the dynamics of fire-dependent ecosystems would be diminished. Furthermore it has important implications for the relative roles of exogenous and endogenous factors in such ecosystems. The authors cited above believe that the structure and diversity of systems regulated by fire frequency, intensity and extent may have non-equilibrial properties associated with decadal to secular variations in global climate.

Johnson and Larsen (1991) provide evidence for climatically-driven fire-histories in the southern Canadian Rockies over the last four centuries. They found that fire frequency fluctuated with climatic changes; for example a period of longer fire cycle (1730-1980) corresponded with glacial re-advance from the early 1700s to the 1940s. A widely held belief in favour of fuel characteristics driving wildland fire histories is that the chance of an area burning increases over time due to the accumulation of dead fuel. However, this assertion was disputed by Johnson and Larsen (1991) who found a lack of consistent spatial variation within the study area. It is interesting to note that Swetnam (1993), although a proponent of the weather school of thought, regards fuel accumulation to be significant in determining fire patterns at the *local* scale. Furthermore, it was found that although patches of vegetation avoid individual fires, no surviving patches were found that had a consistently longer period between fires than adjacent areas that did burn. Similar results to those of Johnson and Larsen (1991) were found by Swetnam and Betancourt (1990) who note that small areas burn after wet springs associated with the low phase of the ENSO, whereas large areas burn after dry springs associated with the high phase of the ENSO; and by Swetnam (1990) who found that in *S. giganteum* groves regionally synchronous fire occurrence was inversely related to yearly fluctuations in precipitation and decadal to centennial variations in temperature. Finally, at the scale of a single fire Fryer and Johnson (1988) found that weather was the single most important variable influencing the 1936 Galatea fire, *as it controls [short-term] fuel moisture*; differences in elevation and vegetation type were found to be insignificant due to the extremely dry conditions and the relative similarities of the fuels the fire burned through. Superficially, the arguments of Clark (1988) and Swetnam (1993) are very similar (i.e. that fire size increases with time between fire events). However, the key point is that Swetnam (1993) suggests that fire comes in low and high frequency periods related to weather patterns. Thus, whereas Clark (1988) is concerned with *spread potential*, Swetnam (1993) is concerned with *ignition potential* (i.e. the potential number of fires).

Bessie and Johnson (1995) assessed the relative significance of weather (wind speed and FMC) and fuel factors (fuel loads, fuel depths, surface area/volume ratio, heat of combustion, and mass density) in the southern Canadian Rocky mountains by creating aggregated fuel and weather variables and using predictions from the models of Rothermel (1972) and Van Wagner (1977a). They found fire behaviour to be more strongly correlated to weather variation (over time) than fuel variation (among stands). The lower threshold below which surface fires could not occur and the upper threshold above which only crown fires occur were defined by the weather variable. By contrast the fuel variable always exceeded zero and therefore could not determine whether or not burning would take place. The weather variable also explained 83% of variation in

fire intensity whereas the fuel variable could only account for 15% of this variance.

Bessie and Johnson (1995) provide two explanations for the dominance of weather over fuel in determining fire behaviour. Firstly weather is more strongly associated with the fundamental processes through which fire spread occurs such as radiative and conductive heat transfer. Moreover FMC largely determines fuel combustability and heat loss rates. By comparison fuel primarily acts as the burn substrate, providing the heat of combustion for the fire (Rothermel, 1972). Secondly, weather largely determines intensity because fire weather is much more temporally variable than the fuel bed. High weather variation and strong links to the fire behaviour mechanisms in the models are such that the weather variations and thus the weather induced intensity variation range over four orders of magnitude.

A crucial point in the debate outlined above is that of FMC being regarded as a weather, and not a fuel, factor. Mutch (1970, p. 1046) points out that historically the occurrence and severity of wildland fires has been viewed in terms of fire climate and "influence of weather factors on fuel moisture". However, if FMC is considered across a range of spatio-temporal scales then the assumption that FMC is principally influenced by weather conditions becomes questionable. Across larger spatio-temporal scales, FMC may well be primarily driven by weather factors, as suggested by Flannigan and Harrington (1988), yet at the scale of the individual fire the assertion of Fryer and Johnson (1988) that weather conditions dictate FMC is debatable, for fuel characteristics play a large part in controlling FMC at smaller temporal scales and FMC will be linked to other variables such as topography, soil type, water table depth and successional stage.

To conclude, the issue of whether fuels or weather drive wildland fire histories and the related debate over the Mutch Hypothesis is extremely problematic. It seems likely that the factors governing the spatio-temporal patterns of fire may vary along a climatic gradient. Christensen (1993) considers that under relatively moist conditions fire spread is regulated by FMC and chemical compositions as well as by micro-scale fuel structure variations. Above threshold moisture limits, variations in stand structure and flammability set the boundaries for fire movement and determined fire intensity. Under the driest conditions, among stand-variations in structure and fuels have little influence on fire behaviour and large-scale topographic features and weather patterns become the dominant features. It seems likely that the significance of environmental trade-offs needs to be considered when evaluating this debate. For example, as precipitation increases fuel load will also increase but flammability will fall as FMCs rise in response to precipitation, although temporal variability will always ensure that FMC sometimes

falls below the critical level. So, it may be expected that fire would reach a maximum regime at an intermediate level of precipitation. Thus, on a climatic gradient from desert or tundra (with low, discontinuous fuels) to rainforest (with less flammable fuels) fire is likely to be prevalent in the driest ecosystems and where the selection pressure is for fine fuel structure, but the load is sufficient to carry a fire.

2.7 The Quantification of Wildland Fire

Questions concerning the quantifiable characteristics of a fire are of significance to those studying the role of fire in ecosystems. The intensity of a fire may determine the scorch height of burnt vegetation, while rate of spread will determine the residence time for lethal fire temperatures at a given point (Whelan, 1995). Furthermore, much of this thesis is concerned with the accurate prediction of the quantitative parameters of wildland fire. For these reasons it seems appropriate to consider how wildland fires are quantified and the inherent problems involved with such quantification. This section is divided into two-subsections: the first considers fire spread and growth, and the second heat generation and fire intensity.

2.7.1 Fire Spread and Growth

The rate of movement of the outer edge of a fire, in a direction normal to the perimeter is termed the *local rate of spread* (Johnson, 1992; Albini, 1993). It is not the increase in perimeter or length of the fire front (Tangren, 1976). Strictly the fire must have established a steady-state behaviour for rate of spread to be meaningful. The local rate of spread may vary greatly along the fire perimeter at any one time, as it is fixed by instantaneous conditions. Thus, it is usually assumed to imply an average value over the minimum period of time, such that variation in instantaneous conditions is immaterial. The forward rate of spread implies either the rate of spread at the front of a wind-driven fire, the upslope rate of spread for a fire in uneven terrain, or the most rapid rate seen at the perimeter of a fire. If the forward rate of spread can be ascertained, then other rates of spread can be estimated in relation to it, and other measures of growth rate may also be calculated (Anderson, 1983; Baines, 1990). Cheney (1990) notes that most fire models calculate rate of spread at the fire front and that most other measures of fire growth are qualified by position on the fire's perimeter.

In homogenous fuels and under unchanging environmental conditions, the local rate of spread can be assumed to be constant for the head, flanks and tail of a given fire. As a result the fire perimeter may be expected to exhibit a steady growth rate, the actively burning area inside the perimeter to increase proportionately and the area burnt per unit

time to increase linearly (Albini, 1993). These relationships are derived from the concept that natural fuel components, after ignition, tend to flame for a period of time proportional to their smallest dimension (Anderson, 1969; Lyons and Weber, 1993). Thus a tree branch burns for longer than a blade of grass. This observation can be interpreted as illustrating the rate at which a pyrolysing wave advances into solid vegetation tissue in 'typical' fire conditions (Albini, 1993; Whelan, 1995).

2.7.2 Heat Generation and Fire Intensity

Possibly the most valuable quantitative parameter of any wildland fire is its fire intensity. It is significant because the ability of living cells to tolerate heat decreases at high fire intensities, and it is also linked to factors such as the scorch height of the vegetation burnt (Whelan, 1995). However, accurate quantification of wildland fire intensity is extremely problematic (Albini, 1976; Cheney, 1990; Whelan, 1995). Albini (1976, p. 75) states:

> ". . . perhaps no descriptor of wildfire behaviour is as poorly defined or as poorly communicated as are measures of fire intensity . . . these measures [are] virtually unobservable but through various empirical relations they can be related indirectly to observable fire phenomena which themselves serve as indirect measures of intensity."

Fire intensity was first defined by Byram (1959) as being the effective radiation temperature of a fire front. Tangren (1976) and some other physicists disagree with the use of the term fire intensity and instead prefer the term *fire power*. However the term fire intensity has become widely used. The most commonly used measure of fire intensity is *Byram's (1959) fireline intensity*:

$$I = H\,w\,R \qquad (2.5)$$

where: I = the fireline intensity ($kW.m^{-1}$), H = the heat yield of the fuel ($J.g^{-1}$), w = the mass of fuel consumed ($g.m^{-2}$), and R = the forward rate of fire spread ($m.sec^{-1}$).

In quantitative terms, fireline intensity can be summarised as the heat release per unit length at the fire front. This is a parameter useful for many purposes and has become widely used to describe wildland fire behaviour (Albini, 1993).

It is important to realise that the energy released is not confined to the leading edge of the fire, but is released over the width of the combustion zone and back behind the fire edge (Tangren, 1976; Cheney, 1990). This is significant because it means that flame characteristics associated with a specific fireline intensity are only applicable to fuel

types with a similar fuel structure (Cheney, 1990).

For modelling the dynamics of vegetation fires, local measures of the rate of heat generation are usually more important than the total heat output rate of the fire. Thus although the rate of heat generated per unit length of fire front (the fireline intensity) is a parameter commonly employed to describe wildland fire, Anderson (1969) and Rothermel (1972) found the rate of heat generated per unit area (the *reaction intensity*) to be both less variable and more useful in the prediction of rate of spread in surface fires. The reaction intensity is the same as the combustion rate in that both describe the heat release per unit area of ground beneath the fuel bed. The reaction intensity curve describes the consumption of fuel as the fire burns across and down through the fuel bed over some point on the ground (Cheney, 1990). In some circumstances, a third measure of intensity, the *total heat output*, is the most appropriate measure. This measure is most useful in the prediction and correlation of convection plume phenomena such as spotting (Briggs, 1969). A final intensity parameter is *convective intensity*, which is defined as that portion of the total heat output used to lift the stack gases and entrained air above the flame zone. Convective intensity is estimated by subtracting conductive and radiant heat losses from the total energy release rate (Chandler *et al.*, 1983).

To predict or estimate any of these measures of fire intensity, vegetation must be classified into burnt and unburnt components. Living plant matter may or may not burn in a surface fire because such matter has a moisture content of between 80 and 200% (Pyne, 1984). By comparison dead plant matter components have a moisture content fixed by the recent history of atmospheric humidity, below a fibre saturation of 30% (Rothermel, 1972; Albini, 1993). If the burning of dead plant matter creates a fire of sufficient intensity (probably best characterised by reaction intensity), then the smaller living plant components will also be burned and will contribute to the local heat release rate. The rate at which any fuel component burns after ignition can be estimated from its minimum dimension (Whelan, 1995). Leaves 0.03mm thick should flame vigorously for about 6 seconds, those 3 mm thick for about one minute (Albini, 1993). At the outer edges of the fire, where ignition has just occurred, large fuel elements have surface temperatures below the ignition limit, and live components may still be losing moisture. The rate of heat transfer is very high at this point and rises to its maximum within the envelope of flame at the fire front. The smaller particles of fuel exposed to the flame envelope are consumed within that regime. Larger pieces continue to burn after the flame structure breaks into smaller fragments, the largest ignited only by such residual burning (Albini, 1993). The size of the coherent flame structure, measured normal to the fire edge, provides the scale of length for determining the local fireline intensity

(Cheney, 1990; Albini, 1993). The length of the flame at the fire front has been correlated to a fractional power of the fireline intensity by a number of authors (e.g. Byram, 1959; Albini, 1976, 1981a, 1993; Nelson and Adkins, 1986; Cheney, 1990; Fuller, 1991).

2.8. Summary

This chapter has considered the mechanics of wildland fire and its spread. Fire itself is driven by the fundamental process of combustion which embraces pre-ignition, pyrolysis, ignition, combustion itself and extinction. These processes are generally well understood. However, the manner in which wildland fire spreads and its complex relationship with the physical environment (especially the wind field, topography and fuels) is poorly understood. The debate concerning the interaction between wildfire behaviour and the physical and biological environments is epitomised by the argument over the validity of the 'Mutch Hypothesis'. The quantification of fire and some of the issues associated with this difficult problem have also been reviewed. Although accurate quantification of wildfire is often critical in explaining the ecological changes fire brings, rigorous quantification is rarely carried out in post-fire ecological studies. The issues presented in this chapter are all of some relevance to the development and application of fire behaviour modelling, as is shown in Chapter 3.

Chapter Three

Modelling the Fire Phenomenon

3.1 Introduction

Understanding of the factors determining fire behaviour has been increased through the development of ever more complex predictive models. Simple models linking fuels, moisture and oxygen as primary determinants of fire intensity have developed into basic empirical predictors (e.g. McArthur, 1966, 1967; Noble *et al.*, 1980) and on to complex computer-aided prediction systems such as BEHAVE (Burgan and Rothermel, 1984) and FIREMAP (Vasconcelos, 1988). This chapter reviews the development of fire modelling, and the various theoretical approaches taken. The role of GIS in fire modelling is considered, and the Yellowstone fires of 1988 are considered as a case-study of large-scale predictive fire modelling. Finally, the way in which fire modelling may develop in the future is discussed through the review of three crucial research areas.

3.2 The Fundamental Problem

In general terms the fundamental problem fire modelling seeks to address is the prediction of the rate of spread of a fire through a fuel bed. Weber (1991a) considers there to be three physical processes integral to fire spread :

- An ignition source which leads to the localised release of reactive gases in a fuel bed, followed by their gas phase combustion, resulting in flames within and around the fuel bed;
- The heat produced in this reaction is transferred by any available mechanism and a portion of it reaches the unburnt fuel;
- The absorption of energy by unburnt fuels which raises the enthalpy to a point where decomposition occurs, releasing fresh reactive gases (whose later combustion is seen as fire spread).

Central to this conceptualisation of fire spread is the feedback loop inherent in fire behaviour; the combustion reaction must release and subsequently transfer enough energy to cause unburnt fuels to ignite. In mathematical terms the fundamental problem can be expressed in a reaction transport formulation of the conservation of energy (Weber, 1991a,b):

$$\frac{\partial H}{\partial t} = - \nabla . q + Q$$

rate of change of enthalpy per unit time = spatial variation of the flux of energy + heat generation (3.1)

Typically the enthalpy (H), the flux (q) and the heat generation (Q) are all functions of one variable, temperature (T). Thus, Equation 3.1 is a partial differential equation, expressing the spatio-temporal changes in temperature.

3.3 Physical, Semi-physical or Empirical ?

Three broad types of fire behaviour model are recognised: physical, semi-physical and empirical, although the nomenclature varies (Chandler *et al.*, 1983; Catchpole and de Mestre, 1986; Beer, 1991; Weber, 1991a). Empirical models are in essence statistical descriptions of wildland fires and make no attempt to include any of the physical mechanisms which drive fire. Semi-physical (or semi-empirical) models are those based on the observation of small-scale experimental fires and the subsequent use of dimensional analysis to maintain a similarity of process across all scales. Physical models are those based on mathematical analysis of the fundamental physical and chemical processes of fire spread and involve no analysis of actual fire events. The most significant models of each type are presented in Table 3.1. This section reviews these three types of models and considers their advantages, disadvantages and 'real world' applicability.

3.3.1 Physical Models

Physical (or theoretical) models of fire spread are those based on the first principles of the physics and thermodynamics of the processes which control fire (Weber, 1991a). Catchpole and de Mestre (1986) argue that for a model to be classed as 'physical' it must incorporate the chemistry of combustion to be predictive, and results must be validated and calibrated by test burning. All physical fire spread models assume that the outcome of the chemical process is known and use variables such as flame height and temperature as model inputs. As a result all current physical models contain some degree of empirical analysis despite being termed 'physical' (Catchpole and de Mestre, 1986). Most physical models are developed from the idea of the steady state energy flux relationship presented in Equation 3.2:

$$Q = \rho r \Delta h \qquad (3.2)$$

where : Q = the net energy per unit area transported across the surface of fire inception; ρ = fuel density; r = rate of spread, and Δh = the difference in thermal enthalpy between

the fuel at its ignition temperature and the virgin fuel. Williams (1977a, p. 1282) considers this expression to be the "fundamental equation of fire spread".

Table 3.1. Examples of the classification of fire spread models according to whether they are empirical, semi-physical or physical. (Weber, 1991a).

Empirical	*Semi-empirical (semi-physical)*	*Physical*
Anderson *et al.*, 1982.	[Frandsen, 1971.] *	Albini, 1967, 1985, 1986.
Green, 1983.	Rothermel, 1972.	Cerkige, 1978.
McArthur, 1966.		Dorrer, 1984.
Noble *et al.*, 1980.		Emmons, 1964.
Stauffer, 1985.		Fons, 1946.
		Frandsen, 1971.
		Fujii *et al.* 1980.
		Grishin, 1984.
		Grishin *et al.*, 1983.
		Hottel *et al.*, 1964.
		Kurbatsky and Telisi, 1977.
		Pagni and Peterson, 1973.
		Steward, 1974.
		Thomas, 1967, 1971.
		Weber, 1989a, 1989b.

* Weber (1991a) classes Frandsen's (1971) model as semi-empirical but most others consider it to be physical.

The major advantage of rigorous physical models is that they are based on known relationships, thereby facilitating their scaling (Chandler *et al.*, 1983; Weber, 1991a). Such scaling allows validation against a much more limited data set than is required for the other types of model. Furthermore, physical models provide an insight into the mechanisms which drive wildland fire spread (Catchpole and de Mestre, 1986). However, the widespread usage of physical models is hindered by two major factors. Firstly, many of the key input variables (e.g. flame height and stack gas viscosity) are almost impossible to measure in the field (Chandler *et al.*, 1983; Beer, 1991), and secondly, as discussed in Chapter Two, the processes of heat transfer are neither temporally nor spatially constant. A model that predicts rate of spread by calculation of flame radiation can only give valid outputs when the fire is being driven by radiative heat transfer. The relative importance of radiation and convection will vary from fire to fire and estimation of their exact combination is not simple (Thomas, 1971; Weber, 1991a).

No genuinely physical fire spread model has been used operationally in the manner of the models of Rothermel (1972) in the USA, Stocks *et al.* (1989) in Canada, or McArthur (1966, 1967) and Noble *et al.* (1980) in Australia. However, two physical models are worthy of closer examination; those of Fons (1946), the first published mathematical model of fire spread, and Frandsen (1971), which forms the basis of Rothermel's (1972) model.

Fons (1946) published a mathematical model which calculated the rate of spread of fire in light forest fuels. Fons (1946) considered the fuel to be an array of equidistant vertical rods of an ambient temperature before the approach of the fire front. At the time when the n-1th row of rods is ignited, its temperature is termed the ignition temperature, and the temperature of row n is at some point between the ambient and ignition temperatures. Catchpole and de Mestre (1986) believe a major weakness in the model of Fons (1946) is the problematic calculation of the value of this intermediate temperature. This nth row is assumed to be in contact with the flames from the n-1th row, and is heated by convection, conduction and radiation until it reaches the ignition temperature. The rate of spread equation derived by Fons (1946) considered the physical characteristics of the fuel particles, fuel bed configuration and meteorological conditions. These were defined in terms of eight fundamental variables (Crock, 1986): (i) film conductance for convection and conductance; (ii) heat transfer factor for radiation; (iii) ignition temperature; (iv) fuel particle spacing; (v) surface-to-volume ratio of the fuel; (vi) specific heat; (vii) fuel density and (viii) fuel temperature. Fons (1946) expressed rate of spread with regard to the fundamental variables as opposed to more standard, field-assessable variables (e.g. slope, wind speed, FMC) because he considered that such standard variables only influence rate of spread through inducing changes in the fundamental variables. The final expression Fons (1946) produced was for rate of spread in an homogeneous light forest fuel :

$$R = \frac{C(f_c + f_r)\sigma L}{YC_p \ln[C_t(T_f - T_o)/(T_f - T_i)]} \qquad (3.3)$$

where : R = rate of spread (ft.hr^{-1})

C = a proportionality constant relating rate of spread in a natural fuel bed to rate of spread in an idealised standard fuel bed;

f_c = film conductance for convection and conductance (BTU.ft^{-2}.hr^{-1});

f_r = heat transfer factor for radiation (BTU.ft^{-2}. hr^{-1});

σ = surface-to-volume ratio (in.$^{-1}$);

L = spacing between particles (in.);

U = density of moist fuel (lbs.ft^{-3});

C_p = specific heat of moist fuel at a constant pressure (BTU.lb^{-1});
C_t = temperature-difference ratio coefficient;
T_p = temperature of flame (°F);
T_o = temperature of a fuel particle far away from the flame (°F);
T_i = ignition temperature of a fuel particle (°F).

Frandsen (1971) applied the conservation of energy principle to a unit volume of fuel ahead of an advancing fire in a homogeneous fuel bed. Frandsen's model is termed as a 'propagating flux model' by Catchpole and de Mestre (1986) because the three elements of heat transfer are not treated separately but are aggregated to form the 'propagating heat flux'. A global energy balance gives rate of spread in terms of the fuel specific heat, the bulk density and the propagating heat flux. The propagating heat flux is a function of the shape of the combustion zone in the fuel bed. The model is based on the premise that the curved interface between burnt and unburnt fuel implies that the term:

$$\int_{-\infty}^{0} \left(\frac{\partial Q}{\partial z}\right) d_z \qquad (3.4)$$

needs to be added to the left hand side of Equation 3.2 (Beer, 1991). This term can be obtained by integrating the equation of energy conservation and represents the effects of the vertical heat flux gradient, the vertical being represented by z and the horizontal direction of the fire front propagation being the $-x$ direction. The final expression derived by Frandsen (1971) is :

$$R = \frac{I_{xig} + \int_{-\infty}^{0} \left(\frac{\partial I_z}{\partial z}\right)_{z_c} d_x}{\rho_{be} \; Q_{ig}} \qquad (3.5)$$

where : I_{xig} = horizontal heat flux absorbed by a unit volume of fuel at the time of ignition (BTU.ft^{-2}.min^{-1}); ρ_{be} = effective bulk density (amount of fuel per unit volume of the fuel bed raised to ignition ahead of the advancing fire, lb.ft^{-3}); Q_{ig} = heat of pre-ignition (the heat required to bring a unit weight of fuel to ignition, BTU.lb^{-1}) and $(\partial I_z / \partial z).z_c$ = the gradient of the vertical intensity evaluated at a plane of constant depth (z_c) of the fuel bed (BTU.ft^{-3}.min^{-1}).

Frandsen (1971) acknowledged that the model does not provide an *a priori* method of determining rate of spread but it does give a way in which the heat source (combustion zone) can be divided from the heat sink (the fuel). The main significance of Frandsen's (1971) model is that it forms the physical base for the Rothermel fire spread model (Catchpole and de Mestre, 1986).

3.3.2 Semi-physical Models

Because of the difficulties inherent in the development and use of rigorous physical models, many models adopt a combination of physical and empirical techniques; such models are termed semi-physical, or semi-empirical (Chandler *et al.*, 1983; Catchpole and de Mestre, 1986). A characteristic of semi-physical models is that they postulate the heat flux and the required heat of ignition without strict regard as to the mode of heat transfer or the mechanism of heat absorption (Beer, 1991). The various constants governing variation in the heat flux and absorption terms are usually derived experimentally. Such models do not describe the processes which contribute to Q (the net energy per unit area transported across the surface of fire inception; Equation 3.2); instead, it is usually termed the propagating flux and is empirically derived as a function of the reaction intensity (Weber, 1991a).

The most important semi-physical model for predicting fire spread is that of Rothermel (1972). The model was developed to predict rate of spread in a continuous stratum of fuel contiguous to the ground (Rothermel, 1972). The model is only briefly outlined below for it is considered in greater detail in Chapter 4. Like the physical model of Frandsen (1971), Rothermel's model is based on the premise of a propagating flux generated by radiative heating. Convective heating ahead of the flame and direct flame contact are not considered (Catchpole and de Mestre, 1986). As described in Section 3.3.1, the inputs which physical models require to calculate the propagating flux are often difficult to measure. Rothermel (1972) avoids these difficulties by assuming that the propagating flux is proportional to the reaction intensity of the fire. This proportionality constant was established for no-wind, no-slope conditions by burning test beds of various sizes and compactnesses. As a result the constant is assumed to depend, in the no-wind, no-slope case, on fuel particle size and packing, and not on other parameters such as fuel bed depth, flame characteristics or chemical fuel properties (Chandler *et al.*, 1983). Corrections for slope and wind have been derived empirically under laboratory conditions. Calibration of the model involves the inclusion of physical parameters such as fuel bed depth, the characteristic surface-area to volume ratio of the fuel bed and fuel heat content (Beer, 1991). The model has been tested in a wide range of laboratory and field conditions including horizontally patchy and vertically stratified fuels (e.g. Brown, 1972; Sneeuwjagt and Frandsen, 1977; Andrews, 1980; Rothermel and Rinehart, 1983; Van Wilgen *et al.*, 1985; Gould, 1988; Van Wilgen, 1988 and Catchpole *et al.*, 1993). These validations are considered more fully in Chapter 4.

3.3.3 Empirical Models

Empirical models are those which make no attempt to involve physical mechanisms and are, in essence, statistical descriptions of test fires (Catchpole and de Mestre, 1986; Weber, 1991a). Empirical models have been used successfully in a range of ecosystems (e.g Noble *et al.*, 1980; Stocks *et al.*, 1989). However, their lack of physical basis means that they can only cautiously be used outside of the test conditions (Chandler *et al.*, 1983; Weber, 1991a; Marsden-Smedley, 1993).

The McArthur fire and grassland meters are a good example of an empirical model that has been developed to the point of operational usage (McArthur, 1966, 1967; Noble *et al.*, 1980). They were developed and tested in south-eastern Australia using a database of over 5000 fires and 500 intensively studied prescribed burns (Chandler *et al.*, 1983). Noble *et al.* (1980) derived mathematical relationships for the simplest meter, the Mark IV grassland fire danger meter :

$$F = 2 \exp [-23.6+5.01 \ln (C_d) + 0.0281 T_a - 0.226 RH^{½} + 0.663 U_{10}^{½}]$$
$$R = 0.13F \qquad (3.6)$$

where : R = Rate of spread (km.hr^{-1}); C_d = degree of curing (%); T_a = air temperature (°C); RH = relative humidity (%); U_{10} = wind velocity (m.sec^{-1}) at mid-flame height and F = fire danger index.

The use of these meters has been very successful in the conditions for which they were designed (Catchpole and de Mestre, 1986; Weber, 1991a). However, their use in other fire environments (e.g. heathland) has been markedly less successful (Marsden-Smedley, 1993). This highlights the prime inadequacy of empirical models - their lack of widespread applicability due to their inability to be extrapolated beyond the conditions in which they were formulated.

3.4 Fire Shape and Fire Simulation Modelling

A different sort of empirical model to those outlined in Section 3.3.3 is that concerned with the simulation of fire behaviour. In such models the objective is to predict the eventual extent of a fire, rather than the rate at which it is spreading (Weber, 1991a). Fire shape and simulation modelling are further considered in the following sub-sections.

3.4.1 Fire Shape Modelling

Green *et al.* (1983) found that the elliptical model provides a satisfactory description of

the perimeter of a free-burning wildland fire (Figure 3.1). The ellipse can serve as: (i) a growth model for the development of a fire burning in homogeneous conditions (constant wind velocity, uniform fuel, flat or uniformly sloping terrain), in either continuous (Anderson *et al.*, 1982) or discontinuous fuels (Green *et al.*, 1983); or, (ii) as a template to be applied to an established model perimeter parameter to generate the shapes to be expected in non-homogeneous conditions (Anderson *et al.*, 1982). Catchpole *et al.* (1992) further extended these concepts to the prediction of the proportions of the fire perimeter burning at given intensities. An outline of the development of the elliptical-fire perimeter model is given below.

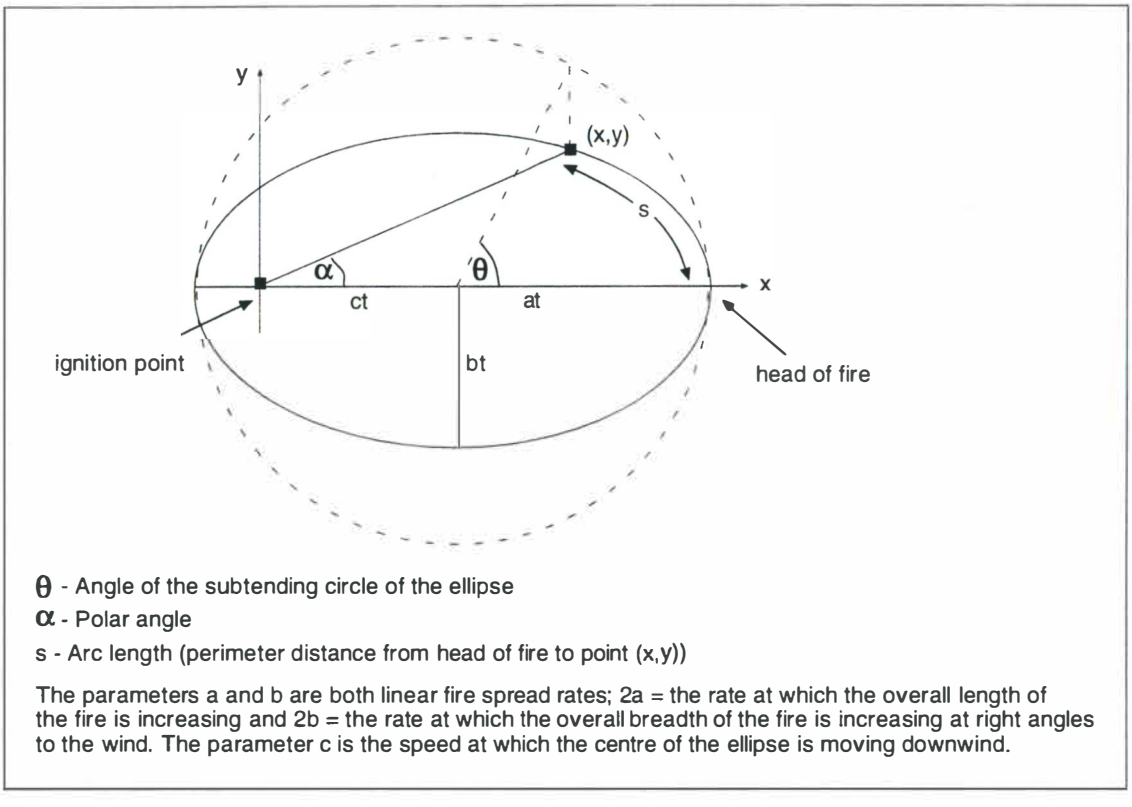

Figure 3.1. Position of the perimeter of a simple elliptically shaped fire at time *t* under uniform wind, fuel, and topographic conditions, with the maximum rate of advance in the x direction. The dotted curve is the subtending circle of the ellipse (Catchpole *et al.*, 1992 and Wallace, 1993).

Peet (1967) studied the shape of low- and mild-intensity fires in the Jarrah forest of Australia. He found that fire shape tended to become more ovoid as the forward rate of spread of the fire increased. Albini (1976) found the same effect and produced a set of idealised fire shapes (Figure 3.2) for wind speeds between 0 and 50 km.hr^{-1}.

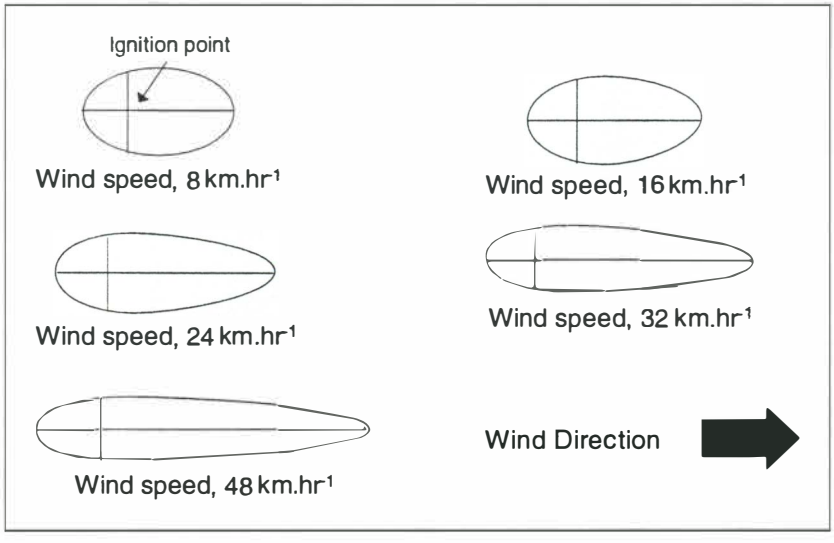

Figure 3.2. Eccentricity of the elliptical fire shape at different wind speeds. The sizes shown are arbitrary (Albini, 1976 and Pyne, 1984).

Van Wagner (1969) was the first to consider mathematically the concept of elliptical shapes in fire spread (Figure 3.3). He examined the shapes of rapidly moving, high intensity fires. Van Wagner (1969) regarded the elliptical shape as overly simplistic but that the approximation was adequate for practical purposes. His final expression was :

$$A = \frac{\pi}{2} (v + w)\ ut^2 \tag{3.7}$$

where : A = fire's area (an ellipse); v = the linear rate of spread at head; u = linear rate of spread at the flanks; w = linear rate of spread at the rear and t = the time since ignition.

Despite the apparent simplicity of Equation 3.7 it requires more information than is usually available. Van Wagner (1969) notes that the ideal situation is where, for a given fuel type, u, v and w are expressed as functions of specific burning conditions. The rate of increase at time t will be given in terms of area per unit time by the first derivative :

$$\frac{\partial A}{\partial t} = \pi(v + w)\ ut \tag{3.8}$$

This shows that the rate of areal increase is not constant but increases over time. However, the acceleration rate at which the area increases is constant and is given by the second derivative with dimensions of area per unit time^2 :

$$\frac{\partial^2 A}{\partial t^2} = \pi(v + w)\ u \tag{3.9}$$

Anderson (1983) studied wind driven fires with velocities of between 3 and 20 km.hr^{-1}. Anderson (1983) found that the shape of the burnt area was best described as a combination of two semi-ellipses, with the two ellipses sharing a common minor axis. The backing fire is described by an ellipse with a shorter minor axis which reflects the

slower rate of spread (Ball and Guertin, 1992).

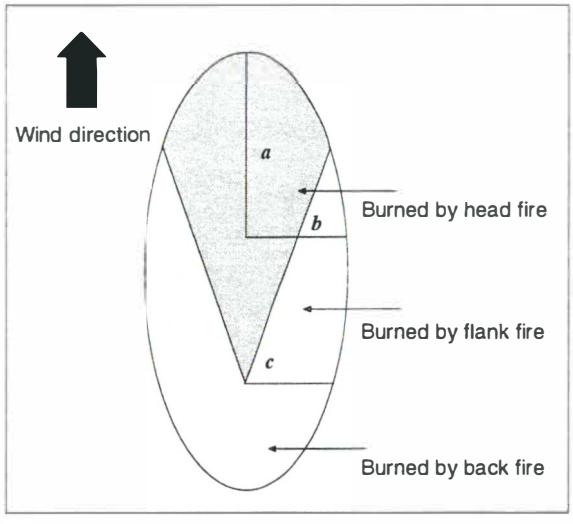

Figure 3.3. Van Wagner's (1967) elliptical fire growth model (Van Wagner, 1969).

Arranging these studies in the order of fire intensity and rate of spread, the fire shape progresses from a circle to an ovoid, to a double-ellipse, to a semi-ellipse (Ball and Guertin, 1992). In summary, the shapes produced by the analytical models of Peet (1967), Van Wagner (1969) and Anderson (1983) described above are estimated by fitting a mathematical shape to the patterns of burnt areas. The models all attempt to calculate fire shape for uniform fuel, moisture, terrain and wind conditions (Ball and Guertin, 1992; Catchpole *et al.*, 1992).

Green *et al.* (1983) tested experimental fires against the fire shape models described above (an ellipse, a double-ellipse and an ovoid), a rectangle and a simulation model developed by Green (1983) to establish which of these models is the best predictor of fire shape. Green *et al.* (1983) showed that the five fire models tested (including the rectangle) all gave reasonable approximations of the fire contours examined. Green *et al.* (1983) consider that the number of parameters used to fix the shapes, rather than the intrinsic properties of the shapes themselves, to be the prime determinant of the goodness-of-fit to real fire maps.

3.4.2 Fire Growth Simulation

To overcome the limitation of analytical models, much use has been made of simulation models to predict the growth pattern(s) of fire. Such models make use of computer graphics to produce a visual representation of the growth of fire over a landscape. Many different theoretical approaches have been taken to fire simulation. These include simulations based on the elliptical models described in Section 3.4.1 (Anderson *et al.*, 1982; Wallace, 1993), cellular automata (Hogewog, 1988; Clarke *et al.*, 1994; Clarke

and Olsen, 1996), fire propagation in arrays (Weber, 1990), Markov chains (Catchpole *et al.*, 1989), percolation modelling (Stauffer, 1985; Beer and Enting, 1990), stochastic contagion techniques (Von Niessen and Blume, 1988), chaotic techniques (Chevrou, 1992) and the discrete events system paradigm (Vasconcelos and Zeigler, 1993; Vasconcelos *et al.*, 1993).

Kourtz and O'Regan (1971) developed a fire growth model which examined the spread characteristics of smouldering ground fires. Kourtz and O'Regan (1971) used a square cell array to plot the spread of the fire over a small area. The spread of the fire was evaluated by calculating the path of least resistance between cells, using Dijkstra's shortest path algorithm (Dijkstra, 1959), without any dependence on neighbouring cells. Although the model provides useful information about ground fire spread, the small array area makes it unsuitable for large-scale fires. However, the assumptions which Kourtz and O'Regan (1971) made about non-homogeneous, discontinuous fuels were developed in the model of Frandsen and Andrews (1979).

Frandsen and Andrews (1979) were concerned with the modelling of fire behaviour in heterogeneous fuel beds. They used hexagonal cells, at a size selected to provide sufficient resolution of the fuel array. It was assumed that each cell was internally homogeneous. The choice of a hexagonal cells carries with it the restriction that fire can only spread in the six cardinal directions of the hexagon, but it has the advantage that neighbouring cells are all equidistant from a focal cell. The sources of the fires used in the model were line fires, and the examination of fire behaviour in non-uniform fuels was through the observation of fire spread distribution. Since the model results were in the form of distribution graphs, no graphical representation of spread was produced. The spatial resolution of the array was a critical factor in Frandsen and Andrews (1979) model, the resolution selected (two feet across) restricted the wind speed to two miles per hour. If the wind size were to increase the cell size would need to increase correspondingly, and this is not practical in a dynamic model (Ball and Guertin, 1992).

French *et al.* (1990) compared the results of three cell-based simulations (two square [Kourtz and O'Regan, 1971; Green, 1983], one hexagonal [Frandsen and Andrews, 1979]) and a non-grid-based alternative based on Huygen's principle (Anderson *et al.*, 1982). In the grid-based representations, the shapes of the fires became distorted because of the grid system and the algorithms used to derive fire shapes. The method employing Huygen's principle assumes that the elliptical shape adequately describes the shape of a fire. By linking an analytical generation of an ellipse to the graphical display of the fire, French and Anderson (1989) managed to approximate the type of fires described by Van Wagner (1969). The French *et al.* (1990) simulation was performed

under homogeneous conditions of no slope, uniform fuel and a constant wind direction. Green's (1983) method was found to be the most general model, but it required significantly more computation than the other algorithms tested. The other grid-based methods executed more quickly but produced serious distortions of fire shapes. French *et al.* (1990) found Huygen's method to execute quickly and produce little distortion, but its application in non-uniform environments was problematic.

Green *et al.* (1990) developed a fire simulation system termed IGNITE. IGNITE uses an array of square cells and is based on the fire spread formulations of Noble *et al.* (1980). The program uses inputs describing fuel loads, vegetation type, topography, and land use and Green *et al.* (1990) consider how these data may be stored in a GIS. The model uses an elliptical ignition template to determine the effect of burning cells on their neighbours. This template is implemented as a look-up table and specifies the time it takes for a burning cell to ignite adjacent cells. Green *et al.* (1990) note that the model assumes that fire spread is a simple epidemic process, with the time delay until ignition for any point in the fuel bed being determined by the path of least time from the fire's starting point.

The use of the look-up table and the description given by Green *et al.* (1990) indicates that the fire is assumed to be linked to the source of ignition for the duration of the fire event. Ball and Guertin (1992) consider this to be an invalid assumption noting that only very small fires retain some connection with the ignition source and that in large fires in complex terrain the fire fronts effectively act as new sources of ignition.

Although Green *et al.* (1990) indicate that the influences of irregular topography are considered in the simulation, all of the examples shown are based on differences in fire shape as a function of fuel structure and no indication is given regarding the influences of slope. Green *et al.* (1990) note that the model can incorporate spotting (randomised ignition) and fire fighting activities. However no information as to how these parameters can be incorporated is provided.

3.5 Spatial Information Systems and Fire Modelling

This section explores the role(s) of spatial information systems in fire modelling. Firstly the broad issue of the integration of GIS and other specialist environmental modelling systems is considered and then the use of GIS within the context of fire modelling is discussed, primarily though the use of a case-study, FIREMAP. It is important to note that other related spatial information systems, such as remote sensing platforms and data, may also be important in fire and environmental process modelling; hence the title

of this section.

3.5.1. The Systems Integration Problem

Computer-based, mathematical models capable of realistically portraying spatially distributed and temporally dependent environmental processes have come to be seen as crucial for the reliable, quantitative assessment of problematic environmental issues (Steyaert, 1992). In recent years there have been important developments in the quantitative description of resources through the linkage of environmental process models to GIS (Johnson, 1990; Abel *et al.*, 1994; Wesseling *et al.*, 1996). Current GIS are valuable as a source of data and data pre-processing for spatial models and for the analysis and display of results (Hamilton *et al.*, 1989; Chou and Ding, 1992). The capability to derive spatial information from a range of sources and to store them in a spatial database has, in a number of cases, simplified the data capture and supply aspect of environmental modelling (Wesseling *et al.*, 1996). However, the effective coupling of environmental process models and GIS has proved problematic. This section looks at two of the crucial issues hindering the effective integration of GIS and spatial process modelling; spatial data availability and the lack of temporal ability in contemporary GIS.

A number of the major problems facing those attempting the effective integration of process models and GIS have concerned the quality of spatial data. Many of the data that have been incorporated into spatial databases in the last fifteen years have been taken directly from cartographic documents. GIS use of such data is very different from their use in the context of a traditional map. Indeed many GIS may be using and manipulating spatial data in a manner for which they were neither intended nor collected (Goodchild, 1992). Therefore, although the digital processing of geographic data brings benefits in terms of processing and analysis, it may also reveal otherwise unapparent flaws in the data (Burrough *et al.*, 1988). Such problems are exacerbated by the fact that the computational and analytical techniques used are often very precise and so any uncertainty or error in the data can cause problems both in the form of erroneous results and subsequently in decisions based upon these results (Goodchild, 1991). In short, reliance on digital data collected from unknown or unreliable sources can lead to uncontrolled error (Johnson, 1990).

Burrough *et al.* (1988, p. 605) consider that the distributed finite element or finite difference approach, widely used in efforts to integrate GIS and other specialist systems, is valid only where "the models are supplied with data that describe spatial variation as accurately as the models can describe the process". Thus, for a process

model to yield consistently useful results each finite element in the substrate must be provided with its own location-specific data. When the finite elements are large in comparison to the heterogeneity of the landscape then model results are likely to be erroneous. Furthermore, choosing small elements and filling them with the same values taken from previously classified data brings no further intrinsic improvements, merely a dangerous illusion of accuracy due to an amelioration in the graphical quality of the output. Thus we have reached a point which Burrough *et al.* (1988) term the 'parameter crisis'; that is, as models get ever more realistic they require both better and more data to drive and control them. GIS is certainly no guarantee of data availability and finding solutions to issues such as the parameter crisis are problematic. They include the :

- collection of more spatial data,
- better use of existing data by using them for interpolating the values of attributes to a suitable grid instead of generalising and clumping,
- use of existing data and knowledge in a manner which enables better substrate models to be constructed.

When complex spatial process models are being used, the issues of what data should be input and in what form are often problematic. This commonly results from a lack of understanding about fundamental processes, scaling from small to large area estimates, methods for the integration and aggregation of data in time and space, and the inter-relationships of data sets in time and space (Steyaert, 1992). GIS can potentially help meet such needs and provide the flexibility for the development, testing, validation and evaluation of spatio-temporal data sets. The ability to be able to convert existing data sets to derivative data sets with provisions for flexible scaling, multiple parameterisations and classifications, grid cell resolutions or spatial aggregations and integrations will need to be developed in the future to support such data sets (Goodchild, 1991, 1992; Chou and Ding, 1992) .

Dynamic models, with temporally variable parameters, are difficult to integrate in most GIS. This is largely because GIS have been developed as tools useful for the query, display and maintenance of static databases storing static phenomena. Contemporary GIS do not explicitly allow temporally dynamic phenomena to be stored and analysed, and nor do they provide efficient facilities for iteration through time (Goodchild, 1991). Sundgren (1975) noted that most interesting systems are dynamic in nature and yet Ariav (1986) noted that despite this most databases merely provide a 'thin' tenseless and temporally inconsistent snapshot of the latest available data.

A spatio-temporal database could model the dynamically changing world; events could be traced and no data be forgotten (Clifford and Warren, 1983). Although the lack of

temporal capacities in GIS has been well documented (eg Armstrong, 1988; Nyerges, 1992; Langran, 1993), the concepts that form the basis of the required software architecture are still needed. The coupling of process models with GIS is required simply because no contemporary GIS has the ability to be able to represent data both spatially and temporally (Nyerges, 1992) or the algorithmic flexibility to process spatio-temporal dynamic models internally (Abel *et al.*, 1994; Wesseling *et al.*, 1996). In a process-modelling environment, a GIS could model temporality by allowing a system to respond to a range of historical or trend-analysis queries from simple analysis such as 'where was this feature ten years ago ?' to more complex queries (Langran, 1993).

3.5.2 GIS and Fire Modelling

Periera and Vasconcelos (1990) reviewed a number of spatial approaches to fire spread modelling. GIS-based fire behaviour modelling differs from these approaches in that it usually involves the use of real, precisely geo-referenced landscapes, as opposed to the aggregated statistical treatment of actual or simulated heterogeneity (Vasconcelos *et al* , 1994). As a result, when the spread of specific fires is attempted, the shapes produced are the result of the underlying models and geometric fire characteristics are not imposed *a priori*. Furthermore, simulation of fire characteristics under alternative fuel management and meteorological scenarios is facilitated by the cartographic data management capabilities which GIS provides (Hamilton *et al.*, 1989; Periera and Vasconcelos, 1990).

GIS can be used to spatially integrate several hazard variables, such as vegetation, topography, soil and fire history, which are only considered from sample areas in traditional fire danger systems (Chuvieco and Salas, 1996). This capacity has been widely used to generate locally oriented GIS-based storage which cover a small area at high resolution (typically 50-100m grid size). Examples of this approach are provided by Cosentino *et al.* (1981), Burgan and Shasby (1984), Yool *et al.* (1985), Salazar and Palmer (1987), McKinsey (1988), Salazar and Power (1988) and Hamilton *et al.* (1989). However, there have been some attempts to create global, low resolution fire danger models (e.g. McKinley *et al.*, 1985 and Werth *et al.*, 1985 - both cited in Chuvieco and Salas, 1996).

The key parameter in both the local and global studies is the vegetation layer. Several studies have explored the use of satellite imagery to generate data for these fuel layers through digital image processing, using Landsat-MSS or TM (Shasby *et al.*, 1981), SPOT HRV (Williamson, 1988) and NOAA-AVHRR (Miller *et al.*, 1986) imagery. Other variables frequently used for such GIS-based danger indices are weather

information, topography and fire history (Chuvieco and Salas, 1996). The following criteria are used to estimate the appropriate combination of the variables :

- the use of qualitative criteria for assigning danger values from the cross-relationships of the different variables
- the adoption of standard danger indices (e.g. BEHAVE; Burgan and Rothermel, 1984)
- the creation of new danger indices, based upon the selective weighting of the danger variables (e.g. Chuvieco and Salas, 1989; de Vliegher, 1992)
- the creation of locally oriented models, where danger weightings for each variable are obtained through multiple-regression analysis for a given region (Chou, 1992).

Holder *et al.* (1990) modelled the spread of specific fire events through the integration of two Canadian fire spread models using raster data and cellular diffusion processes in an analytical GIS, SPANS. The models Holder *et al.* (1990) employed required three sets of input information; digital topographic data, meteorological data and fuel class data. Three study areas were chosen, at a range of spatial scales. However, fire simulation was only attempted at the smallest area where the highest resolution data were available. Layers calculated in SPANS for the most significant environmental variables were used as inputs for the fire growth model(s), and then calculations were transferred to SPANS for graphical display.

Vasconcelos (1988), Periera and Vasconcelos (1990), Vasconcelos and Periera (1992), Vasconcelos and Guertin (1992) and Vasconcelos *et al.* (1990, 1994) were able to demonstrate the feasibility of using a GIS to model fire behaviour by developing the FIREMAP system. FIREMAP is based on a coupling of the BEHAVE fire modelling system (Burgan and Rothermel, 1984; Andrews, 1986) which is based on Rothermel's (1972) fire spread model, and the MAP GIS (Tomlin, 1986). Vasconcelos (1988) and Vasconcelos and Guertin (1992) used FIREMAP to compare model predictions with the growth of an actual fire in Ivins Canyon, central Arizona. The BEHAVE system estimates the quasi-steady state linear rate of spread of the flaming front for surface fires in homogeneous conditions. Fire intensity (expressed as fireline intensity, reaction intensity, heat per unit area and flame length) is also calculated. The structure of the FIREMAP system is shown in Figure 3.4. The process for fire spread simulation in FIREMAP comprises three main phases (Vasconcelos, 1988). Initially the GIS is used to divide the study area into internally homogeneous cells, and to disaggregate the geographic information into layers equivalent to the different inputs required by the BEHAVE system. This overcomes the spatial and temporal limitations inherent to the fire model which restrict the application of BEHAVE to spatially uniform conditions.

Thus, the approach taken by FIREMAP does not violate the model's assumptions and provides a method of simulating the actual spread of a fire over real terrain (Vasconcelos *et al.*, 1990).

Following the processing of the input data into suitable layers, the data are supplied to BEHAVE. A fire vector is then processed for each landscape cell, in a distributed and accurately geo-referenced manner. Results are subsequently written to the appropriate cells and output in cartographic form.

The third phase uses the MAP SPREAD algorithm (Vasconcelos *et al.*, 1994). A travel-time map is derived by dividing the values in the rate of spread map by the cell size (which is constant for the whole firescape). This produces a map which illustrates the time required for flames to cross a given cell. One cell is selected as the ignition point and overlaid with the flame front time map. Subsequently, the SPREAD algorithm processes the data for the time interval selected for the given simulation. Results of the simulation include location, shape and size of burned areas and fire perimeter at user-specified intervals. The system can cope with changes in the meteorological conditions at the beginning of each iteration. Maps of all characteristics calculated by FIREMAP and BEHAVE may also be produced (Vasconcelos, 1988).

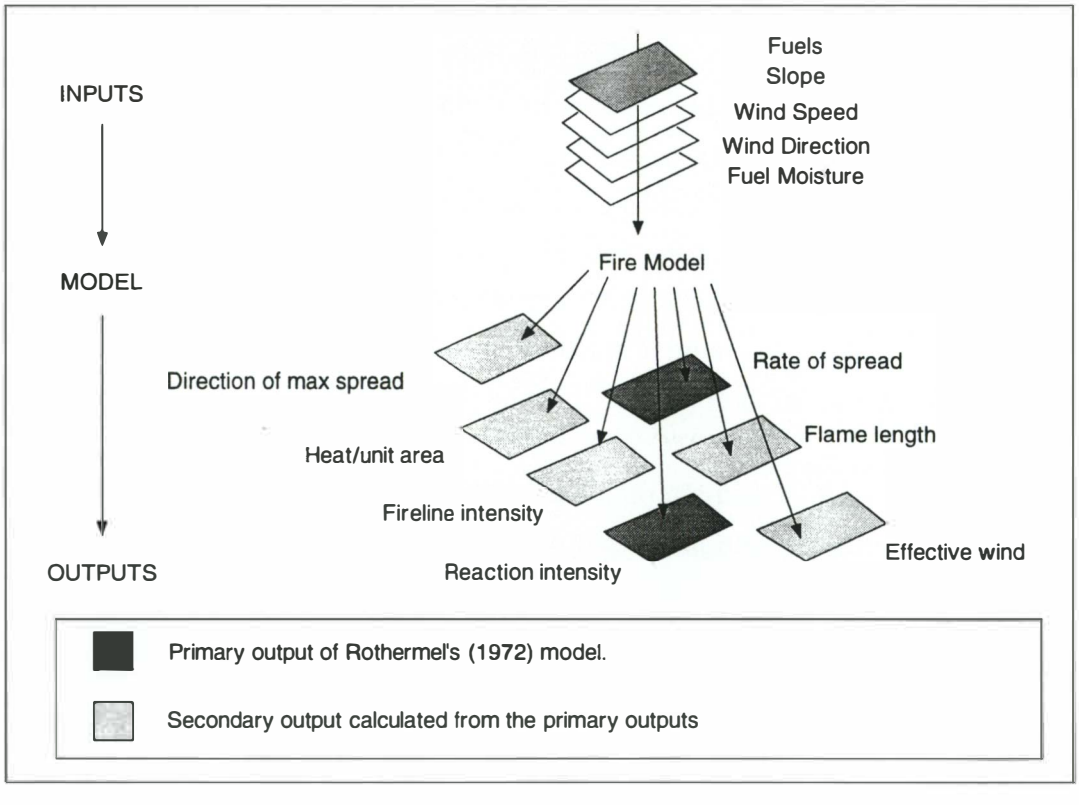

Figure 3.4. Structure of the FIREMAP fire simulation system. (Vasconcelos and Guertin, 1992).

Within each constant weather interval, all cells are assumed to burn in the same

direction, which can be updated between time intervals. Additionally, the fire perimeter must be manually updated at the end of each iteration so that only those cells burning at the fire front remain burning to influence the next time period (Vasconcelos and Guertin, 1992).

3.6 Case-study: Fire Modelling the 1988 Yellowstone Park Fires

The Yellowstone Park Fires of July-August 1988 were among the most severe in the western states of the USA during the 20th century. In total, 11% (570 000 ha.) of the Greater Yellowstone Area (GYA), and approximately 45% (400 000 ha.) of Yellowstone National Park (YNP) were burnt (Schullery, 1989). Fire behaviour projections were used in the management of the various fire complexes; the way in which fire behaviour was predicted and the accuracy of these predictions is the focus of this section.

Yellowstone National Park has a 'prescribed natural burn policy'. This policy had been implemented in the early 1970s to allow (some) natural fires to take their course (Elfring, 1988). However, the fires of July 1988 were larger and more dangerous than any previously and so were declared 'wildfires'. The large-scale of the 1988 YNP fires was the result of a number of complex, inter-related factors. Drought conditions were a major factor; not only did they enhance burning, but they also rendered fire control dangerous and, in many cases, impossible. Furthermore, drought conditions favoured the development of unpredictable spot fires. As drought conditions increased, so too did fire activity. In early August fire spread averaged about 1.5 km per day; by September runs of 12 to 25 km per day were common (Schullery, 1989; Rothermel, 1991a). As a result of the prolonged drought condition soil moisture was exceptionally low (3%) causing correspondingly low litter moisture levels (Potts and Morris, 1989; Rothermel, 1991a). Hartford and Rothermel (1991) found that although humidity rose to a nightly maximum of 70-90 % the FMC of dead *Pinus contorta* (lodgepole pine) litter only varied between 3-4% at mid-afternoon and reached a maximum of 10-11% in the early morning. Furthermore, such prolonged drought conditions decreased variability within the fuel complex as a whole; fuel particles of all sizes became potential heat sources rather than partial heat sinks. Most large fires have historically been related to extended drought conditions.

The intense drought conditions generated fires of a size that were not impeded by small-scale changes in micro-climate, land-forms, or fuel beds, and that could not be contained using standard suppression techniques. However, landscape heterogeneity did influence fire behaviour at small spatial scales causing a mosaic of different burn

intensities (Christensen *et al.*, 1989). Although significant, Romme and Despain (1989) note that the YNP fires of 1988 were similar to fires in the early 18th century with regard to heat released, flame height and rate of spread. Past human actions, mainly fire suppression and associated fuel accumulation, had some influence on the size and behaviour of the fires in 1988, but these large fires were the result of wind and drought conditions, as well as of normal successional dynamics following the last major fire approximately 280 years ago (Christensen *et al.*, 1989; Romme and Despain, 1989).

Fire behaviour analysts were requested to attempt to project the eventual magnitude of the fires in YNP by the end of the fire season and to develop a worst-case scenario. Three major issues confronted the fire analysts:

- eight major, independent fire complexes had to be considered. These were often inaccessible, limiting both available data and management options.
- predictions were required over time-frames of several weeks whereas weather forecasts are only accurate for 3-5 days.
- no quantitative fire behaviour model could be used; BEHAVE, the standard US fire system, was inappropriate as it can not deal with either crown fires or spotting. As a result qualitative analysis had to relied upon.

Prediction of the fires was based on two crucial relationships; those between fuels and fire behaviour, and between weather and fire behaviour. Fire behaviour was related to five *P. contorta* stand types, based on age (Romme and Despain, 1989; Despain, 1990) and to six weather scenarios (Rothermel, 1991a). These six scenarios embraced a range of conditions from fire subduing precipitation to strong frontal winds with the potential to fan the fire to uncontrollable intensities and rates of spread. The occurrence of each state was predicted using both forecasts and the analysis of past fire weather records.

As illustrated in Figure 3.5 there are large disparities between the predicted and the actual final extent of the fire complexes at the 15th and 31st of August. By late August three new and unpredicted fire complexes had developed; the Hellroaring, Storm Creek and Huckleberry Fires. In the Snake Complex the Falls Fire had spread as predicted and joined with the Red and Shoshone Fires and, as expected, this combined fire was held on the north-west flank. However, it spread extensively to the east and later joined the Mink Fire. This growth was not expected and Rothermel (1991a) attributed it to winds more westerly and stronger than those forecast. The Mink Fire did behave as expected and burnt out to the east of YNP. The growth of the Clover Mist fire complex was largely contained within YNP, but, although, as predicted, it held on the southern half of its eastern flank, it grew to the north-east out of YNP and into the Shoshone National Forest, Wyoming. The Fan Fire continued to hold within YNP and remained static after

mid-August. Finally, the North Fork Fire grew more than had been predicted and by August 31 had grown as far north-east as Canyon Village. Furthermore, it spread west fanned by nocturnal easterly wind, beyond the boundaries of YNP into Targhee Forest.

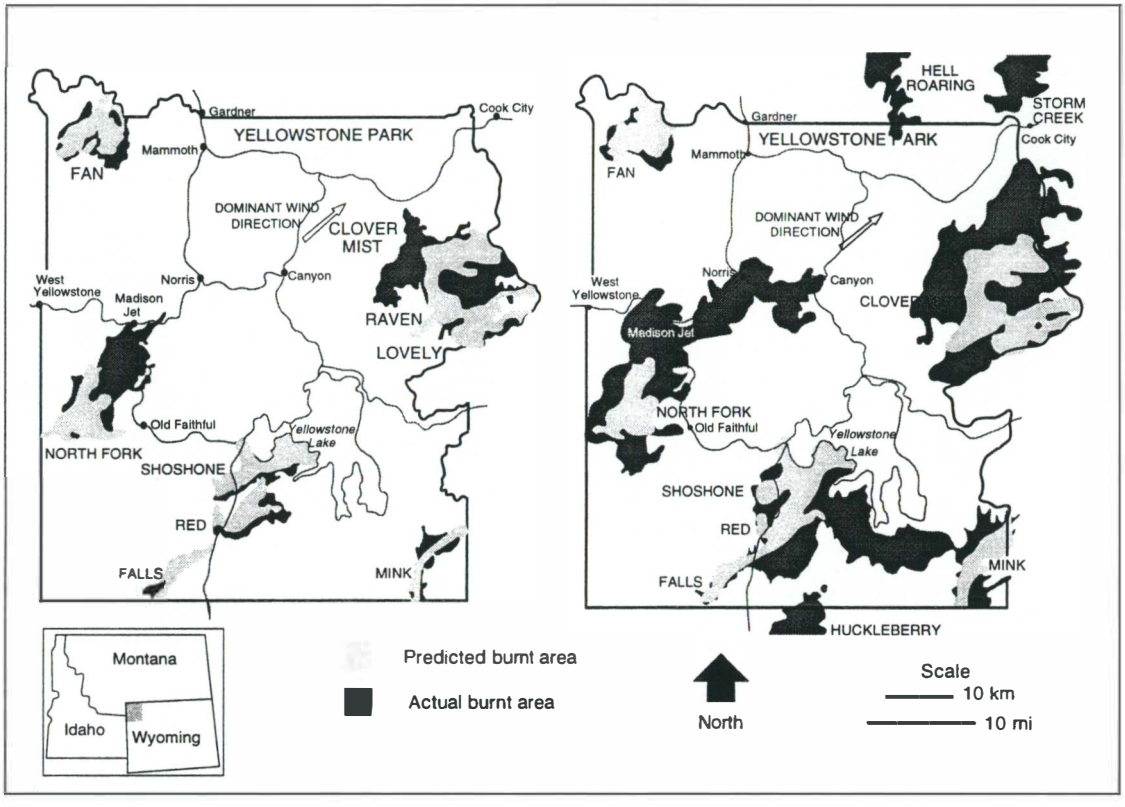

Figure 3.5 Comparison of actual fire events with predicted values using weather forecasts by August 15 (left) and August 31 (right). Light grey areas indicate the predicted area burned while dark grey areas indicate the actual burnt area. (Rothermel, 1991a).

Accurate prediction of the eventual size and shape of the fires proved almost impossible. Rothermel (1991a) concluded that although in late July fire growth predictions could have been made for two week periods for August, September and October, it would have been impossible to predict when the fire season would end. The error in final extent could have been extremely large, because, as illustrated by the 1988 fires, the largest fire growth often occurs at the end of the season. A worst-case scenario would have identified a much larger extent of a fire growth, but the final size would have remained unpredictable. The inaccuracy of long-range forecasts (over periods of two weeks) made accurate long-term predictions extremely difficult, and as a result a great deal of research has since focussed on long-range weather forecasting techniques (e.g. Fujioka and McCutchin, 1989) and examination of atmospheric conditions conducive to fire spread (e.g. Haines, 1988; Werth and Ochoa, 1990). Rothermel (1991a) concludes that although reasonable estimations of weather trends are possible, the level of information needed for day-by-day fire prediction is infeasible. Another hindrance was the lack of any model to predict crown fire behaviour. Indeed, little

research had addressed the issue since the seminal work of Van Wagner (1977). As a result a method for predicting the intensity and rate of spread of crown fires was developed (Rothermel, 1991b). A final research effort stimulated by the Yellowstone fires is an attempt to use climatological records to determine the probability of weather conditions occurring which would end the fire season. This may allow a worst-case fire behaviour scenario to be developed with a probability of season-ending weather incorporated.

This section has examined a major fire complex and looked at efforts to manage and predict its behaviour. It is obvious that the fire behaviour was extreme and complex and proved very difficult to predict accurately. It has also highlighted some of the current inadequacies in understanding of fire behaviour and how these make fire management a problematic process. It is obvious that the sophisticated models described in Section 3.3 were not applicable due to both the nature of the predictions required and the accuracy with which parameters could be collected and/or estimated.

3.7 Fire Modelling : The Future

Contemporary fire modelling techniques are at an impasse; Fosberg *et al.* (1993; p. 127) consider that: "current capability in fire modelling rests on two models: Rothermel's rate of fire spread model, and the Byram fireline intensity model", both of which are over 25 years old. Three major areas are the focus of current fire modelling research and development: (i) improved understanding of fire-related phenomena; (ii) the development of rigorous physical fire spread models; and, (iii) the development of regional to global scale fire monitoring and modelling frameworks. This section briefly considers all three of these issues.

3.7.1 Understanding Fire-dependent Phenomena

At present, the occurrence of a number of the phenomena associated with vegetation fires can not be predicted *a priori* (Albini, 1993). These include the onset and demise of crown fires, the occurrence and intensity of fire whirls, and remnant unburned strips of vegetation after major fire events (Albini, 1984). Phenomena such as these are unlikely to admit to prediction *a priori*, but they may be explained after the event. However, in order to offer even a simple explanation of these phenomena it is necessary to have an understanding of the events that are causally linked. Once the phenomenology is understood, causal mechanisms may be posited, modelled and tested. Without knowledge of the phenomenology, modelling cannot reveal the underlying mechanisms driving the event.

A good example of a poorly understood fire-phenomena is crown fires: Strauss *et al.* (1989) found that despite the fact that only 1% of all fire events are large-scale crown fires, they are responsible for 80-96% of the total area burnt. Apart from that of Van Wagner (1977), little research has considered these events and as a result they are poorly understood and, at present, no technique exists to model their behaviour (see Section 3.5). Although Rothermel (1991b) attempted to formulate a model for the prediction of the behaviour and size of crown fires, it was merely a series of statistical correlations based on the **surface**-fire spread model of Rothermel (1972) rather than a rigorous physical model. Furthermore, the model of Rothermel (1991b) is unable to predict the rate of spread of plume-dominated crown fires, that is those crown fires associated with low wind speeds and the development of a strong convection column, or plume that towers above the fire rather than leaning over before the wind. However, Rothermel (1991b) does provide techniques which enable the onset of plume-dominated crown fires to be predicted.

Crown fires are but one example of a poorly understood fire-related phenomena, other important examples include fire spread on down-slopes (Van Wagner, 1988), fire whirls (Soma and Saito, 1991) and unburned crown strips (Wade and Ward, 1973; Haines, 1982; Albini, 1993). Progress in understanding the phenomenology of such events will lead to progress in predictive modelling. However, it is first necessary to gather information on the sequence of events to be linked and explained. Gathering any information on phenomena as transient as crown fire processes and fire whirls poses both physical and situational problems; fires of large-scale and/or extreme intensity are rare and often inaccessible. Yet, it is only through a better understanding of such complex phenomena that contemporary fire modelling techniques can be developed and improved.

3.7.2 The "New Generation" of Fire Spread Models

Current operational fire models are all either empirical or semi-physical (e.g. McArthur, 1996, 1967; Rothermel, 1972; Stocks *et al.*, 1989). Weber (1991a) notes that many of the crucial questions about fire behaviour cannot be answered within the framework of contemporary fire models, as they are often specific to the experimental conditions in which they were developed. As a result, there has been a growing recognition in the fire modelling community that a new generation of rigorous physical fire spread models is required.

An interesting example of a 'new generation' fire behaviour model is that of Grishin *et al.* (1983) who propose a wind-driven forest fire model which considers the basic

physical and chemical processes of heating, drying, pyrolysis and combustion. The model is concerned with a single spatio-temporal dimension and uses first-order Arrhenius kinetics to describe pyrolysis and combustion. Grishin *et al.* (1983) assume that turbulent transport processes in the vegetation can be modelled using turbulent exchange. As an example, the heat flux (q) may be expressed as:

$$q = \lambda_T \frac{\partial T}{\partial x} \tag{3.9}$$

where : λ_T = effective turbulent conductivity or eddy diffusivity and T = temperature.

The energy-equation is then written as:

$$\left(\sum_{i=1}^{4} \rho_i \varphi_i c_{pi} + \rho_{cp}\right)\frac{\partial T}{\partial t} + \rho_{cp} W \frac{\partial T}{\partial x} = \frac{\partial}{\partial x}\left(\lambda_T \frac{\partial T}{\partial x}\right) - H(T - T_\infty) + \textit{reaction terms} \tag{3.10}$$

The summation term includes dry organic matter, liquid water, condensed pyrolysis products and the mineral composition of the forest fuels. Note that convective cooling is included with the term $H(T-T_\infty)$. This emphasises the fact that the model of Grishin *et al.* (1983) does not incorporate the hydrodynamic aspects of heat flow, only the combustion.

Numerical analysis was used by Grishin *et al.* (1983) in the solution of their time-dependent model. The structure of the fire front is part of the solution and the development of the front is modelled from the point of conception until a quasi-steady spread rate is reached. The results of Grishin *et al.* (1983) imply that rate of spread decreases rapidly with an increase in FMC, and that critical FMCs exist above which combustion will not occur. This is analogous to the critical conditions produced by the ignition/extinction theory and is a general feature of any model which incorporates a kinetic scheme (Williams, 1985; Weber, 1991a).

The inclusion of a model chemical kinetic scheme by Grishin *et al.* (1983) is a major advance and possibly indicative of the future direction of fire modelling. A similar model including chemical kinetic effects and heat transfer was developed by Weber (1991b). A key feature of the models of Grishin *et al.* (1983) and Weber (1991b) is the inclusion of conditions under which a fire will not burn. However, the further development of such models is hindered by the difficulties involved in the measurement of many of the processes and parameters included in such models (see Section 3.3.1). Despite these problems, the coupling of such fire spread models with further fire chemistry studies seems a promising and fruitful step towards the development of a 'new generation' of fire models.

3.7.3 Global and Regional Scale Fire Monitoring and Modelling

The third direction in which fire modelling seems likely to develop is its integration within regional-global scale fire monitoring and modelling frameworks. Current directions in the integration of spatial information technology with meso-scale fire monitoring were discussed in Section 3.5.2. However, new global scale fire information systems are likely to require a new approach to fire modelling to be taken. Current fire behaviour models are essentially valid for the conditions used in their formulation; generalisation of such 'episodic' models to larger scales and aggregation of the results under a wide-range of conditions is not practical (Malingreau *et al.*, 1993). This section considers the development of such fire information systems and briefly reviews the Vegetation Fire Information System (VFIS) concept proposed by Malingreau *et al.* (1993), the integration of fire behaviour models and sophisticated micro-climatic and atmospheric models.

Malingreau *et al.* (1993) put forward the concept of a global VFIS; the framework of such an information system is shown in Figure 3.6. An early, and much simpler, example of a VFIS is the 'Fire Behaviour Information Integration System' developed by Kessell and Cattelino (1978) for use in southern California chaparral wildlands. This system integrated remotely-sensed information, gradient fuel models and a number of computer routines to simulate fire behaviour and consequences. However, the fire information system of Kessell and Cattelino (1978) was operational at a scale significantly smaller that that outlined by Malingreau *et al.* (1993) and it is with this issue of scale where the difficulties in the VFIS lie. The development of a system such as the VFIS would require an ecosystem-scale approach to be taken. From this perspective, it is the ecosystem characterisation, in terms of fuel situation and fire occurrence, that would drive the selection and activation of the stylised interpretative model of fire behaviour and fire emissions. The final result of such a complex series of operations would be the production, on a regular basis, of estimates of the contribution of individual parcels of land (i.e. cells or pixels) to the gas fluxes associated with burning. Malingreau *et al.* (1993) consider that the VFIS would need to include the following elements:

- A data base organised into a GIS; this data-base would include vegetation parameters relevant to the fuel situation in a given cell (e.g. fuel types) and to the burning practices normally associated at the local level,
- A meteorological data base,
- A satellite observation system that could detect a 'fire pixel' and activate the initiation an appropriate fire model,
- A suite of fire behaviour and fire emission models on call,

• A fire model that could incorporate the various sources of information, produces the required fire-related parameters for a particular site on the globe and keeps a record of the fire history of that site,

• A user-driven statistical integrator capable of summarising the results over space and time according to particular needs,

• A suite of testing procedures that could be used to validate the model output.

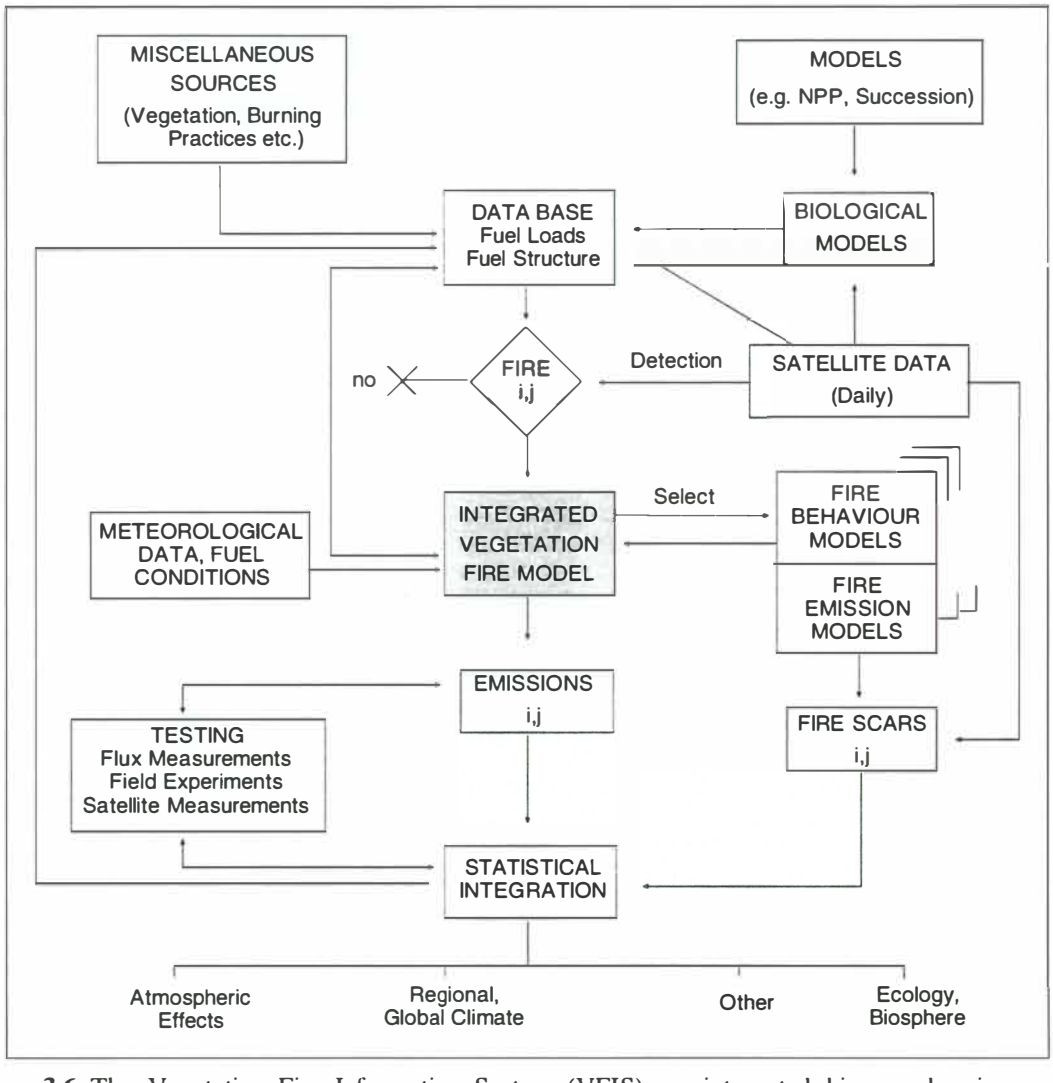

Figure 3.6 The Vegetation Fire Information System (VFIS): an integrated biomass burning model (Malingreau *et al.*, 1993).

An operational VFIS is far from reality and will require significant research and technology development before it becomes a practical possibility. However, it does provide an indication as to the type of integration fire modelling, spatial information systems and fire management techniques may achieve in the future. Furthermore, the successful development of a system such as the VFIS would provide a solid framework for better quantification of issues of global change related to biomass burning. Most obviously, improved description of current sources of aerosols and atmospheric

trace gases alongside estimates of past history will provide inputs to models of climate and atmospheric chemistry change. Conversely, the VFIS has the potential to provide a framework for relating fires to future climate change through an organisation of present knowledge related to fire frequency and environmental conditions.

Another development involving the integration of fire models with sophisticated environmental process models is the merging of sophisticated climatic and atmospheric models with 'new generation' fire spread models. Stokstad (1996) reviews the development of a system that links models of fire behaviour and atmospheric wind movements to simulate the processes which occur following ignition in forest fires. The model described by Stokstad (1996) appears to provide a framework in which the interactions between fire behaviour and wind dynamics can be better understood and analysed. A second example of the integration of fire and weather modelling is provided by Zack and Minnich (1991) who used Arc/Info to create and edit topographic and meteorological information and perform analyses on the combined effect of slope and the estimated surface wind field with a slope-wind interaction model (KRISSY). Zack and Minnich (1991) consider that such a framework may allow for the creation of data layers suitable for input into fire modelling architectures or the production of maps to aid in fire management.

3.8 Summary

This chapter has reviewed the directions which fire spread modelling has taken over the last twenty to thirty years. It has been shown that the models which are currently in widespread operational use (e.g. Byram, 1959; McArthur, 1966, 1967; Rothermel, 1972 and Stocks *et al.*, 1989) are all either empirical or semi-physical. As a result there has been a growing awareness that new modelling techniques are required. Furthermore, it has become apparent that the integration of technologies such as spatial information systems with fire behaviour models may allow for more effective spatially-based and explicit fire modelling, simulation and management. Analysis of fire prediction efforts during the Yellowstone Park Fires of 1988 illustrated some of the problems facing predictive fire behaviour modelling and areas where research is necessary. There appear to be three major areas in which fire behaviour modelling is likely to advance; firstly, a better understanding of fire-dependent phenomena such as crown fires is necessary to enable predictive modelling of such events; secondly, a 'new generation' of rigorous fire models needs to be developed; and, thirdly, the integration of fire modelling techniques with spatial information technology such that regional to global-scale modelling and monitoring of fire events may occur.

Chapter Four

Analysis of Rothermel's Firespread Model

4.1 Introduction

The purpose of this chapter is to provide an overview of the fire spread model developed by Rothermel (1972). Initially the fire spread model is reviewed and its assumptions and limitations considered. Following this, a more detailed sensitivity analysis of the Rothermel model is considered and finally the application of the fire model in ecosystems outside those in which it was designed and calibrated is discussed.

4.2 The Rothermel Fire Spread Model

The fire spread model developed by Rothermel (1972) provides a means of estimating the rate at which a fire will spread through a uniform fuel array that may contain particles of various sizes. Although it was developed to predict surface fire behaviour, it was not developed for a specific fuel type (Andrews, 1988). In essence it is a rate of spread model, but it also computes the reaction intensity, which can be used to calculate more widely used parameters such as fireline intensity and flame length.

This section explores the Rothermel (1972) model, firstly through providing a brief outline of the conditions it was designed for and some of the assumptions and limitations associated with that design. Secondly the actual rate of spread expression, and its derivation are explored in some detail. The interactions between fuel model, topography and environmental parameters, and the mathematical fire spread model of Rothermel (1972) are numerous and complex and it is beyond the scope of this work to review them completely.

4.2.1 A Brief Overview, Assumptions and Limitations

The mathematical fire spread model of Rothermel (1972) was developed to predict the rate of spread of a fire at the flaming front in an environment specified by fuel, weather and topography descriptors (Fujioka, 1985). The model is based on that of Frandsen (1971) which considers radiative heat transfer and the law of the conservation of energy. The model treats the spread of fire as a series of ignitions where the heat transfer from each successive strip of fuel raises the next strip to ignition temperature,

thus propagating fire. Rothermel (1972) divides the necessary input variables for the model into three broad classes (Table 4.1).

Table 4.1 Classes of input parameters for the Rothermel model.

Fuel Particle Properties	*Fuel Array Arrangement*	*Environmental Parameters*
Heat content	Loading by size class (live and dead)	Wind speed
Mineral content	Mean size within each class	Fuel moisture content (FMC)
Particle density	Mean depth of the fuel bed	Slope steepness (%)

The primary driving force in the calculations is the dead fuel less than 6 mm (¼ inch) in diameter; these are the fine fuels that carry the fire (Vasconcelos, 1988). Fuels larger than 76 mm (3 inches) in diameter are not included in the calculations at all (Andrews, 1986). The most important descriptors are fuel bed depth, load in each size-class and the surface-area to volume ratio of the fuel bed (Andrews, 1988).

The model describes fire spreading through surface fuels (defined as those up to 2 metres tall and contiguous to the ground) such as grass, brush, litter and logging slash. In general, the model is not applicable to crown fires, where fire spreads aerially, independent of the surface fuel (Andrews, 1986). However, one exception is chamise type brush fields; these are characterised by many stems and are reasonably contiguous to the ground, thus making fire spread through them suitable for modelling as a surface fire (Rothermel, 1972). The fire spread model can identify conditions severe enough for spotting, and crowning (Vasconcelos, 1988) and Rothermel (1983) notes that despite the fact that it does not incorporate spotting, this does not appear to affect the prediction of fire behaviour. It cannot be applied to ground fires such as smouldering duff or fires in peat bogs (Andrews, 1986).

Rothermel's fire spread model was designed to simulate a fire that has stabilised into a quasi-steady spread state. Most fires begin from a single source and spread outward, growing in size and assuming an elliptical shape with the major axis in the direction most favourable to spread. When the fire is large enough so that the spread of any portion is independent of influences caused by the opposite side, it can be assumed to have stabilised into a line fire. A line fire behaves like a reaction wave with temporally steady progress in uniform fuels (Rothermel, 1972).

The Rothermel fire spread model is primarily intended to describe fires advancing steadily away from the source of ignition. As such, its use is problematic in fires whose behaviour is influenced by the pattern of ignition (Rothermel and Rinehart, 1983;

Andrews, 1986). The model can be used to predict the behaviour of some prescribed fires, such as those where strip head firing ignition techniques are used. Rothermel and Rinehart (1983) note that it has been widely used to provide an indication of the potential severity of prescribed fires. Unplanned ignitions that are allowed to burn because they meet fire prescriptions criteria are similar to wildland fires and as such are predicted better by the model (Andrews and Rothermel, 1982).

Fuel type, FMC, wind and slope are assumed to be constant during the time when the predictions are to be applied (Rothermel, 1972, 1983; Rothermel and Rinehart, 1983; Andrews, 1986). However since wildland fires rarely burn in spatially uniform conditions, the fuel model and the length of the prediction are crucial parameters. The more uniform the conditions, the longer the prediction time can be (Andrews, 1986). This problem can be circumvented by partitioning the landscape into a series of internally homogeneous cells and applying the fire spread model to each cell.

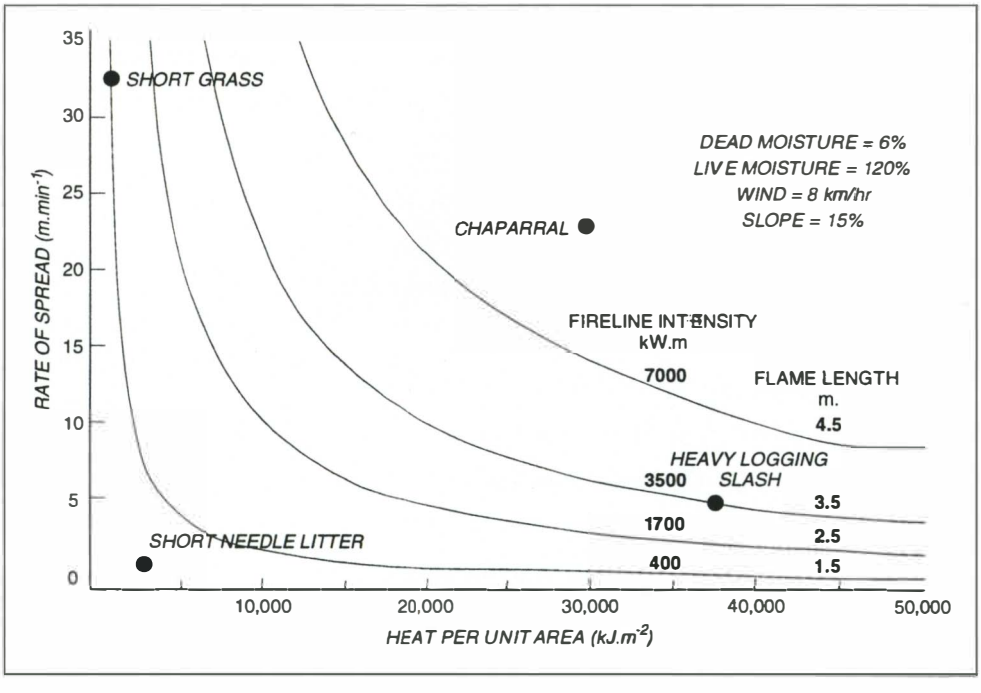

Figure 4.1 Predicted fire behaviour plotted on a fire characteristics chart for four fuel model under the same moisture, wind and slope conditions. (Andrews, 1988).

Andrews (1988) notes that because the Rothermel model gives several descriptions of fire behaviour its utility is increased. Andrews and Rothermel (1982) developed a series of charts of fire characteristics based on the relationships between rate of spread, heat per unit area, flame length and fireline intensity. Figure 4.1 illustrates the ability of the fire model to give realistic fire behaviour predictions for a wide range of fuel types under the same wind, slope and FMC conditions. The grass fuel has a high rate of spread, but a low heat per unit area. Conversely, heavy logging slash has a low rate of

spread, but a very high heat per unit area. Short needle litter results in a slow-spreading, low-intensity fire; 1.8m high south Californian chaparral results in a fast-spreading, high-intensity fire.

4.2.2 The Basic Equation of the Fire Model

The formulae used in Rothermel's (1972) fire spread model are many and complex, and it is beyond the objective of this work to describe and explain them fully. However an understanding of the basic relationships is useful and aids in interpretation of the results; a full presentation of the equations and input variables which comprise Rothermel's fire spread model is presented in Appendix 1, along with the metric revisions of Wilson (1980).

The theoretical basis for the fire spread model was developed by Frandsen (1971). The terms of Frandsen's (1971) equation were unable to be solved analytically and so it was necessary to define new terms, reformulate the expression, and design new experimental methods to evaluate the individual terms (Burgan and Rothermel, 1984). The final form of the rate of spread expression derived by Rothermel (1972) is:

$$R = \frac{I_R \ \xi(1 + \phi_w + \phi_s)}{\rho_b \varepsilon Q_{ig}} \qquad (4.1)$$

where : R = the forward rate of spread of the flaming front (m.min^{-1});

I_R = the reaction intensity (kJ.m^{-2}.min^{-1});

ξ = the propagating flux ratio (dimensionless);

ϕ_w = wind coefficient (dimensionless);

ϕ_s = slope factor (dimensionless);

ρ_b = bulk density (kg.m^{-3});

ε = effective heating number (dimensionless);

Q_{ig} = heat of pre-ignition of the fuel (kJ.kg^{-1}).

If fire spread is conceptualised as a series of ignitions, then it will move through a fuel bed at the rate at which adjacent potential fuel can be heated to ignition temperature. Only a small proportion of the heat released in the flaming front reaches the unignited fuel; instead, the majority of the heat is carried upward by convection or is radiated in other directions (Burgan and Rothermel, 1984). Thus, the numerator in Equation 4.1 represents the amount of heat received by the potential fuel, while the denominator represents the amount of heat required to bring this fuel to the ignition temperature.

Reaction Intensity (I_R)

Reaction intensity (I_R) is a measure of the energy release rate per unit area of combustion. The direction of energy release is not implied; the reaction intensity describes the **total** energy production rate per unit area at the fire front. It is affected by the size of the individual fuel particles, the compactness of the fuel bed, the FMC, and the mineral content fraction of the fuel (Burgan and Rothermel, 1984; Burgan, 1987). Rothermel (1972) assumes this last parameter to be constant for all fuel types. Reaction intensity is calculated through the following function :

$$I_R = \Gamma' w_n h \eta_m \eta_s \tag{4.2}$$

where : Γ' = the potential reaction velocity (min^{-1})

w_n = net load ($kg.m^{-2}$)

h = fuel heat content ($kJ.kg^{-1}$)

η_s = moisture damping coefficient (dimensionless)

η_e = mineral damping coefficient (dimensionless)

The net load (w_n), and the moisture (η_s) and mineral (η_m) damping coefficients are defined as:

$$w_n = \frac{w_0}{1 + s_t} \tag{4.3}$$

$$\eta_m = 1 - 2.59\left(\frac{m_f}{m_x}\right) + 5.11\left(\frac{m_f}{m_x}\right)^2 - 3.52\left(\frac{m_f}{m_x}\right)^3 \tag{4.4}$$

$$\eta_s = 0.174 s_e^{-0.19} \tag{4.5}$$

where : w_o = ovendry fuel loading ($kg.m^{-2}$); s_t = fuel total mineral content (dimensionless); s_e = fuel effective (silica-free) mineral content (dimensionless); m_f = fuel moisture content (dimensionless); m_x = fuel moisture of extinction (dimensionless).

The influence of the heat content (h) on fire behaviour is easily understood; fire potential increases with heat content and *vice-versa* (Burgan, 1987). The heat content is usually assumed to be a constant of 18608 $kJ.kg^{-1}$ (Burgan and Rothermel, 1984). Burgan (1987) notes that the three key parameters in Equation 4.2 are the potential reaction velocity (Γ'), ovendry bulk density (ρ_b) and fuel bed depth (δ). Γ', as described below, is a function of the relative packing ratio (β/β_{op}) and the surface-area to volume ratio (σ), while ρ_b is a function of the fuel load and the fuel bed depth. Γ' will always peak when the packing ratio (β; the proportion of within-fuel volume that is occupied by fuel elements) is optimum (i.e. $\beta=\beta_{op}$), but I_R may peak at a packing ratio higher than optimum. This occurs because the addition of more fuel per unit volume (ρ_b and β

increasing) will continue, for a while, to increase the total energy release rate (despite the fact that the combustion rate for individual particles is declining) because there are more fuel particles burning. Finally, however, the fuel bed becomes so compact, and the potential reaction velocity (Γ') is slowed sufficiently that the total rate of heat output (I_R) begins to decrease. In summary:

- The reaction intensity (I_R) is a function of the potential reaction velocity (Γ'), which depends upon the packing ratio (β; Equation 4.7) and the fuel particle surface-area to volume ratio (σ).
- I_R will eventually decrease with increased packing ratio (β) as the potential reaction velocity (Γ') falls.
- The reaction intensity does not necessarily peak at the optimum packing ratio as the potential reaction velocity (Γ') does.

The potential reaction velocity (Γ') is defined as the ratio of the efficiency of the fire to the reaction time (Burgan, 1987). As such it is a measure of the actual rate of fuel consumption (i.e. a measure of the speed of the combustion reaction). The reaction velocity is defined as:

$$\Gamma' = \Gamma'_{max}\left(\frac{\beta}{\beta_{op}}\right)^{A} \exp\left[A\left(1 - \frac{\beta}{\beta_{op}}\right)\right] \tag{4.6}$$

where: Γ'_{max} = the rate of fuel consumption when the packing bed is optimum ($\beta=\beta_{op}$), (dimensionless).

β/β_{op} = the ratio of the actual packing ratio (β) to the optimum packing ratio (β_{op}). β_{op} is constant for any σ value.

A = an arbitrary variable dependent upon σ (dimensionless).

$$\beta = \frac{\rho_b}{\rho_p} \tag{4.7}$$

β_{op}, Γ'_{max} and A are all empirical intermediate variables and are listed in Appendix 1.

The potential reaction velocity increases as β/β_{op} increases from 0 to 1, at which point Γ' is at a maximum ($\beta=\beta_{op}$), and then decreases again as the fuel bed is more tightly packed; this is shown in Figure 4.2. By definition, at the optimum packing ratio the potential reaction velocity (Γ') equals the maximum reaction velocity (Γ'_{max}). The reaction velocity (Γ') is at a maximum when the fuel bed density is optimised to provide the best fuel/air ratio. This occurs when the relative packing ratio is 1 (i.e. $\beta = \beta_{op}$; Burgan, 1987). The influence of the surface-area to volume ratio of the fuel bed (σ) on the exponent A, produces a series of reaction velocity curves for varying levels of σ. In essence this shows that fuel is consumed more rapidly in fine fuels. The manner in which Γ' changes with β/β_{op} is a function of the trade-off described in the previous

discussion on reaction intensity (I_R). In summary:

• Γ' increases rapidly to a maximum value at β_{op}, and then decreases as the packing ratio (β) increases.

• Γ' peaks at higher values as the surface-area to volume ratio of the fuel bed (σ) increases.

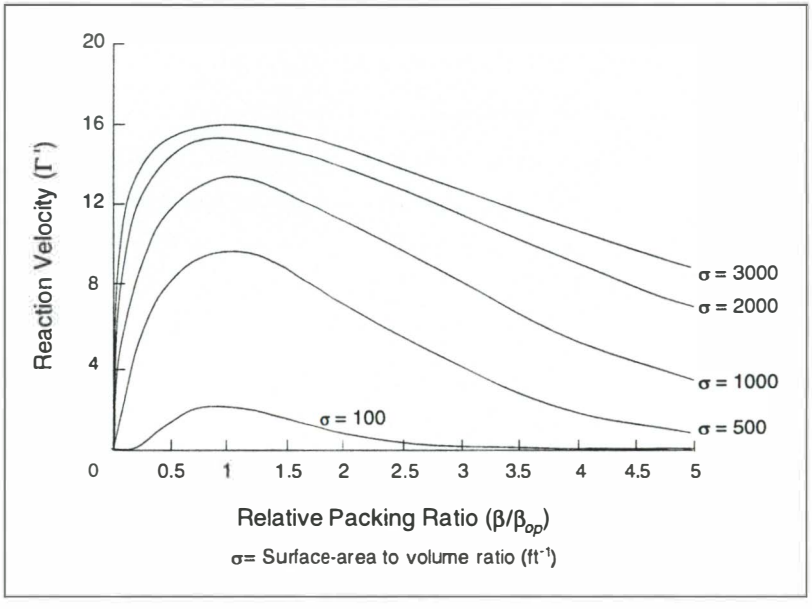

Figure 4.2 The relationship between the potential reaction velocity (Γ') and the relative packing ratio (β/β_{op}).

The Propagating Flux Ratio (ξ)

The propagating flux ratio (ξ) describes the portion of the total heat release rate from a fire which is transferred and absorbed by the fuel ahead of the fire, raising its temperature to ignition. This parameter is required because the reaction intensity is the total heat release per unit area of the fire front in all directions, not just in the direction of the adjacent potential fuel (Burgan and Rothermel, 1984). Physical models usually attempt to estimate the propagating flux through the evaluation of physical processes, the flux being determined by observable properties of the flaming front (Catchpole and de Mestre, 1986). However, the Rothermel model avoids the difficulties associated with measuring flame properties by assuming that the reaction intensity is directly proportional to the propagating flux. As a result the Rothermel model does not describe the processes which contribute to the net energy per unit area transported across the surface of inception (Q in Equation 3.2). ξ is calculated under zero-state conditions (i.e. no slope and no wind) and as such is solely a function of fuel characteristics:

$$\xi = (192 + 7.9095\sigma)^{-1} \exp[(0.792 + 3.7597\sigma^{0.5})(\beta + 0.1)] \quad (4.8)$$

Values for ξ can range from zero (no heat reaches adjacent fuels) to one (all of the heat

reaches the adjacent fuels). However, in surface fires realistic field values range from 0.01 to 0.2 (Burgan and Rothermel, 1984). It tends towards 0 as either β or σ decreases, that is, as the fuel bed gets more 'fluffy' (a high number of fine elements/fuel volume) or the fuel particle size increases (Burgan, 1987). Figure 4.3 illustrates how the propagating flux ratio (ξ) increases as the surface-area to volume ratio (σ) decreases for various packing ratios. It is important to notice that ξ increases more rapidly as σ increases in tightly packed fuel beds such as litter than in loosely packed fuel beds such as grass. The proportion of the heat produced in the combustion zone that actually contributes to fire propagation varies from 0 to 20 percent, depending on fuel particle size and fuel bed compactness. In summary, ξ increases when either β or σ increases.

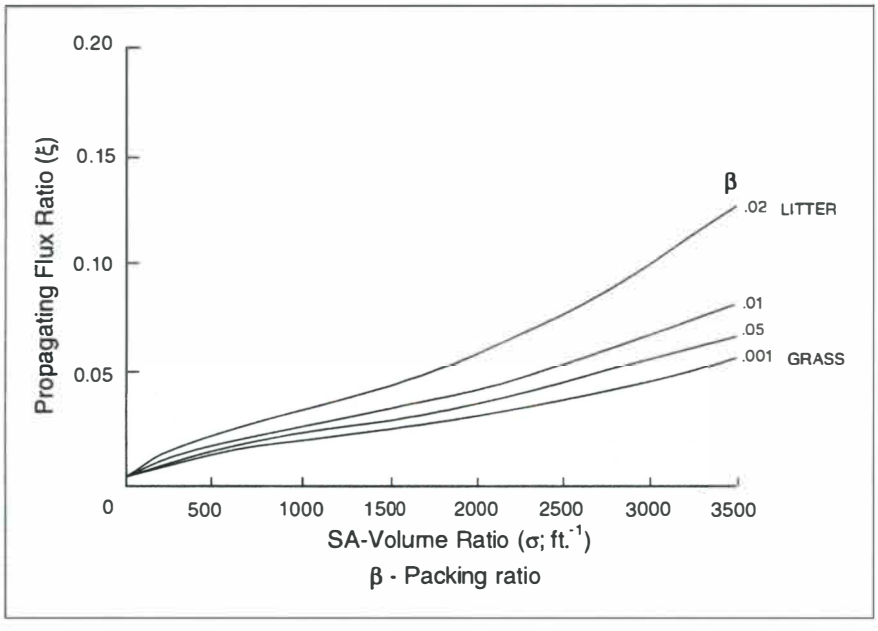

Figure 4.3 The relationship between the propagating flux ratio (ξ) and the surface-area to volume ratio (σ) (Burgan, 1987)

The Wind Coefficient (ϕ_w)

The wind coefficient (ϕ_w) is a dimensionless multiplier that accounts for the increased rate of spread resulting from the improved radiant and convective heat transfer and increased oxygen flow in wind-driven fires. It is influenced by the surface-area to volume ratio of the fuel bed (σ), the packing ratio (β), and the wind speed (U). ϕ_w is a power function which Rothermel (1972) derived from McArthur's (1968) seminal research and is of the form:

$$\phi_w = C(3.281U)^B\left(\frac{\beta}{\beta_{op}}\right)^{-E} \qquad (4.9)$$

where : ϕ_w = the wind correction factor (dimensionless); U = the wind speed at mid-flame height (m.min^{-1}); β/β_{op} = the ratio of actual to optimal packing ratio

(dimensionless) and C, B and E are constants related to the surface-area to volume ratio (σ).

Figure 4.4 shows that as the surface-area to volume ratio (σ) increases wind speed (U) is raised to an increasingly larger power (B) and ϕ_w increases correspondingly. C decreases as σ increases, but not such that it can counteract the effect of U^B. Figure 4.4 also illustrates that the wind coefficient increases more rapidly in lightly loaded fuel beds (i.e. those whose β/β_{op} ratio is low).

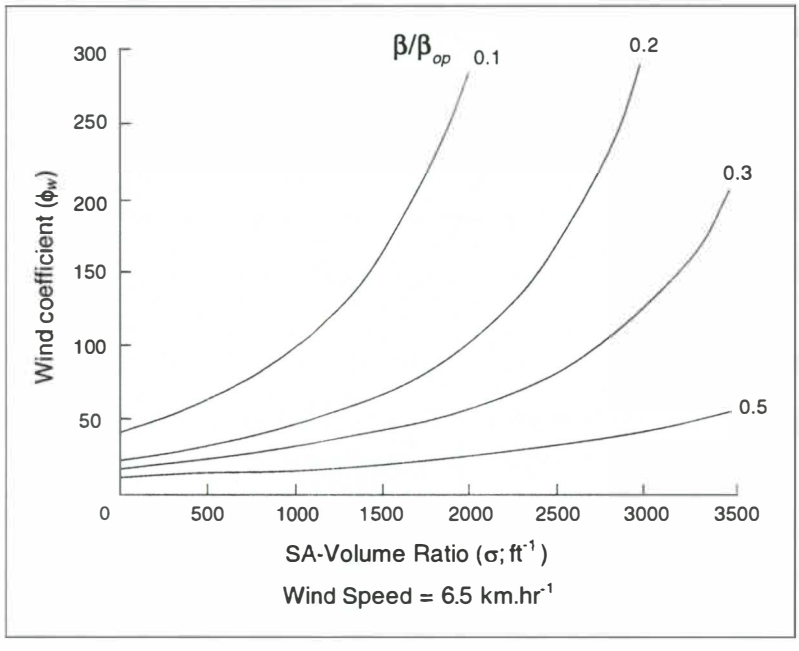

Figure 4.4 The nature of the relationship between the wind coefficient (ϕ_w) and the surface-area to volume ratio (σ). β/β_{op} is the ratio of the packing ratio to the optimum packing ratio (Burgan, 1987).

Figure 4.5 shows that ϕ_w decreases rapidly as β/β_{op} increases, but, as fuel beds become more and more tightly packed, the rate of decrease in ϕ_w slows. Although wind speed generally increases fire spread rate and intensity because of improved radiant and convective heat transfer and oxygen flow, there are limits to these effects and at high wind speeds rate of spread may be reduced (McArthur, 1966; Basher *et al.*, 1990; Section 2.5.2). Although the Rothermel model does not predict reduced spread rates at high wind speeds, it does identify when the maximum spread rate is reached (Burgan and Rothermel, 1984). In summary:

- ϕ_w increases with wind speed (U)
- for a given wind speed (U), ϕ_w increases with the surface-area to volume ratio (σ; i.e. the effects of wind are more pronounced in fine fuels)
- for a given wind speed (U), ϕw increases as β/β_{op} decreases (i.e. as the fuel becomes more 'fluffy')

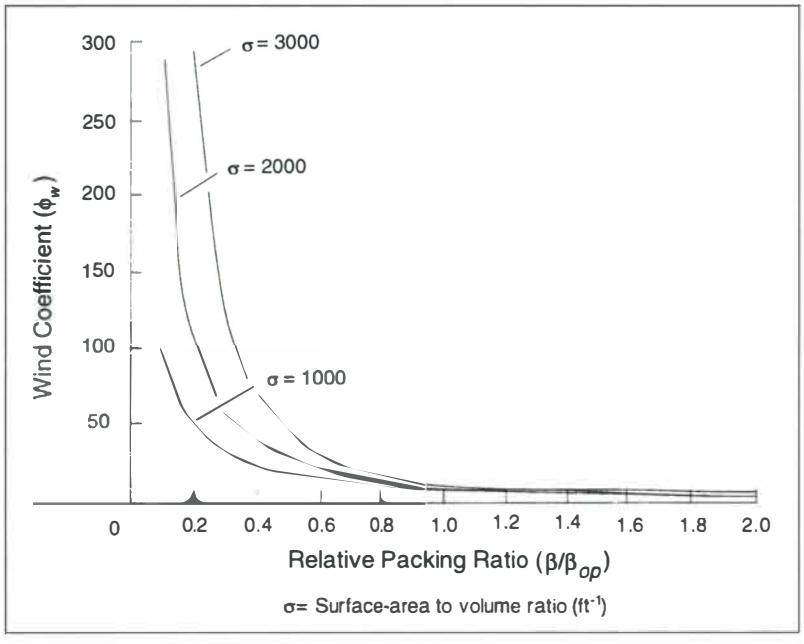

Figure 4.5 The nature of the relationship between the wind coefficient (ϕ_w) and the relative packing ratio (β/β_{op}) (Burgan, 1987).

Beer (1993) notes that Rothermel (1972) based his value for *B* on a paucity of data (three points from the data of Thomas, 1965; cited in Beer, 1993), and considers the relationship between wind speed and rate of spread to be inadequately described by Equation 4.9. Furthermore, in some fuels *B* may be greater than one, meaning that fire may spread at a rate in excess of the wind speed (Weber, 1991a). Beer (1993) proposes the following relationships between wind-driven rate of spread (*V*), zero-wind rate of spread (V_0) and wind speed (U; m.sec^{-1}):

$$\frac{V}{V_o} - 1 = a\left(\frac{U}{U'}\right)^{0.5} \qquad where : \frac{U}{U'} < 1 \tag{4.10}$$

$$\frac{V}{V_o} - 1 = a\left(\frac{U}{U'}\right)^{3} \qquad where : \frac{U}{U'} > 1 \tag{4.11}$$

where : U' = *a* constant reference wind speed and a = a dimensionless constant (suggested value is 15).

Beer (1993) found that with values of U' = 2.5 m.sec^{-1} and $a \approx 15$, the functions presented above perform in a similar manner to existing models. However, a problem with these functions is the evaluation and definition of V_o, the no-wind spread rate.

The Slope Coefficient (ϕ_s)

The slope coefficient (ϕ_s) is affected by the slope steepness (tan ϕ) and the packing ratio (β) of the fuel bed. As the slope increases from 0%, where it has no influence on fire

spread rate, the rate of spread increases steadily. The mechanism producing this effect is similar to that for wind; the heat transfer efficiency is improved because the flames are closer to unburned fuels (Section 2.5.3). Negative slopes are not accepted by the model; instead downslopes are considered equivalent to zero-slopes. Furthermore, Rothermel's (1972) model considers the various effects that slope and wind speed have on fire spread to be independent. Therefore, the model assumes that any wind is blowing directly upslope, and, as a result, wind and slope both have an increasing effect on fire spread in the same direction (Andrews, 1986).

Ovendry Bulk Density (ρ_b)

Ovendry bulk density (ρ_b), a measure of the amount of fuel, is determined by dividing the fuel load by the fuel bed depth (Vasconcelos, 1988). Bulk density is defined as :

$$\rho_b = \frac{w_0}{\delta} \qquad (4.12)$$

where w_o = fuel load (kg.m^{-2}) and δ = fuel bed depth (m).

In the Rothermel model particle density (ρ_p) is usually assumed to be a constant and as a result bulk density (ρ_b) is the primary variable describing fuel bed compactness. In essence, it may be defined as the fraction of the fuel bed occupied by fuel (Brown, 1981). The significance of bulk density in the denominator of Equation 4.1 should be noted. Increasing the bulk density tends to decrease the rate of spread because the total heat sink (as expressed through the denominator) is increased. However, this effect is mediated by the influence of fuel load on the reaction intensity, and bulk density on the propagating flux ratio (Burgan and Rothermel, 1984).

The Effective Heating Number (ε)

The effective heating number (ε) is a measure of the proportion of a fuel particle that is heated to ignition temperature at the time flaming combustion starts and is a function of the surface-area to volume ratio (σ):

$$\varepsilon = \exp\left(\frac{-4.528}{\sigma}\right) \qquad (4.13)$$

For example, when large fuel particles burn, the centre of the log may be cool relative to the surface that is on fire. Thus, only the outer shell of the particle is heated to the ignition temperature (320 °C) at the time flaming combustion commences. This proportion is a function of the size of the fuel particle and is markedly higher for fine

fuels, thus it increases with the surface-area to volume ratio (σ). Multiplication of the bulk density (ρ_b) by the effective heating number (ε) provides an estimate of the amount of fuel that must be heated to ignition temperature as the fire progresses (i.e. the amount of fuel in the heat sink).

Heat of Pre-Ignition (Q_{ig})

The heat of pre-ignition (Q_{ig}) quantifies the amount of heat required to raise the temperature of one unit of moist wood from ambient temperature to the temperature at which it will ignite. The amount of heat required to raise the temperature of one unit of dry wood from ambient temperature to ignition temperature is reasonably constant and can be calculated in advance. FMC (m_f), however, is not constant and it strongly affects, in a direct proportional relationship, the amount of heat required to dry the fuel particle. The heat of pre-ignition is defined as :

$$Q_{ig} = 581 + 2594 m_f \qquad (4.14)$$

Although the product of bulk density (ρ_b) multiplied by the effective heating number (ε) quantifies how much fuel weight must be heated to pre-ignition, the heat of pre-ignition (Q_{ig}) quantifies how much heat is required to do this. Thus the product of the bulk density, the effective heating number and the heat of pre-ignition ($\rho_b \varepsilon Q_{ig}$) is the total amount of heat per unit volume of the fuel bed that must be supplied by the propagating flux (Burgan and Rothermel, 1984).

The Moisture and Mineral Damping Coefficients (η_m and η_s)

The final important components of the rate of spread expression (Equation 4.1) produced by Rothermel (1972) are the moisture and mineral damping coefficients (Equations 4.4 and 4.5). The following discussion will be concerned solely with the moisture damping coefficient (η_m) since η_s is in essence constant. Rate of spread is directly proportional to the moisture damping coefficient (η_m), which is incorporated into the model as a multiplier of the reaction intensity. Equation 4.4 shows that the moisture damping coefficient is a simple cubic and is derived from what Rothermel (1972) terms the 'fuel moisture ratio', that is m_f / m_x. Figure 4.6 shows that the cubic described by Equation 4.4 is one of simple monotonic decline.

The extinction FMC (m_x) is a parameter which may have a significant influence on fire behaviour. In essence, it can be defined as the dead fuel moisture content at which a fire will no longer spread with a uniform flame front and for which the model predicts a

zero spread rate (Burgan, 1987). Predicted fire intensity and spread rate will increase when the difference between the actual fuel moisture and the dead fuel extinction moisture increases; this occurs as dead fuels become drier. Increasing the dead fuel moisture will have the opposite effect. Figure 4.6 shows that fire behaviour predictions are most responsive to changes in the dead fuel moisture content when the fuels are relatively dry or relatively wet (i.e. the response of a fuel model to changes in moisture is non-linear).

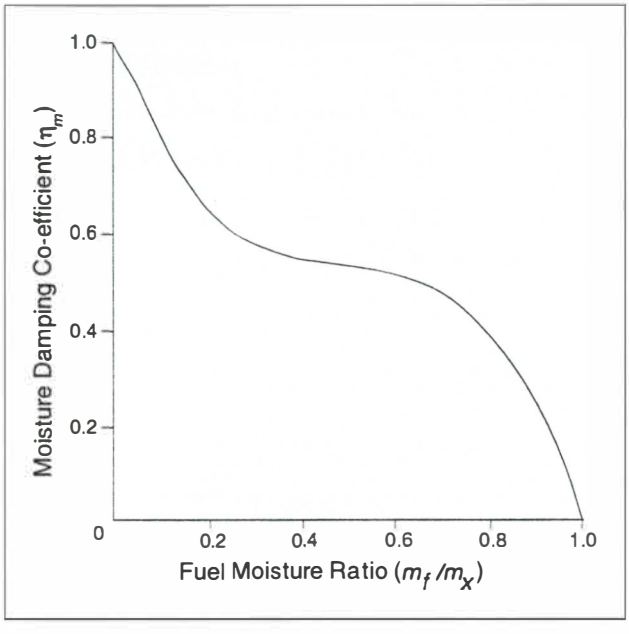

Figure 4.6 The relationship between the moisture damping coefficient and the fuel moisture ratio. (Burgan, 1987).

Little research has addressed the moisture content of extinction and so it is usually assumed to be constant across all fuel types (Brown, 1972; Andrews, 1980; Malanson and Travaud, 1988). However, Brown (1972) notes that there appear to be relationships between environmental conditions, fuel parameters and m_x, although these have not been experimentally analysed. Rothermel (1972) notes that for litter fuels of ponderosa pine needles, m_x is about 0.3; for other dead fuels it lies between 0.1 and 0.4.

The mineral damping coefficient (η_s) is based on the research of Philpot (1968) who studied the thermal decomposition of inorganic minerals in wildland fuels. Philpot (1968) found that silica did not affect the thermal decomposition rate and so the mineral damping coefficient is derived from the silica-free mineral content of the fuel (s_e) as shown in Equation 4.5.

4.3 Sensitivity Analysis of the Rothermel Fire Spread Model

Sensitivity analysis was performed to test how the Rothermel model reacts to changes in the input variables. This analysis enables an examination of the way in which the model may react to different 'real-world' changes. The sensitivity analysis was performed using a specially written Fortran 77 routine which allowed the variable of interest and secondary variables to be altered incrementally; the program is included in Appendix 2. The results of the sensitivity analysis are presented in the order that Rothermel (1972) presents the parameters in his model formulation. Sensitivity analysis was performed using the tall grassland fuel model of Rothermel (1972) and Burgan and Rothermel (1984). The default FMC was 0.1, the default moisture content of extinction (m_x) was 0.5; slope was held at zero and wind speed at 10 km.hr^{-1}. Total and effective mineral content (s_e and s_t), and the low heat content (h), were not considered as Rothermel (1972) and Burgan and Rothermel (1984) consider these values to be constants.

The first step in evaluating the Rothermel model was to analyse the relationships between the input variables and the terms in the final rate of spread Rothermel expression. These relationships are shown in Table 4.1.

Table 4.1 A schematic representation of the relationships between the input variables and the terms in the final expression of the Rothermel (1972) fire behaviour model.

	Terms in the Rothermel Spread Expression						
Input Variables	I_R	ξ	ϕ_w	ϕ_s	ρ_b	ε	Q_{ig}
Loading (w_o)	■	■	■	■	■		
Heat content (h)	■						
Fuel particle density (ρ_p)	■	■	■	■			
Fuel particle surface-area to volume ratio (σ)	■	■	■			■	
Fuel bed depth (δ)	■	■	■	■	■		
Fuel moisture content (m_f)	■						■
Total mineral content (s_t)	■						
Silica-free mineral content (s_e)	■						
Wind speed (U)			■				
Angle of slope ($\tan\phi$)				■			

4.3.1 Fuel Load

Fuel load (w_o) is a key variable in the Rothermel fire spread model, it influences all of the terms in the spread function except for the effective heating number (ε) and the heat of pre-ignition of the fuel (Q_{ig}). In general terms, as load increases so rate of spread will increase to the point where the packing ratio is optimised. Beyond this point further increases in fuel load will cause a decrease in rate of spread (Figure 4.7). Increasing depth does not change the shape of the load-rate of spread curve. Instead it moves it up the y-axis and increases the difference between rate of spread at high and optimal fuel loadings.

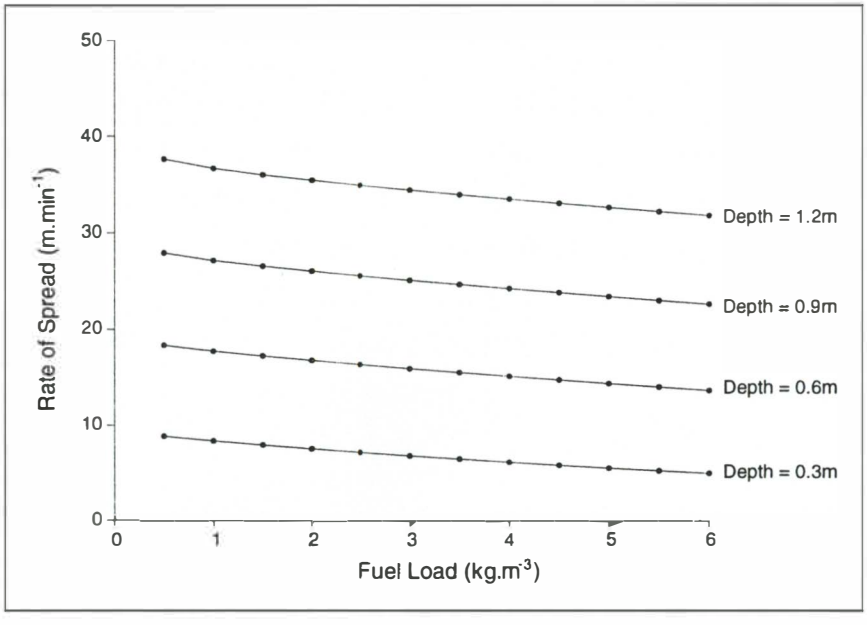

Figure 4.7 The relationship between fuel load (w_o) and rate of spread within the Rothermel model.

The conceptual basis of the Rothermel model is that rate of spread equates to the ratio of the amount of heat received by the potential fuel ahead of the fire to the heat required to ignite this fuel (Equation 4.1). While fuel load indirectly influences all of the terms in the numerator of Rothermel's final expression, a change in fuel load has a far greater influence on the denominator (the heat required to ignite the fuel ahead of the front) through its influence on the ovendry bulk density (ρ_b). Bulk density is the only term in the final rate of spread equation on which fuel load has a direct influence. Although load influences reaction intensity (I_R), the propagating flux (ξ), the wind coefficient (ϕ_w) and the slope coefficient (ϕ_s), this influence is through intermediate variables i.e. the packing ratio (β) for the propagating flux, and the wind and slope coefficients, and net load (w_n) for the reaction intensity. Increasing the fuel load (while holding depth constant) increases the packing ratio (β). This will:

- Increase the reaction velocity (Γ') until the packing ratio is optimum.

Then as load is increased further, Γ' will begin to decrease. Thus, increasing load can either increase or decrease the numerator (Figure 4.2).

• Increase the propagating flux (ξ; Figure 4.3), and therefore increase the numerator of the spread equation,

• Decrease the wind coefficient (ϕ_w), very rapidly at first, and then more slowly as the fuel bed becomes more tightly packed (Figure 4.5), and therefore decrease the numerator.

• Decrease the slope coefficient (ϕ_s) in a manner similar to the wind coefficient. However, compared to the effect of wind, the effect of slope is small.

4.3.2 Fuel Particle Density

Fuel particle density (ρ_p) influences the four variables which comprise the numerator of Rothermel's rate of spread expression (i.e. the potential fuel ahead of the fire); as a result an increase in fuel particle density causes a corresponding increase in rate of spread. However, as described in Section 4.2.1 the fuel particle density (ρ_p) is usually held as a constant and the fuel bed bulk density (ρ_b) used as the primary measure of fuel bed compactness. Fuel particle density does not have a direct influence on any of the rate of spread expression terms. Instead it influences them all through the packing ratio (β; Equation 4.7).

4.3.3 Fuel Particle Surface-Area to Volume Ratio

Fuel particle surface-area to volume ratio (σ) describes the coarseness (or fineness) of a fuel and is another very important input to the Rothermel model. This parameter a fundamental input to the Rothermel model firstly because the model assumes that the fine fuels that carry the flaming fire front that the model describes, and secondly because other parameters (e.g. fuel load) are weighted using the surface-area to volume ratio.

The surface-area to volume ratio influences four of the terms in the final rate of spread expression; the reaction intensity (I_R), the propagating flux ratio (ξ), the wind coefficient (ϕ_w) and the effective heating number (ε). Figures 4.8 shows that in the ranges of the variables indicated, rate of spread is a positive function that exhibits rapidly changing values for high surface-area to volume ratios (σ) and to low-moderate wind speeds (U). For a given wind speed (U), the function grows with the surface-area to volume ratio until it reaches a critical value of σ at which point it increases at a decelerated rate; the result is that the rate of spread function is convex in particular sub-domains (Fujioka, 1985). The shape of the relationship makes physical sense; the fire

front is carried by fine fuels and so an increased fineness of fuel will cause an increased heading rate of spread. However, there is a point at which the fuel particles become so fine that they can not support fire and so heading rate of spread decreases again. It is this critical point which is most affected by changes in fuel load.

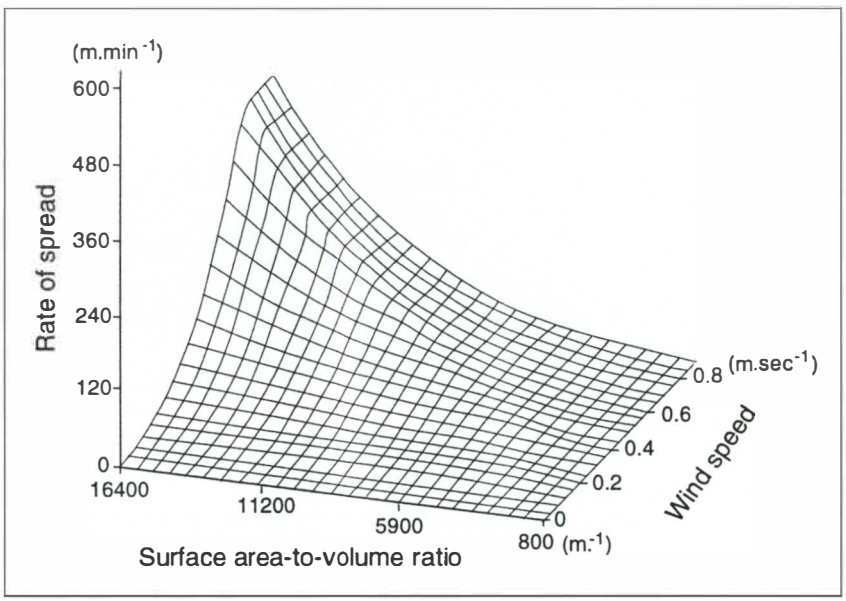

Figure 4.8 The rate of spread function for variable surface-area to volume ratio (σ) and wind speed (U), with other independent variables held constant (Fujioka, 1985).

Increasing the surface-area to volume ratio (σ) will:

- Increase the reaction velocity (Γ'), and thus the numerator in loosely packed fuels. The point of maximum reaction velocity will be shifted to lower packing ratios (Figure 4.2). These changes reflect the fact that fine fuels burn best when loosely packed and coarser fuels burn better when more tightly packed (Burgan, 1987).
- Increase the propagating flux (ξ; Figure 4.3) and thus the numerator.
- Increase the wind coefficient (ϕ_w) significantly for fuel beds with a low packing ratio (β), but not much for tightly packed fuel beds (Figure 4.4). As a result the numerator would increase.
- Increase the effective heating number (ε) which would increase the denominator, thus producing an opposing effect to the three listed above. This will be minor, however, and the general trend is that for increasing σ, spread rate will increase in loosely packed fuels and decrease in tightly packed fuels.

4.3.4 Fuel Bed Depth

Table 4.1 shows that fuel bed depth (δ) influences the same terms as fuel load (w_o; Section 4.3.1). However, a comparison of Figures 4.7 and 4.9 shows that fuel bed depth has a different influence on rate of spread in that as fuel bed depth increases, rate of

spread increases correspondingly.

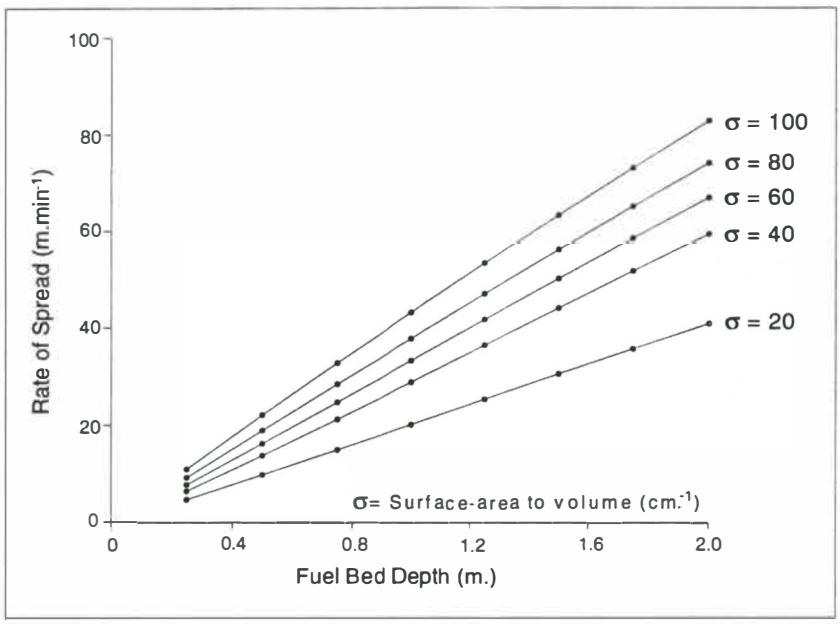

Figure 4.9 The influence of fuel bed depth (δ) on rate of spread based on the Rothermel fire spread model.

An increase in fuel bed depth causes a linear increase in rate of spread through changes to the packing ratio (β). The only parameter fuel bed depth directly influences is the packing ratio (β), as shown in Equation 4.7. The other variables fuel bed depth influences (ϕ_s, ϕ_w, ξ, I_R) are through changes in the packing ratio. Increasing the fuel bed depth (while holding load constant) decreases the packing ratio (β). This will :

- Increase the reaction velocity (Γ') where the packing ratio (β) is greater than optimum, and decrease it when reaction velocity is sub-optimal (Figure 4.2). Therefore, a change in depth may either decrease or increase this term of the numerator.
- Decrease the propagating flux ratio (ξ; Figure 4.3), and the numerator.
- Increase the wind coefficient (ϕ_w; Figure 4.5), and thus the numerator.

4.3.5 Wind Speed

Wind speed is perhaps the single most important environmental factor influencing the behaviour of a wildland fire. However, as described in Section 4.2.1 the accurate modelling and assessment of the relationships between wind speed and the fire parameters that the Rothermel model seeks to quantify has been problematic.

Rate of spread is known to increase with wind speed (Section 2.5.2; Figure 2.5) and the Rothermel model predicts an exponential increase in rate of spread as wind speed increases (Figure 4.10)

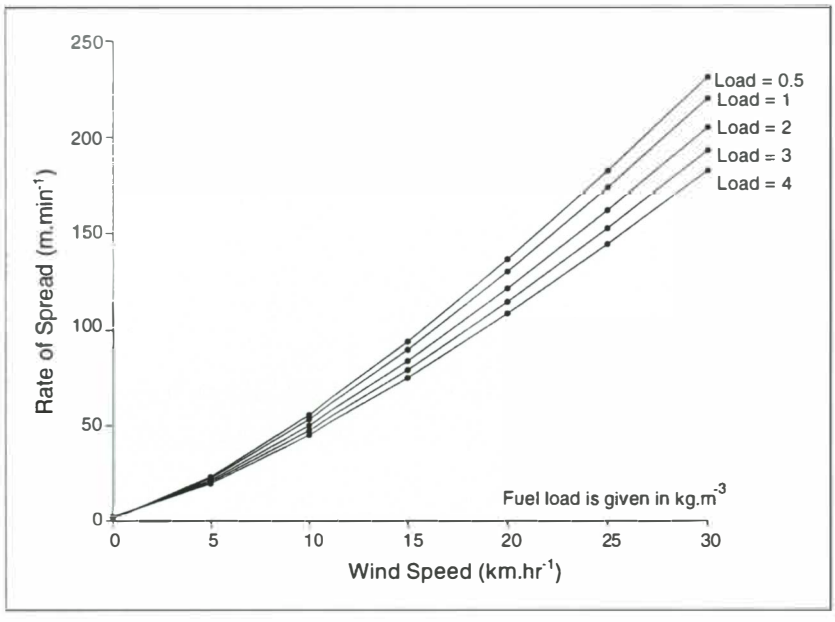

Figure 4.10 The relationship between wind speed (U) and rate of spread as described by the Rothermel (1972) fire spread model.

If the fuel load is increased then it can be seen that the rate of spread is somewhat decreased and growth in the rate of spread flattens. Load reduces the effect of wind speed through its influence on air circulation by increased fuel compactness (the packing load). It also illustrates that there is an optimal fuel load above and below which rate of spread will decrease (Burgan, 1987; Sections 4.3.1 and 4.3.4).

4.3.6 Fuel Moisture Content

Within most fuel beds fuel moisture content is a parameter which exhibits significant spatial and temporal variation, and it is one which plays a key role in establishing whether a wildland fire will ignite and whether later combustion will be successful. The relationship between FMC and rate of spread is one of truncated exponential decay as is seen in Figure 4.11.

Rate of spread decreases rapidly as FMC increases from zero to a point where m_f is greater than the moisture content of extinction (m_x); in this analysis m_f was set at 0.5 and so when $m_f > 0.5$ then the forward rate of spread is zero. The relationship between m_f and m_x is described by the moisture damping coefficient (η_m) and is explored more thoroughly in Section 4.2.1 (Figure 4.6).

Figure 4.11 illustrates the importance of the inter-relationship between FMC and wind speed; where FMC is low and wind speeds are high the Rothermel model predicts extreme fire behaviour (e.g. where FMC = 0, and U = 20 km.hr^{-1} then rate of spread ≈

3.6 m.sec^{-1}). However, as FMC increases and wind speed decreases, rate of spread significantly decreases such that when FMC = 0.4 and wind speed = 10 km.hr^{-1} rate of spread ≈0.3 m.sec^{-1}; this is a twelve-fold decrease from the example described above. However, wind speed does not alter the point of extinction and so, regardless of the wind speed, fire spread is not possible (i.e, rate of spread = 0) when $m_f < m_x$.

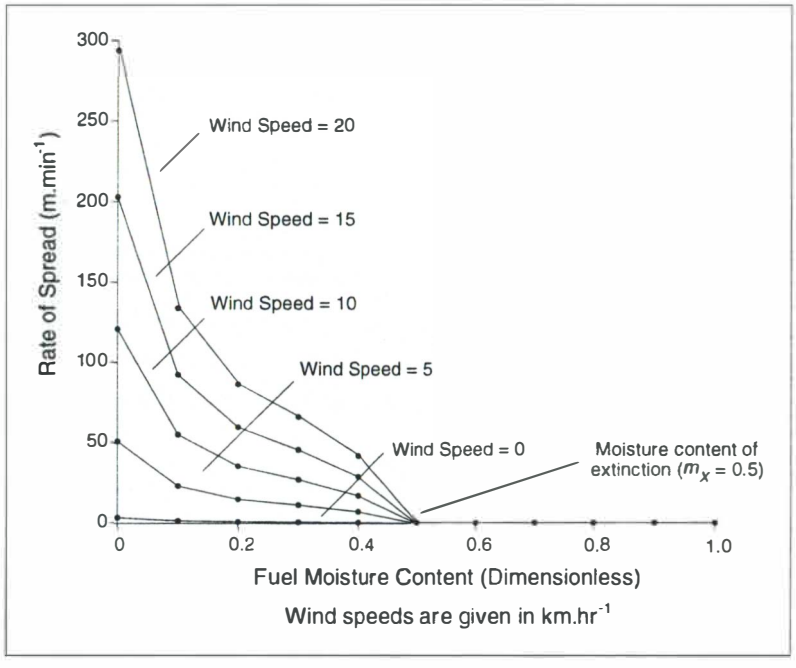

Figure 4.11 The relationship between FMC (m_f) and forward rate of spread.

4.3.7 Slope Angle

The effect of an increase in slope steepness on rate of spread is similar to that of an increased wind speed (Section 2.5.3; Figure 2.7). However, unlike parameters such as fuel moisture content and micro-climatic conditions, slope is not temporally variable at scales relevant to fire behaviour, and so its influences are less well understood (Van Wagner, 1988). As Figure 4.12 shows, within the Rothermel model there is a weak relationship of exponential growth between upslope angle and forward rate of spread. However, it is evident that the relationship presented in Figure 4.12 is greatly mediated by the fuel moisture content and so as FMC increases the difference between rate of spread at 0° and 45° becomes significantly less. It is important to note that the relationship between rate of spread and slope is significantly weaker that that between rate of spread and wind speed (Burgan, 1987). This is despite their hypothesised similarity in physical effect (Sections 2.5.2 and 2.5.3; Figure 2.6). The significant difference between the effects of wind and upslopes is the increased mixing of air by wind; it is this effect which accounts for the greater influence of wind speed on rate of spread.

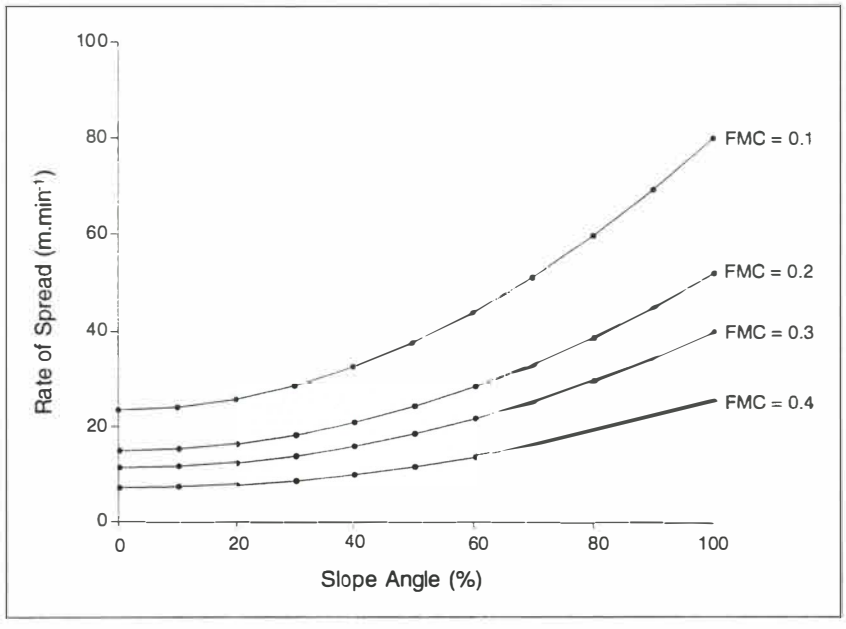

Figure 4.12 The relationship between up-slope steepness (%) and rate of spread as postulated by Rothermel (1972).

4.4 Field Evaluation of the Rothermel Model

This section will examine six evaluations (five field and one experimental) of the Rothermel fire spread model. The six evaluations were conducted across a wide range of fuel types, from logging slash to Australian grassland to South African fynbos. Two of the evaluations are concerned with the application of the Rothermel model to South African ecosystems and these will be considered in the same section. The evaluations are considered in chronological order, and this section only considers evaluation of rate of spread; for information on the other output parameters (e.g. flame length and reaction intensity) the reader is directed to the source material. It is hoped that the inclusion of this section will highlight the problems associated with the application of the Rothermel model in ecosystems outside those for which it was designed and, in addition, show some of the problems in the formulations and (inter-) relationships which make up the model.

4.4.1 Heavy Logging Slash : Brown (1972)

Brown (1972) evaluated the Rothermel model in two types of slash fuels; *Pseudotsuga menziesii* (douglas fir) and *Pinus ponderosa* (ponderosa pine). It was found that the mathematical model generally predicted higher rates of spread than those observed (Figure 4.13). Brown (1972) considers there to be three key reasons behind these constant over-estimations : (i) assumptions regarding the nature of the fuel bed; (ii) the

moisture content of extinction (m_x) chosen for the fuel, and; (iii) the method of weighting input parameters by fuel surface-area to volume ratio.

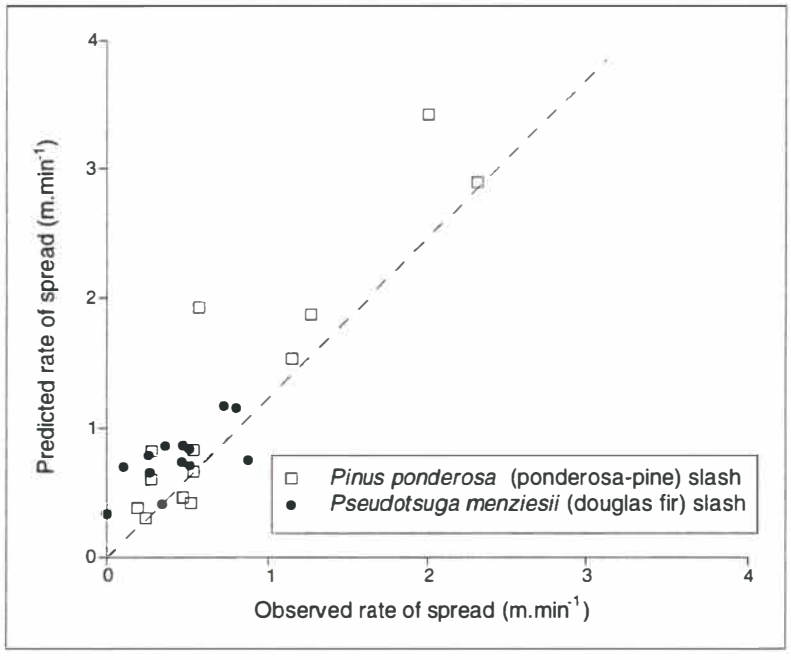

Figure 4.13. Observed vs. predicted rate of spread in heavy *pseudotsuga menziesii* and *Pinus ponderosa* logging slash; the dotted line is the line of exact agreement. From the data of Brown (1972).

Brown (1972) found the disparities between predicted and observed rates of spread to be highest where the packing ratio and fuel load were low. Discontinuity in the arrangement of the fuel particles and a corresponding decrease in the supply of heat for pre-ignition may occur as a result of the spacing between the fuel particles. Brown (1972) notes that spacing was greatest in the least compact fuels; the branching habit and manner of needle growth created gaps between particles, even though the slash was distributed evenly in the fuel bed. Such gaps may have been large enough to necessitate a substantial propagating heat flux to ignite unburnt particles. By contrast, the Rothermel model was developed primarily using fuel beds composed of evenly spaced particles without such large gaps between them. Deviations for the plots having higher loads were less, possibly because the higher fire intensities generated in such plots provided sufficient heat flux for a nearly uniform rate of particle ignitions (Brown, 1972). Fires in the low loading plots generally burned more sporadically because particle ignitions were not occurring at a uniform rate.

Rate of spread is directly proportional to the moisture damping coefficient (η_m), which is a multiplier of the reaction intensity. Brown (1972) used a constant of 0.24 for m_x. However, subsequent analysis showed that values of 0.11 for *P. ponderosa* and 0.13 for *P. menziesii* were more realistic. If the m_x values used by Brown (1972) were too high, then this may explain some of the disparity between the predicted and observed values.

Brown (1972) found that fuel beds with higher loading developed more intense fires; m_x may be expected to increase with intensity as more energy is available to preheat fuels from ambient to ignition temperatures. More porous fuel beds showed larger deviations between observed and predicted rates of spread; such discontinuities tend to lower m_x.

Finally, Brown (1972) considered that the weighting of fuel bed parameters by the characteristic surface-area to volume ratio of the fuel bed may have caused some over-estimation of rate of spread. Brown (1972) notes that although fine fuels tend to carry the flaming front the surface-area to volume ratio weighting technique employed in the Rothermel model may over-estimate their importance through .

4.4.2 North American Grassland Fuels : Sneeuwjagt and Frandsen (1977)

Sneeuwjagt and Frandsen (1977) evaluated the accuracy of the predictions of the Rothermel model in North American grasslands (Figure 4.14). It was found that 45% of the predictions in 'average' wind speed conditions lay within ±25% of the observed rate of spread and that 75% lay within ±50% of the observed rate of spread. Their data also suggested that the Rothermel model tended to over-estimate at high (30% above 'average') wind speeds and under-estimate at low (30% below 'average') wind speeds.

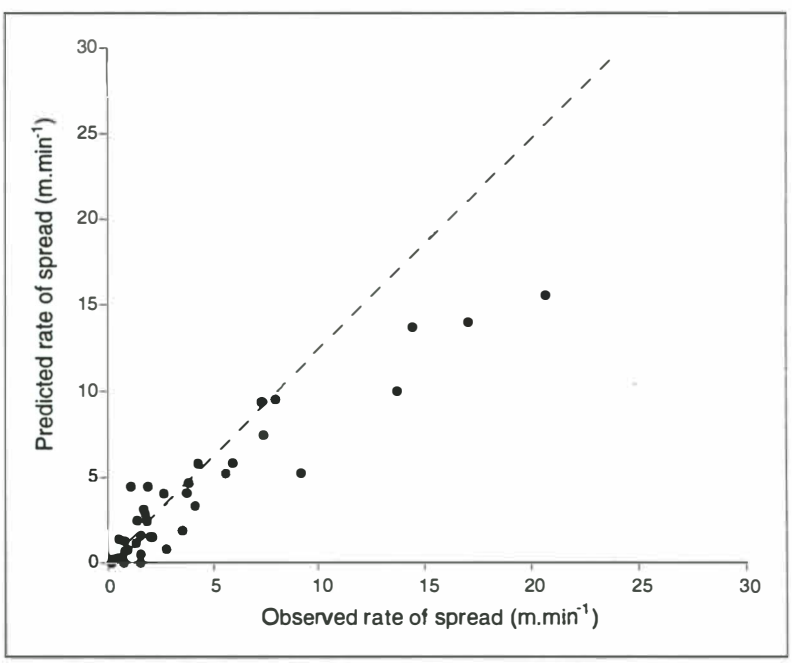

Figure 4.14 Observed vs. predicted rate of spread at 'average' wind speed in North American grasslands; the dotted line is the line of exact agreement. From the data of Sneeuwjagt and Frandsen (1977).

Sneeuwjagt and Frandsen (1977) also compared the predictions of the Rothermel fire spread model with those of the fire model of McArthur (1966). It was found that the

McArthur model tended to over-predict (median: +35%) in 'average' wind speeds whereas Rothermel's model tended to under-estimate (median: -10%) in similar conditions. 55% of McArthur's predictions were within ±50% of the observed rate of spread while 70% of Rothermel's predictions fell within this limit. A major difference between the models of McArthur and Rothermel, which may explain their different performances, is that the sole fuel parameter included in McArthur's model is the degree of curing, whereas the fuel bed is described considerably more rigorously in Rothermel's model.

Sneeuwjagt and Frandsen (1977) conclude that due to the semi-physical nature of the Rothermel fire spread model it is superior to the regression and empirical fire spread models of McArthur (1966) and Peet (1967). However, Sneeuwjagt and Frandsen (1977) note that the predictive utility of the Rothermel model would be improved by a better understanding of the role of fuel geometry and wind in establishing the moisture content of extinction (m_x); the model does not account for changes in the dead-fuel moisture content of extinction as a response to fluctuations in other environmental parameters.

4.4.3 South African Fynbos and Savanna : Van Wilgen *et al.* (1985) and Van Wilgen and Wills (1988)

Van Wilgen *et al.* (1985) evaluated the use of Rothermel's (1972) fire spread model in South African fynbos (sclerophyllous shrubland vegetation) using a fuel model previously developed for this vegetation type by Van Wilgen (1984). Van Wilgen *et al.* (1985) found that fire in fynbos spread faster and with greater intensity than fires in most other shrublands, despite similarities in biomass (*cf* Hobbs and Gillingham, 1984). These higher rates of spread and fire intensities reflect differences in vegetation structure. Significant relationships were found between the predicted and observed rates of spread, although Van Wilgen *et al.* (1985) consider that the fuel model of Van Wilgen (1984) was found to under-estimate all the fire behaviour parameters it was used to predict (Figure 4.15). Van Wilgen *et al.* (1985) attributed this under-estimation to problems with evaluation of fuel bed depth. However, the data presented in Table 4.3 question the conclusion that the fuel model under-predicts rate of spread.

Van Wilgen *et al.* (1985) concluded that mountain fynbos exhibited too many horizontal and vertical discontinuities to allow satisfactory fire behaviour prediction with any fire model, including that of Rothermel (1972). Fynbos is structurally highly heterogeneous and even superficially homogeneous stands (such as those used in this study) exhibit large variations in biomass and structure. Furthermore fynbos is found in

mountain areas with varied and rugged terrain and a correspondingly heterogeneous wind field; in addition, the techniques used in lighting prescribed fires and controlling wildfire in fynbos produce interactions between the heading, flanking and backing fires. These factors are all problematic for the successful application of the Rothermel model.

Van Wilgen *et al.* (1990) used a modification of the Rothermel model to test hypotheses concerning the roles of vegetation structure and fuel chemistry in excluding fire from forest patches in fynbos (macchia) shrubland. This modified version of the Rothermel model allows accurate prediction in vegetation where vertical discontinuities are evident through the accommodation of separate fuel models for up to three strata and the calculation of rate of spread for individual strata, which may vary in cover (Kessell *et al.*, 1978). It was found that modelling the behaviour of fire in fynbos was complicated by patches of forest vegetation of low flammability embedded in the fynbos. Van Wilgen *et al.* (1990) note that the structural differences between fynbos and forest are sufficient to explain the inability of fires to penetrate such forest patches. Furthermore live forest vegetation has a higher FMC and a lower crude fat and energy content than the fynbos shrubland, resulting in a comparatively lower flammability.

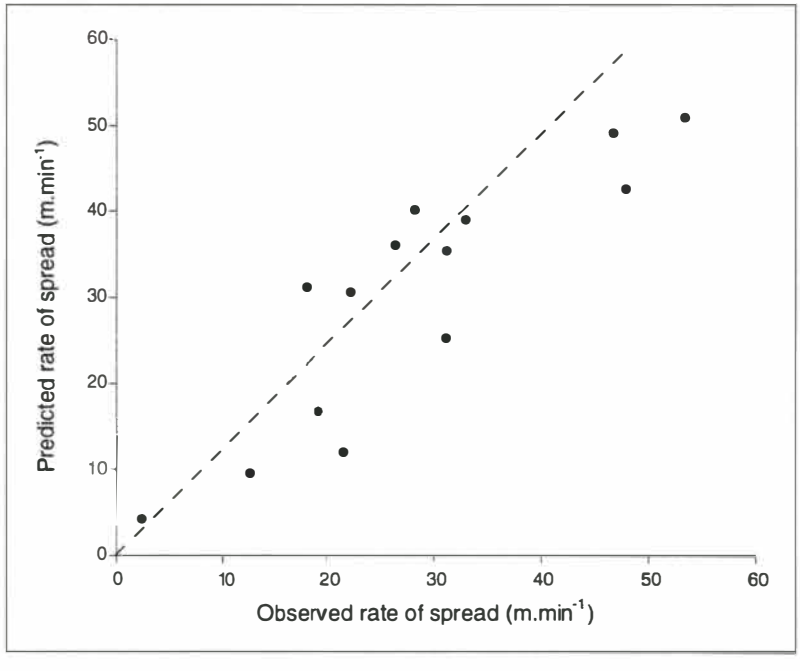

Figure 4.15 Observed vs. predicted rate of spread in South African fynbos; the dotted line is the line of exact agreement. From the data of Van Wilgen *et al.* (1985).

Van Wilgen and Wills (1988) tested the BEHAVE system in South African savanna vegetation; BEHAVE (Burgan and Rothermel, 1984) is the standard US fire behaviour prediction tool-kit and is based upon Rothermel's (1972) fire spread model. Predictions of fire behaviour were compared with observed fire behaviour in 10 experimental fires

(Figure 4.16). Rate of spread was well predicted by the BEHAVE system. Disparities between observed and predicted rates of spread were not large, although Van Wilgen and Wills (1988) conclude that the model tended to over-predict rate of spread. Van Wilgen and Wills (1988) consider that the BEHAVE system may be applied with more success in savanna vegetation than in mountain fynbos. This is a result of the structural simplicity of the savanna; such spatial uniformity enables easier use of the Rothermel model.

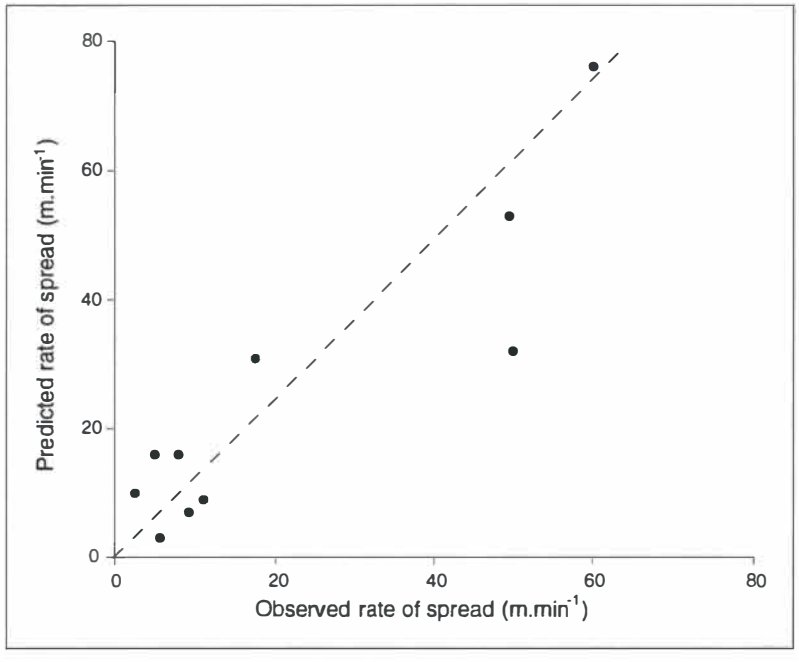

Figure 4.16 Observed vs. predicted rate of spread in South African savanna vegetation; the dotted line is the line of exact agreement. From the data of Van Wilgen and Wills (1988).

4.4.4 Australian Grassland Fuels : Gould (1988)

Gould (1988) tested the Rothermel model in 75 experimental fires in *Eriachne burkittii* (kerosene grass) grassland in Northern Territory, Australia. Rate of spread predictions were not as successful as those of Van Wilgen and Wills (1988) despite the apparent similarities between the fuel beds (Figure 4.17). 33% of the predicted rates of spread were within ±25% of the observed rate of spread and 32% of the predicted rates of spread fell beyond 50% under-prediction (i.e. the prediction was less than half the observed).

Gould (1988) found that a key component in the disparities between the observed and predicted rates of spread was error in field assessment of the surface-area to volume ratio of the fuel bed. An over-estimation of surface-area to volume ratio in the fuel bed would cause an over-prediction of rate of spread and *vice-versa*.

Gould (1988) used a σ of 97.7 cm^{-1} giving the constant B (in the wind coefficient (ϕ_w); Equation 4.9) a value of 1.90. The result of raising wind speed to this power is to significantly increase the predicted rate of spread at high wind speeds. Gould's (1988) observed rate of spread data suggest that the rate of spread increases directly with wind speed (i.e. it is a function of wind speed raised to a power approaching 1). If the surface-area to volume ratio was adjusted within the range of the measured σ, the power function in the wind correction factor would exceed the 1.56 threshold of Rothermel (1972). Gould's observed data indicate that the wind correction factor may be incorrectly formulated and that the surface-area to volume ratio weighting may be invalid.

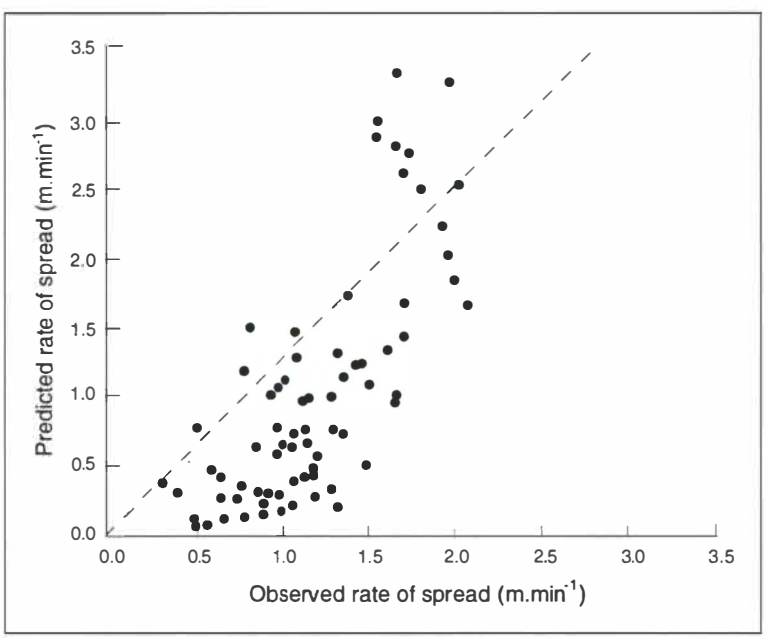

Figure 4.17 Observed vs. predicted rates of spread in Australian grassland fuels; the dotted line is the line of exact agreement. From the data of Gould (1988).

The data of Gould (1988) confirmed the prediction of the Rothermel model that rate of spread *in grass* would not be influenced by fuel load and thus do not support Luke and McArthur's (1986) argument that rate of spread in a specific grass type is directly proportional to fuel load.

Gould (1988) concludes that the Rothermel model predicts the rate of spread reasonably well at head fire speeds of up to 2 $m.sec^{-1}$. However, the model generally under-predicted at low rates of spread, and tended to over-predict when rates of spread were high. The rate of spread shifted in the direction predicted by Rothermel's model for a change in either fuel height, or bulk density, but in both cases the change was less than predicted. The change in rate of spread with increasing wind speed suggested that the function relating rate of spread to wind speed was incorrect for grassland fuels. The function used in the Rothermel model would cause the model to under-predict at low

wind speeds and over-predict at high wind speeds.

Cheney *et al.* (1993), after conducting a number of experimental burns in similar grassland, agree with many of the findings of Gould (1988); they agree that there is no evidence to suggest that it is valid to use the surface-area to volume ratio to adjust the wind exponent, B, for different fuel types. Cheney *et al.* (1993) found the exponent B to remain under 1.0 in all the fuel types they assessed. This figure was considerably different from the values for B suggested by McArthur (1966) of 2, and Rothermel (1972) of between 1.56 and 2.22 (depending on the surface-area to volume ratio of the grass). Furthermore, Cheney *et al.* (1993) found that grass type characterised by either species group or surface-area to volume ratio did not significantly influence the rate of spread and that rate of spread in grassland is not proportional to the fuel load.

4.4.5 Experimental Mixed Fuel Complexes : Catchpole *et al.* (1993)

Catchpole *et al.* (1993) note that two main problems have become apparent since the Rothermel model was originally developed. The first is a simple inconsistency; the Rothermel model and the US National Fire Danger Rating System (NFDRS) both attribute high fire intensities to large fuel sizes. However, the Rothermel model weights the energy release component by the fuel bed surface-area to volume ratio, whereas the NFDRS weights the energy release component by fuel load (Bradshaw *et al.*, 1983). Consequently intensity predictions from the two systems are not equivalent. Secondly, Albini (1976) notes that the surface-area weighting used is not self-consistent; this is equally true of weighting by fuel load. If a homogeneous fuel is regarded as consisting of two equal portions, and the weighting technique applied, the model produces a fuel with only half the original loading. Rothermel (1972) considers the fuel parameters, including loading, of a mixed fuel to be a weighted average of the parameters of the component fuels. Thus, the characteristic loading for a mix consisting of fuel loading w_1 of fuel type 1 and w_2 of fuel type 2 is $w_{tot} = f_1 w_1 + f_2 w_2$, where f_1 and f_2 are the fractions of the total surface-area contributed by the fuel types. If a homogeneous fuel of loading w is regarded as consisting of equal proportions $w_1 = w_2 = \frac{1}{2}w$, then $f_1 = f_2 = \frac{1}{2}$ and so $w_{tot} = \frac{1}{2}w_1 + \frac{1}{2}w_2 = \frac{1}{2}w_{tot}$. To avoid this problem in practice the fuels are divided into size-classes with a large mean difference in fuel diameter, and all fine fuels are placed in a single size-class for which an average surface-area to volume ratio is calculated. These two problems indicate an underlying difficulty in the weighting method used by Rothermel's model (Catchpole *et al.*, 1993).

Catchpole *et al.* (1993) tested the Rothermel model in a series of laboratory fuel beds comprising of either excelsior (wood wool), 6.35 mm sticks, or a mixture of the two. A

series of comprehensive tests was performed both in the absence and presence of wind. Various characteristics of the fire, including rate of spread and fireline intensity, were compared with predictions from the Rothermel model. The results of these experiments have important implications for the use of the Rothermel model in mixed and stratified fuel beds.

Results of the rate of spread experiments showed that the predictions for the single fuel fires do not agree very well (Figure 4.18). Catchpole *et al.* (1993) note that the Rothermel model is over-sensitive to fuel bed depth and attribute some of the estimation error to this. It was found that in wind-driven fires the ratios of rate of spread predicted in the three fuel types agreed quite well with the observed ratios, but that in zero-wind fires agreement was poor. For the other parameters tested (reaction time, reaction intensity and fireline intensity) the model provided inadequate predictions.

The Rothermel model produced very different predictions for all parameters depending on whether the fuel bed was a mixed or component one. Catchpole *et al.* (1993) conclude that there appear to be serious problems with the surface-area weighting technique used in the Rothermel model to handle mixed fuel beds.

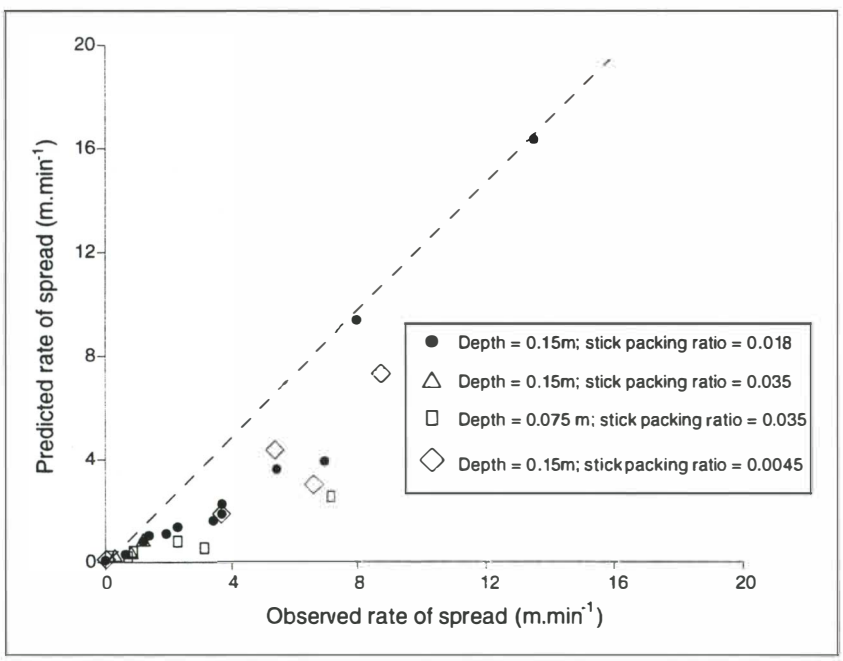

Figure 4.18 Observed vs. predicted rates of spread in various mixed experimental fuel beds. From the data of Catchpole *et al.* (1993).

The behaviour of fire in a mixed fuel bed, compared to that in component fuels, was strongly influenced by whether the fire was wind-driven or not. Catchpole *et al.* (1993) consider that this may be due to the effect of different heat transfer processes. This may mean that the basic assumption of the Rothermel model, that the propagating flux in a

wind-driven fire can be easily related to the propagating flux of a zero-wind fire, is fundamentally flawed.

Catchpole *et al.* (1993) note that in many of the experimental fuel beds used, the loading of large diameter fuel compared with that of fine fuel was 3:1. This ratio is significantly greater than is found in most wildland fuels. The ratios were exaggerated by Catchpole *et al.* (1993) in order to highlight some of the problems of using the Rothermel model in mixed fuel beds. For the same reason Catchpole *et al.* (1993) used two fuels (excelsior and sticks) of widely different sizes. It was found that in mixed fuels with lightly packed sticks the fire behaves similarly to a fire in fine fuels only, with the sticks burning behind the main fire front. However the spread rate is considerably reduced by the presence of the sticks. Unlike Brown (1972), Catchpole *et al.* (1993) found no evidence that non-uniform packing has any effect on fire behaviour.

4.4.6 Summary of Field Evaluations of the Rothermel Model

Table 4.3 shows a summary of the evaluations presented in the preceding sections. Of 194 test fires the model over-predicted rate of spread in 74 and under-predicted the remainder.

Table 4.3 Summary statistics on predicted and observed rates of spread.

Fuel Type	*Number of observations*	*Number over-predicted*	*Number under-predicted*	*Mean error* (m.sec^{-1})*	r^2
Logging slash (Brown, 1972)	26	23	3	+0.41	0.80
Grassland (Sneeuwjagt & Frandsen, 1977)	42	19	23	+2.11	0.92
South African fynbos (Van Wilgen *et al.*, 1985)	14	5	9	+3.51	0.77
South African Savanna (Van Wilgen & Wills, 1988)	10	5	5	+3.47	0.82
Grassland (Gould, 1988)	75	22	53	†	0.55
Experimental Complex (Catchpole *et al.*, 1993)	27	0	27	-0.97	0.83
All studies combined ‡	194	73	120	+1.14‡	0.85‡

* = (predicted - observed)/n

† This value could not be calculated as the paper of Gould (1988) did not include raw data.

‡ Gould (1988) not included.

The degree of under- and over-prediction is evaluated by dividing the absolute

difference of the predicted and observed values by the larger of the two values (Andrews, 1980). As shown in Figure 4.19, 36% of the observations lie within 25 percent of under- and over-prediction. Rate of spread observations of 33 (27%) of the 119 fires fell beyond 50 percent of over- and under-predictions; that is, the prediction is more than twice or less than half the observation.

The mean prediction for all fires was 1.14 $m.min^{-1}$, ranging from +3.47 for South African savanna to -0.97 in the experimental fuel beds used by Catchpole *et al.* (1993). 75.6 percent of the absolute differences were less than 1 $m.min^{-1}$ and 89.9% were less than 5 $m.min^{-1}$. The r^2 values were obtained through linear regression of predicted onto observed rates of spread. This analysis yields information on the precision of the model; an r^2 of 1 would indicate an exact functional relationship. The r^2 values for the various fuel beds range from 0.55 (Gould, 1988) to 0.92 (Sneeuwjagt and Frandsen, 1977). The r^2 value of all data combined was 0.85 ($p<0.01$). This value is similar to that found by Andrews (1980) and is indicative of a strong relationship between the predicted and observed values.

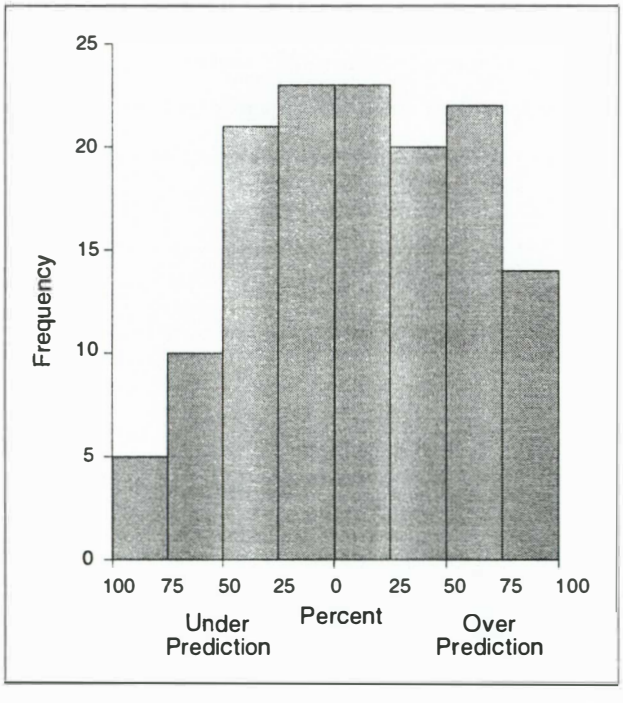

Figure 4.19 Frequency distribution of percentage under-prediction (100*[obs-pred]/obs) or over-prediction (100*[pred-obs]/pred) of rates of spread. Gould (1988) is not included as there is no raw data available for his tests.

Brown (1972), Gould (1988), and Catchpole *et al.* (1993) all found problems with the use of the surface-area to volume ratio to weight other parameters. Gould (1988) also found the estimation of the surface-area to volume ratio to be problematic and that errors in its estimation could cause either an under or over-prediction of rate of spread.

Brown (1972), Sneeuwjagt and Frandsen (1977) and Andrews (1980) consider that agreement between the observed and predicted rates of spread may be improved if estimation(s) of the moisture content of extinction were improved. The assignment of a moisture content of extinction is problematic and it is the only model input that can not be measured directly.

4.5 Summary

This chapter has reviewed the fire spread model of Rothermel (1972). This model was developed to predict the rate of spread and intensity of surface fires in wildland fuels. The development and limitations of the model were considered and a sensitivity analysis was performed on the model; the input variables which predictions of rate of spread were most sensitive to were found to be fuel moisture content, wind speed and the surface-area to volume ratio of the fuel bed. The performance of the Rothermel model in a number of ecosystems outside those in which was designed and validated was considered. It was seen that the Rothermel fire spread model can be effectively used to predict fire behaviour in wildland fuels. In 119 experimental fires, nearly 40 percent of the observations were within 25 percent of over- or under-prediction. However, problems were identified with the parameterisation of the moisture content of extinction and the weighting of fuel bed parameters by the surface-area to volume ratio.

Chapter Five

The PYROCART Simulation Model

5.1 Introduction

This chapter describes the conceptualisation, development and testing of the fire-spread simulation model (PYROCART) to the point at which it could be validated by *a posteriori* prediction of the Cass fire of May 1995. Initially the conceptual basis and the structure of the modelling system are reviewed. Then the model is tested in five artificial landscapes ranging in complexity from a completely homogeneous landscape to one in which the fuel bed and terrain were spatially heterogeneous and the wind field temporally variable. The model output in each of these conditions is presented and the way in which the fire shapes produced conform to theoretical expectations is briefly discussed. Throughout this chapter wind speeds are referred to in units of $km.hr^{-1}$; while the author recognises that this is not a SI unit it is the unit most widely referred to in the fire modelling literature.

5.2 An Introduction to the Fire Modelling System -

Chapter 3 illustrated that most predictive fire spread models assume that the fuel bed is both horizontally continuous and spatially homogeneous. Real fuel beds, however, are spatially heterogeneous and often both vertically and horizontally discontinuous. Moreover, they are discontinuous at almost any scale relevant to fire spread modelling. Whether, they consist of trees, bushes or tussocks, fuels in the 'real world' are normally not continuous but discrete, at the scale of individual plants. Even where litter provides virtually continuous fuel cover, this cover can be extremely patchy, displaying significant variations in depth or concentration. At larger scales, changes in vegetation type lead to similar variations in fuel concentrations. Fuels that are both continuous and homogeneous comprise only one end of a spectrum, the other end being fuels concentrated in patches and separated by bare ground.

Within PYROCART the landscape is represented, using the raster data model, as a geo-referenced rectangular array of 'cells' with each cell in the array representing a discrete area of the land surface. Associated with each cell (location) are 'states' that represent relevant environmental information such as vegetation type and slope. Theoretically, therefore individual cells may represent single plants or whole patches of vegetation

depending on the spatial resolution of the cells. However, in the modelling system developed in this research cells are unlikely to be applicable to a full continuum of spatial scales. For example, at very small scales issues such as the amount of bare ground surrounding every plant would become problematic. Given the duration of a fire, fuel and topography are essentially temporally constant and so have no temporal component. However, wind speed and wind direction have both a spatial and a temporal resolution, at scales smaller than the fire duration. Regardless of the spatial resolution of the array each cell is considered to be internally homogeneous with regard to fuel, topography and wind variables. In formal terms, this type of landscape model is a *cellular automata* (Hogewog, 1988). This approach mirrors both traditional quadrat sampling methods and pixel-based satellite imagery.

The use of GIS allows the issues raised by spatially non-uniform landscapes to be resolved. Furthermore, the use of the raster data model is equivalent to the cellular automata model outlined above. Each cell is geo-referenced and contains a single value describing the state of that cell. The fire model can be applied to each cell individually and thus assumptions of spatial uniformity are not violated.

5.3 The Fire Spread Model

This section is concerned with the development and structure of the fire spread model. The model is considered in two parts: firstly the overall structure of the model is outlined and the way in which Arc/Info and the Fortran 77 routines were integrated is discussed; secondly, the nature of the spread routine itself is analysed. The version of Fortran that was used was 'f77' Version 3.0.1 from Sun, a superset of standard Fortran 77 (Sun Soft, 1994).

5.3.1 The Structure of the Fire Model

As discussed in Section 3.5 the integration of environmental modelling systems and GIS has proved extremely problematic. The nature of the integration used in this thesis has been widely termed 'loose coupling' (Fedra, 1993; Wesseling *et al.*, 1996). The basic structure of loosely coupled modelling frameworks is shown in Figure 5.1. It can be seen that the model reads input data from GIS files and produces some of the output in a format which allows processing and display within the GIS. Loose coupling is appropriate when a model is being linked to a GIS as an experiment or as part of an exploratory process, or where there are particular computational requirements that are not provided by the GIS (as was the case in this model, in which the ability to be able to rapidly process large arrays was crucial). The major advantage of loose coupling is that

if code is available for the environmental model, then it can often be used with only minimal modification; Wesseling *et al.* (1996) note that loose coupling has often been used by disciplines with a strong mathematical tradition. However, Fedra (1993) notes that loosely coupled integration is cumbersome and error prone, especially with regard to the data transfer process.

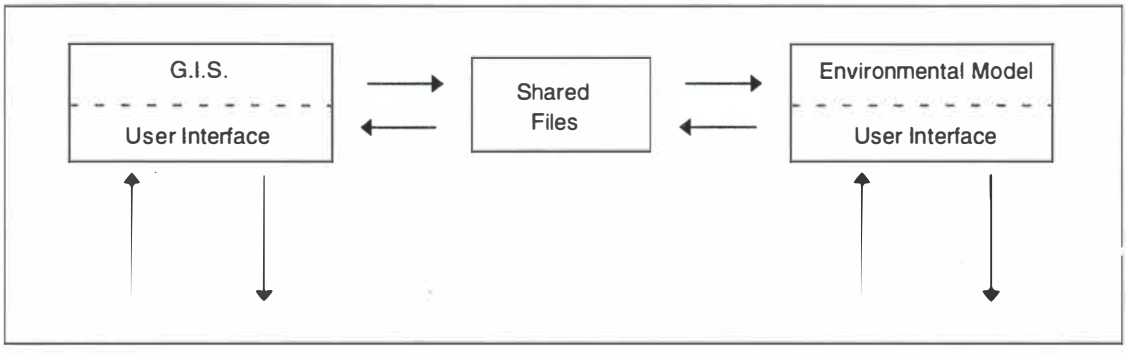

Figure 5.1 The nature of loosely coupled integration between a GIS and a spatial [environmental] model. (Fedra, 1993).

This approach is very similar to that taken by Vasconcelos (1988) and Vasconcelos *et al.* (1990, 1992). The overall structure of the model is shown in Figure 5.2. Data concerning fuel class, slope, wind speed and wind direction are stored in Arc/Info GRIDs. These are extracted to ASCII files using the Arc/Info command <<*gridascii*>>. Once in ASCII format these data layers are readable into the main Fortran 77 routine. After completion of the Fortran 77 routine, the final array, which contains information on the burn status of each cell, is written to an ASCII file in a format suitable to be read into Arc/Info. These ASCII files are then converted to Arc/Info GRIDs using the Arc/Info command <<*asciigrid*>>. Arc/Info is then used for analysis (e.g. calculation of areal statistics) and display of the fire shapes.

Within the model, time increases in discrete increments (each equivalent to one iteration of the main loop) and both spatial and temporal resolution can be set within the model. During each time interval, relevant variables are calculated and the status of every 'affected' cell is updated. Table 5.1 illustrates both the states a cell may be in at any point in time and the nature of the changes that a cell may undergo over one time interval. Cells may only burn in two iterations if they are *diagonally* adjacent to a fire source (i.e. they share a corner and not an edge).

Table 5.1 States and possible outcomes for any cell over one iteration.

Cell Code	*Cell State*	*Possible Change(s)*
0	Unburnt	0, 2, 3
1	Burnt	None
2	Burn at the next time increment	1
3	Burn in two time increments	2
4	Ignition Point	None

Figure 5.3 shows that the main body of the program is concerned with calculating rate of spread in cells, testing whether fire will spread from burning cells into their unburnt neighbours and as a result updating the STATUS array. This array contains information on the 'burn status' of every cell in the landscape matrix. Finally, the routine writes out ASCII files suitable for import to Arc/Info. The routine used to produce the fire spread shapes shown in this Chapter is presented in Appendix 2.

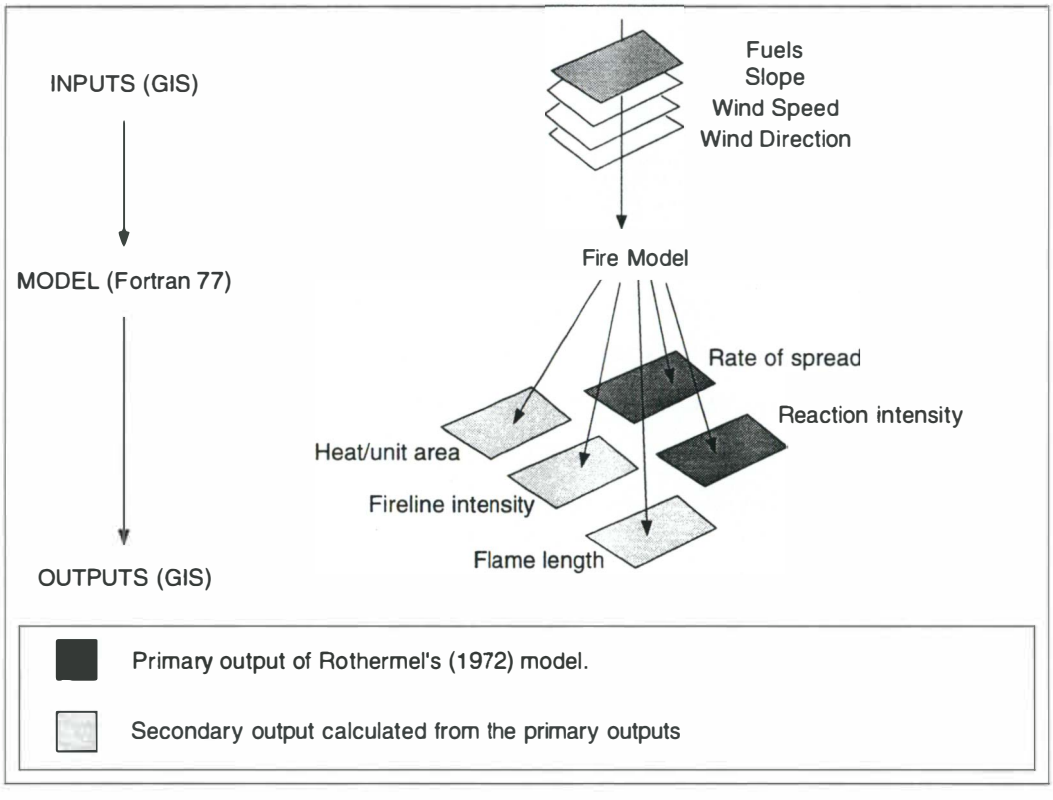

Figure 5.2 The structure of the PYROCART fire model.

5.3.2 The Spread Algorithm

As discussed in Section 3.4.1 it is usually assumed that the area directly affected by a burning piece of fuel is an ellipse, in which the source lies in one focus, the major axis is parallel to the wind direction, and the eccentricity of the ellipse increases as a

function of the speed of the prevailing wind (Anderson, 1983; Catchpole *et al.*, 1992; see Figure 3.1). Green *et al.* (1990) translate this into an expression which calculates the rate of spread R (in m.min^{-1}) in an arbitrary direction θ (in degrees from north) :

$$R(\theta) = \frac{F(1 - e)}{[1 - e\cos(\theta - \omega + 180)]} \quad (5.1)$$

where : F = forward rate of spread (in m.min^{-1}), e = the eccentricity of the spread ellipse, and ω is the direction from which the prevailing wind is blowing.

The eccentricity e of the spread ellipse is usually defined as:

$$e^2 = 1 - \frac{1}{l^2} \quad (5.2)$$

where : l = the length to breadth ratio of the ellipse.

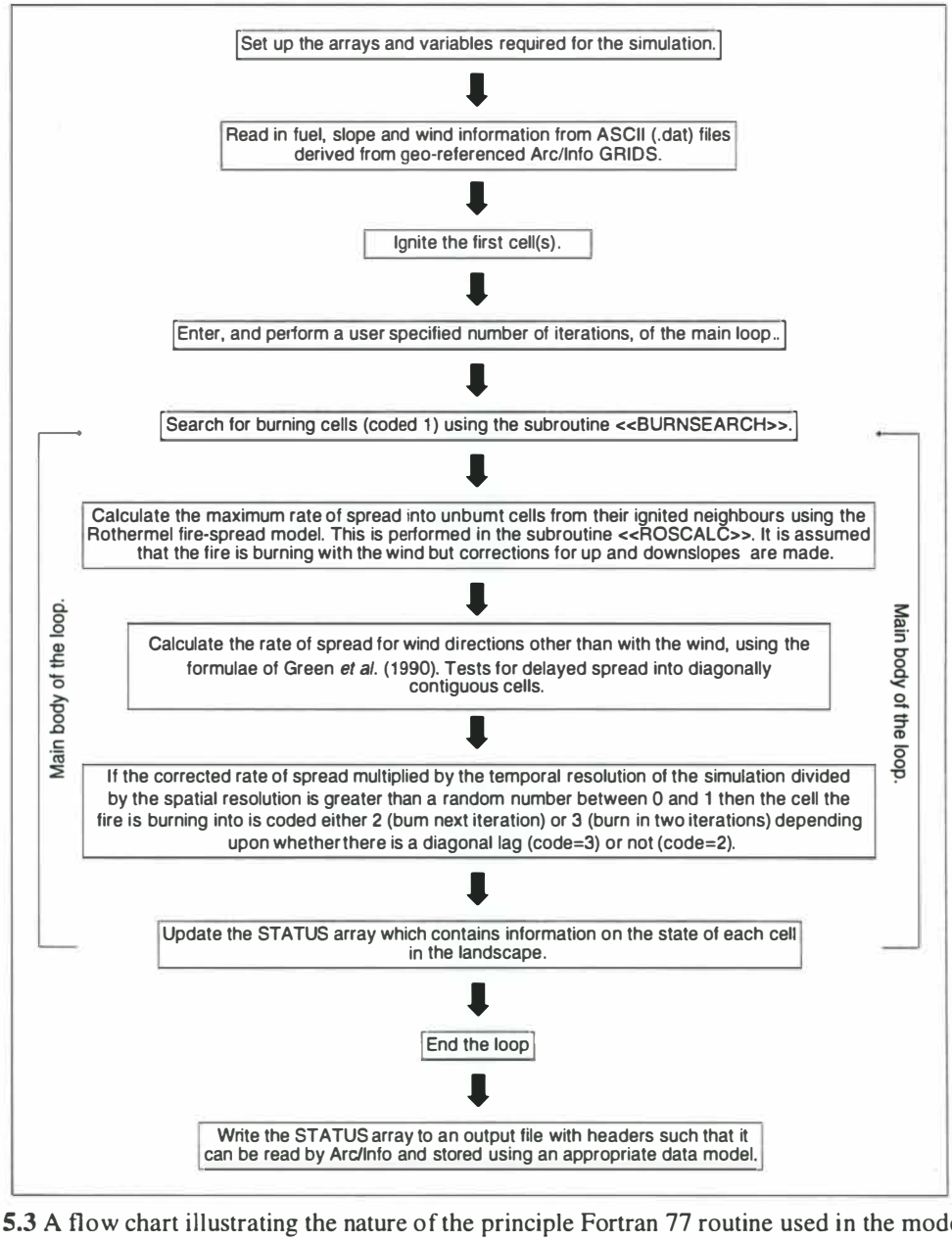

Figure 5.3 A flow chart illustrating the nature of the principle Fortran 77 routine used in the model.

In fire modelling applications, empirical formulae have been derived to estimate fire-spread eccentricity for different fuel types. The two formulae derived by Green *et al.* (1990) are for forest and grassland fuels and are presented below (Equations 5.3 and 5.4).

$$e = \sqrt{[1 - \exp(0.0058 - 0.0324w^{1.2})]} \qquad \text{FOREST} \qquad (5.3)$$

$$e = \sqrt{1 - 0.826w^{-0.928}} \qquad \text{GRASSLAND} \qquad (5.4)$$

where : w = wind speed (km.hr^{-1}). If $w \leq 1$, then e is assumed to be 0 (for both Equations 5.3 and 5.4).

The ways in which the two different expressions of eccentricity affect final fire shape is shown in Figure 5.4. These simulations were performed under identical, homogeneous conditions (wind speed *(w)* = 10 km.hr^{-1}) with the only difference between them being the expression used to calculate eccentricity of the spread ellipse *(e)*; the shapes are those produced after 75 iterations at the same temporal resolution. The ellipse produced using the forest expression is less elliptical than that produced using the grassland expression. This is because using the forest expression yields higher flanking rates of spread than the grassland expression (Figure 5.5).

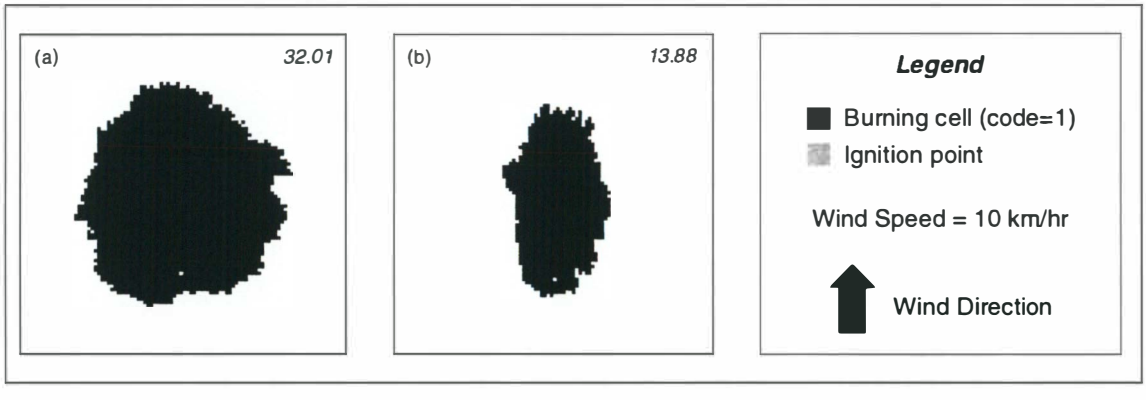

Figure 5.4 The effect of the different eccentricity (*e*) expressions of Green *et al.* (1990) on final fire shape; (a) the shape produced using the forest expression (Equation 5.3); and (b) the shape produced using the grassland expression (Equation 5.4). The numbers in each simulation represent the % of the array burnt (i.e. coded 1).

Despite the fact that relative rate of fire spread decreases for flanking and backing fires as wind speed increases (Figure 5.5), the absolute rate of spread of a backing fire may be higher at high wind speeds. This is because the adjusted rate of spread is calculated from the heading rate of spread which increases exponentially with wind speed (Equation 5.1). To counter the problem of excessively high backing rates of spread at high wind speeds an arbitrary limit was set on rate of spread at 135° and 180° to the wind. The limit was set at the rate of spread for that angle at a wind speed of 5 km.hr^{-1}.

In summary, the adjusted rate of spread model is a function of wind speed (which determines the eccentricity of the ellipse), the forward rate of spread and the difference between the direction from which the prevailing wind is blowing (ω) and the direction in which fire is spreading (θ); the adjustment of rate of spread is at a maximum where the difference between ω and θ is 0° (i.e. the fire is travelling into the wind) and at a minimum where the difference is 180° (i.e. the fire is travelling with the wind). Green (1983) studied the model presented in Equation 5.1 in detail and Green *et al.* (1983) confirmed its validity by testing the shapes it produced against the final shape of a number of experimental fires.

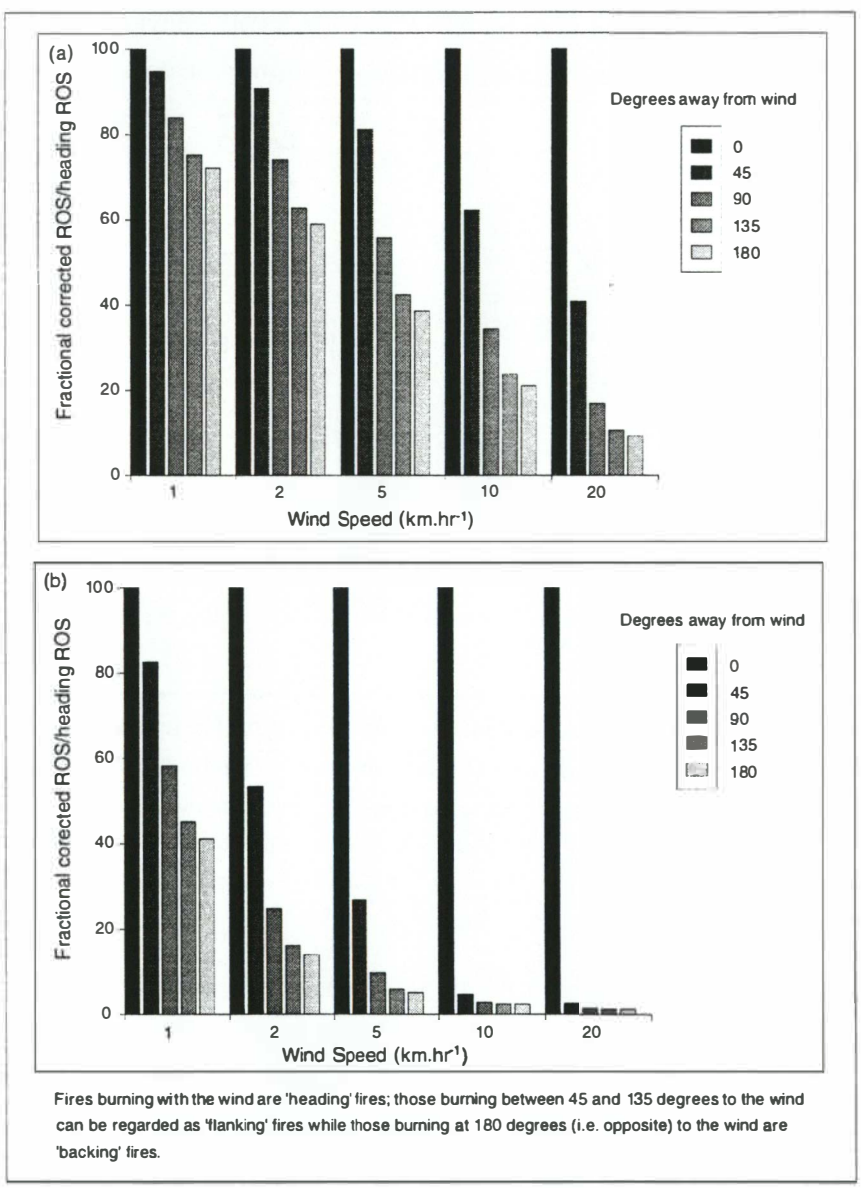

Figure 5.5 Corrected flanking and backing rates of spread (ROS) as a function of wind speed and the angle between wind direction and fire spread direction using the expressions of Green *et al* (1990). Graph (a) shows corrected rate of spread in woodland (Equation 5.3) and graph (b) shows corrected rate of spread in grassland (Equation 5.4).

In the model, wind-corrected rate of spread was calculated by determining the vector from the cell currently burning to the cell into which fire was potentially spreading, with wind speed and wind direction read from the cell into which fire was spreading.

Following calculation of corrected rates of spread an evaluation of whether fire spreads into the neighbouring unburnt cell occurs. This is a relatively simple, probabilistic procedure. The adjusted rate of spread is multiplied by the temporal resolution of the simulation (in minutes); this value is then divided by the spatial resolution of the data layers (where appropriate this is corrected for diagonally contiguous cells; cell size*$\sqrt{2}$). The final value is then compared with a randomly generated number between 0 and 1 and if the spread value exceeds the random number the cell is ignited.

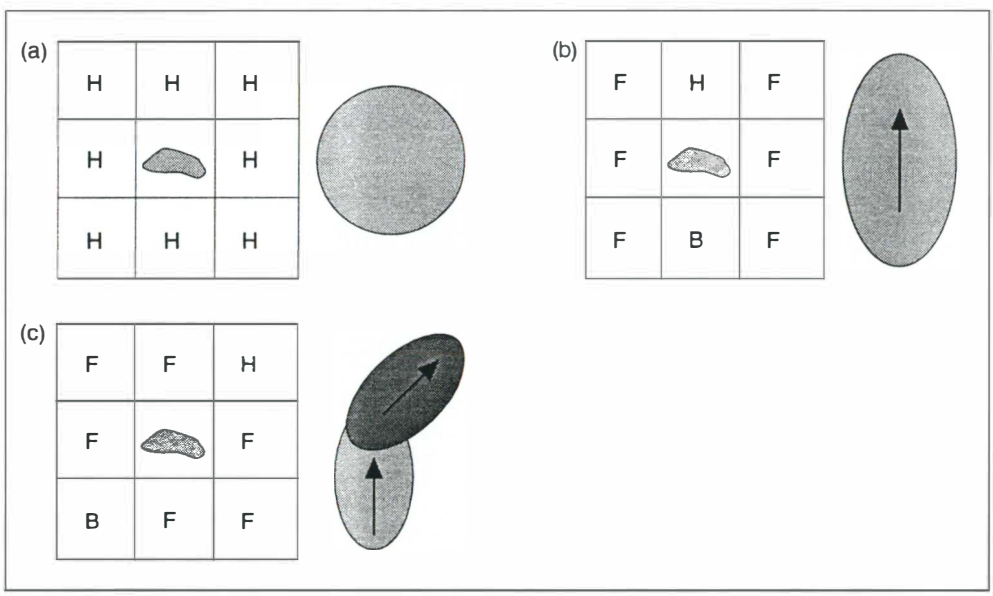

Figure 5.6 Representation of fire spread within a 3x3 cellular matrix. The letters in the cells are for head fires (H), flanking fires (F), and backing fires (F). All conditions are uniform with the exception of wind speed. In (a) the wind speed is zero, in (b) the wind speed is constant blowing up the page, and in (c) the wind speed is constant with the wind and blowing diagonally form lower left to upper right (Ball and Guertin, 1992).

Figure 5.6 illustrates the manner in which wind speed and direction affect the nature of fire spread into each cell. In Figure 5.6a wind speed is zero and so fire spreads into each neighbouring cell as a heading fire; as a result a circular fire shape is predicted. The fire shape depicted in Figure 5.6b is wind-driven; with a wind blowing up the page. As a result fire does not spread into neighbouring cells solely as a heading fire. Instead fire spreads into cells between 45° and 135° to the wind as flanking fires and into cells directly opposed to the prevailing wind direction (180°) as a backing fire. The third case (Figure 5.6c) illustrates the effect of a change in the prevailing wind direction. As can be seen a second ellipse is formed with its major axis aligned with the new wind direction. There is a corresponding shift in the cells fire spreads into as a fronting,

flanking or backing fire.

Although the Rothermel model treats rate of spread down slopes as being equivalent to rate of spread on flat surfaces (zero-slope) recent research has shown this assumption to be invalid (Van Wagner, 1988; Section 2.5.3). Thus, PYROCART includes the downslope correction expression of Van Wagner (1988). This is :

$$SF = 1 - 0.0330A + 0.00749A^2 \quad (5.5)$$

where : SF = the downhill spread-rate factor, to be applied as a multiplier on the estimated level rate, and, A = the slope angle as degrees from the horizontal.

The equation yields a minimum of 0.64 (64%) of the level spread rate at 22° and regains the level spread rate again at approximately 45°. The nature of the function is shown in Figure 5.7. Van Wagner (1988) attributes increased rate of spread on steep downslopes to the influence(s) of uneven air pressure on both sides of the flame, and to the minute downward movement of partially burnt fuel matter.

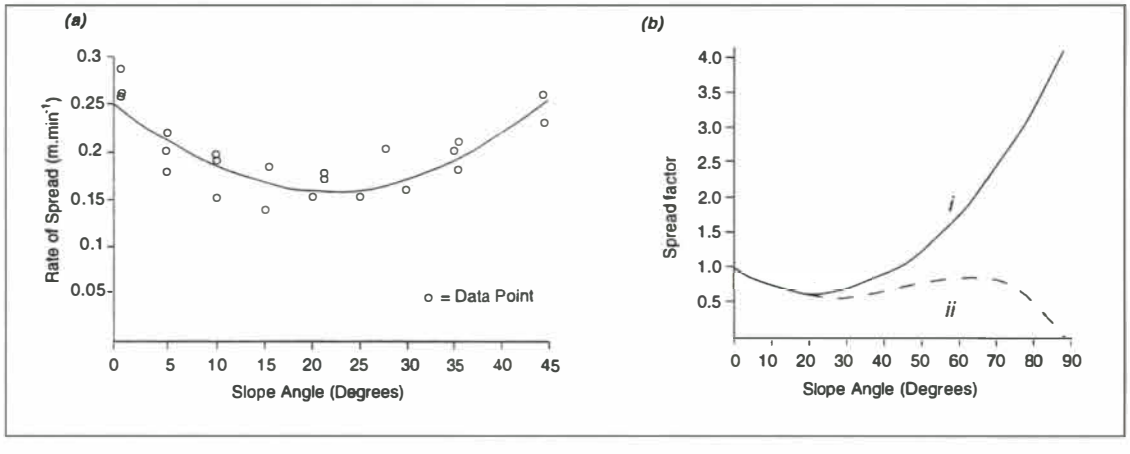

Figure 5.7 (a) Rate of spread (adjusted to 10% moisture) vs. downslope angle for 22 downslope laboratory fires, with fitted parabolic curve. (a) Graph of spread factor given by Equation 5.5 from 0° to 90° slope (i) as given for spread down slope and (ii) multiplied by cosA for horizontal projection. (Van Wagner, 1988).

5.4 Testing Zero State and Simple Homogeneous Conditions

The first stage in the development of the fire simulation model was evaluating its behaviour in simple, homogeneous conditions. In this case it was assumed that the terrain was totally flat, and there was a monotypic fuel bed fuel (the 'tall grass' fuel model of Rothermel, 1972); both wind speed and direction were held constant across each simulation. The model was tested using a number of wind speeds to assess whether the model would predict an initially circular fire shape which became an ever more elongate ellipse as wind speed increased. Furthermore, as wind speed increases a

larger proportion of the array should also burn as rate of spread increases.

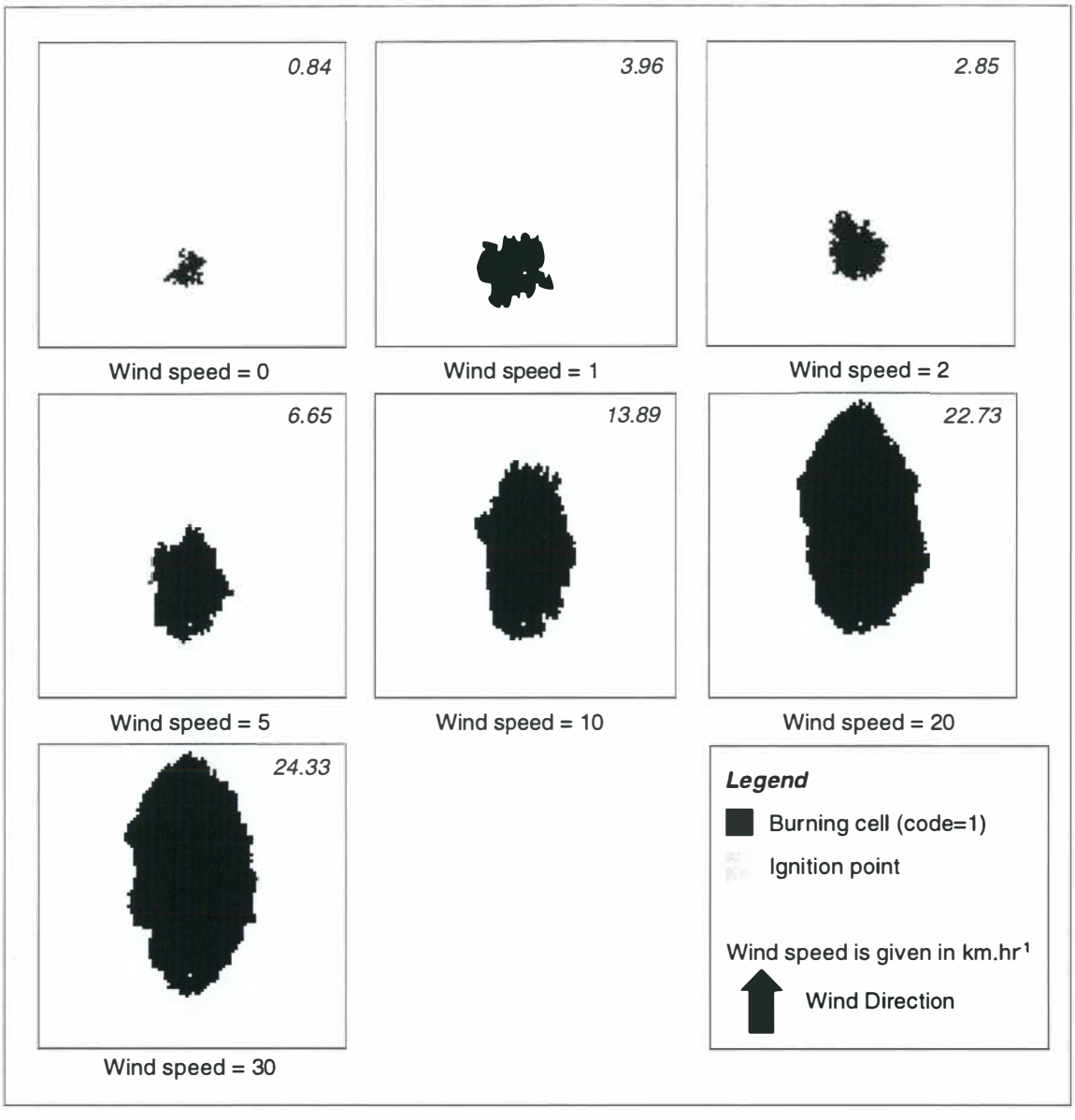

Figure 5.8 The fire shapes produced by PYROCART in simple homogeneous (no-slope, constant fuel and wind) conditions after 75 iterations. The numbers in the top right of each simulation denote the % of the array burnt.

Because fire spread is assessed only at multiples of 45° angles to the wind, the final spread shapes produced at wind speeds above zero are distorted by the square cell matrix. The fire shapes presented in Figure 5.8 generally show a more angular leading edge than might otherwise be expected. This is a result of the raster data structure which cannot represent the true continuous nature of an actual fire. Thus, the shapes predicted by analytical models such as those of Peet (1967), Van Wagner (1969) and Anderson (1983) (all modified elliptical forms) are not well reproduced by the model in terms of having a smooth edge. However, if the effect of the raster data structure is ignored, then the shapes conform to those predicted by the elliptical fire shape model.

Furthermore Ball and Guertin (1992), who employed a similar spread algorithm, found that a simple cosine correction of the flanking and backing algorithm is an oversimplification of fire behaviour and may lead to some distortion in the eventual shape of the fire perimeter. In the cellular neighbourhood, angles are multiples of 45° which adds to the inaccuracy of flanking adjustment using a simple cosine formulation.

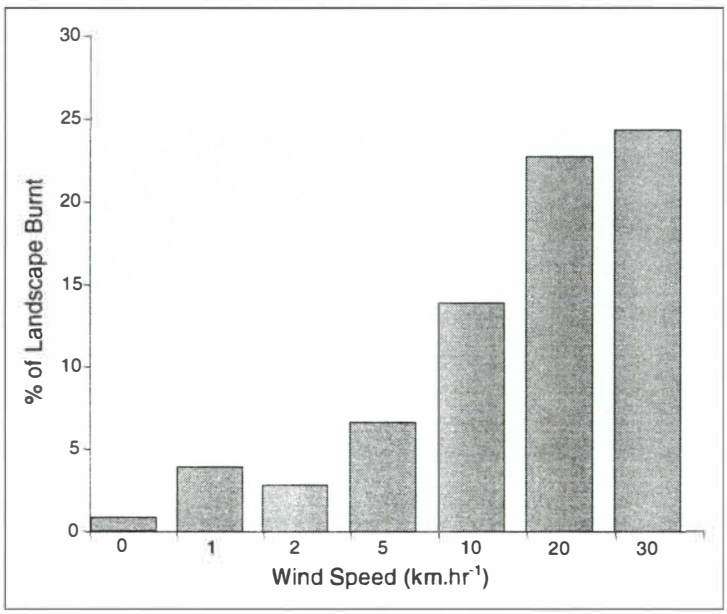

Figure 5.9 The number cells burnt at each wind speed after 75 iterations as a percentage of the number of cells burnt after 75 iterations with a wind speed of 30 km.hr^{-1}.

Two crucial issues are highlighted when the fire shapes presented in Figure 5.8 and the data in Figure 5.9 are examined. Firstly, the number of cells burnt at a wind speed of 2 km.hr^{-1} is considerably smaller (29%) than the number of cells burnt at a wind speed of 1 km.hr^{-1}. This difference is an artefact of the spread rate corrections of Green *et al.* (1990). Equations 5.3 and 5.4 calculate the eccentricity of the ellipse as a function of wind speed with ellipse eccentricity increasing with wind speed (w). For wind speeds of less than or equal to 1 km.hr^{-1} e is assumed to equal zero and so spread is not corrected in any direction. However, at a wind speed of 2 km.hr^{-1} e is not assumed to equal zero and so the fire is forced in the direction of the wind with flanking and backing fires assuming very low rates of spread. As a result the number of cells burnt with a wind speed of 2 km.hr^{-1} is significantly lowered. The second important point is that the eccentricity (e) of the fire shapes increases. This is shown in Figure 5.10 which presents analytical solutions for eccentricity against wind speed in both grassland and forest fuels. It can be seen that in grassland fuels eccentricity rapidly tends towards one; the zero eccentricity at low wind speeds is a function of the restrictions imposed in the model of Green *et al.* (1990). Although, in forest fuels fire shapes less rapidly approach an eccentricity of one the trend is similar to that seen in grassland fuels. The fire shapes presented in Figure 5.9 show that eccentricity does increase with wind speed. However

in these shapes length-to-breadth ratio is constrained by both the cellular nature of the model and the size of the landscape itself and so the analytical solutions presented in Figure 5.10 are distorted.

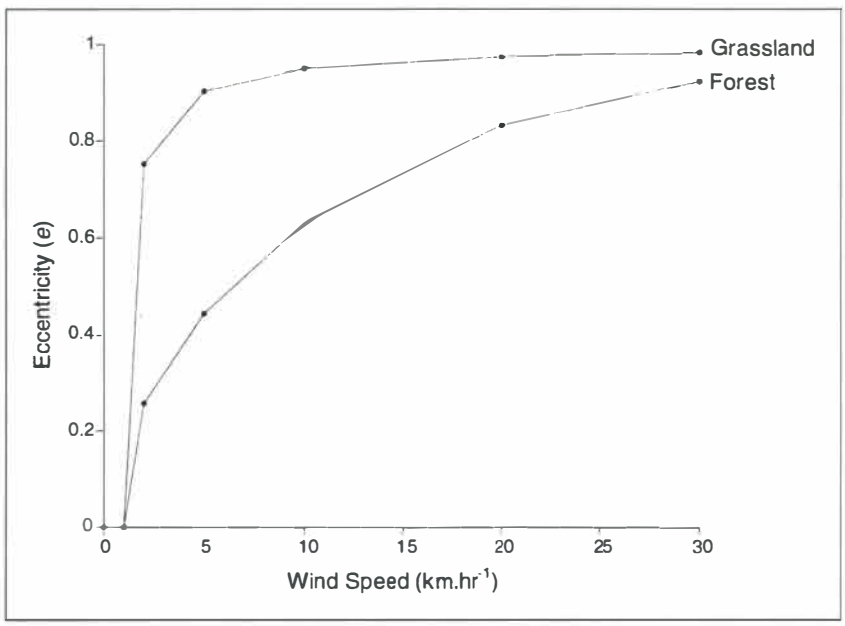

Figure 5.10 Analytical solutions for wind speed (w) against the eccentricity (e) of the spread ellipse in grassland and forest fuels.

5.5 Simulating Fire Spread in Complex Heterogeneous Landscapes

After the PYROCART modelling system was found to produce acceptable results in homogeneous conditions, it was necessary to evaluate its operation in more complex, heterogeneous conditions. This process was performed incrementally in four levels of spatial heterogeneity:

- variable terrain, constant fuels and wind,
- variable fuels, constant terrain and wind,
- homogeneous fuels and terrain with a pre-ordained wind shift,
- variable terrain and fuels with pre-ordained wind shifts.

The fire shapes produced in heterogeneous landscapes are compared to those produced in homogeneous conditions using the Sørensen Coefficient (Greig-Smith, 1983). The Sørensen Coefficient is used here to test for presence/absence similarity between two landscapes and is defined as :

$$s = \frac{2a}{2a + b + c} \tag{5.6}$$

where : s = the Sørensen Coefficient; a = the number of cells burnt in both fires; b = the number of cells burnt in the homogeneous fire only; c = the number of cells burnt in the heterogeneous fire only.

The final value for the coefficient lies between 0 and 1 with a value of 1 indicating a complete congruence and a value of 0 representing no overlap. The Fortran routine used for the similarity analyses is presented in Appendix 2.

5.5.1 Fire Spread in Irregular Terrain

The first level of spatial complexity on which the model was checked was a synthetic landscape (100*100 cells) with irregular terrain but with a constant single fuel (the tall grass model of Rothermel, 1972) and wind direction. The landscape used is shown in Figure 5.11. In theory it would be expected that the fire shapes produced in these conditions would be different from those presented in Section 5.4. Upslopes may be expected to increase the rate of spread of the fire as the flame is tilted towards the fuel bed. Conversely, downslopes less than 45° decrease the rate of spread as the flame tilts away from the downhill fuels and radiative pre-heating diminishes (Section 2.5.3; Figure 2.6). However, although the effect of upslopes on rate of spread is included in the Rothermel model with the incorporation of a slope factor correction (ϕ_s) and downslope influences through the inclusion of the correction factor of Van Wagner (1988) these have a relatively small effect on the rate of fire spread when compared to FMC or wind (Sections 4.3.5 and 4.3.6).

Slope is derived from the elevation layer by calculating the difference between the elevation in the burning cell and the cell into which the fire will spread and then dividing the difference by the distance between the centres of the two cells. In the cases of diagonally contiguous cells the distance is equal to the cell resolution *$\sqrt{2}$. These calculations were necessary because using Arc/Info to calculate slope from the DTM of the firescar would provide only the maximum slope within the cell and not the slope between two cells in any of the eight cardinal directions in which fire can spread in a raster grid.

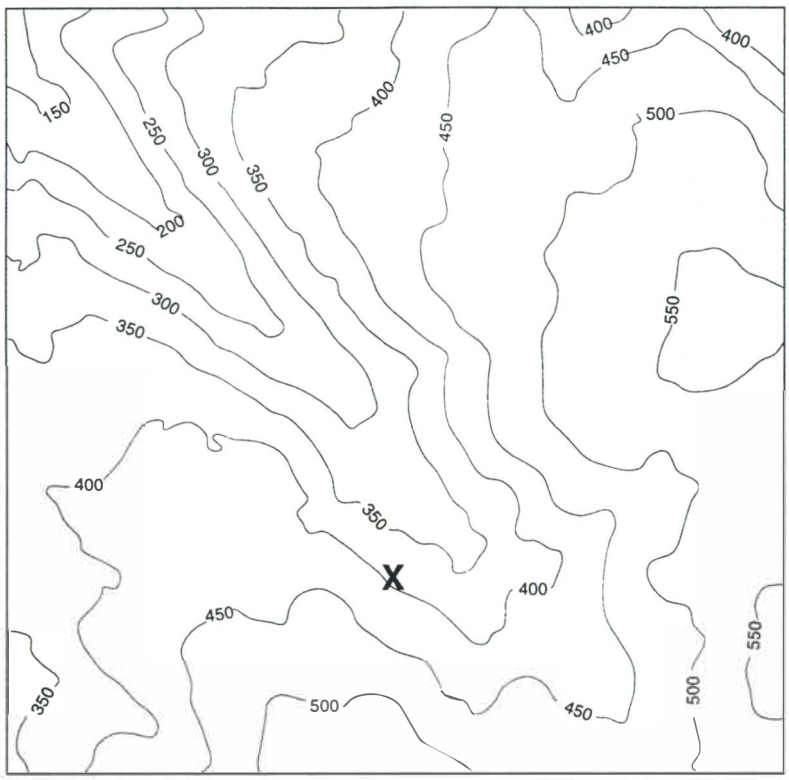

Figure 5.11 The landscape used to test the performance of the fire spread model in irregular terrain. The contour lines are at intervals of 50m; **X** denotes the ignition point.

The difference between the fire shapes presented in Section 5.4 (Figure 5.8) and those produced for irregular terrain (Figure 5.12) are small. This is because the slopes between cells were usually less than 10% and so had a limited effect on rate of spread. At wind speeds above 5 $km.hr^{-1}$ wind speed and direction become the dominant influences and the effect of slope becomes negligible. The slightly lower number of cells burnt at high wind speeds compared to the homogeneous simulations (Section 5.4) is attributable to lowered rates of spread due to the predominantly downhill progression of the fire. However, at low wind speeds the fire can be seen to spread up-slope preferentially and as a result the approximately circular shape expected at these wind speeds (where e~0) is distorted and a higher number of cells is burnt than in homogeneous conditions.

A comparison of the fire shapes, using the Sørensen coefficient, produced under homogeneous conditions and in spatially variable terrain is presented in Table 5.2. The values for the coefficient range between 0.34 and 0.95 and increase with wind speed. This increase in similarity is clearly apparent when Figures 5.9 and 5.12 are compared. At low wind speeds slope is the most important control on fire behaviour, but as wind speed increases, wind speed and direction exert an ever stronger influence. The values of b and c emphasise the nature of the changes caused by variable terrain. The relatively

high values of c (compared to b) at wind speeds of 0-1 km.hr^{-1} reflects the preferential upslope burning of the fire. The difference between b and c diminishes as wind speed increases and the wind vector becomes the dominant influence on fire shape.

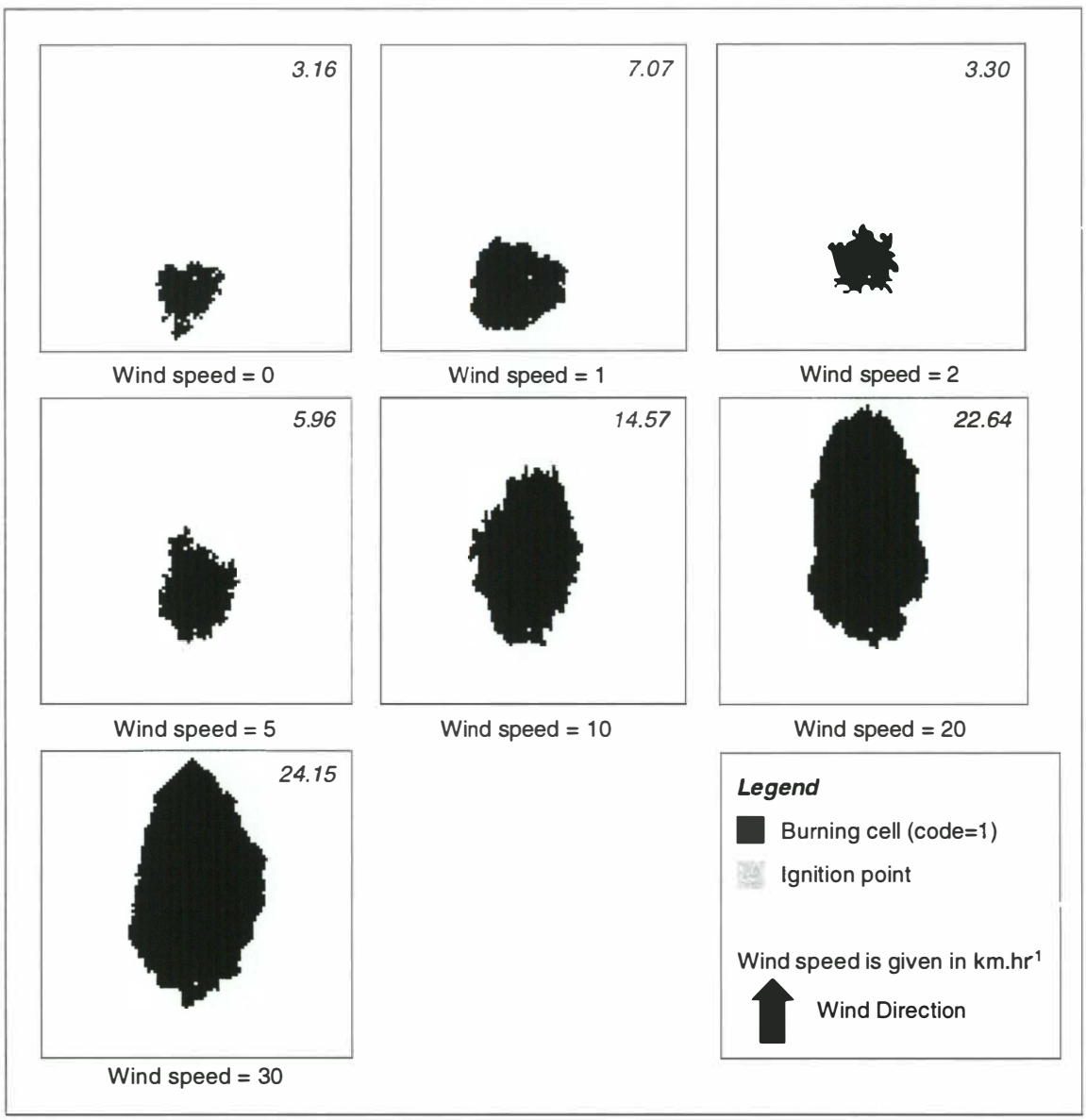

Figure 5.12 The shapes produced by PYROCART in variable terrain. The numbers in the top right of each simulation denote the % of the array burnt.

Table 5.2 Sørensen similarity index coefficient values for fire shapes produced in homogeneous conditions compared with those produced where the terrain is variable.

Wind Speed (km.hr^{-1})	*a*	*b*	*c*	*Sorensen Coefficient*
0	67	17	247	0.34
1	366	29	332	0.67
2	231	48	96	0.76
5	525	124	66	0.85
10	1290	81	148	0.92
20	2094	158	136	0.93
30	2266	120	126	0.95

a - Number of cells burnt in both landscapes.
b - Number of cells burnt in homogeneous landscape only.
c - Number of cells burnt in heterogeneous landscapes only.

Figure 5.13 compares the percentage of the array burnt under the five scenarios in which PYROCART was tested against wind speed. In both of the simulations in which terrain was spatially non-uniform, its influence at low wind speeds is clearly visible.

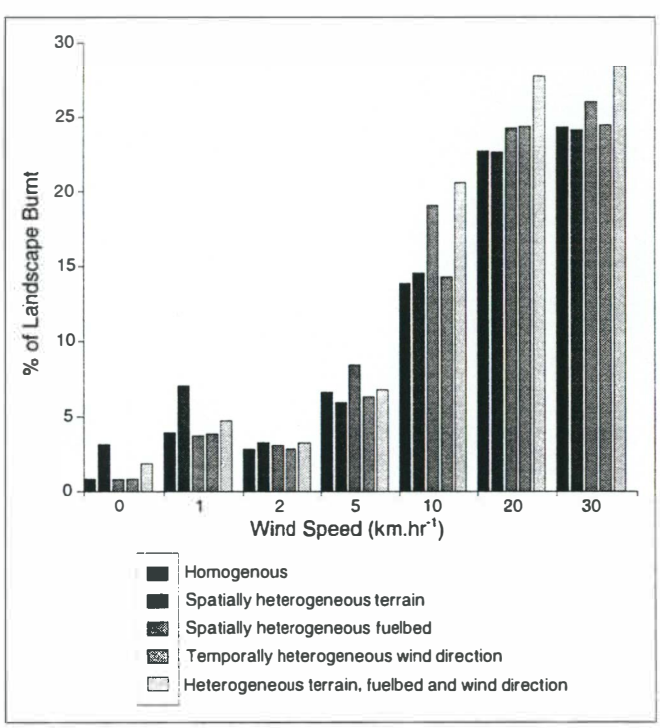

Figure 5.13 A comparison of the proportion of the landscape burnt at each wind speed after 75 iterations for each of the five scenarios PYROCART was evaluated in.

Across the five simulations the shapes are most similar (in terms of % of the landscape burnt) at a wind speed of 2 km.hr^{-1}. This is because of the extremely low flanking and backing rates of spread at this wind speed; the shapes are least similar at wind speeds of 0 and 1 km.hr^{-1} due to the zero eccentricity assumptions of Green *et al.* (1990). As wind

speed increases, however, the importance of slope diminishes and variables such as fuels become more important. Finally at the highest wind speeds (20 and 30 km.hr^{-1}) wind speed and direction become the dominant influences on fire shape.

5.5.2 Fire Spread in Spatially Heterogeneous Fuels

The presence of spatially heterogeneous fuels leads to spatially heterogeneous rates of fire spread. As a result the elliptical template of fire spread is likely to be greatly modified; a spatially variable fuel bed is likely to have a more significant influence on fire shape than spatially variable terrain. The artificial 'fuelscape' comprised an array (100*100) of 9 different fuel types, including unburnable patches of fuel ($m_f > m_x$). The fuelscape is shown in Figure 5.14. The fuel models were all taken from Rothermel (1972); two brushland and chaparral models were used with different FMCs. . The fuel models for this fuelscape are presented in Appendix 3. Figure 5.15 shows rate of spread against wind speed for these fuel models.

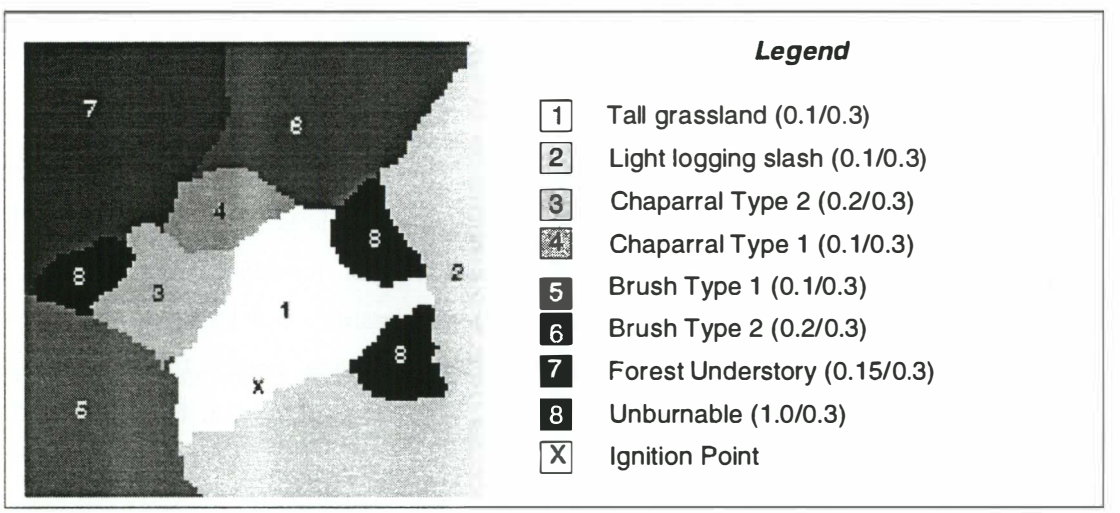

Figure 5.14 The artificial fuelscape used to test the performance of the fire spread model in spatially non-uniform fuels. The numbers in parentheses denote FMC and the moisture content of extinction.

The differences between the fire shapes in homogeneous conditions and in the presence of a variable fuel bed are significant; not only is the elliptical shape greatly modified (Figure 5.15) but the number of cells burnt is altered (Figure 5.13). At low wind speeds (0-1 km.hr^{-1}), the fire is largely restricted to the tall grassland patch and so the shapes produced by PYROCART are similar to those produced at the same wind speed in homogeneous conditions (Section 5.4; Figure 5.8). However, at higher wind speeds both the final shape and the number of cells burnt differ from the simulations performed in the homogeneous environment (Figure 5.16; Table 5.3). The greatest disparity between the shapes produced in homogeneous conditions and those produced in the spatially varying fuel bed above occurs at higher wind speeds (10-30 km.hr^{-1}). Fire has

spread preferentially into some fuel types. The highly flammable chaparral (Figure 5.14) has burnt rapidly and the rapid movement of fire into this fuel can be seen in the 5 km.hr^{-1} simulation as can the spread of the head fire into the brush type 2 fuel bed.

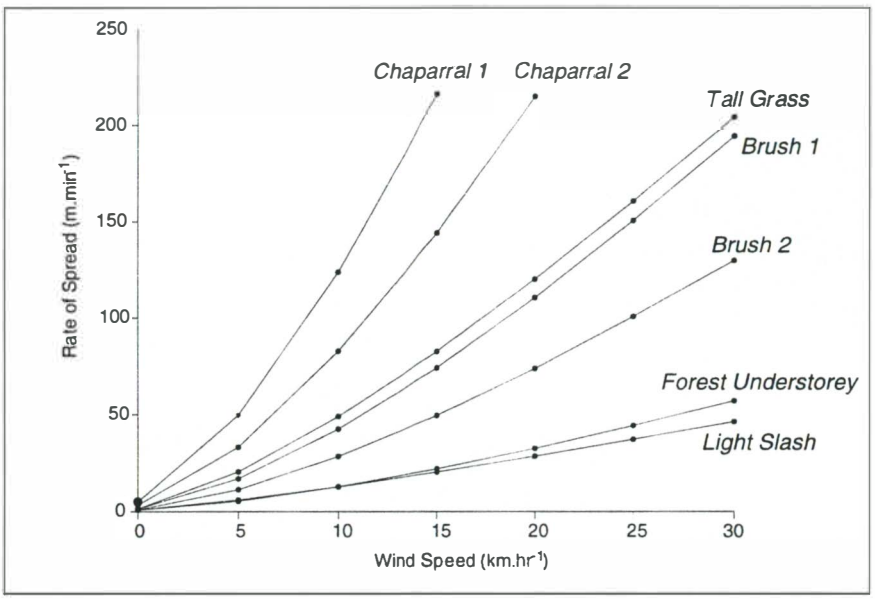

Figure 5.15 Rate of spread plotted against wind speed for the fuel models of Rothermel (1972) used in Sections 5.5.2 and 5.5.4.

At no wind speed has the fire has been able to spread effectively into the area of litter and understorey as either a flanking or heading fire. This fuel type is of low flammability (Figure 5.15) compared to the other fuel models. Most of the tall grassland area has burnt except for the far right of the patch. For two reasons fire has largely failed to propagate into the area of light logging slash; firstly, the light logging slash fuel model is of low flammability (Figure 5.15) and secondly, fire is spreading into this fuel bed as flanking (135°) and backing (180 °) fires, and thus the rates of fire spread are very low.

The Sørensen coefficients presented in Table 5.3 show that there is a relatively high degree of similarity between the fire shapes produced in homogeneous conditions and those produced in conditions where the fuel bed is spatially non-uniform. The high Sørensen coefficient value (0.99) for zero wind speed reflects the fact that fire is limited to the tall grassland patch in the spatially non-uniform scenario. This similarity is also reflected in the values of *b* and *c* at this wind speed. At wind speeds of 5 and 10 km.hr^{-1} the value of *c* is relatively much higher than *b*. This is due to the rapid propagation of fire through flammable fuel beds. The decrease in *c* at higher wind speeds (20-30 km.hr^{-1}) is a result of less flammable fuel beds (e.g. litter and understorey) inhibiting fire spread).

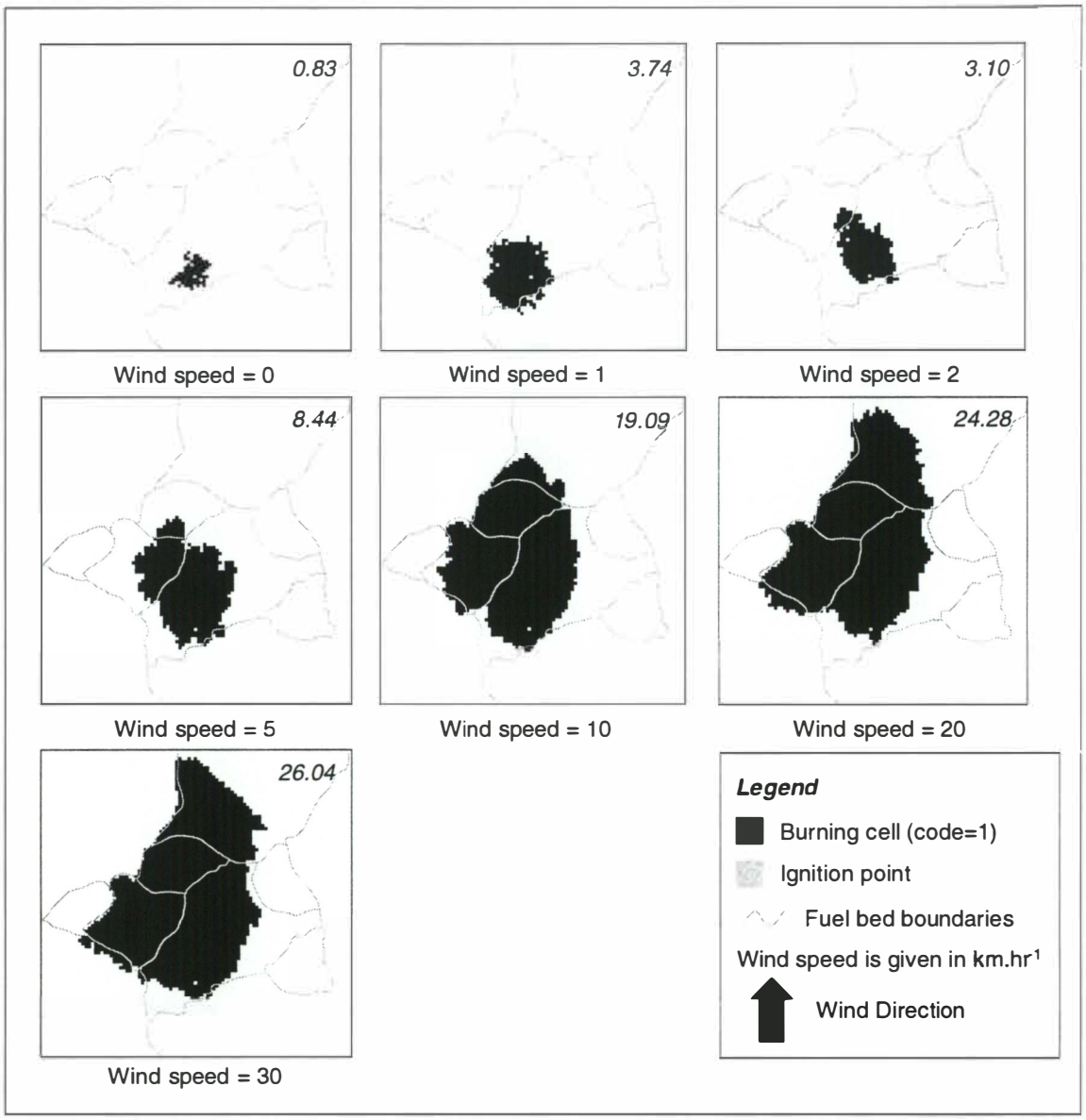

Figure 5.16 The fire shapes produced by the model in a spatially heterogeneous fuel bed with flat terrain and a constant wind direction. The numbers in the top right of each simulation denote the % of the array burnt.

In conclusion, the introduction of a spatially varying fuel bed has a profound effect on the eventual shape of the fire perimeter and thus, the eventual burnt area. This is a direct result of a spatially heterogeneous rate of spread, and the inability of flanking and backing fires to spread into some fuel types. In short, the eventual shape and extent of the fire reflects the properties of the fuel complex.

Table 5.3 Sørensen similarity index coefficient values for fire shapes produced in homogeneous compared with fire shapes produced in a spatially non-uniform fuel bed.

Wind Speed (km.hr^{-1})	*a*	*b*	*c*	*Sorensen Coefficient*
0	83	1	0	0.99
1	329	64	39	0.86
2	261	21	48	0.88
5	599	61	237	0.8
10	1319	57	565	0.81
20	1926	325	476	0.83
30	2116	307	461	0.85

a - Number of cells burnt in both landscapes.
b - Number of cells burnt in homogeneous landscape only.
c - Number of cells burnt in heterogeneous landscapes only.

5.5.3 Fire Spread in an Heterogeneous Wind Field

The effects of wind shifts in a simple homogeneous environment (the same as that used in Section 5.4) are studied in this section. The wind field is the same as that illustrated in Figure 5.6. (i.e. a shift of 45° to the west (180° shifting to 225°); this occurred 66% of the way through the simulation (i.e. after 50 of the 75 iterations). The fire shapes produced in these conditions are presented in Figure 5.17. The effects of a shift in fire shape are clearly visible when Figures 5.8 and 5.17 are compared.

Theoretically the result of a wind shift during the fire should be the modified elliptical shape predicted by Anderson (1983) and Ball and Guertin (1992; Figure 5.6). However, this shape is not entirely what happens as shown in Figure 5.18. This is because the modified elliptical model does not allow for what were previously flanking cells to become heading cells; as a result the double-ellipse is less clearly defined than in Figure 5.6. However, Figure 5.18 which shows the shape predicted by PYROCART where the prevailing wind changes direction and compares this with the modified elliptical model of Anderson (1983) and Ball and Guertin (1992), and shows that the shape predicted is significantly different from that presented in Figure 5.6. This is because flanking and backing fires are not extinguished and so previously flanking firefronts become head fire fronts and *vice versa*. However, that the shift in wind has a significant effect is confirmed when the cells coded to burn in future iterations are examined (i.e. code=2 or code=3); these are located primarily on the eastern (right) perimeter of the fire indicating that it is spreading preferentially with the 'new' wind direction (225°). At high wind speeds divergence between the shapes predicted by PYROCART and the model(s) of Anderson (1983) and Ball and Guertin (1992) is

greatest because of the over-estimation of flanking and backing rates of spread. Figure 5.13 shows that there is very little difference between the percentage of the array burnt where there is a wind shift as compared to the totally homogeneous scenario.

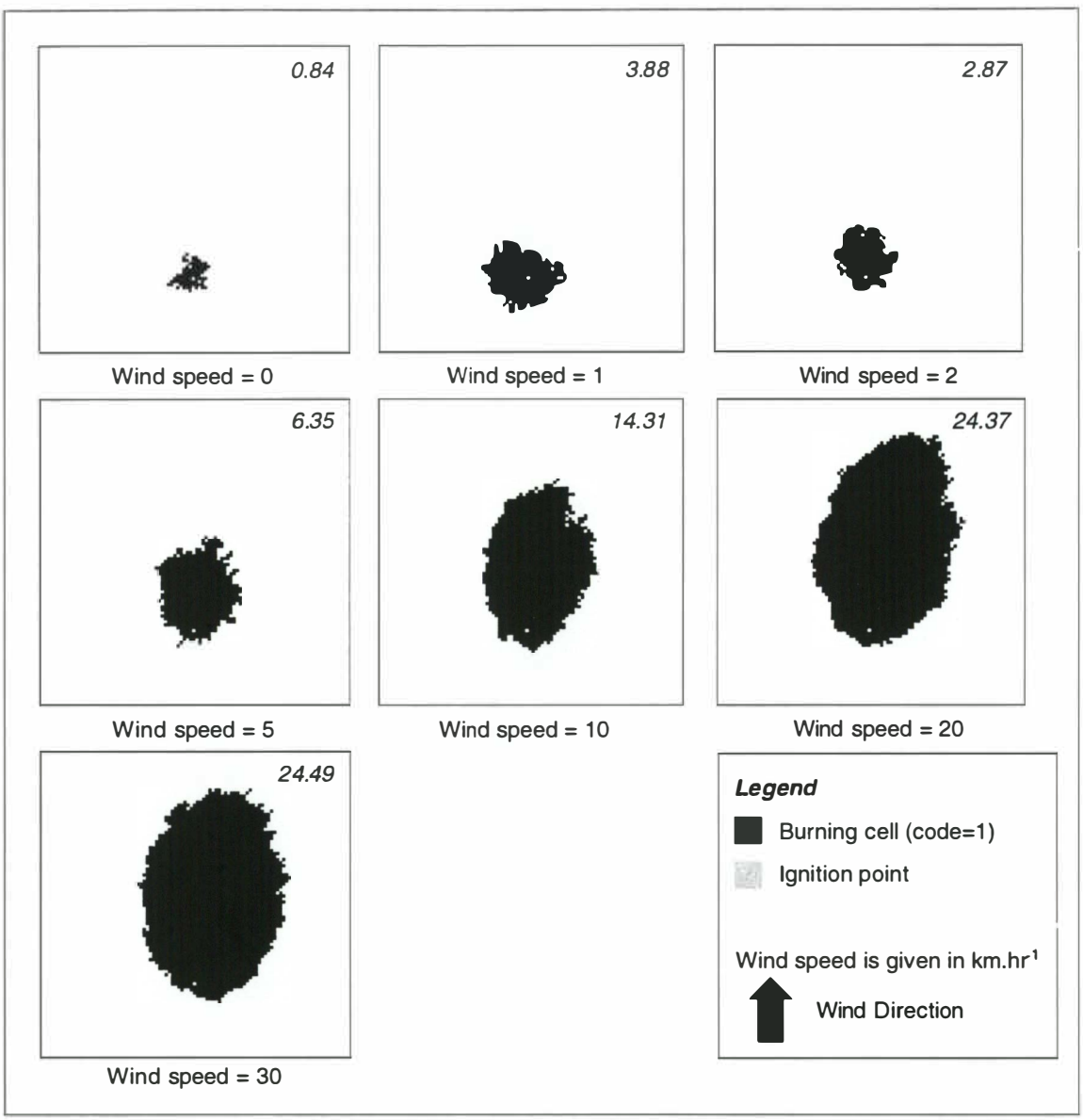

Figure 5.17 The fire shapes predicted by PYROCART after 75 iterations in an homogeneous environment with a 45° wind shift to the west after 66% of the simulation time. The numbers in the top right of each simulation denote the % of the array burnt.

The Sørensen coefficient values presented in Table 5.4 reflect the disparities between the fire shapes produced in the homogeneous scenario (Figure 5.8) and those illustrated in Figure 5.17. In the absence of any wind the shapes are identical. However, as wind speed increases the differences between the shapes tends to increase. At wind speeds of 5 and 10 km.hr^{-1} a larger proportion of the landscape has been burnt in the wind-shift scenario. This is a result of flanking cells becoming heading cells. At higher wind speeds (20-30 km.hr^{-1}) the values of *b* and *c* are similar indicating that the fire is clearly

spreading with the new wind direction. However, the shift in wind direction results in the fire spreading at a slightly increased areal rate compared to the homogeneous wind scenario.

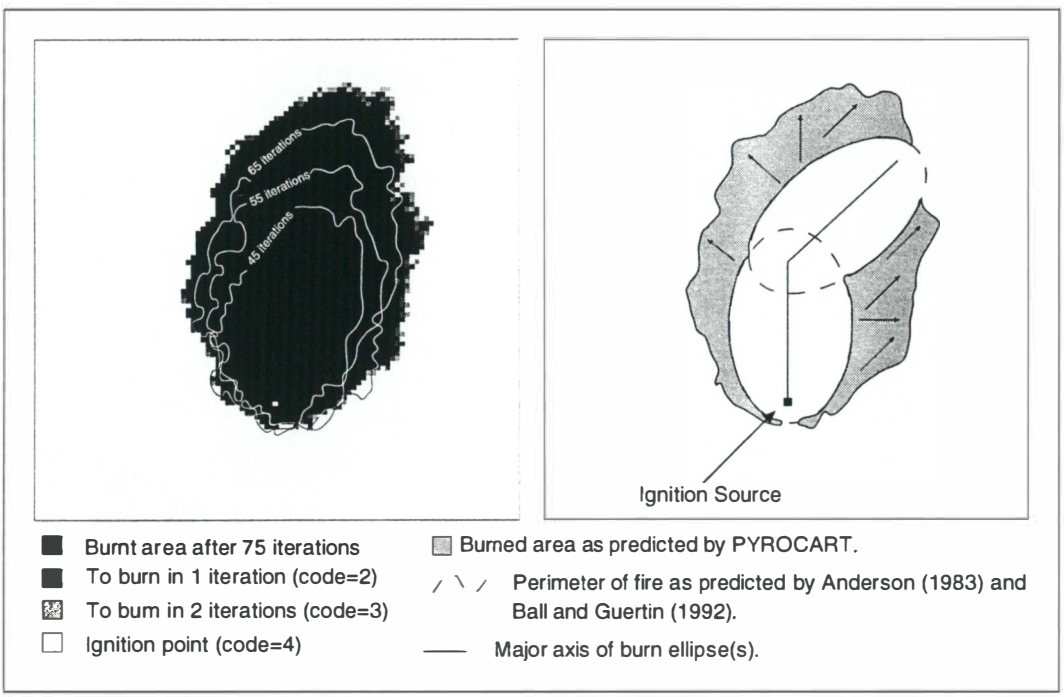

Figure 5.18 A comparison of the shapes produced by PYROCART with those predicted by Anderson (1982) and Ball and Guertin (1992) in an environment with a wind shift of 45° to the west. The fire shape is that produced by PYROCART after 45, 55, 65 and 75 iterations with a wind speed of 20 km.hr^{-1}. Arrows illustrate where flanking spread has produced a deviation from the shape predicted by Anderson (1983) and Ball and Guertin (1992).

Table 5.4 Sørensen similarity index coefficient values for fire shapes produced in homogeneous conditions compared with fire shapes produced where the wind is temporally non-uniform.

Wind Speed (km.hr^{-1})	*a*	*b*	*c*	*Sorensen Coefficient*
0	84	0	0	1
1	308	84	73	0.8
2	236	45	47	0.84
5	551	101	77	0.86
10	1200	177	231	0.86
20	1850	413	548	0.79
30	1944	461	474	0.81

a - Number of cells burnt in both landscapes.
b - Number of cells burnt in homogeneous landscape only.
c - Number of cells burnt in heterogeneous landscapes only.

In conclusion, although there are problems with the shapes produced by the PYROCART model in conditions where wind is temporally variable these can be

partially explained by the nature of the flanking and backing routines used in the model as illustrated in Figure 5.18. The differences between the shapes produced by the PYROCART model and the shapes predicted by Anderson (1983) and Ball and Guertin (1992) are most obvious at the highest wind speeds (20-30 $km.hr^{-1}$). These differences are attributable to previously flanking fires becoming head fires, and the over-prediction of flanking and backing rates of spread at these wind speeds.

5.5.4 Fire Spread in Spatially Non-uniform Fuels, Terrain and Wind

Spatial heterogeneity in both the fuel bed and the terrain in which it is located provides a challenge for accurate fire spread simulation. The end result of such heterogeneity is a greatly modified elliptical fire shape. The fire shapes illustrated in Figure 5.19 were produced in conditions of spatially non-uniform terrain (Figure 5.11) and fuels (Figure 5.14) and temporally non-uniform wind direction (a wind shift 45° to the west after 66% of the simulation). The effect of a temporally variable wind field is likely to be more significant where other environmental factors are spatially variable (e.g. terrain, fuel load, FMC). In such circumstances a variable wind direction may force the fire into patches of fuel that may not have been burnt if fire were to spread into them as either a flanking or backing fire. However, in an otherwise homogeneous landscape (where all cells predict the same fronting/flanking/backing spread rate) the effect of a wind shift is likely to be less significant (Figure 5.17).

At low wind speeds (0-5 $km.hr^{-1}$), where the fire is largely restricted to the grassland area, slope appears to be the dominant influence on fire spread and shape. However, the effect of slope is reduced compared to the situation where terrain is variable but fuel is homogeneous by the presence of a less flammable fuel (light logging slash) upslope of the ignition point which acts to retard fire spread. However, at higher wind speeds where the fire is able to spread into neighbouring fuel patches wind direction and fuel type combine to influence the fire shape and the influences of slope become relatively unimportant. The change in wind direction has an important influence in that the fire is driven into the more flammable brush type 2 fuel bed and away from the less flammable litter and understorey fuel beds. An increased proportion of the tall grass area is burnt and one of the unburnable patches of fuel is clearly visible where the wind speed is in excess of 20 $km.hr^{-1}$. However, despite the change in wind direction fire spreads rapidly into the highly flammable chaparral fuel bed(s).

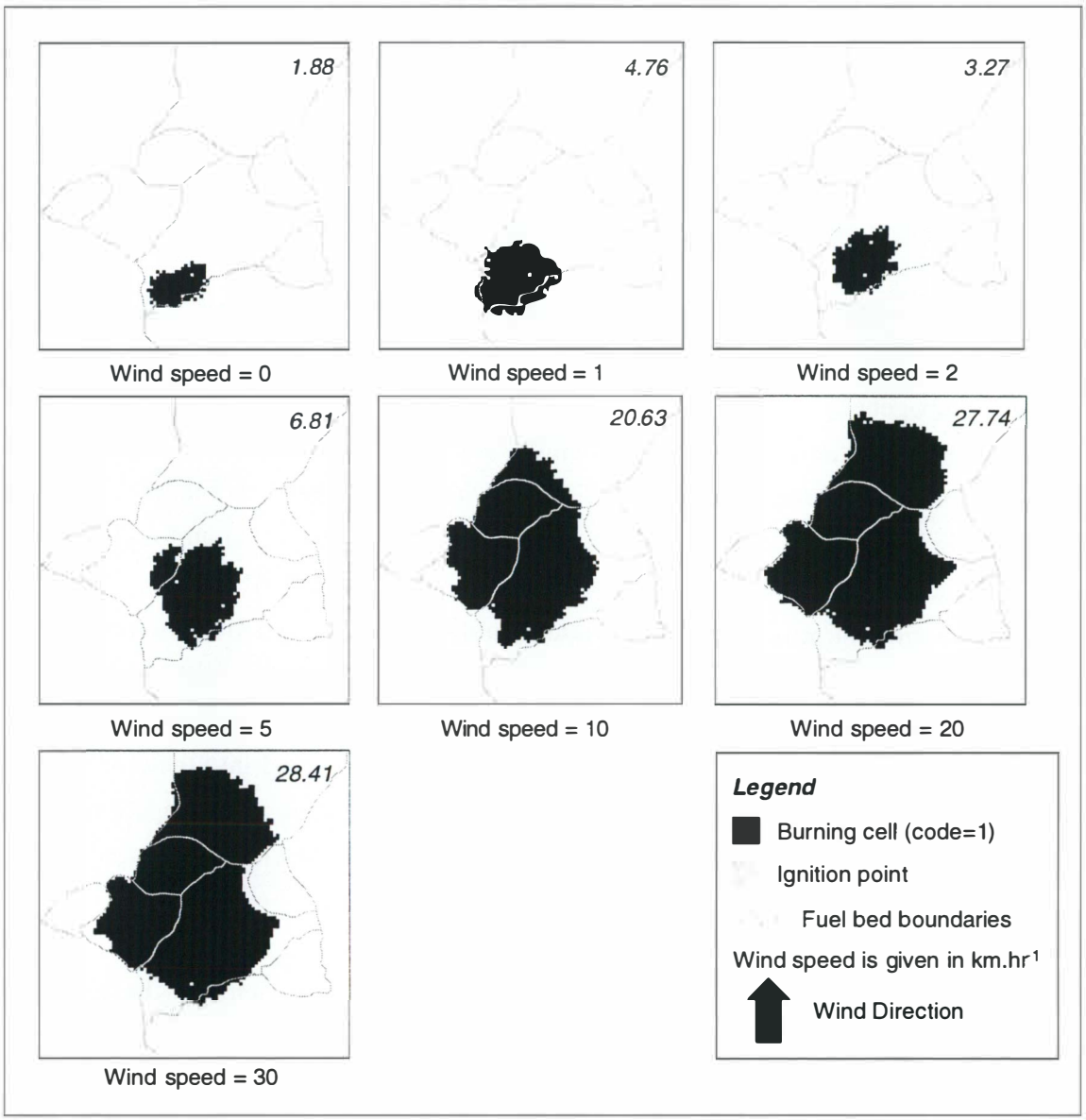

Figure 5.19 The fire shapes produced by PYROCART in an environment with a spatially non-uniform fuel bed and terrain and temporally non-uniform wind direction. The numbers in the top right of each simulation denote the % of the array burnt.

The Sørensen coefficient values presented in Table 5.5 compare the fire shapes presented in Figure 5.19 with those produced in the other four scenarios. These data illustrate the comparative importance of each component effect by showing the relative size of differences in burnt areas. Thus, a high Sørensen coefficient value represents a high importance for that environmental factor at a given wind speed. At zero wind speeds all of the factors have a significant influence on fire shape. Comparison between the heterogeneous terrain scenario and the conditions considered in this section yield a Sørensen coefficient value of 0.67 indicating that the fuel bed is of considerable significance. The significance of slope at zero wind speeds is also visible when Figures 5.12 and 5.19 are compared. The relative importance of variable slope remains high

until wind speeds are in excess of 5 $km.hr^{-1}$. However, at these low-moderate wind speeds the other environmental factors are also significant as is reflected by their Sørensen coefficient values. At wind speeds above 5 $km.hr^{-1}$ spatial heterogeneity in the fuel bed becomes the dominant influence on fire shape; this is reflected in the high Sørensen coefficient values for the variable fuel Sørensen coefficient values. The Sørensen coefficient values for the are also high suggesting that the other environmental factors also remain of high importance. However, at these high wind speeds it is difficult to comment on the relative importance of the various environmental factors as the effects of wind speed overcome the influences of environmental heterogeneity in factors such as slope. Comparison of Figure 5.16 and 5.19 indicates that the apparently high significance of variations in the fuel bed may be justified as the fire burns into patches of varying flammabilities.

Table 5.5 Sørensen similarity index coefficient values for spatially non-uniform fuels and terrain and temporally non-uniform wind fire shapes against the four other scenarios.

Wind Speed ($km.hr^{-1}$)	*Homog*	*Slope*	*Fuels*	*Wind*
0	0.45	0.67	0.44	0.45
1	0.81	0.79	0.80	0.81
2	0.72	0.87	0.66	0.79
5	0.85	0.84	0.78	0.89
10	0.79	0.82	0.91	0.77
20	0.80	0.81	0.91	0.84
30	0.82	0.83	0.91	0.84

Homog - Homogeneous conditions (Section 5.4)
Slope - Heterogeneous terrain (Section 5.5.1)
Fuels - Heterogeneous fuel bed (Section 5.5.2)
Wind - Shift in wind direction (Section 5.5.3)

5.7 Conclusions

This chapter has considered the performance of the PYROCART fire model in a range of environmental conditions from simple homogeneity to complex environments, where fuels and terrain are spatially variable and wind direction is temporally non-uniform. The nature of the integration between the GIS and the environmental model was described and it fits into the category of loose coupling. The model produced theoretically acceptable fire shapes in all environments. However, the shapes produced in an environment with wind shifts were somewhat different from those predicted by Anderson (1983) and Ball and Guertin (1992). These differences were more prominent at high wind speeds and reflect both over-prediction of flanking and backing rates of spread, and the manner in which after the change in wind direction the flanking

firefront becomes the heading front and *vice versa*. Analysis of the similarity between shapes produced in homogeneous and heterogeneous conditions was performed using Sørensen's similarity coefficient. It was evident that at low wind speeds environmental factors such as slope and fuels controlled the fire shape. However, as wind speed increased, wind speed and direction became the variables which controlled fire behaviour and thus fire shape, although fuels still exert an important influence (e.g. unburnable patches).

Chapter Six

Model Validation

6.1 Introduction

This chapter is concerned with the validation of the PYROCART simulation model using the Cass fire of May 1995 and is divided into three broad sections. Firstly, the study site is described; secondly, the methodology required to estimate Rothermel model parameters for the PYROCART system such that the Cass fire could be simulated *a posteriori* is reviewed; thirdly, the results of the validation are presented and discussed, as are the problems involved with the use of the model.

6.2 The Cass District

The Cass River basin lies at the northern end of the Craigieburn Range in the middle part of the Waimakiriri watershed, in western Canterbury, central South Island. The University of Canterbury's Cass field station, which was the base for field research, is situated at a latitude of 43°02' S and a longitude of 171°45' E within the Cass River basin. The field station is equidistant from the east and west coasts of the South Island being 105 kilometres from both Christchurch and Greymouth. The Cass field station lies at an altitude of 590 metres above sea level and the surrounding terrain rises to between 1200 and 1800 m.

The fire which is the focus of this thesis occurred on the west bank of the Cass River primarily on Waterfall Terrace, the lower flanks of Mounts Misery and Horrible, Horrible Bog and Misery Swamp (Figure 6.1; Plate 6.1 in back envelope).

6.2.1 The Geomorphology of the Cass Basin

The geomorphic history of the Cass region is complex, with the area having been affected by repeated glacial activity and, since the last glaciation, by intense erosional and fluvial action. Early glacially eroded topography is rare and Soons (1977) notes that there is little evidence of the presence of early to mid-period Pleistocene landforms in the area; the only remaining forms resulting from direct ice action are found on rock surfaces that have been more recently overrun by ice (e.g. Mounts Horrible and Misery

and Romulus and Remus). The most significant contemporary erosional processes are fluvial action and rock shatter by freeze-thaw cycling (Soons, 1977).

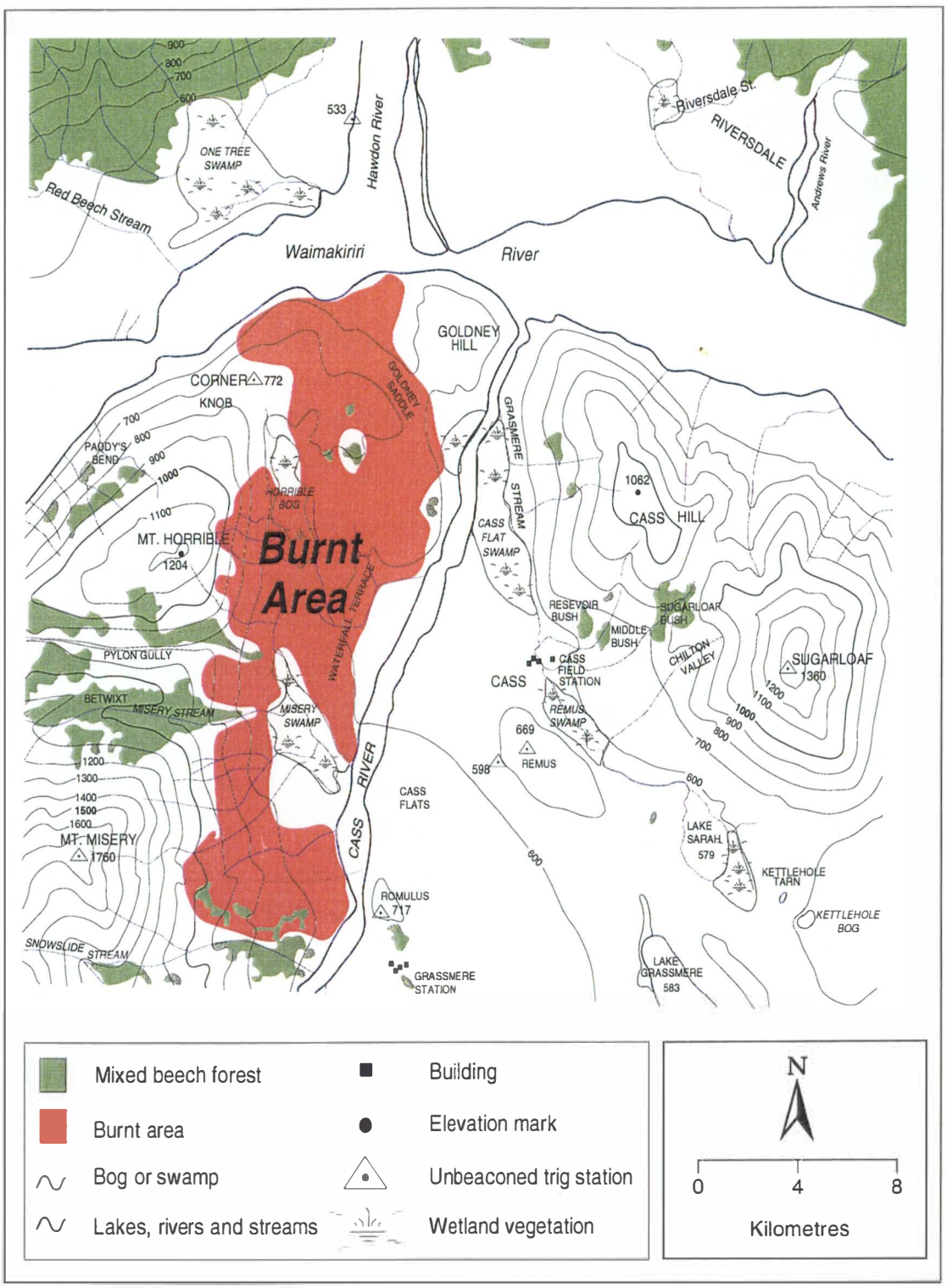

Figure 6.1 A map of the Cass region showing the location of the study site and the extent of the May 1995 fire (west bank of the Cass River).

The geomorphology of the west bank of the Cass River reflects the many dynamic processes which have altered the landscape. During the Blackwater Advance a large

tongue of ice split off from the main Waimakiriri Glacier through the saddle of Pylon Gully into the Cass Basin (Gage, 1977). Shanks *et al.* (1990) note that it seems likely that ice flowed over Mount Horrible, as is evidenced by the striated bedrock at the summit and associated roche moutonée features. Post-glacial erosion has deposited steep, coarse cone screes beneath shattered greywacke and argillite bluffs on the slopes of Mount Horrible, Mount Misery and the sideslopes of Pylon Gully (McArthur, 1964, 1975).

Misery Stream and the unnamed stream that runs from Pylon Gully drain into Misery Swamp from incised gullies cut into the glacially-smoothed slopes. The swamp was formed when the streams which now feed the swamp were dammed by fan formation to the south (Howard, 1985). It is bounded to the east by Waterfall Terrace, which is a bedrock roche moutonée extension of Romulus (Shanks *et al.*, 1990). Horrible Bog, to the north of Waterfall Terrace, is a large swamp complex occupying a depression in the extensive morainic deposits which cover the region. The swamp formed in the gully floor as a result of drainage of the existing underfit stream through Pylon Gully being impaired by fan deposition from Mount Horrible (Shanks *et al.*, 1990).

The dynamic nature and the extreme topographic variation within this environment has important implications for fire behaviour. Not only does the spatial variability of the terrain directly influence fire behaviour but such spatial variability also influences the vegetation mosaic through the creation of micro-climates, and the wind field through the processes of topographic forcing.

6.2.2 The Vegetation of the Cass Basin

The vegetation of the west bank of the Cass River, and indeed the Cass locality as a whole, has been highly modified since human colonisation of the area. As a result many of the communities seen in the area have been 'induced' by anthropic influences such as repeated burning and grazing. Burrows (1960) notes that this modification of the plant communities has mainly consisted of a considerable reduction in the *Nothofagus solandri* var *cliffortioides* (mountain beech) forest and alpine tussockland above the treeline, and of an increase in bare shingle, short tussockland and scrub communities. These profound modifications are thought by Burrows (1960) to have largely occurred before the European settlement of the area, possibly around 300 years ago and probably as a result of a series of catastrophic fire events. The following section describes the vegetation as it is now, noting where so-called 'induced' communities are evident. The description of the vegetation found on the west bank of the Cass River is based largely on that of Shanks *et al.* (1990).

Waterfall Terrace is characterised by a very variable, disturbance-induced montane shrubland with a high diversity of species. In essence the shrubland is a mosaic of *Cassinia leptophylla* (tauhinu), *Leptospermum scoparium* (manuka), *Corokia cotoneaster* (korokio), *Dracophyllum longifolium* (turpentine plant), *Hebe brachisyphon* and *Hebe odorata* and two *Coprosma* species, *C. propinqua* and *C.* aff. *parviflora* (aff 'T'). There are also scattered pockets of *N. solandri* var *cliffortioides*, *Podocarpus nivalis* (snow totara) and *Festuca novae-zelandiae* (tussock), as well as a wide variety of other less common small shrubs, herbs and grasses. A feature of the glacial gravel deposits which cover the area are the numerous depressions with exposed subsoils; these depositions favour frost heave and thereby prevent the establishment of vegetation. At the southern end of Waterfall Terrace there is a large area dominated by a community comprising *Discaria toumatou* (matagouri), *C. leptophylla* and *F. novae-zelandiae*.

There is extensive *L. scoparium* scrub on Corner Knob and similar assemblages are found at the base of Pylon Gully and the flanks of Mounts Horrible and Misery. The original *N. solandri* var *cliffortioides* forest on these areas was burnt in the nineteenth century (considerably later than much of the rest of the area) and has been replaced by tussockland which has subsequently been invaded by mixed scrub communities (Burrows, 1960; Molloy, 1977). Shanks *et al.* (1990) consider that in the absence of further fire events *N. solandri* var *cliffortioides* will continue to invade and reclaim these 'induced' shrublands.

The streams running through Misery Swamp are characterised by adventive-dominated communities with small areas of the native *Carex secta* (pukio) present. At the southern end a dense area of adventive grass grows between isolated *Schoenus pauciflorus* tussocks; Shanks *et al.* (1990) note that all that is left of the red tussockland that once covered the area are a few scattered red tussock and *Olearia virgata* var. *rugosa.* A tall, dense *D. toumatou*-dominated community grows on the toe of a large debris fan which runs from the mid-slopes of Mount Misery into Misery Swamp.

Horrible Bog is considerably less modified than Misery Swamp. *Carex flaviformis* grows in the dampest areas with *S. pauciflorus*, *Rytidosperma gracile*, *Carex sinclairii* and, elsewhere, a few scattered *L. scoparium*, *H. odorata* and *C. leptophylla.*

6.2.3 The Fire History of the Cass Region

Fire has been an important disturbance agent in the Cass region since at least the last glaciation (Molloy, 1977). This section briefly considers the fire history of the Cass

district with regard to three broad time periods; (i) the pre-human fire history (up to c1000 AD); (ii) the Polynesian fire history (c1000 AD to c1850 AD); and (iii) the European fire history (c1850 AD until the present day). The way in which changes in the fire regime have affected the vegetation seen in the landscape is also considered.

There is evidence of periodic fire events in the Cass Basin long before human settlement of New Zealand. These fires are likely to have been the result of lightning strikes as the area has no history of Late Quaternary volcanism (Molloy, 1977). Cox and Mead (1963) and Grant-Taylor and Rafter (1971) found evidence of periodic fires in the Canterbury dating back 6500 BP; charcoals are also known to occur in Late Pleistocene deposits but these have not been successfully dated.

An early radio-carbon-dated charcoal deposit from the Cass region was reported by Grant-Taylor and Rafter (1971) and Molloy and Cox (1973) from the summit of Sugarloaf (4610 years BP); the charcoal was primarily composed of deposits of *Phyllocladus alpinus* (mountain toatoa). In the mid-1970s several buried soils complete with charcoals were found on Mount Misery, opposite Romulus (Molloy, 1977). The sequence provides evidence of at least four major fire events ranging from glacial times to the first recorded European fire (1857). The surface soil and two buried soils contain evidence of *N. solandri* var *cliffortioides* charcoal, whereas the lowest buried soil contains charcoal derived solely from *P. alpinus*. The Sugarloaf charcoal is consistent with contemporary treeline vegetation in the Cass region. However, Molloy (1977) considers it more likely that it represents a higher abundance of *P. alpinus* at the time of the fire rather than the current snow-tussock grassland. Molloy (1977) interprets the Mount Misery sequence as indicative that *Phyllocladus* shrubland dominated the landscape until approximately 7000 years BP after which time its abundance was decreased by natural fire; such clearance may have enabled the subsequent expansion of *N. solandri* var *cliffortioides*. The presence and age of these charcoal deposits indicates that although fire was an infrequent occurrence in pre-settlement times, it was an important disturbance agent in the Cass district. Furthermore, they provide important evidence as to the character and composition of the vegetation of the area prior to human settlement.

Charcoals from the Craigieburn Ranges and Porters Pass are indicative of widespread fire between 500 and 100 years ago (Cumberland, 1962; Molloy *et al.*, 1963). Molloy (1977) considers it likely that these fires were lit by early Polynesian hunters to facilitate hunting and land clearance. Charcoal derived from Polynesian burning is widespread under forest vegetation throughout the Cass locality. Although several areas were seemingly unfavourable to fire, they still suffered significant perturbation (e.g.

parts of Mounts Horrible and Misery in the Cass Valley). Most of the charcoal samples collected from the Cass area have been found in forested areas. Further samples have been located under scrub and grassland both above and below the timber line (c. 1370 m ASL); areas where charcoal is notably absent include the Cass fan, the fan of the Craigie Burn and in the tussock-covered alluvial flats of the Waimakiriri River (Molloy, 1977).

The Polynesian burning of the Cass Basin and surrounding regions has fundamentally changed the face of the Cass landscape and the vegetation assemblages seen on it. Burrows (1960) regards the most significant change to be the replacement of forested land and snow-tussock grassland by scrub, fescue-tussock and bare scree slopes. Other features of the Cass landscape which reflect Polynesian burning include the lowering of the tree line, widespread hybridization in the flora and accelerated erosion rates (Molloy, 1977).

The first recorded European fire in the Cass area occurred in 1857 and from then the frequency of burn events increased to the 1960s, from which point it decreased. This European burning has not had the same influence on the landscape as the Polynesian fires, with the notable exceptions of the lower Cass Valley on the northern flanks of the Craigieburn, Black and Academia Ranges (Molloy, 1977). Those areas which have remained unburnt since the late 19th century and that have not been subjected to heavy grazing pressure have slowly reverted through mixed scrubland communities back to *N. solandri* var *cliffortioides* forest (Burrows, 1960).

Traditionally, high levels of erosion in the eastern South Island high country have been attributed to the farming practices, especially burning and grazing, employed by early European pastoralists (Whitehouse, 1984). However, recent research has shown that this view may not be entirely accurate (Whitehouse, 1984; McSaveney and Whitehouse, 1989). McSaveney and Whitehouse (1989) note that although erosion has increased following deforestation and grassland depletion as a result of fire and grazing, a significant proportion of the established anthropic erosion occurred in the first 500 years of Polynesian occupation, prior to European settlement. Furthermore, early surveys of soil erosion in the South Island equated bare ground and sparse vegetation cover with soil erosion, and soil erosion with anthropic erosion (e.g. Cumberland, 1944, 1945). As a consequence, they found much anthropic erosion over large areas of the eastern South Island high country. Within these same areas it is now recognised that there are areas where sparse vegetation cover is neither anthropic, nor related to high levels of soil erosion, and areas where soil erosion is not anthropic (McSaveney and Whitehouse, 1989). Thus, although the burning practices of European pastoralists in the

area may have induced some erosion through deforestation and grassland depletion, the view that all soil erosion in the eastern South Island high country is due to such practices is erroneous, as is the view that all soil erosion in this area is anthropic.

Little evidence is available from which to assess the effects of European fires on alpine communities. Some areas above the tree line in the Craigieburn Ranges have certainly been subjected to fire. Such areas are characterised by degraded alpine grasslands dominated by species whose abundance increases after fire (e.g. *Celmisia lyallii, C. spectabilis* and *Poa colensoi*).

6.3 A Pyrogeography of the May 1995 Cass Fire

On the 27-28 May 1995 a large fire burnt 580 hectares of vegetation on the west bank of the Cass River (Figure 6.1; Plate 6.2). The fire occurred during a period of strong north-westerlies. Such wind conditions would have both dried the fuels and fanned the fire when it was in progress. The most severely burnt areas were stands of shrubs including *D. toumatou*, *L. scoparium*, *C. leptophylla* and two species of *Coprosma*, *C. propinqua* and *C.* aff. *parviflora* (aff 'T'). The fire appears to have been relatively fast moving; there is evidence in some shrubs of the canopy burning and burning fragments falling and subsequently igniting areas of ground cover. Where shrubs were more widely spaced the fire burnt the canopies and the ground layer immediately underneath them, but the grass between the shrubs was largely unburnt (Kelly, 1995). In areas of *F. novae-zelandiae*, the tussocks were often burnt to their base, while shorter exotic grasses such as *Agrostis capillaris* (browntop) remained unburnt.

Outliers of colonising *N. solandri* var *cliffortioides* were largely killed by trunk scorching (Plate 6.4). However, in larger patches the outer trees were burnt while those in the middle of the patch remained unharmed; evidently the fire failed to propagate as successfully in the beech stands as in the shrubland. As a result most of the larger stands have escaped serious damage (Plate 6.3). One stand of *N. solandri* var *cliffortioides* to the south of Corner Knob remained entirely unburnt as flames swept around both sides of it. In Horrible Bog fire damage was also relatively minor, with only small amounts of dry plant matter being burnt. A large grassy fan with a number of old *D. toumatou* shrubs on it also avoided major damage as the fire burnt higher on the flanks of Mount Misery.

Plate 6.2 View of the fire scar looking south from the top of Knobbly Hill. Baldy Peak and the Cass Range are visible in the background as are the flanks of Mount Misery. In the middleground Waterfall Terrace and the largely unburnt Misery Swamp are visible.

Plate 6.3 Tongues of unburnt *Nothofagus solandri* var *cliffortioides* extending from Pylon Gully and Betwixt. Mount Misery forms the backdrop.

Two sites of botanical interest may also have been affected by the fire; the first is a patch of *Nothofagus fusca* (red beech) which was colonising Corner Knob (Burrows and Lord, 1993) and the second is an area of the native fern *Botrychium australe*, described by Kelly (1994). It seems likely that some of the colonising *N. fusca* will have been killed. However, Kelly (1995) considers it unlikely that the *B. australe* population will have been severely damaged, due both to the presence of large underground storage organs.

Plate 6.4 Severely burnt *Nothofagus solandri* var *cliffortioides* on the south side of Corner Knob. The trees shown in this plate have all been killed by trunk scorching.

Thus, the areas most severely affected by the fire were the extensive shrubland mosaic that dominates Waterfall Terrace and the lower flanks of Mounts Horrible and Misery. In some places stands of mature *N. solandri* var *cliffortioides* have been severely

damaged, notably on the slopes below Pylon Gully, and on the southern slopes of Corner Knob. Kelly (1995) considers that the fire will have set back the successional process by approximately 100 years in these areas. The fire will, therefore, have a range of impacts on the vegetation mosaic it burnt through. A large area of regenerating shrubland and significant stands of *N. solandri* var *cliffortioides* and colonising *N. fusca* are likely to have been killed. However, ruderal species (such as *B. australe* and some shrub species) may benefit from reduced competition with woody plants.

6.4 Methodology

This section will describe: (i) slope and wind data collection; (ii) vegetation mapping and fuel cell modelling; and (iii) GIS data processing required prior to running the PYROCART model to recreate the Cass fire. The construction of the Fortran 77 routines which drive the simulation have already been considered in Chapter 5; thus, the methods considered in this section are primarily concerned with parameterisation of the Rothermel model.

6.4.1 Topography and Wind Data Collection

The topography of the fire-scar was evaluated using x,y,z data obtained through a combination GPS surveying of the area and stereo aerial photography. Eighteen control points were surveyed across the data site using the Trimble ProXL GPS system. These points were differentially corrected using data from the DOSLI base-station in Christchurch and post-processed using Trimble's PathFinder software. The accuracy of this surveyed data were well in excess of the spatial resolution of the fire spread model (50m). The horizontal accuracy of the control points is:

$$h = 1.0+3*10^{-6} d \qquad (6.1)$$

where : h = horizontal accuracy (m) and d = the base to rover distance (m).

Using equation 6.1, the horizontal accuracy of the control points was estimated to be approximately 1.12 metres. The vertical accuracy of the control points is 2 to 5 times worse than the horizontal. Thus, these surveyed data were well in excess of the spatial resolution of the fire spread model (50m).

These x,y,z data were then exported to the Virtuozo package (Virtuozo, 1996) at the University of Auckland. Virtuozo is a digital virtual photogrammetry system which creates a DTM and an ortho-photo from a stereo pair of aerial photographs by using digital stereoscopy algorithms. Thus, a DTM of the fire-scar was created using a stereo pair of air photos of the study area and from Virtuozo the DEM was exported to Arc/

Info where it was stored as a geo-referenced lattice.

The wind field of the fire-scar was analysed under north-west conditions similar to those under which the fire took place. Readings of wind speed and direction were taken over four five minute periods at 9 sites across the fire-scar using an anemometer and a wind vane; these sites were chosen to cover the range of landscape units on the fire-scar and are illustrated in Figure 6.2. Relationships between the wind vector at the various sites were derived and from these wind speed and direction surfaces interpolated and stored in Arc/Info. The quintic interpolation of Akima (1978) was used to ensure a reasonably smooth surface and because of the relative sparseness of data points.

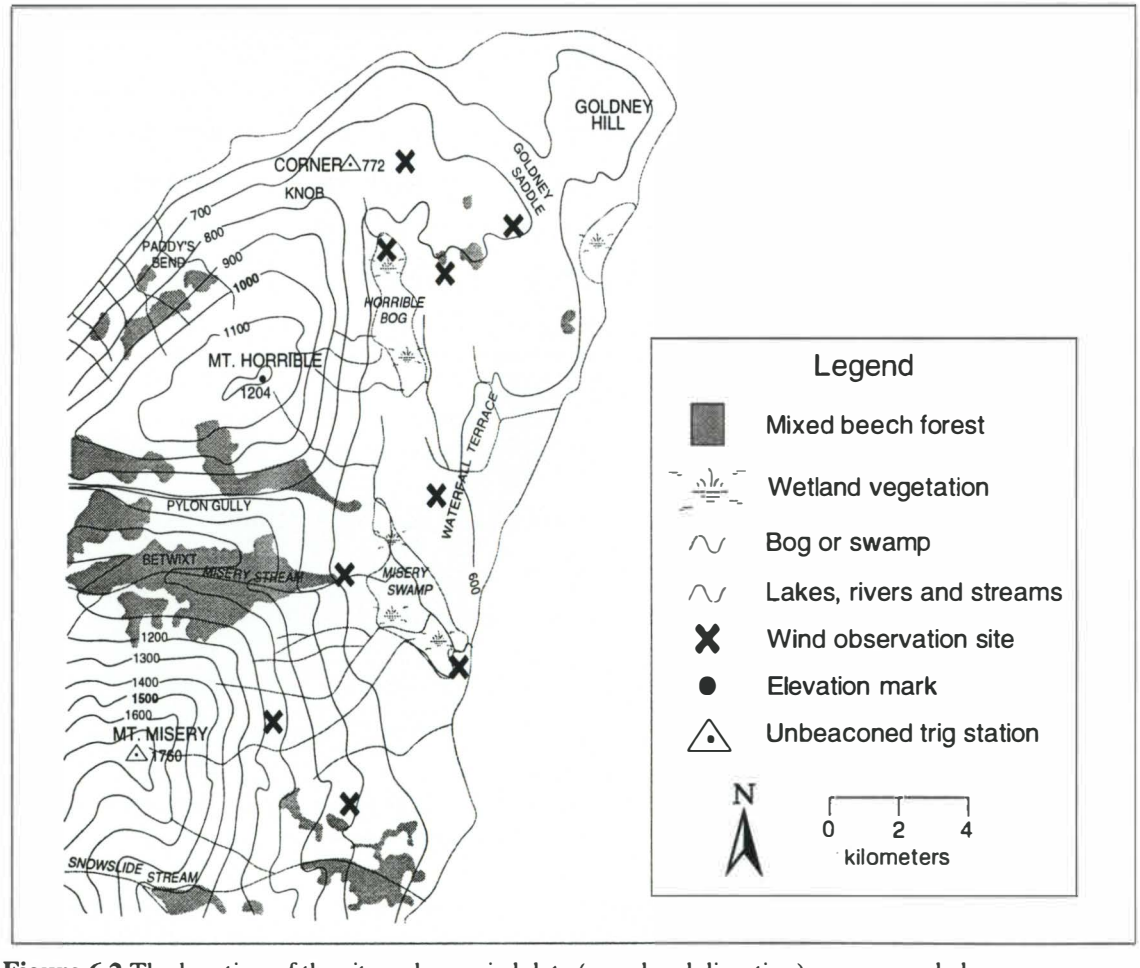

Figure 6.2 The location of the sites where wind data (speed and direction) were recorded.

Data layers representing the standard deviation in wind speed and direction across the field site were also created. These were used to simulate random variations in wind speed and direction across the firescar. At the point where wind speed/direction are calculated the model re-calculates the value to be ±1.5*the standard deviation multiplied by a random number between 0 and 1. The standard deviation is multiplied by 1.5 such that the calms and gusts in wind speed and the variations in wind direction fall within 90% confidence intervals of the real wind speed and direction.

6.4.2 Vegetation Analysis and Fuel Modelling

A detailed map of the vegetation cover of the fire-scar area was constructed, based on an aerial photograph of the burnt area blown up to Al size (approximately 1:8000 scale). Initially polygons were drawn onto the air photo, based on known vegetation boundaries and the grey-scale shading and texture on the photo. These polygons were then ground-truthed, corrected where necessary, and coded. Eleven vegetation types were recognised ranging from simple monospecific stands of *N. solandri* var *cliffortioides* to more complex shrubland mosaics containing a number of different species. The fuel types are briefly described in Table 6.1. Finally, the vegetation map was digitised and geo-referenced in Arc/Info using control points established through the use of a Global Positioning System (GPS).

Given the requirements of the Rothermel (1972) fire spread model, it was necessary to construct a number of stylised 'fuel models'. As the Rothermel model had not been previously trialled in New Zealand, it was necessary to construct fuel models for each vegetation type described in Table 6.1. A brief review of fuel modelling is provided before description of the methodology which was employed in order to orientate the reader.

A fuel model is a:

> "stylised quantitative description of a certain vegetation type and contains information on those components of the vegetation structure which are important for fire behaviour". (Brown, 1981, p. 667).

A number of such models exist for a wide range of North American vegetation types. A schematic representation of fuel model considerations and characteristics is presented in Figure 6.3.

Table 6.1 A brief description of the 11 vegetation classes recognised on the fire-scar.

Fuel Type	Description
(1) Mixed Shrub	This is a widespread and variable fuel class. It is comprised of a mixture of woody shrub species such as *C. leptophylla*, *D. toumatou*, *Coprosma* spp., *Dracophyllum* spp. and *L. scoparium*. Ground cover is provided by *F. novae-zelandiae* and exotic grasses.
(2) Wet Mixed Shrub	This fuel type is similar to (1) but is found in moister areas such as gullies and on south-facing slopes. It is denser than (1) and contains some additional species, especially *Hebe* spp. Ground cover is similar to (1) although *Schoenus* is sometimes present.
(3) Beech	Variously-aged monospecific stands of *N. solandri* var *cliffortioides*.
(4) Bog	*Schoenus*-dominated bog vegetation with few, if any, woody shrubs present. Standing water is common in this fuel type.
(5) Manuka Shrubland	*L. scoparium*-dominated shrubland. This fuel class dominates the flanks of Mounts Horrible and Misery. Other woody shrub species may be present in low densities. Ground cover is similar to (1). This fuel class has a significantly higher standing biomass than either (1) or (2).
(6) Matagouri Shrubland	*D. toumatou*-dominated shrubland. This fuel class is common on the lower flanks of Mount Misery and on the large alluvial fan fan running from Misery Stream to the Cass River. This fuel type is almost monospecific, apart from exotic grasses.
(7) Light mixed shrub	Similar species composition to (1) but with a significantly lower standing biomass.
(8) Grassland	This fuel class comprises exotic grasses, *F. novae-zelandiae*, and, in some places, *Schoenus*. The dominant species is spatially variable but the fuel type is characterised by the absence of woody shrub species.
(9) Wetland	This is a fuel class intermediate between (2) and (4). It is epitomised by low, sparse shrubs (especially *Hebe*) growing in thick stands of *Schoenus*. Good examples of this fuel class are found on Waterfall Terrace.
(10) Beech-mixed shrub	This is mixed shrubland with a significant component of *N. solandri* var *cliffortioides* in it. It is mainly found around the perimeter of beech stands where the beech appears to be (re-)colonising new areas.
(11) Bare ground	These are patches of bare ground. On such patches standing biomass is very low. *Gaultheria* is common, as are stunted shrubs of a number of species including *N. solandri* var *cliffortioides*.

When fuel models are constructed the dead vegetation is divided into various 'time lag' (TL) classes. Herbaceous and woody fuels are considered separately. Data are collected for each fuel class and type combination and is then aggregated using a complex weighting process which is outlined in Rothermel (1972), Burgan and Rothermel (1984) and Burgan (1987).

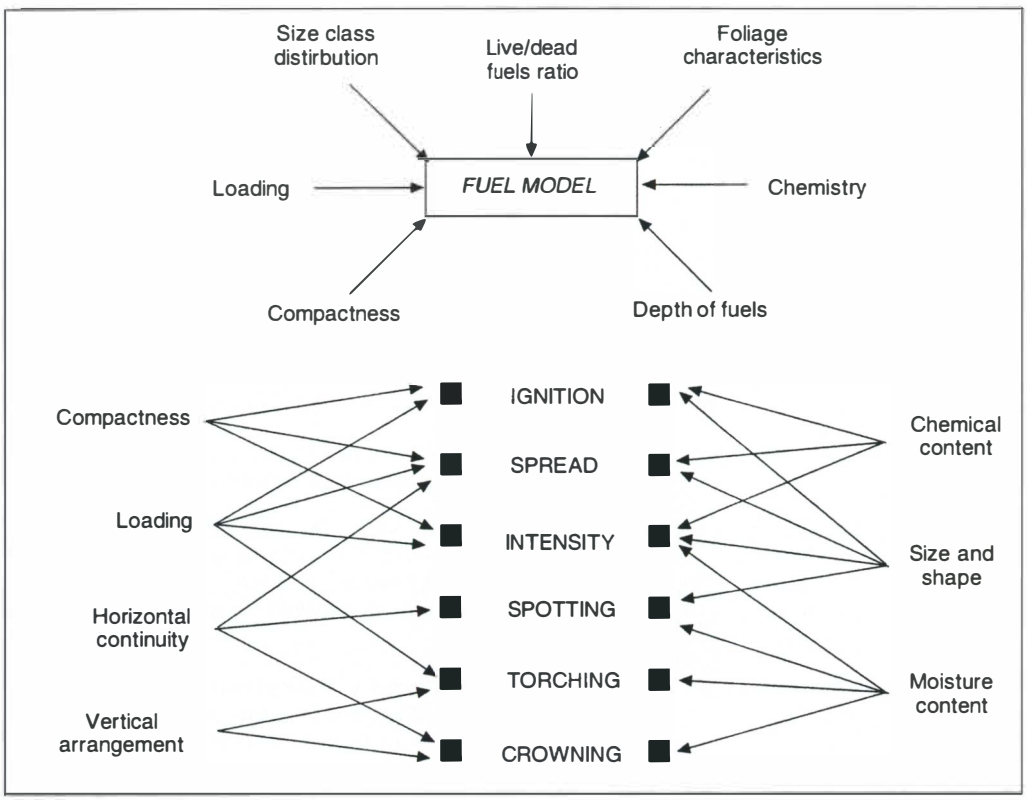

Figure 6.3 Fuel model considerations and characteristics (Pyne, 1984).

The TL divisions for the dead fuels are an attempt to simplify the variable rate(s) at which dead fuels dry. Based on their TL periods four categories of fuel particles and fuel beds are recognised (Table 6.2). Fuels are committed to one of these categories as a function of their diameter, in the case of particles, or their depth in the case of fuel beds. The concept of TL periods is based around that of equilibrium moisture content (EMC; Section 2.5.1). EMC is defined as the value that the actual moisture content would approach if the fuel particle were exposed to constant atmospheric conditions for an indefinite length of time. Each TL period describes the moisture exchange to the amount of 63% (1-1/EMC) of the departure from the EMC. The actual duration required to achieve EMC depends on the properties of the fuel, including its size and diffusivity (Pyne, 1984; Bond and Van Wilgen, 1996).

Table 6.2 Timelag fuel categories (Pyne, 1984).

Timelag (hr)	*Fuel Particle Diameter (mm/in.)*	*Fuel Bed Depth (mm/in)*
1	0-6 (0-0.25)	Fuelbed surfaces
10	6-25 (0.25-1)	Down to 15 (0.75)
100	25-76 (1-3)	16-102 (0.75-4)
1000	76-203 (3-8)	102-305 (4-12)

Of the nine fuel-related parameters required as input to the Rothermel model, three were assumed to be constants, as suggested by Burgan and Rothermel (1984), either because they have a very small effect in their naturally occurring range or are difficult to assess accurately. These parameters and their assumed values are shown in Table 6.3. Burgan and Rothermel (1984) also assume the surface-area to volume ratio of 10-hr TL and 100-hr TL fuels are constants. However for the purposes of this study, they *were* assessed.

Table 6.3 Constant fuel parameters and their assumed values (Burgan and Rothermel, 1984).

Fuel Parameter	*Assumed Value*
Particle density (ρ_p)	512 kg.m^{-3}
Total mineral content (s_t)	0.0555 (fractional)
Effective mineral content (s_e)	0.01 (fractional)

Fuel modelling was carried out for this study in the following way. After the creation of the vegetation map the composition of each of the fuel types was measured. Each vegetation class was assessed on the basis of basal area and net abundance such that % composition of each plot could be calculated on the basis of standing biomass. Thus, the basal diameter of 30 specimens of each species represented in a fuel class was measured, the mean basal area calculated and termed the 'standard unit' for that species. The exception was exotic grasses for which the 'standard unit' was based on the average number of upright tillers per metre-squared plot, based on the average of thirty samples. This approach was taken as it was believed that the simplest way to build fuel models for each fuel class was to construct a fuel model for each major species and subsequently aggregate these using weighted averages (either number of standard units, or % abundance by basal area) for each vegetation class.

Assessment of each vegetation class consisted of surveying three randomly located 10m by 10m plots for the basal diameter of each plant except grasses for which the number of upright tillers was counted. For especially abundant species smaller sub-samples (usually 4 at 0.5m by 0.5m or 4 at 1m by 1m) were surveyed; the numbers of grass upright tillers were assessed in this manner. After all plots were surveyed, % abundance (by basal area) and the number of standard units per 10m by 10m plot could be calculated from the average of the three samples and where appropriate scaled to the metre-squared level. Within each plot the proportions of herbaceous, woody and dead fuel(s) were calculated on the basis of standard units.

For each species one specimen was 'dissected' in the laboratory in order to assess load,

surface-area to volume ratio and FMC; the specimen dissected was selected to be as close as possible to the standard unit size so that the data obtained were directly comparable to the data from the survey plots. Before dissection each whole (above-ground) plant was weighed to estimate the total load for each species 'standard unit'. The specimen was then divided into functional categories (e.g. leaves, branches, boles etc.); these were then classed according to their TL division. The biomass of each TL size class within each functional category was then weighed. FMC was assessed for each TL division by weighing a sample and then drying it for 24 hours at 80 C, re-weighing it and using the weight loss to calculate the FMC. Antecedent weather conditions are not included in the fuel moisture assessment required for the Rothermel model. However, a problem with fuel modelling after the event was the adequate parameterisation of variables such as fuel moisture. For, whereas fuel load and fuel bed depth were estimated on the basis of an 'average' fuel unit, fuel moisture is extremely temporally variable. As a result fuel moisture was estimated from material that was available at the time of fuel modelling. While it is recognised that there are likely to be differences between the fuel moisture at the time of assessment and the fuel moisture at the time of the fire this was unavoidable.

Estimation of the surface-area to volume ratio was also carried out on the basis of functional category and TL division (see above). This was a time consuming task and in some cases assumptions had to be made in order to obtain reasonable data within a realistic time-frame (e.g. branch units were assumed to be cylindrical etc.).

Brown (1970) gives a series of equations for the estimation of the surface-area to volume ratio (σ) according to whether the particle falls into the class of 'needles, grasses and lichens' or 'hardwood leaves'. Following Brown's (1970) methods, surface-area and volume were both measured on the same particles to facilitate accurate determination of σ and, where possible, surface-area was determined on particles at a low FMC. For the category of 'grasses, lichens and leaves', σ can be assessed using the expression:

$$\sigma = \frac{S}{V} = \frac{LP + 2A}{LA} = \frac{P}{A} + \frac{2}{L} \qquad (6.2)$$

where : S = surface-area of particle (cm^2); V = volume of particle (cm^3); L = length of particle (cm); P = average perimeter of particle taken normal to length (cm) and A = average cross-sectional area of particle taken normal to length (cm^2).

End areas of long, narrow particles contribute little to σ, as can be seen by examining

the second term in Equation 6.2. Thus, the formula used for such particles was:

$$\sigma = \frac{P}{A} \tag{6.3}$$

Brown (1970) notes that grass stalks may be assumed to approximate cylinders and so Equation 6.3 simplifies to:

$$\sigma = \frac{P}{A} = \frac{2\pi r}{\pi r^2}$$

$$= \frac{4}{d} \tag{6.4}$$

where : d = average diameter of particle (cm)

The leaves of species such as *Corokia cotoneaster* and *Coprosma* sp. were also assessed using an alternative formula provided by Brown (1970) :

$$\sigma = \frac{S}{V} = \frac{2Sa + tPa}{tSa} \tag{6.5}$$

where : Sa = surface-area on one side of leaf (cm^2); t = average thickness of leaf (cm) and Pa = perimeter of leaf outline (cm).

Diameter and thickness was assessed for all these particles using a micrometer caliper; a ruler or tape measure was used for all other surface-area to volume ratio measurements. Having collected σ values for each TL category, the characteristic surface-area to volume ratio of the species could be calculated using the technique described in Burgan and Rothermel (1984). In essence, this technique uses a weighted averaging system based on the surface-area within each TL class as a proportion of the total surface-area; since the largest proportion of surface-area usually falls within the 1-hr TL and 10-hr TL classes, the fine fuels receive the highest weighting. This is appropriate as the Rothermel model considers the passage of the flaming front which is itself carried by the finest (1-hr TL and 10-hr TL) fuel particles. For all woody species, multiple 1-hr TL classes were used; this technique is used where there were two different types of particles in the 1-hr TL class (e.g. twigs and leaves).

Fuel bed depth was assessed by calculating the average height of 30 specimens of each of the species represented in the fuel models. The final fuel bed depth was estimated to be 70% of the maximum depth, as described by Burgan and Rothermel (1984).

Fuel modelling for *N.solandri* var *cliffortioides* was problematic as it was not possible to dissect and evaluate a specimen of this species. Thus, the fuel model was estimated from data obtained from a variety of sources such as data on the structure of individual beech trees at Cass (Maister, 1970; Burrows, 1977), from general data on the beech in

New Zealand (Wardle, 1984) and from published US fuel models for natural forest vegetation.

After fuel models were compiled for one standard unit for each species represented in the various fuel classes the standard unit values were aggregated on the basis of the number of standard units present per square-metre (load) and by % abundance based on basal area (FMC, depth and surface-area to volume ratio). All units were calculated in metric units in accordance with Wilson's (1980) metric revision of the fire spread model of Rothermel (1972). The full fuel models for the various vegetation classes are listed in Appendix 3.

6.4.3 Post-collection GIS Data Processing

In order that the data collected for the vegetation, topography and wind field of the fire-scar could be input into the fire spread model, it was necessary that all the layers be processed and corrected in Arc/Info. For the vegetation layer this involved rasterisation of the digitised (vector) polygon coverage of vegetation class. For wind speed and direction, grids were interpolated on the basis of the point samples. Topographic data were already in raster form as this was how they had been exported from Virtuozo to Arc/Info. All layers were rasterised at a spatial resolution of 50m.

After the data had been rasterised the four layers (elevation, wind speed, wind direction and vegetation) were geo-referenced and clipped such that the co-ordinate pairs (x_{min},y_{min}) and (x_{max},y_{max}) were the same. If 'no data' were available for a given cell it was coded 9999. Finally, the raster layers were converted to ASCII files that could be read by the Fortran 77 routines that controlled the simulation model (as per Chapter 5).

6.5 Data Layers and Data Preparation for Model Validation

The following sections are concerned with the parameterisation of the PYROCART model such that it could be used to recreate the Cass fire of May, 1995. As such the section is not concerned with the methodology used to estimate the parameters, but with the nature of the parameters themselves. The major focus of the section is the fuel models and mapping. However, wind and slope layers are also presented and discussed.

6.5.1 Vegetation Data

Although 11 fuel classes were represented in the original vegetation layer, after rasterisation to a cell size of 50m only 9 remained. Those omitted were beech-mixed

shrub (10) and bare-ground (11). The abundance of the nine remaining fuel classes is shown in Figure 6.4. The total number of cells in the layer is 5332 (124 rows*43 columns). Of these 5332 cells 1892 are coded NODATA; these NODATA cells are all found either on the east bank of the Cass River or the north side of State Highway 73 and are not located on the firescar itself.

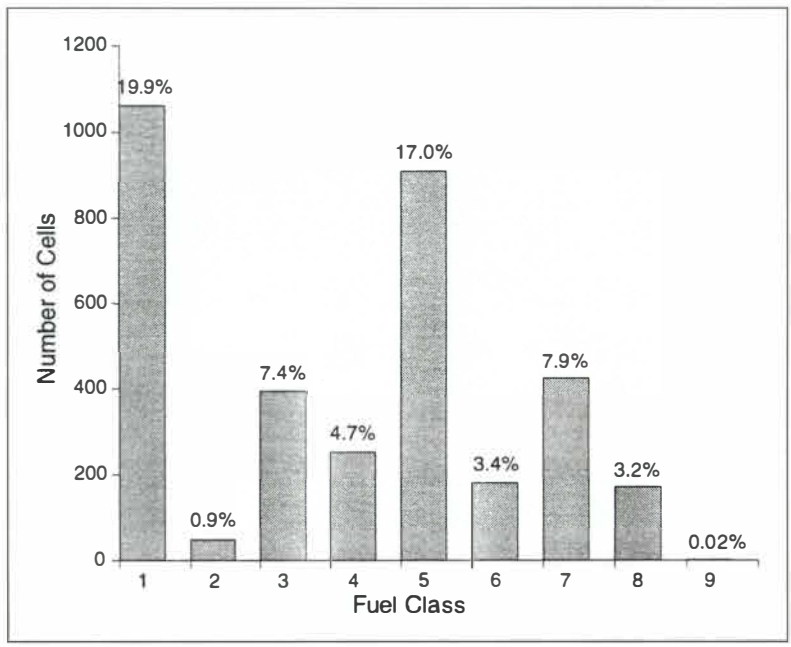

Figure 6.4 The abundance of the different vegetation classes in the vegetation layer. The vegetation classes are those presented in Table 6.1; the values above the bars are the percentage of the grid cells filled with these vegetation class. 1892 (35.6%) of the cells were coded NODATA.

Despite the loss of fine-grain data in rasterising the data coverage, major vegetation features are still visible. These include Horrible Bog, Misery Swamp, the patches of mountain beech on Corner Knob, the large matagouri-covered fan and the manuka shrubland which covers much of the flanks of Mounts Misery and Horrible. The complexity of the vegetation mosaic on Waterfall Terrace is also evident (Figure 6.5).

Preliminary tests of fire spread characteristics (Figure 6.6) illustrate that the nine different fuel types can be divided into three coarse groups based on their rate of spread. The first group includes the species with the highest rate of spread (manuka shrubland (5), mixed shrub (1) and light mixed shrub (7)). The ability for fire to propagate rapidly through these fuel beds is reflected in their high fine fuel component (reflected in the surface-area to volume ratio). Manuka shrubland burns at a significantly higher rate than either mixed shrubland or light mixed shrubland due to the greater fuel bed depth.

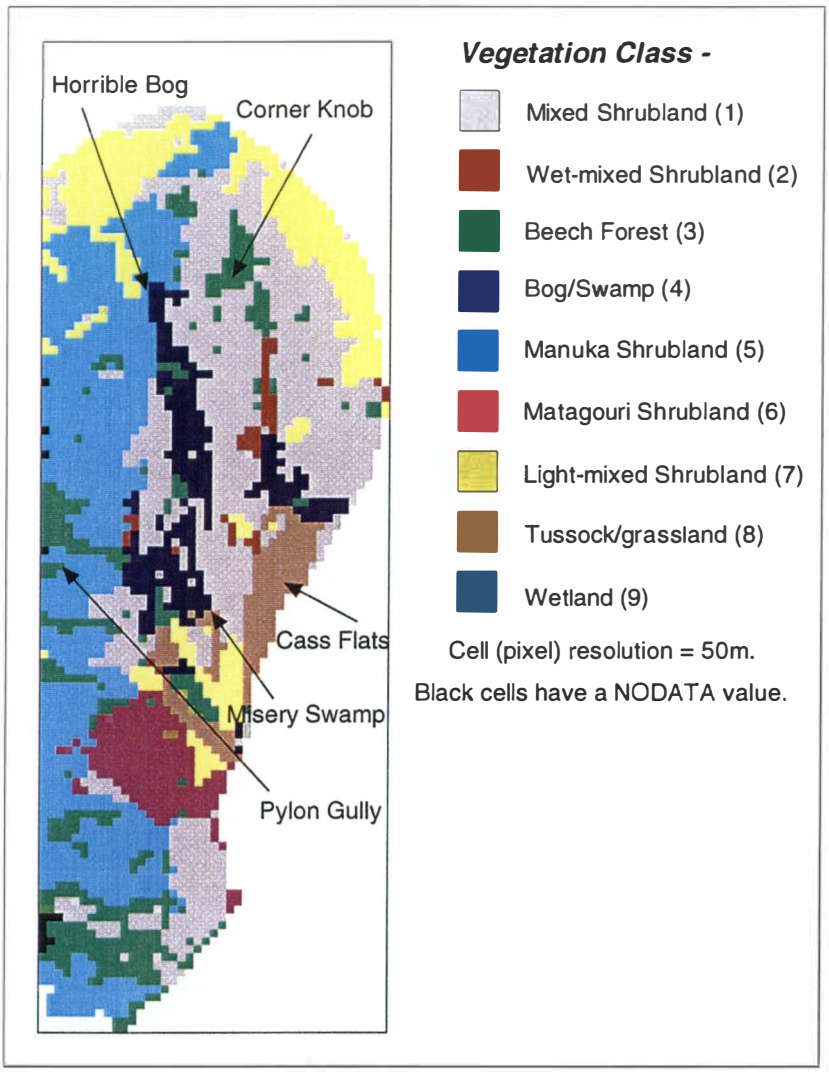

Figure 6.5 The vegetation layer as input into the PYROCART model (spatial resolution = 50m).

The second group of fuel models are those with an intermediate rate of spread (tussock/grassland (8), wet mixed shrubland (2) and matagouri shrubland (6)). These fuel types burn less rapidly than the first group for a number of reasons. The tussock/grassland fuels burn significantly slower than the two grass models of Rothermel (1972) due to a shallower fuel bed and higher FMC. Wet mixed shrubland burns slowly because of an unfavourable FMC (m_f) to FMC of extinction (m_x) ratio. Matagouri shrubland also has a relatively low rate of spread; this reflects an inability for fire to propagate between matagouri plants rather than an inability for individual matagouri to burn. The third group includes wetland, bog and beech. All three of these fuel types burn poorly due to an unfavourable FMC (m_f) to FMC of extinction (m_x) ratio and low surface-area-to-volume ratios (σ).

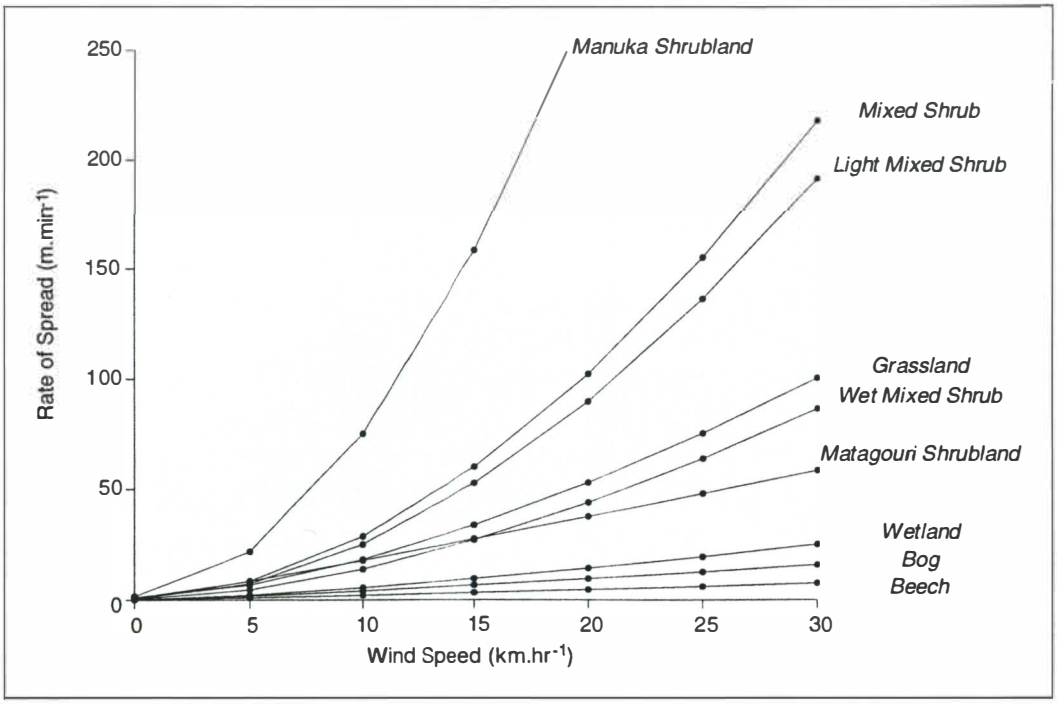

Figure 6.6 Rate of spread plotted against wind speed for the nine fuel models used in the PYROCART validation.

6.5.2 Slope and Wind Data

The terrain over which the fire spread is complex and slope ranges from 0 to over 40 degrees, with a mean slope angle of 10 to 15 degrees (Figure 6.7). As shown in Sections 2.5.3 and 5.3.1, and Figure 2.7, slope has a significant effect on fire spread, with slope spreading preferentially upslope and being reduced on downslopes. Large flat areas are evident on the grassy flats beside the Cass River and on Waterfall Terrace and Horrible Bog; slope increases on the flanks of Mount Misery and Horrible and on Corner Knob.

Data layers representing wind speed and direction were derived from the field observations of these two variables. The wind speed layer is relatively simple with the highest wind speeds being evident on the exposed top of Corner Knob and the areas of lowest wind speed being those sheltered in the floor of the basin (e.g. Horrible Bog and parts of Waterfall Terrace). Wind speeds in the data layer range between 1.8 and 6.55 $m.sec^{-1}$ (6.5-23.6 $km.hr^{-1}$). The wind direction layer is more complex with some areas where direction shows high variability at small spatial scales evident; such areas are frequently associated with those of low wind speed. Wind directions in the data layer vary from westerly (274°) to north-westerly (319°).

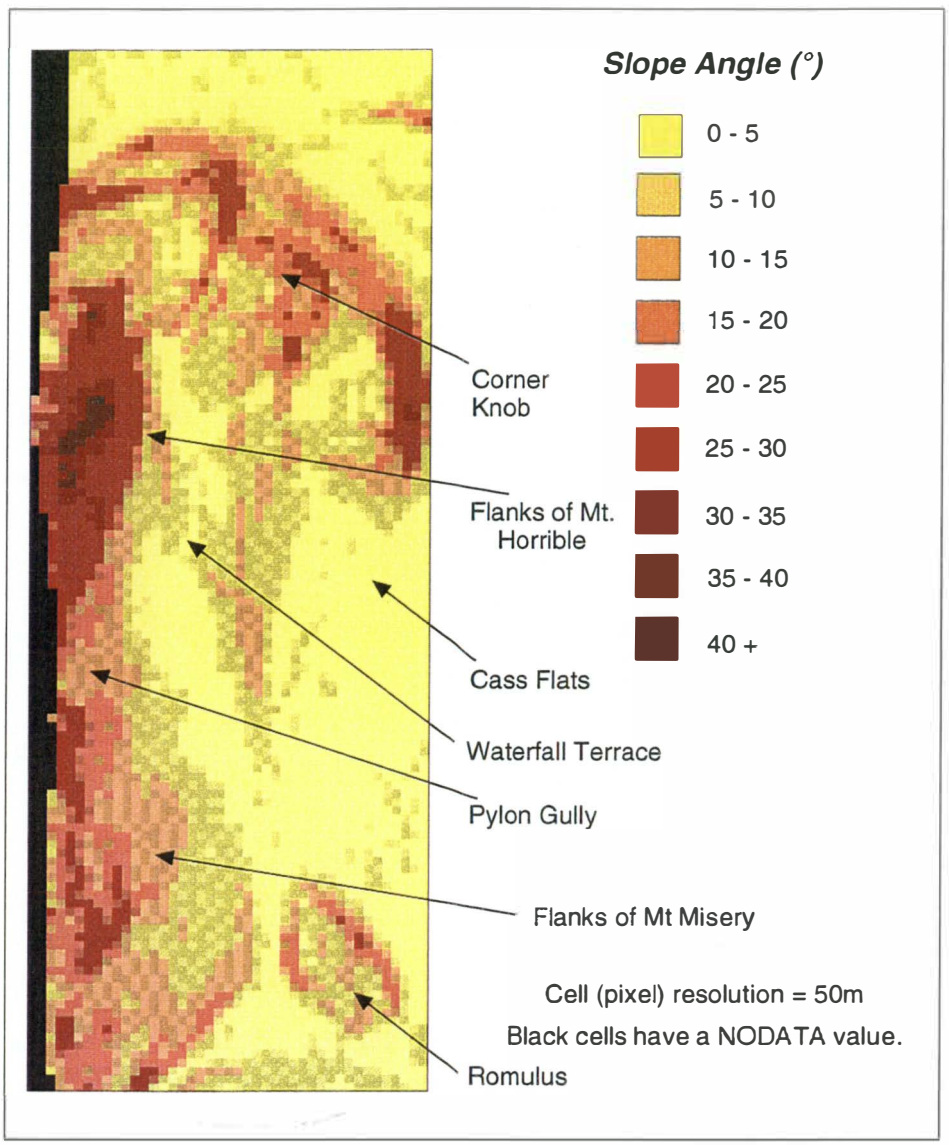

Figure 6.7 The slope layer as input into the PYROCART model (spatial resolution = 50m).

The temporal resolution used in the *a posteriori* recreation of the Cass fire was crucial. It was estimated by calculating the average of rate of spread for all fuel types at the maximum possible wind speed (including gusts). This average was divided by the spatial resolution (50) and a temporal resolution selected such that assuming an average rate of spread at maximum wind speed there was a 50% chance of a fronting fire propagating into a neighbouring cell (i.e.[ROS x temporal resolution]/spatial resolution ~ 0.5).

6.6 Validation of the PYROCART Simulation of the Cass Fire

This section considers the validation of the PYROCART fire model. Initially the overall accuracy of the model is discussed in qualitative terms. Following this initial

discussion the accuracy of the model in a range of environmental conditions, such as fuel type and slope steepness is considered. Such an analysis allows an evaluation of the strengths and weaknesses of the fire modelling system to be carried out.

6.6.1 Description of the PYROCART Fire Shapes

Although a temporal validation of the shapes produced using PYROCART is not possible an examination of the way in which the shapes change over time is useful. However, it is evident from the temporal extent of the fire (165 minutes) that the model tends to over-predict rates of spread. Fire shapes at half hourly intervals are presented in Figure 6.9 and in the back pocket; the final extent of the fire is presented in Figure 6.8 to facilitate comparison between the predicted and the real fires. Figure 6.10 plots the cumulative number of cells burnt against time.

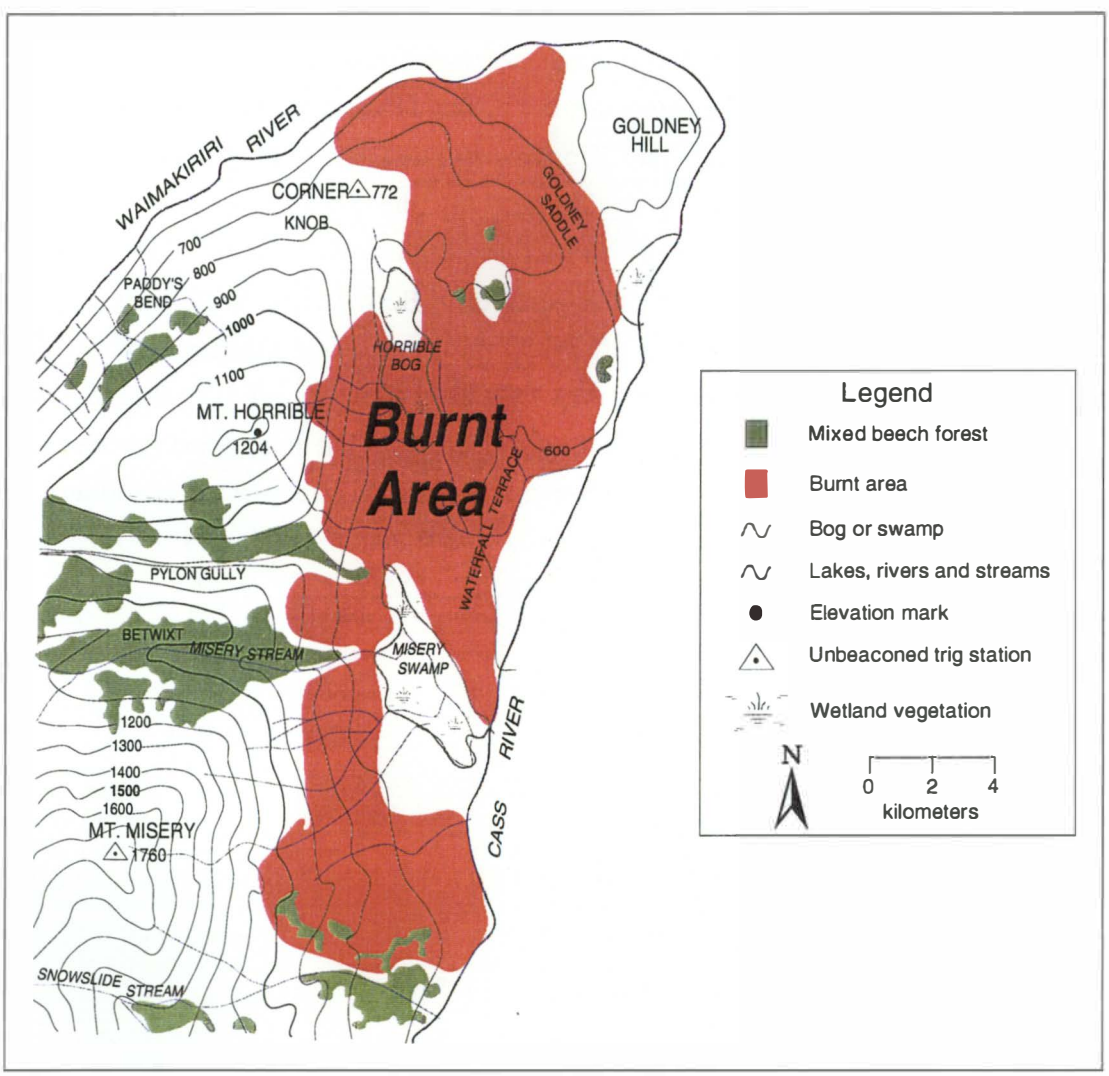

Figure 6.8 Extent of the Cass fire of May 27-28, 1995.

A single ignition point for the fire was used. Therefore at the start of the first iteration

this cell was the sole source of fire spread. After 30 minutes fire had spread to the top of Corner Knob and was progressing through the light mixed fuel bed around its flanks. A patch of unburnt *N. solandri* var *cliffortioides* is visible. The south face of the fire front appears to have been slowed by Horrible Bog and the large patch of Mountain Beech on Corner Knob. After 60 minutes the fire has progressed around the flanks of Corner Knob and has spread along the flanks of Mount Horrible. The rapid progression along Mount Horrible is due to the flammable nature of the fuel on these sites. Unburnt patches of *N. solandri* var *cliffortioides* are visible on Corner Knob and the fire has largely failed to propagate into Horrible Bog. By 90 minutes the fire has spread further along the flanks of Mount Horrible and has also moved into the grassland on the Cass Flats; Horrible Bog still remains largely unburnt. The fire shape after 120 minutes has become more complex. Both Horrible Bog and the swampy patches at the toe of Corner Knob remain unburnt and fire spread progress has been impeded by Misery Swamp and the strips of *N. solandri* var *cliffortioides* extending from Pylon Gully. In one place, however, fire has burnt through the mountain beech and moved rapidly into the more flammable *L. scoparium*. The fire shape after 150 minutes has formed a patchwork of burnt and unburnt areas of varying sizes. Horrible Bog remains largely unburnt as does Misery Swamp. Fire spread has been impeded by the *D. toumatou* covered fan extending from Mount Misery. Apart from these areas small unburnt areas of *N. solandri* var *cliffortioides* are visible on Pylon Gully, Betwixt and Waterfall Terrace. The final fire shape is similar to that after 150 minutes with a mosaic of burnt and unburnt areas is visible. The fire has been halted by the area of *N. solandri* var *cliffortioides* opposite Romulus at the south of the firescar. The matagouri fan remains largely unburnt as do Misery Swamp and Horrible Bog. Small areas of grassland and *N. solandri* var *cliffortioides* remain scattered across the fire site. The largest of these are found extending from Pylon Gully and on Waterfall Terrace.

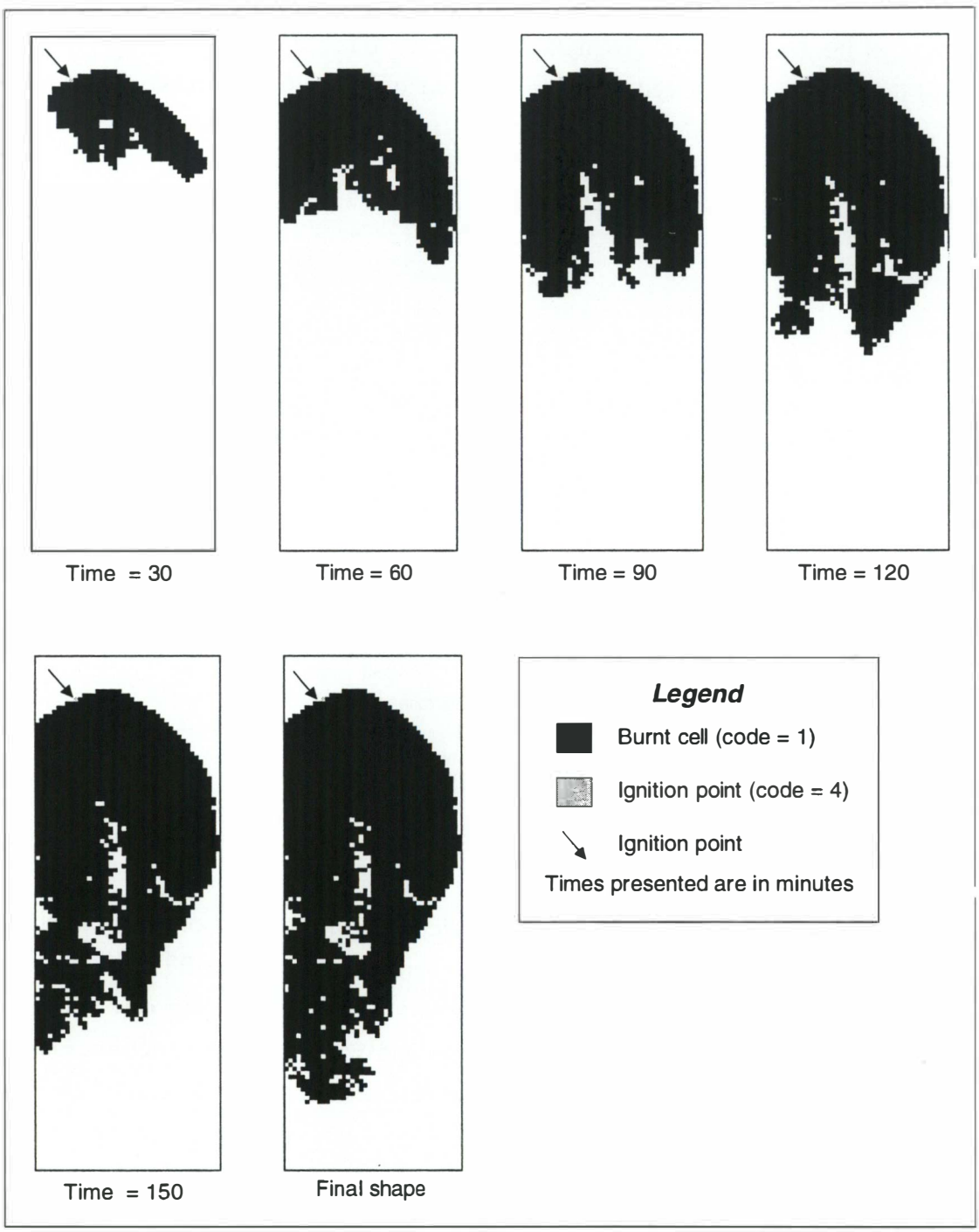

Figure 6.9 *A posteriori* simulation of the May 1995 Cass Fire produced by PYROCART. These fire shapes were used in the validation of the fire spread model.

Figure 6.10 shows that the fire progression (in terms of number of cells burnt) was temporally (if not spatially) consistent. The only major change in gradient on the slope occurs at about 150 iterations (75 minutes). It is probable that this decrease in the progression of the fire reflects the less flammable fuel beds through which the fire was spreading (e.g. Misery Swamp, Horrible Bog, and patches of *N. solandri* var *cliffortioides)* and the flatter terrain and lower wind speeds of Misery Swamp and

Waterfall Terrace. Sections 2.7.1 and 3.4 described the nature of the constant rate of increase of the fire perimeter (implying a quadratic function). However, this constant rate of increase is not reflected in the linear nature of Figure 6.10. It is possible that the artificial NODATA boundary surrounding the fire scar has forced the fire to spread as an *irregular* line-fire (*cf* Section 4.2.1).

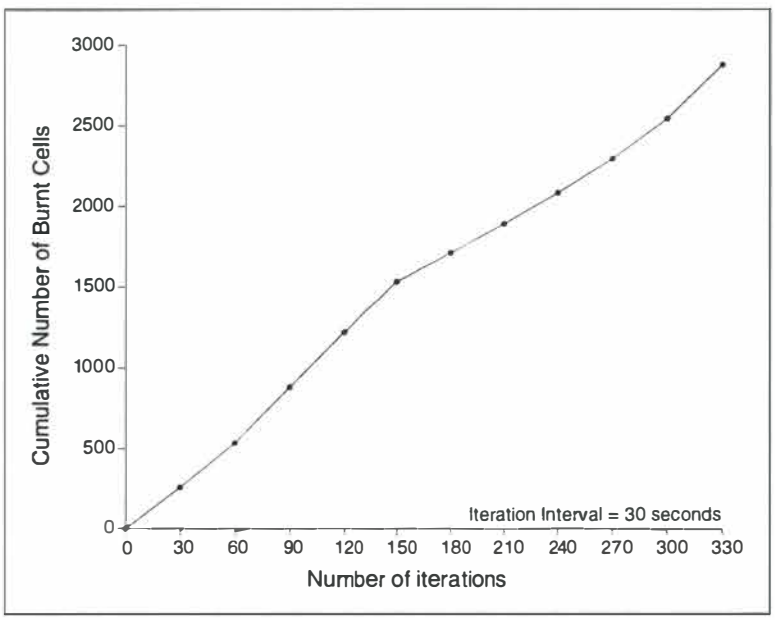

Figure 6.10 Cumulative number of cells burnt against iterations (time).

6.6.2 Analysis of the PYROCART Fire Shapes

Sørensen coefficients (Equation 5.6) were calculated in order to compare the shapes predicted by the PYROCART model with the eventual shape of the 1995 Cass fire. The performance of the model was considered both as a whole and then across the fuel classes and in categories of slope, wind speed and wind direction. Such an analysis allows the strengths and weaknesses of the models performance to be more rigorously evaluated.

Table 6.4 Sørensen coefficient values comparing the PYROCART output and the shape of the Cass fire.

Overall Accuracy	*a*	*b*	*c*	*Sørensen Coefficient*
	2043	854	213	0.793

a - Number of cells that burnt in reality and that were predicted to burn.
b - Number of cells that were predicted to burn but did not.
c - Number of cells that were not predicted to burn but which did.

Table 6.4 shows that the level of matching between the fire which occurred at Cass and the fire as predicted by PYROCART is 79.3%. The high level of *b* (the number of cells that the model predicted would burn, but which did not) indicates that the model tends

to over-predict the extent of the fire. However, in isolation this value is of little value as it conveys no information about the nature of the correlation between model predictions and reality in different environmental conditions. The over-prediction of the model may reflect two issues: firstly, the Rothermel model may over-predict rates of spread in the fuel models that were used; and, secondly, the lack of an adequate fire extinction routine may cause areas such as the stands of *N. solandri* var *cliffortioides* on Corner Knob to burn through infilling. The high surface-area volume ratios of the fuel bed may have been especially significant in the over-prediction of rates of spread. Gould (1988) found that at surface-area volume to ratios similar to those measured, rate of spread is corrected excessively with regard to wind speed and that as a result the model may tend to over-predict rate of spread at some wind speeds. The evaluation of moisture content of extinction is also problematic. Andrews (1980) notes that this parameter is assessed subjectively and Brown (1972) and Sneeuwjagt and Frandsen (1977) found that small differences in the extinction moisture content can have significant influences on the model predictions. A further important point is that the spread of the fire is constrained by artificial NODATA boundaries; the inability of the fire to spread beyond these boundaries may have artificially elevated the accuracy of the model.

Prediction Accuracy Within Individual Fuel Classes

The first set of environmental predictors that were tested were the fuel classes. The values of the Sørensen coefficient for each fuel class are presented in Table 6.5. It can be seen that there is a wide range in the coefficient for different fuel types. The highest Sørensen coefficient for an individual fuel type is for wet mixed shrubland (0.945) and the lowest meaningful value is for grassland (0.379). Although wetland has a coefficient value of 0 this is not interpretable as only a single cell contained this fuel type.

Table 6.5 Sørensen coefficient values for individual fuel classes. The fuel classes are presented in order of their prediction accuracy.

Fuel Class	*a*	*b*	*c*	*Sørensen Coefficient*
Wet mixed shrubland (2)	43	5	0	0.945
Mixed shrubland (1)	844	107	33	0.923
Manuka dominated shrubland (5)	548	272	3	0.799
Light mixed shrubland (7)	265	156	0	0.773
Mountain Beech (3)	132	66	33	0.748
Bog (4)	112	40	68	0.675
Matagouri dominated shrubland (6)	48	70	36	0.475
Grassland (8)	39	127	1	0.379
Wetland (9)	0	1	0	0

a - Number of cells that burnt in reality and that were predicted to bum.
b - Number of cells that were predicted to burn but did not.
c - Number of cells that were not predicted to burn but which did.

Across all fuel types except bog (4) the fire spread model tended to over-predict the number of burnt cells. This is reflected in the values of *c* being comparatively higher than those of *b*. The over-prediction is probably a reflection of two factors; firstly, the temporal resolution may be too coarse and, secondly, the Rothermel model may over-predict rate of spread in the fuel types that were used.

The individual fuel type whose burnt area was the most poorly predicted was grassland (8). The area of grassland that was predicted to be burnt was greatly over-predicted. There are two large expanses of grassland; the largest of these (110 cells; 65%) is found in the Cass Flats with the remaining 60 (35%) located at the southern end of Misery Swamp. Figure 6.8 shows that PYROCART predicted that these areas would be burnt with the exception of some scattered pockets of unburnt grassland in Misery Swamp. However, the grasslands on the Cass Flats remained completely unburnt along with much of Misery Swamp. The level of the over-prediction is illustrated in the *b* value (127). In proportional terms, of the 170 grassland cells 75% were predicted to burn but did not. This inaccuracy in predicting fire spread in grassland areas is probably a reflection of the vegetation abutting the Cass Flats and the over-prediction of flanking and backing rates of spread. An area of bog and wet mixed shrubland is found at the toe of the terrace adjacent to the grassland. Field observation shows that this areas was unburnt and may have prevented fire from spreading onto the Cass Flats. However, these areas of vegetation are not large enough to be included in the fuel layer at the spatial resolution at which the model was run (50m).

Although those cells described by the mountain beech fuel model have a reasonably high Sørensen coefficient value (0.748), a number of problems were found with the

application of fuel modelling techniques to this fuel class. As described in Section 6.4.2 the fuel model was a composite, constructed from a range of data sources. The key problems lay with the effective parameterisation of fuel bed depth, ovendry fuel loading and surface-area to volume ratio. Thus, although the Sørensen coefficient is reasonably high and the model predicted fire spread within this fuel class more accurately than within other fuel classes the fuel model used remains unsatisfactory. For example, the model failed to predict the unburnt patches of *N. solandri* var *cliffortioides* on Corner Knob and over-predicted fire spread in the tongues of this fuel type extending from Pylon Gully. The model, however, did predict the inhibiting effects of the large stand of mountain beech at the southern end of the fire scar. Fundamentally, the problem lies with the use of the Rothermel model to describe fire spread in this specific fuel type. Rothermel (1972, p. iii) describes the model as being designed for the prediction of:

> "rate of spread and intensity in a continuous stratum of fuel that is contiguous to the ground. The initial growth of a forest fire occurs in the surface fuels (fuels that are supported within 6 feet of less of the ground)."

Thus, the use of the model to describe fire spread in this fuel type breaks one of the fundamental assumptions of the model (Chapter 4). Furthermore, Van Wilgen *et al.* (1985) had some similar problems with the fuel bed depth parameter when applying the model to South African mountain fynbos and Catchpole *et al.* (1993) consider that the Rothermel model may be over-sensitive to fuel bed depth.

The bog fuel class (4) differs from the other fuel classes in that PYROCART *under*-predicted the number of cells in this fuel class that burnt. This under-prediction is visible in the Horrible Bog and Misery Swamp area. The PYROCART model predicted that these areas would remain largely unburnt. However, in reality these areas burnt to a greater extent that was predicted. This may reflect difficulties in describing whether cells are burnt or unburnt as well as the spatial resolution of the data set. In an environment such as Horrible Bog the area described by a single cell (50m) comprises a patchwork of burnt and unburnt areas. Such micro-scale variations in the pattern of burning are not predicted by PYROCART. This problem reflects both the grain of the spatial data and the Boolean nature of the output produced by the model (i.e. cells may be either burnt or unburnt, they can not be partially burnt). The issue of micro-scale variations in burn pattern is of less significance in areas described by fuel classes such as mixed shrubland as the pattern of the burn was spatially more uniform.

Prediction Accuracy by Slope Angle

This sub-section is concerned with an analysis of the accuracy of the predictions made

by PYROCART on slopes of differing steepness. Table 6.6 presents the Sørensen coefficient values for varying slope angles.

Table 6.6 Sørensen coefficient values for slope classes of differing steepnesses.

Slope Angle (degrees)	*a*	*b*	*c*	*Sørensen Coefficient*
0-5	213	211	51	0.619
5-10	586	193	114	0.792
10-15	486	140	39	0.844
15-20	324	81	9	0.878
20-25	160	62	5	0.827
25-30	102	34	1	0.854
30-35	64	13	0	0.908
35-40	21	11	0	0.792
40-45	22	0	0	1.0

a - Number of cells that burnt in reality and that were predicted to burn.
b - Number of cells that were predicted to burn but did not.
c - Number of cells that were not predicted to burn but which did.

There is a smaller range in the Sørensen coefficient values for slope than was the case for the individual vegetation (*cf* Table 6.5). The model predictions were least accurate on slopes between 0° and 5°, whilst the highest level of prediction accuracy was for the steepest slopes (40-45°). The level of over-prediction declines markedly on steeper slopes. The reasons for this increased accuracy on steeper slopes are considered below.

Table 6.6 shows a general trend of the accuracy of the model predictions increasing with slope steepness. However, it is difficult to assess the performance of the model solely with respect to slope steepness as vegetation and slope are confounded. On flatter areas such as Waterfall Terrace, Misery Swamp, Horrible Bog and the Cass Flats the vegetation mosaic is much more spatially complex than is the case on the steeper slopes (e.g. the flanks of Mounts Horrible and Misery). Thus, it is necessary to describe the nature of the vegetation on slopes of different steepnesses in order to understand the model predictions on varying slopes.

Table 6.7 shows that the number of fuel classes decreases with slope. On slopes between 0° and 5° 8 of the 9 fuel classes are represented and on slopes between 5 and 10 all fuel classes are represented. However on the steepest slopes (40°-45°) only 2 fuel classes are represented.

Table 6.7 Cross-tabulation between slope steepness and fuel class.

	Vegetation Class								
Slope (°)	*MS*	*WMS*	*MTB*	*BOG*	*MAN*	*MATS*	*LMS*	*GLD*	*WLD*
0-5	145	2	37	149	15	4	39	116	0
5-10	429	23	78	91	104	73	92	54	1
10-15	307	18	112	12	162	85	105	0	0
15-20	110	4	74	0	179	15	93	0	0
20-25	33	0	22	0	135	2	50	0	0
25-30	17	0	17	0	89	1	15	0	0
30-35	2	1	5	0	60	0	9	0	0
35-40	4	0	5	0	23	0	0	0	0
40-45	1	0	0	0	21	0	0	0	0

MS	Mixed Shrubland	*BOG*	Bog	*LMS*	Light Mixed Shrub
WMS	Wet Mixed Shrubland	*MAN*	Manuka Shrubland	*GLD*	Grassland
MTB	Mountain Beech	*MATS*	Matagouri Shrubland	*WLD*	Wetland

The interaction between slope and fuel class is epitomised by the the two extremes of slope steepness (0°-5° and 40°-45°). Fuel class diversity is extremely high on the flattest slopes. As described above this reflects the diversity of the vegetation mosaic on such sites. Of the cells with a slope steepness between 0 and 5 degrees 52% contain either bog or grassland fuel types and as discussed earlier PYROCART showed a low predictive power for these two fuel types. Thus, it is difficult to attribute the models relatively poor performance on flat terrain to slope steepness alone. On the steepest slopes fuel class diversity is at a minimum; of the 22 cells that have a steepness between 40° and 45° 21 contained manuka-dominated shrubland and 1 contained mixed shrubland. Table 6.5 shows that both of these fuel classes have a high Sørensen coefficient value (0.799 and 0.923 respectively). Thus, the accuracy of the prediction provided by PYROCART can again be seen to be a result of the interactions of more than one environmental variable.

Prediction Accuracy by Wind Speed and Wind Direction

This section is concerned with an analysis of the accuracy of the predictions provided by the PYROCART model in the differing conditions of wind speed and wind direction found across the validation area. Table 6.8 presents the Sørensen coefficient values for wind speed classes.

Table 6.8 Sørensen coefficient values for wind speed classes

Wind Speed (km.hr^{-1})	*a*	*b*	*c*	*Sørensen Coefficient*
< 9	480	83	54	0.875
9-11†	287	141	26	0.775
11-13†	308	198	38	0.723
13-15	272	208	50	0.678
15-17	173	169	6	0.664
17-19†	164	21	9	0.916
19-21	216	20	35	0.887
21-23	131	4	8	0.956

a - Number of cells that burnt in reality and that were predicted to burn.
b - Number of cells that were predicted to burn but did not.
c - Number of cells that were not predicted to burn but which did.
† Denotes wind speeds derived from quintic interpolation alone (i.e. no real data)

As was the case for fuel type and slope the model over-predicts burnt areas at most wind speeds; the sole exception being wind speeds between 19-21 km.hr^{-1}, and 21-23 km.hr^{-1}. It is difficult to discern clear trends in the Sørensen coefficient values for varying wind speeds. Although the predictions of the PYROCART model appear to be more accurate at each end of the wind speed distribution this is complicated by the nature of the analysis of the wind field. The lower Sørensen coefficient values for wind speeds between 11 and 17 km.hr^{-1} may reflect inaccuracies in the interpolation of the wind point samples across the fire scar rather than problems within the fire spread model. Analysis of the Sørensen coefficient values for wind direction classes is subject to the same constraints as analysis of wind speed classes. Table 6.9 presents the coefficient values for wind direction classes.

Table 6.9 Sørensen coefficient values for wind direction classes.

Wind Direction (degrees)	*a*	*b*	*c*	*Sørensen Coefficient*
265-270	67	8	0	0.944
270-275	151	14	13	0.918
275-280	228	7	31	0.923
280-285	198	35	33	0.853
285-290	170	108	49	0.584
290-295	293	142	27	0.776
295-300	544	289	39	0.768
300-305	140	114	8	0.696
305-310	117	74	13	0.729
310-315	74	49	12	0.708
315-320	49	4	1	0.951

a - Number of cells that burnt in reality and that were predicted to burn.
b - Number of cells that were predicted to burn but did not.
c - Number of cells that were not predicted to burn but which did.

Apart from the model over-predicting burnt area in all wind direction classes except 275°-280° no clear trends are apparent and the accuracy of prediction is above 70% for all but one wind direction class (285°-290°; s=58.4%). Problems with interpolation of point samples similar to those described above may help explain some of the inaccuracies in the predictions made by the fire spread model.

Summary of Similarity Analysis

Similarity analysis of the nature outlined above allows an evaluation of the model with respect to the individual key environmental parameters. This is more useful than an overall similarity analysis as it enables the strengths and weaknesses of the model to be identified.This subdivision of the environmental factors is necessary because the model is being validated against a single event (i.e. n=1). Fuel class and slope angle appear to be the environmental descriptors with the most influence on the predictions made by the fire spread model. Wind speed and direction did not show clear trends in prediction accuracy; it is probable that this reflects problem with interpolation of point data across the firescar rather than more fundamental problems in either PYROCART or the Rothermel model. Analysis of the prediction accuracy on slopes of differing steepnesses illustrated the way in which the various environmental descriptors interact to control fire behaviour.

It is difficult to comment on the relative accuracy of the PYROCART model compared to other similar models. The only comparable model is that developed by Vasconcelos (1988). Although little quantitative validation is presented in this study from the data presented it is possible to calculate a Sørensen coefficient value of 0.81 (a=218; b=54; c=68) for Vasconcelos predicted against Vasconcelos observed. These figures indicate that the model of Vasconcelos (1988) has a similar level of prediction accuracy to the PYROCART fire spread model. However, the model of Vasconcelos (1988) tended to under-predict the extent of the burnt area whereas the PYROCART model tended to over-predict the burnt area. Although the overall Sørensen coefficient values of the two models are similar it is difficult to compare them due to the differences in the two models and the conditions in which they were validated. The crucial differences are firstly, the fire which Vasconcelos used to validate her model occurred in a considerably less complex landscape than that in which PYROCART was validated (e.g. 3 vs. 9 fuel types) and wind speed and wind direction were assumed to be constant; and, secondly, the fuel models which Vasconcelos (1988) used were taken directly from the US National Fire Danger Rating System and had been rigorously tested in a range of fire situations. This last difference is likely to be the most significant because, as described above, errors in prediction by the PYROCART model

are likely to reflect problems in parameterising the model. The only fair comparison between the model presented in this thesis and that of Vasconcelos (1988) would be to run the data set used to validate PYROCART on the model of Vasconcelos (1988) and *vice versa*.

6.7 Summary

This chapter has been concerned with the PYROCART fire spread model developed in this research. The methods required to parameterise the model were presented and the outputs of the model and the accuracy of its predictions were considered. Similarity analysis using Sørensen's similarity index was carried out both for the overall level of accuracy as well as for individual environmental descriptors. The Sørensen coefficient value for the overall match was 0.793. The fire spread simulation model of Vasconcelos (1988) was found to have a similar prediction accuracy. The similarity analysis for the individual environmental descriptors suggested that within PYROCART fuel class and slope are the two most important environmental variables. The model tended to over-predict the burnt area and the data is suggestive of the model over-predicting rates of spread in most fuel types. Furthermore, the analysis suggests that simple interpolation of wind data point samples may cause some inaccuracies in the predictions made by the model.

Chapter Seven

Conclusions

7.1 A Re-examination of the Research Objectives

In Chapter 1 three major research objectives were presented. These were:

- testing the applicability of fire spread models developed overseas to New Zealand ecosystems,
- investigating the controls on fire behaviour through the use of a case study,
- assessing the applicability of a Geographic Information System (GIS) for predicting the spatial behaviour of fire.

The PYROCART model developed in this research has as its conceptual base the fire spread model of Rothermel (1972). Thus, discussion and analysis of this model has been an important component of the thesis. Furthermore, the use of the model allowed an evaluation of the parameterisation techniques involved with its use. Due to the lack of temporal data describing the spread of the Cass fire of 27-28 May, 1995 it was only possible to validate PYROCART with respect to the spatial extent of the fire. For the purpose of predicting the eventual extent of the fire, the PYROCART fire spread performed well. For further analysis of its applicability to New Zealand fuels, controlled burns would be required such that real rates of spread could be compared with those predicted by the model. Parameterisation of the Rothermel model was not simple and a number of difficulties were encountered. Fuel modelling the *N. solandri* var *cliffortioides* fuel type was especially problematic. However, as discussed in Chapter 6, this was largely due to the extension of the model beyond the fuel types for which it was designed.

Figure 7.1 provides a synthesis of the manner in which wildland fires occur as a result of a series of complex physical and biological interactions at a range of temporal and spatial scales. An understanding of the the physical and chemical processes controlling fire is important because of the feedback loop between the fire and the ecosystem in which it occurs. The nature of the controls governing fire behaviour has been a central component of this thesis. Not only have they been laid out both in general terms (Chapter 2) and through the use of a case study (Chapter 6) but an understanding of the controls has been crucial both to understanding the Rothermel model and to making many of the assumptions implicit in the fire spread model developed in this research.

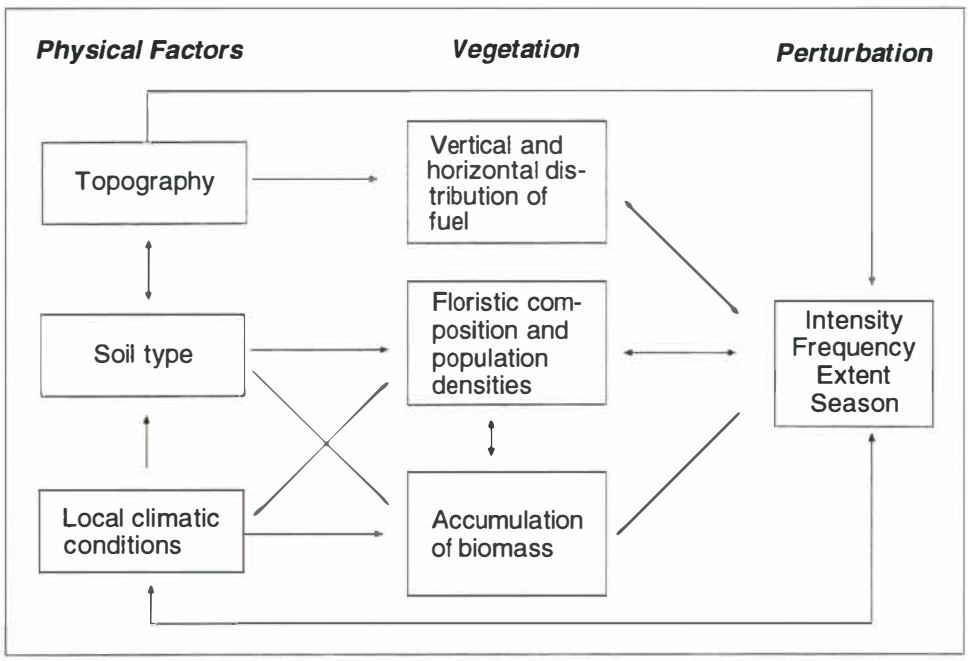

Figure 7.1 A schematic diagram summarising the interactions between fire, and the biological and physical environments (Whelan, 1995).

The third research objective was to assess the applicability of GIS for predicting the spatial behaviour of fire. One of the key issues currently facing the development of GIS and environmental modelling is the integration of spatially-based environmental modelling systems and GIS. Chapters 3 and 5 illustrated some of the problems facing such effective integration. In summary, the two major problems are the availability and accuracy of suitable spatial data and the lack of 'temporality' in most contemporary GIS. The lack of GIS functionality for sophisticated process modelling has been highlighted in this thesis by the use of a 'loosely coupled' integration framework. The fire spread model itself was run outside the GIS in an external programming environment and the GIS itself was used for the storage and display of model data. However, GIS does have much to offer fire spread modelling. The ability to store data in a cellular form, and the ability to be able to simply and rapidly manipulate and display spatial, if not temporal, data have a number of advantages over non-GIS approaches. Furthermore, GIS has the ability to facilitate the collation of data from a range of sources such as remotely-sensed images, maps, aerial photography and tabular data in a common, geo-referenced database. Finally, the use of a GIS environment allows the accurate representation of complex, spatially non-uniform variables and provides spatially explicit results at several points in time.

7.2 Limitations and Future Development of the PYROCART Model

PYROCART is a direct implementation of Rothermel's fire spread model, and the predictions it makes are subject to the limitations and assumptions of this model. However, there are a number of differences between the PYROCART system and simple elliptical fire models based upon the outputs of the Rothermel model. Spatial homogeneity in the fire environment is a fundamental assumption of the Rothermel model. However, the use of a cellular automata model to describe the landscape, in which each cell is internally homogeneous, allows the assumptions of spatial homogeneity to be circumvented. Thus, the approach used in this thesis does not violate any of the assumptions of the Rothermel model and provides a means of simulating fire spread in a spatially heterogeneous landscape. However, PYROCART also incorporates the algorithms of Van Wagner (1988) and Green *et al.* (1990) and so it is subject to their constraints. Again, the cellular automata model and the general structure of the fire model ensure that any assumptions implicit in these models are not violated.

At present PYROCART has only a limited potential for *in situ* fire management. The major issue inhibiting the active use of the model for fire management are the sophisticated and complex input data required. These include vegetation and terrain maps, wind data, as well as the accurate parameterisation of fuel models. A second problem is the lack of quantitative data concerning the rate of fire spread in New Zealand fuels, both indigenous and exotic. This lack of data means that the rates of spread predicted by the PYROCART model cannot be validated or compared with 'real world' data sets. Furthermore, the lack of quantitative data concerning rates of fire spread in New Zealand fuels makes the evaluation of the temporal resolution at which the model should operate problematic. Despite the problems outlined above PYROCART may be used to make predictions on the influences of environmental change under differing land management scenarios. Such predictions may be of more use than actual *in situ* fire management as they allow the consequences of different land management options to be rigorously evaluated. For example, a functioning fire prediction model could complement reserve managment plans such as those outlined by Calder *et al.* (1992) and Wilson (1993). Again, however, the use of the model in such a way would require the collection of data describing the landscape as well as the development of more sophisticated fuel models. Other applications where a model such as PYROCART may be of practical value are population viability analyses of endangered species in fire-prone ecosystems (e.g. Brooker and Brooker, 1994; Lindenmayer and Possingham, 1995, 1996; Southgate and Possingham, 1995), restoration management in ecosystems where the fire regime has been modified by human action (e.g. Baker, 1994; Wilson *et al.*, 1995) and to assess the influences of disturbance on fundamental ecological processes such as competition and seed dispersal

(e.g. Green, 1989).

Some of the improvements that PYROCART could incorporate to increase its functionality are :

- inclusion of the capacity to predict spot fire activity,
- inclusion of the capacity to predict the onset of crowning,
- better, more reliable simulation of wind patterns,
- inclusion of more realistic fire extinction criteria, and,
- inclusion of ability to model the effects of firebreaks.

Morris (1988) developed a simple method for computing spotting distances from wind-driven surface fires based on the spotting models of Albini (1979, 1981b, 1983). The model of Morris (1988) has been included in a recent revision of BEHAVE and was found to predict spotting distances accurately. The inclusion of such a module into the modelling system developed in this thesis would pose no major difficulties. The ability to predict the onset of crowning is much more problematic. Firstly, there is limited knowledge as to when crowning is likely to occur in forest fuels, and secondly the only model which predicts crowning behaviour (Rothermel, 1991b) has not been subjected to rigorous field testing.

Zach and Minnich (1991) showed how a GIS and a diagnostic wind field model could be integrated and produce outputs suitable for sophisticated fire modelling. Given the importance of wind in the processes of fire spread and combustion improved simulation of wind patterns would aid in the prediction of wildland fire events. The importance of accurate wind field modelling is emphasised by the nature of the similarity analysis for both wind speed and wind direction classes. The data presented in Section 6.6.2 suggests that simple interpolation of point data may not provide wind data of sufficient accuracy or spatial grain.

The inclusion of a more sophisticated extinction criterion within the model, operational at both the level of individual cells and the fire as a whole, would be a significant improvement; the lack of such a criterion in PYROCART reflects the lack of validated, quantitative research on fire extinction. If such an extinction criterion were to be included within PYROCART then problems such as the infilling of unburnt areas and the excessive backing and flanking rates of spread may be resolved. A possible example of such a fire extinction model is provided by Wilson (1985, 1990) who developed a probabilistic model of fire extinction based on the Rothermel model. This model was designed to reflect the energy balance of the fire near the marginal limits of sustained burning. Similar fire extinction models have also been developed by Grishin *et al.*

(1983) and Weber (1991b). However, these models all remain unvalidated and are subject to the parameterisation difficulties associated with physical models (Chapter 3). Wilson (1988) published an expression describing the relationship between fireline intensity and flame length to the width of the firebreak that could be breached, via contact, by a fire of a given fireline intensity, in a particular grass fuel type. Such a model could be developed to find similar relationships in other fuel beds and to provide a framework to calculate the impedance to fire spread corresponding to field features dependent on their characteristics and on the intensity of the fire. The ability to be able to predict the influence of fire breaks on fire behaviour would be of use to those wishing to actively manage fire behaviour and reduce fire extent.

7.3 Conclusions

The model developed and presented in the research detailed in this thesis goes beyond the simple display of spatial information. Instead GIS is used to aid in the simulation of the temporally and spatially dynamic process of fire spread. However, the integration of GIS and spatial process models is problematic and it is probable that this issue will remain at the forefront of GIS research (see Goodchild *et al.*, 1996). The current lack of functionality in many contemporary GIS means that spatial process modelling must be performed outside the GIS itself.

It has been seen that overseas fire spread models may have some applicability to New Zealand ecosystems. However, a lack of quantitative data on the rate of fire spread in both indigenous and exotic fuels means that it is difficult to validate such models. The collection of data on rates of fire spread is crucial if fire spread models formulated overseas are to be validated and used in New Zealand.

Finally, this research has emphasised the nature of the interactions between fire and the biological and physical environment. These complex interactions occur at a range of scales and in a number of cases are poorly understood. Further research into these relationships, both in New Zealand and overseas, is crucial if fire spread modelling is to continue to improve.

References

Abel, D.J., Kilby, P.J. and Davis, J.R. 1994. The systems integration problem. *International Journal of Geographical Information Systems* **8** : 1-12.

Agee, J.K. 1993. *Fire Ecology of Pacific Northwest Forests*. Island Press, Washington, D.C.

Akami, H. 1978. Bivariate interpolation and smooth surface fitting for irregularly distributed data points. *ACM Transactions for Mathematical Software* **3** : 148-159.

Albini, F.A. 1967. Physical models for fire spread in brush. *11th Symposium (International) on Combustion.* The Combustion Institute, Pittsburg. pp. 553-560.

Albini, F.A. 1976. *Estimating Wildland Behaviour and Effects*. USDA Forest Service, General Technical Report, INT-30.

Albini, F.A. 1979. *Spot Fire Distance from Burning Trees - A Predictive Model.* USDA Forest Service General Technical Report, INT-56.

Albini, F.A. 1980. *Thermochemical Properties of Flame Gases from Fine Wildland Fuels.* USDA Forest Service Research Paper, INT-243.

Albini, F.A. 1981a. A model for the wind-blown flame from a line fire. *Combustion and Flame* **43** : 155-174.

Albini, F.A. 1981b. *Spot Fire Distance from Isolated Sources - Extensions of a Predictive Model.* USDA Forest Service Research Note, INT-309.

Albini, F.A. 1983. *Potential Spotting Distance from Wind-driven Surface Fires.* USDA Forest Service Research Paper, INT-309.

Albini, F.A. 1984. Wildland fires. *Scientific American* **72** : 590-597.

Albini, F.A. 1985. A model for fire spread in wildland fuels by radiation. *Combustion Science and Technology* **42** : 229-258.

Albini, F.A. 1986. Wildland fire spread by radiation - a model including fuel cooling by

natural convection. *Combustion Science and Technology* **45** : 101-113.

Albini, F.A. 1993. Dynamics and modelling of vegetation fires : observations. In : Crutzen, P.J. and Goldammer, J.G. (eds) *Fire in the Environment : The Ecological, Atmospheric, and Climatic Importance of Vegetation Fires.* John Wiley and Sons, New York. pp. 39-53.

Albini, F.A. and Stocks, B.J. 1985. Predicted and observed rates of spread of crown fires in immature jack pine. *Combustion Science and Technology* **48** : 65-76.

Anders, E; Wolbach, W.S. and Gilmour, I. 1991. Major wildland fires at the Cretaceous-Tertiary boundary. In : Levine, J.S (ed) *Global Biomass Burning.* MIT Press, Cambridge MA. pp. 485-492.

Anderson, D.H., Catchpole. E.A., De Mestre, N.J. and Parkes, T. 1982. Modelling the spread of grass fires. *Journal of the Australian Mathematical Society (Series B)* **23** : 451-466.

Anderson, H.E. 1969 *Heat Transfer and Fire Spread.* USDA Forest Service Research Paper, INT-69.

Anderson, H.E. 1970. Forest fire ignability. *Fire Technology* **6** : 312-322.

Anderson, H.E. 1983. *Predicting Wind-driven Wildland Fire Size and Shape.* USDA Forest Service Research Paper INT-305

Andrews, P.L. 1980. Testing the fire model. In : Martin, R.E. (ed) *Proceedings of the 6th Conference on Fire and Forest Meteorology*, April 22-24, Seattle, WA. Society of American Foresters. pp. 70-77.

Andrews, P.L. 1986. *BEHAVE : Fire behaviour prediction and fuel modeling system - BURN subsystem , Part One.* USDA Forest Service General Technical Report INT-194.

Andrews, P.L. 1988. Use of the Rothermel Model for fire danger rating and fire behaviour prediction in the United States. In : Cheney, N.P. and Gill, A.M. (eds) *Proceedings of the Conference on Bushfire Modelling and Fire Danger Rating Systems,* Canberra, 11-12 July, 1988. CSIRO, Canberra. pp. 1-8.

Andrews, P.L. and Rothermel, R.C. 1982. *Charts for Interpreting Wildland Fire*

Behaviour Characteristics. USDA Forest Service General Technical Report, INT-131.

Ariav, G. 1986. A temporally oriented data model. *ACM Transactions on Database Systems* **11** : 499-527.

Armstrong, M.P. 1988. Temporality in spatial databases. In : *Proceedings of GIS/LIS '88*, San Antonio, Texas, 30 November - 2 December, 1988. pp. 880-889.

Baines, P.G. 1988. The effects of topography on the wind field. In : Cheney, N.P. and Gill, A.M. (eds) *Proceedings of the Conference on Bushfire Modelling and Fire Danger Rating Systems*, Canberra, 11-12 July, 1988. CSIRO, Canberra. pp. 101-107.

Baines, P.G. 1990. Physical mechanisms for the propagation of surface fires. *Mathematical and Computer Modelling* **13** (12) : 83-94.

Baker, W.L. 1994. Restoration of landscape structure altered by fire suppression. *Conservation Biology* **8** : 763-769.

Ball, G.L. and Guertin, D.P. 1992. Improved fire growth modelling. *International Journal of Wildland Fire* **2** : 47-54.

Barney, R.J., Fahnestock, G.R., Herbolsheimer, W.G., Miller, R.K., Philips, C.B. and Pierovich, J. 1984. Fire Management. In : Wenger, K.F. (ed) *Forestry Handbook* (2nd edition). John Wiley and Sons, New York. pp. 189-251.

Basher, L.R., Meurk, C.D. and Tate, K.R. 1990. *The Effects of Burning on Soil Properties and Vegetation : A Review of the Scientific Evidence Relating to the Sustainability of Ecosystems and Land Use in the Eastern South Island Hill and High Country*. DSIR Land Resources Technical Report 18.

Beer, T. 1991. Bushfire rate-of-spread forecasting : deterministic and statistical approaches to fire modelling. *Journal of Forecasting* **10** : 301-317.

Beer, T. 1993. The speed of a fire front and its dependence on wind speed. *International Journal of Wildland Fire* **3** : 193-202.

Beer, T and Enting, I. 1990. Fire spread and percolation modelling. *Mathematical and Computer Modelling* **13** (11) : 77-96.

Bessie, W.C. and Johnson, E.A. 1995. The relative importance of fuels and weather on fire behaviour in subalpine forests. *Ecology* **76** : 747-762.

Bond, W.J. and Midgley, J.J. 1995. Kill thy neighbour: an individualistic argument for the evolution of flammability. *Oikos* **73** : 79-85.

Bond, W.J. and Van Wilgen, B.W. 1995. *Fire and Plants.* Chapman and Hall, London.

Bradshaw, L.S., Deeming, J.E., Burgan, R.E. and Cohen, J.D. 1983. *The 1978 National Fire Danger Rating System: Technical Documentation.* USDA Forest Service General Technical Report, INT-169.

Brain, C.K. and Sillen, A. 1988. Evidence from the Swartkrans cave for the earliest use of fire. *Nature* **336** : 464-466.

Briggs, G.A. 1969. *Plume rise.* US Atomic Energy Commission TID-25075.

Brooker, L.C. and Brooker, M.G. 1994. A model for the effects of fire and fragmentation on the population viability of the Splendid Fairy-wren. *Pacific Conservation Biology* **1** : 344-358.

Brown, J.K. 1970. Ratios of surface area to volume for common fine fuels. *Forest Science* **16** : 101-105.

Brown, J.K. 1972. *Field Test of a Rate-of-Fire Spread Model in Slash Fuels.* USDA Forest Service Research Paper, INT-116.

Brown, J.K. 1981. Bulk densities of nonuniform surface fuels and their application to fire modeling. *Forest Science* **27** : 667-683.

Browne, M.L. 1977. Meteorological conditions at a controlled burn. *New Zealand Journal of Forestry* **22** : 147-154.

Burgan, R.E. 1987. *Concepts and Interpreted Examples in Advanced Fuel Modeling.* USDA Forest Service General Technical Report, INT-238.

Burgan, R.E. and Rothermel, R.C. 1984. *BEHAVE - Fire behaviour Prediction and Fuel Modeling System - FUEL Subsystem.* USDA Forest Service General Technical Report, INT-167.

Burgan, R.E. and Shasby, M.B. 1984. Mapping broad-area fire potential from digital fuel, terrain and weather data. *Journal of Forestry* **82** : 228-231.

Burrough, P.A., Van Beursen, W. and Heuvelink, G. 1988. Linking spatial process models and GIS : a marriage of convenience or a blossoming partnership ? In : *Proceedings of GIS/LIS '88*, San Antonio, Texas, 30 November - 2 December, 1988. pp. 598-607.

Burrows, C.J. 1960. Recent changes in vegetation of the Cass area, Canterbury. *New Zealand Geographer* **16** : 57-70.

Burrows, C.J. 1977. Forest vegetation. In : Burrows, C. (ed) *Cass : History and Science in the Cass District, Canterbury, New Zealand.* Department of Botany, University of Canterbury. pp. 233-259.

Burrows, C.J. and Lord, J.M. 1993. Recent colonisation of *Nothofagus fusca* at Cass, Canterbury. *New Zealand Journal of Botany* **31** : 139-146.

Byram, G.N. 1958. *Some Basic Thermal Processes Controlling the Effects of Fire on Living Vegetation.* USDA Forest Service Research Note, SE-114.

Byram, G.M. 1959. Combustion of Forest Fuels. In : Davis, K.P. (ed) *Forest Fire : Control and Use*. McGraw and Hill, New York. pp. 65-89.

Calder, J.A., Bastow Wilson, J., Mark, A.F. and Ward, G. 1992. Fire, succession and reserve management in a New Zealand snow tussock grassland. *Biological Conservation* **62** : 35-45.

Catchpole, T. and de Mestre, N. 1986. Physical models for a spreading line fire. *Australian Forestry* **49** : 102-111.

Catchpole, E.A., Hatton, T.J. and Catchpole, W.R. 1989. Fire spread through non-homogeneous fuel modelled as a Markov process. *Ecological Modelling* **48** : 101-112.

Catchpole, E.A., Alexander, M.E., and Gill, A.M. 1992. Elliptical-fire perimeter- and area-intensity distributions. *Canadian Journal of Forest Research* **22** : 968-972.

Catchpole, E.A., Catchpole, W.R. and Rothermel, R.C. 1993. Fire behaviour experiments in mixed fuel complexes. *International Journal of Wildland Fire* **3** : 45-57.

Cerkige, H.M. 1978. Propagation of fire fronts in forests. *Computation and Mathematics with Applications* **4** : 325-332.

Cheney, N.P. 1981. Fire behaviour In : Gill, A.M., Groves, R.H. and Noble, I.R. (eds) *Fire and the Australian Biota*. Australian Academy of Science, Canberra. pp. 151-177.

Cheney, N.P. 1990. Quantifying bushfires. *Mathematical and Computer Modelling* **13** (12) : 9-15.

Cheney, N.P., Gould, J.S. and Catchpole, W.R. 1993. The influence of fire, weather and fire-shape variables on fire-spread in grasslands. *International Journal of Wildland Fire* **3** : 31-44.

Chevrou, R.B. 1992. Modelisation de la progression des feux de foret, phenomene chaotique. *Revue Forestiere Francais* **44** : 435-445.

Chou, H.-C. and Ding, Y. 1992. Methodology of integrating spatial analysis/modeling and GIS. In : Breshnan, P., Corwin, E. and Cowen, D (eds) *Proceedings of the Fifth International Symposium on Spatial Data Handling,* Charleston, South Carolina, 3-7 July, 1992. pp. 514-524.

Chou, Y.H. 1992. Management of wildland fires with a geographical information systems. *International Journal of Geographical Systems* **6** : 123-140.

Christensen, N.L. 1985. Shrubland fire regimes and their evolutionary consequences. In : Pickett, S.T.A. and White, P.S (eds). *The Ecology of Natural Disturbance and Patch Dynamics*. Academic Press, San Diego. pp. 86-97.

Christensen, N.L. 1993. Fire regimes and ecosystem dynamics. In : Crutzen, P.J. and Goldammer, J.G. (eds) *Fire in the Environment : The Ecological, Atmospheric, and Climatic Importance of Vegetation Fires*. John Wiley and Sons, New York. pp. 233-244.

Christensen, N.L., Agee, J.K., Brussard, P.F., Hughes, J. and nine others. 1989. Interpreting the Yellowstone fires of 1988. *Bioscience* **39** : 678-686.

Chuvieco, E. and Congalton, R.G. 1989. Application of remotely-sensed and geographical information systems to forest fire hazard mapping. *Remote-sensing of Environment* **29** : 147-159.

Chuvieco, E. and Salas, J. 1996. Mapping the spatial distribution of forest fire danger using GIS. *International Journal of Geographical Systems* **10** : 333-345.

Clark, J.S. 1988. Effect of climate change on fire regimes in northwestern Minnesota. *Nature* **334** : 223-225.

Clark, J.S. and Robinson, J. Paleoecology of fire. In : Crutzen, P.J. and Goldammer, J.G. (eds) *Fire in the Environment : The Ecological, Atmospheric, and Climatic Importance of Vegetation Fires*. John Wiley and Sons, New York. pp. 193-215.

Clarke, K.C., Brass, J.A. and Roggan, P.J. 1994. A cellular-automata model of wildfire propagation and extinction. *Photogrammetric Engineering and Remote Sensing* **60** : 1355-1367.

Clarke, K.C. and Olsen, C. 1996. Refining a cellular automata model of wildfire propagation and extinction. In : Goodchild, M.F., Steyaert, L.T., Parks, B.O. and four others. *GIS and Environmental Modeling: Progress and Research Issues*. GIS World Books, Fort Collins. pp. 333-339.

Clifford, J. and Warren, D.S. 1983. Formal semantics for time in databases. *ACM Transactions on Database Systems* **8** : 214-254.

Coley, P.D., Bryant, J.P. and Chapin, F.S. 1985. Resource availability and plant anti-herbivore defence. *Science* **230** : 895-899.

Coley, P.D. 1988. Effects of plant growth rate and leaf life time on the amount and type of anti-herbivore defence. *Oecologia* **74** : 531-536.

Cope, M.J. and Chaloner, W.G. 1985. Wildfire : an interaction of biological and physical processes. In : Tiffney, B.H. (ed). *Geological Factors and the Evolution of Plants*. Yale University Press, Conneticut. pp. 257-277.

Cosentino, M.J., Woodcock, C.E. and Franklin, J. 1981. Scene analysis for wildland fire-fuel characteristics in a Mediterranean climate. In : *Proceedings of 15th International Symposium on Remote Sensing of Environment.* Ann Arbor, MI, ERIM. pp. 635-646.

Cox, J.E. and Mead, C.B. 1963. Soil evidence relating to post-glacial climate on the Canterbury plains. *Proceedings of the New Zealand Ecological Society Conference* **10** :

28-38.

Crock, M.J. 1986. A brief history of fire behaviour modelling and its future prospects in Australia. In : Roberts, B (ed) *Third Queensland Fire Research Workshop*, Lawes, 1-3 October, 1988. pp. 33-52.

Cumberland, K.B. 1944. *Soil Erosion in New Zealand: A Geographical Perspective.* Soil Conservation and Rivers Control Council, Wellington.

Cumberland, K.B. 1945. Burning tussock grassland : a geographic survey. *New Zealand Geographer* **1** : 149-164.

Cumberland, K.B. 1962. Climatic change or cultural interference ? New Zealand in moa hunter times. In : McCaskill, M. (ed). *Land and Livelihood.* Geographical Society, Christchurch. pp. 88-142.

Dayandra, P.W.A. 1977. Stochastic models for forest fires. *Ecological Modelling* **3** : 309-313.

Daubenmire, R. 1968. Ecology of fire in grasslands. *Advances in Ecological Research* **5** : 209-267.

de Vliegher, B.M. 1992. Risk assessment for environmental degradation caused by fires using remote-sensing and GIS in a Mediterranean region (Southern Euboia, Central Greece). In : *Proceedings of the Integrated Geological Applications of Remote Sensing (IGARSS '92) Conference*. May 26-29. Houston, Texas. pp, 44-47.

Despain, D.G. 1990. *Yellowstone Vegetation : Consequences of Vegetation in a Natural Setting*. Roberts Reinhard, Boulder.

Despain, D.G. and Sellers, R.E. 1977. Natural fires in Yellowstone National Park. *Western Wildlands* **4** : 20-24.

Dijkstra, E.W. 1959. A note on two problems in connection with graphs. *Numerical Mathematics* **1** : 269-271.

Dorrer, G.A. 1984. A model of the spreading of a forest fire. *Heat Transfer - Soviet Research* **16** : 39-52.

Elfring, C. 1989. Yellowstone : fire storm over fire management. *Bioscience* **39** : 667-673.

Ellis, R. 1994. *Predicting the Fine Fuel Moisture Content in Gorse.* Unpublished B. For. Sc. Dissertation, School of Forestry, University of Canterbury.

Emmons, H. 1964. Fire in the forest. *Fire Research Abstracts Review* **5** : 163-178.

Flannery, T.F. 1994. *The Future Eaters : An Ecological History of the Australasian Lands and People.* Reed Books, Chatterswood, N.S.W.

Fons, W.L. 1946. Analysis of fire spread in light forest fuels. *Journal of Agricultural Research* **72** (3) : 93-121.

Ford-Robertson, F.C. 1971. *Terminology of Forest Science, Technology, Practice and Products* (English language version). American Society of Foresters, Washington, D.C.

Fosberg, M.A., Mearns, L.O. and Price, C. 1993. Climate change-fire interactions at the global scale : predictions and limitations of method. In : Crutzen, P.J. and Goldammer, J.G. (eds) *Fire in the Environment : The Ecological, Atmospheric, and Climatic Importance of Vegetation Fires.* John Wiley and Sons, New York. pp. 123-139.

Foster, T. 1976. *Bushfires : History, Prevention, Control.* Reed Books, Sydney.

Frandsen, W.H. 1971. Fire spread through porous fuels through the conservation of energy. *Combustion and Flame* **16** : 9-16.

Frandsen, W.H. and Andrews, P.L. 1979. *Fire Behaviour in Non-uniform Fuels.* USDA Forest Service Research Paper, INT-232.

French, I.A., Anderson, D.H. and Catchpole, E.A. 1990. Graphical simulation of bushfire spread. *Mathematical and Computer Modelling* **13** (12) : 67-71.

Fujii, N., Hasegawa, J., Pallop, L. and Sakawa, Y. 1980. A non-stationary model of fire spreading. *Applied Mathematical Modelling* **4** : 176-180.

Fujioka, F. M. 1985. Estimating wildland fire rate of spread in a spatially non-uniform environment. *Forest Science* **31**: 21-29.

Fujioka, F.M. and McCutchin, M.H. 1989. Long range fire weather forecasting. In : *Proceedings of the 14th Annual Climate Diagnostics Workshop*, 16-20 October, 1989. La Jolla, California. NOAA National Weather Service. pp. 410-415.

Fuller, M. 1991. *Forest Fires : An Introduction to Wildland Fire Behaviour, Management, Fire Fighting and Prevention.* John Wiley & Sons. New York.

Gage, M. 1977. Glacial Geology. In : Burrows, C. (ed) *Cass : History and Science in the Cass District, Canterbury, New Zealand.* Department of Botany, University of Canterbury. pp. 67-79.

Gill, A.M. 1981. Post-settlement fire history in the Victorian landscape. In : Gill, A.M., Groves, R.H. and Noble, I.R. (eds) *Fire and the Australian Biota.* Australian Academy of Science, Canberra. pp. 77-98.

Gitay, H., Bastow-Wilson, J, Lee, W.G. and Allen, R.B. 1991. *Chionochloa rigida* tussocks 13 years after spring and autumn fire, Flagstaff, New Zealand. *New Zealand Journal of Botany* **29** : 459-462.

Goodchild, M.F. 1991. Spatial analysis with GIS : problems and perspectives. In : *Proceedings of GIS/LIS '91*, Atlanta, Georgia, 28 October-1 November, 1991. pp, 40-49.

Goodchild, M.F. 1992. Data models and data quality : problems and perspectives. In : Goodchild, M.F., Parks, B.O. and Steyaert, L.T. (eds). *Environmental Modelling With GIS.* Oxford University Press, New York and London. pp. 94-105.

Goodchild, M.F., Parks, B.O. and Steyaert, L.T (eds) 1992. *Environmental Modelling With GIS.* Oxford University Press, New York and London.

Goodchild, M.F., Steyaert, L.T., Parks, B.O and four others (eds). 1996. *GIS and Environmental Modeling: Progress and Research Issues.* GIS World Books, Fort Collins.

Gould, J.S. 1988. Validation of the Rothermel fire spread model and related fuel parameters in grassland fuels. In : Cheney, N.P. and Gill, A.M. (eds) *Proceedings of the Conference on Bushfire Modelling and Fire Danger Rating Systems,* Canberra, 11-12 July, 1988. CSIRO, Canberra. pp. 51-64.

Grant-Taylor, T.L. and Rafter, T.A. 1971. New Zealand radiocarbon age measurements 6. *New Zealand Journal of Geology and Geophysics* **14** : 364-402.

Greig-Smith, P. 1983. *Quantitative Plant Ecology (3rd Edition).* University of California Press, Berkeley.

Grishin, A.M. 1984. Steady-state propagation of a high-level forest fire. *Soviet Physics Doklady* **29** : 917-919. (English Translation).

Grishin, A.M., Gruzin, A.D. and Zuverev, V.G. 1983. Mathemical modelling of the spread of high-level forest fires. *Soviet Physics Doklady* **28** : 328-330. (English Translation)

Green, D.G. 1983. Shapes of similar fires in discrete fuels. *Ecological Modelling* **20** : 21-32.

Green, D.G. 1989. Simulated effects of fire, dispersal and spatial pattern on competition within forest mosaics. *Vegetatio* **82** : 139-153.

Green, D.G., Gill, A.M. and Noble, I.R. 1983. Fire shapes and the adequacy of fire-spread models. *Ecological Modelling* **20** : 33-45.

Green, D.G., Tridgell, A. and Gill, A.M. 1990. Interactive simulation of bushfires in heterogeneous fuels. *Mathematical and Computer Modelling* **13** (12) : 57-66.

Grubb, P.J. 1992. A positive distrust in simplicity - lessons from plant defences and from competition among plants and among animals. *Journal of Ecology* **80** : 585-610.

Habeck, J.R. and Mutch, R.W. 1973. Fire-dependent forests in the Northern Rocky Mountains. *Quaternary Research* **3** : 408-424.

Haines, D.A. 1982. Horizontal roll vortices and crown fires. *Journal of Applied Meteorology* **21** : 751-763.

Haines, D.A. 1988. A lower atmosphere severity index for wildland fire. *National Weather Digest* **13** (2) : 23-27.

Hamilton, M.P., Salazar, L.A. and Palmer, K.F. 1989. Geographic information systems : providing information for wildland fire planning. *Fire Technology* **5** : 5-23.

Hartford, R.A. and Rothermel, R.C. 1991. *Fuel Moisture as Measured and Predicted during the 1988 Yellowstone Fires.* USDA Forest Service Research Paper, INT-396.

Heinselman, M.L. 1973. Fire in the virgin forests of the Boundary Water Canoe Area, Minnesota. *Quaternary Research* **3** : 329-382.

Hennicker-Gotley, G.R. 1936. A forest fire caused by falling stones. *Indian Forestry* **62** : 422 - 423.

Hobbs, R.J. and Gimmingham, C.H. 1984. Studies on fire in Scottish heathland communities. I : Fire characteristics. *Journal of Ecology* **72** : 223-240.

Hogewog, P. 1988. Cellular automata as a paradigm for ecological modelling. *Applied Mathematics and Computation* **27** : 81-100.

Holder, G.H., Van Wyngaarden, R., Pala, S and Taylor, D. 1990. Flexible analysis through the integration of a fire growth model with an analytical GIS. In : *Proceedings of the GIS 1990 Symposium*, Vancouver, B.C. pp. 152-158.

Hottel, H.C., Williams, G.C. and Steward, F.R. 1965. Modelling of firespread through a fuel bed. *10th Symposium (International) on Combustion.* The Combustion Institute, Pittsburg. pp. 997-1007.

Hottel, H.C., Williams, G.C. and Kwentus, G.K. 1971. Fuel preheating in free burning fires. *13th Symposium (International) on Combustion.* The Combustion Institute, Pittsburg. pp. 963-970.

Howard, G. 1985. Late Quaternary geomorphology of the Upper Rakaia and Waimakiriri Valleys : notes for the New Zealand Geological Society post-conference trip. *Geological Society of New Zealand Miscellaneous Publication* **32B** : 71-111.

Jackson, W.D. 1968. Fire, air, water and earth: an elemental ecology of Tasmania. *Proceedings of the Australian Ecological Society* **3** : 9-16.

Johnson, E.A. 1992. *Fire and Vegetation Dynamics : Studies from the North American Boreal Forest.* Cambridge Studies in Ecology, Cambridge University Press, Cambridge.

Johnson, E.A. and Larsen, C.P.S. 1991. Climatically induced change in fire frequency in the southern Canadian Rockies. *Ecology* **72** :194-201.

Johnson, L.B. 1990. Analysing spatial and temporal phenomena using geographic information systems: A review of ecological applications. *Landscape Ecology* **4** : 31-43.

Kemp, K.K 1992. Spatial models for environmental modeling with GIS. In : Breshnan, P., Corwin, E. and Cowen, D (eds) *Proceedings of the Fifth International Symposium on Spatial Data Handling,* Charleston, South Carolina, 3-7 July, 1992. pp. 524-533.

Kelly, D. 1994. Demography and conservation of *Botrychium australe*, a peculiar, sparse, mycrorrhizal fern. *New Zealand Journal of Botany* **32** : 139-146.

Kelly, D. 1995. The cass fire (27-28 May 1995) and its effect on vegetation. *Journal of the Canterbury Botanical Society* **29** : 25-28.

Kemp, E.M. 1981. Pre-Quaternary fire in Australia. In : Gill, A.M., Groves, R.H. and Noble, I.R. (eds) *Fire and the Australian Biota.* Australian Academy of Science, Canberra. pp. 3-21.

Kessell, S.R. and Cattelino, P.J. 1978. Evaluation of a Fire Behaviour Information Integration System for Southern California Chaparral Wildlands. *Environmental Management* **2** : 135-159.

Kessell, S.R., Potter, M.W., Bevins, C.D., Bradshaw, L. and Jeske, B.W. 1978. Analysis and application of forest fuels data. *Environmental Management* **2** : 347-363.

King, N.K. and Vines, R.G. 1969. Variation in the flammability of the leaves of some Australian forest species. CSIRO (Aust.) Division of Applied Chemistry, Mimeo. Report.

Komarek, E.V. Sr. 1969 The natural history of lightning. *Tall Timbers Ecology Conference* **3** : 139-183.

Kourtz, P.H. and O'Regan, W.G. 1971. A model for a small forest fire to simulate burned and burning areas for use in a detection model. *Forest Science* **17** : 163-169.

Kruger, F.J. and Bigalke, R.C. 1984. Fire in fynbos. In : Booysen, P. de V and Tainton, N.M. (eds). *Ecological Effects of Fire in South African Ecosystems*. Spreinger-Verlag, Berlin. pp. 67-114.

Kurbatsky, N.P. and Telitsin, G.P. 1977. *Theoretical and experimental analysis of radiation mechanisms for the spread of forest fires.* USSR Academy of Sciences, Siberian Branch, Krasnoyarsk.

Langren, G. 1993. *Time in Geographic Information Systems.* Taylor and Francis, London and Washington DC.

Le Houerou, H.N. 1974. Fire and vegetation in the Meditteranean basin. *Proceedings of the Tall Timbers Fire Ecology Conference* **13** : 237-277.

Lindenmayer, D.B. and Possingham, H.P. 1995. Modelling the effects of wildfire on the viability of metapopulations of the endangered Australian species of marsupial, Leadbetter's possum. *Forest Ecology and Management* **74** : 197-222.

Lindenmayer, D.B. and Possingham, H.P. 1996. Ranking conservation and timber management options for Leadbetter's possum in southeastern Australia using population viability analysis. *Conservation Biology* **10** : 235-251

Lobert, J.M. and Warnatz, J. 1993. Emissions from the Combustion Process in Vegetation. In : Crutzen, P.J. and Goldammer, J.G. (eds) *Fire in the Environment : The Ecological, Atmospheric, and Climatic Importance of Vegetation Fires.* John Wiley and Sons, New York. pp. 15-39.

Luke, R.H. and McArthur, A.G. 1986. *Bushfires in Australia.* Australian Government Publishing Service, Canberra.

Lyons, P.R.A. and Weber, R.O. Geometrical effects on flames spread rate for wildland fine fuels. *Combustion Science and Technology* **89** : 153-165.

Maister, B.J. 1970. *The development of production curves and the study of the growth habit of Nothofagus solandri var cliffortioides trees.* Botany Honours Part III Project, University of Canterbury.

Malanson, G.P. 1987. Diversity, stability and resilience: effects of fire regime. In : Trabaud, L. (ed). *The Role of Fire in Ecological Systems.* SPB Academic Publishing, The Hague. pp. 49-65.

Malanson, G.B. and Butler, D.R. 1984. Avalanche paths as fuel breaks: implications for fire management. *Journal of Environmental Management* **19** : 229-238.

Malanson, G.P. and Trabaud, L. 1988. Computer simulation of fire behaviour in garrigue. *Applied Geography* **8** : 53-64.

Malingreau, J.P., Albini, F.A., Andrae, M.D. and nine others. 1993. Group report : Quantification of fire characteristics from local to global scales. In : Crutzen, P.J. and Goldammer, J.G. (eds) *Fire in the Environment : The Ecological, Atmospheric, and Climatic Importance of Vegetation Fires.* John Wiley and Sons, New York. pp. 315-335.

Markgraf, V., McGlone, M. and Hope, G. 1995. Neogene paleoenvironmental and paleoclimatic changes in southern temperate ecosystems - a southern perspective. *Trends in Ecology and Evolution* **10** : 143-147.

Marsden-Smedley, J.B. 1993. *Fire Characteristics and Fire Behaviour in Tasmanian Buttongrass Moorlands.* Parks and Wildlife Service. Department of Environment and Land Management. Hobart, Tasmania.

McArthur, A.G. 1962. *Control Burning in Eucalypt Forests.* Australian Forestry and Timber Bureau, Leaflet No. 80, Canberra.

McArthur, A.G. 1966. *Weather and Grassland Fire Behaviour.* Australian Forestry and Timber Bureau, Leaflet No. 100, Canberra.

McArthur, A.G. 1967. *Fire Behaviour in Eucalypt Forests.* Australian Forestry and Timber Bureau, Leaflet No. 107, Canberra.

McArthur, A.G. 1968. The Tasmanian Bushfires of 7 February 1967 and associated fire characteristics. In: *The Second Australian Conference on Fire.* Australian Fire Protection Association, Melbourne. pp. 25-48.

McArthur, A.G. 1977. *Grassland fire danger meter Mark V.* Country Fire Authority of Australia. (published as a linear slide rule).

McArthur, D.A. and Packham, D.R. 1971. Radiation from an ethylene diffusion flame. *Combustion and Science Technology* **2** : 299-306.

McArthur, J.L. 1964. *A Geomorphological Study of the Cass Drainage Basin.* Unpublished M.A. Thesis, Department of Geography, University of Canterbury.

McArthur, J.L. 1975. Some observations on periglacial morphogenesis in the Southern Alps, New Zealand. *Geografiska Annaler* **57A** : 213-224.

McCaw, L. 1988. Measurement of fuel quantity and structure for bushfire research and management. In : Cheney, N.P. and Gill, A.M. (eds) *Proceedings of the Conference on Bushfire Modelling and Fire Danger Rating Systems,* Canberra, 11-12 July, 1988. CSIRO, Canberra. pp. 147-155.

McKendry,P.J. and O'Connor, K.F. 1990. *The Ecology of Tussock Grasslands for Production and Protection.* Unpublished Report for the Department of Conservation.

McKinsey, D. 1988. Priority ranking for prescribed burning in the Cuyamaco Rancho State Park using a geographic information system. In : *Proceedings GIS/LIS Symposium, 1988*, November 30-December 2, San Antonio. Volume 2. pp. 961-970.

McGlone, M.S. 1981. Forest fire following holocene tephra fall. In : Howorth, R.; Froggat, P.; Vucetich, C.G. and Collen, J.D. (eds) *Proceedings of tephra workshop*, June 30th - July 1st 1980. Victoria, University of Wellington, Wellington, pp. 80-86..

McGlone, M.S. 1989. The polynesian settlements of New Zealand in relation to environmental and biotic changes. In : Rudge, M.R. (ed) Moas, Mammals and Climate in the Ecological History of New Zealand. *The New Zealand Journal of Ecology* (Supplement) **12** : 115-129.

McLean, D.M. 1991. Impact winter in the global K/T extinctions. No definitive evidence. In : Levine, J.S. (ed) *Global Biomass Burning.* MIT Press, Cambridge, MA. pp. 493-503.

McRae, R.H.D. 1992. Prediction of area prone to lightning ignition. *International Journal of Wildland Fire* **2** : 123-129.

McSaveney, M.J. and Whitehouse, I.E. 1989. Anthropic erosion of mountain land in Canterbury. In : Rudge, M.R. (ed) Moas, mammals and climate in the ecological history of New Zealand. *New Zealand Journal of Ecology (Supplement)* **12** : 151-165.

Merton, P. 1986. *Investigation of Two Pakihi Mires in South Westland.* Unpublished B. For. Sc. Dissertation, School of Forestry, University of Canterbury.

Mitchell, T.L. 1848. *Journal of an Expedition into the Interior of Tropical Australia.*

Brown, Green and Longman, London.

Meurk, C.D. 1978. Alpine phytomass and primary productivity in Central Otago, New Zealand. *New Zealand Journal of Ecology* **1** : 27-50.

Miller, W.A, Howard, S.M., and Moore, D.G. 1986. Use of AVHRR data in an information system for fire management in the Western United States. In : *Proceedings of the 20th International Symposium on Remote-Sensing of the Environment.* Nairobi, Kenya. Volume 1, pp. 67-79.

Molloy, B.P.J. 1977. The fire history. In : Burrows, C. (ed) *Cass : History and Science in the Cass District, Canterbury, New Zealand.* Department of Botany, University of Canterbury.

Molloy, B.P.J., Burrows, C.J., Cox, J.E., Johnston, J.A. and Wardle, P. 1963. Distribution of subfossil forest remains, eastern South Island, New Zealand. *New Zealand Journal of Botany* **2** : 143-176.

Monk, C.D. 1968. Successional and environmental relationships of the forest vegetation of north central Florida. *USDA Division of Forestry Bulletin* **13** : 49-66.

Moore, L.B. 1955. The plants of tussock grassland. *Proceedings of the New Zealand Ecological Society* **3** : 7-8.

Morris, G.A. 1988. *A Simple Method for Computing Spotting Distances form Wind-driven Surface Fires.* USDA Forest Service Research Note, INT-374.

Mutch, R.W. 1970. Wildland fires and ecosystems - a hypothesis. *Ecology* **51** : 1046-1051.

Nelson, R.M. and Adkins, C.W. 1986. Flame characteristics of wind driven surface fires. *Canadian Journal of Forest Research* **16** : 1293-1300.

Noble, I.R., Barry, G.A.V., and Gill, A.M. 1980. McArthur's fire-danger meter expressed as equations. *Australian Journal of Ecology* **5** : 201-203.

Nyerges, T.L. 1992. Understanding the scope of GIS; its relationship to environmental modeling. In : Goodchild, M.F., Parks, B.O. and Steyaert, L.T. (eds). *Environmental Modelling With GIS.* Oxford University Press, New York and London. pp. 74-95.

O'Connor, K.F. 1982. The implications of past exploitation and current developments to the conservation of South Island tussock grasslands. *New Zealand Journal of Ecology* **5** : 97-107.

O'Connor, K.F. 1984. Stability and instability of ecological systems in New Zealand mountains. *Mountain Research and Development* **4** : 15-29.

O'Connor, K.F. 1993. The influence of science on the use of tussock grasslands. *Review Journal of the Tussock Grasslands and Mountainland Institute* **43** : 15-78.

Pagni, J. and Peterson, G. 1973. Flame spread through porous fuels. *14th Symposium (International) on Combustion*, The Combustion Institute, Pittsburg. pp. 1099-1107.

Payton, I.J. and Brasch, D.J. 1978. Growth and nonstructural carbohydrate response in *Chionochloa rigida* and *C. macra* and their short-term response to fire. *New Zealand Journal of Botany* **16** : 435-460.

Payton, I.J. and Mark, A.F. 1979. Long-term effects of burning on growth, flowering and carbohydrate reserves in narrow-leaved snow tussock (*Chionochloa rigida*). *New Zealand Journal of Botany* **17** : 43-54.

Peet, G.B. 1967. The shape of mild fires in Jarrah forest. *Australian Forestry* **31** : 121-127.

Periera, J.M.C and Vasconcelos, M.J. 1990. Fire propagation in heterogeneous environments and a new spread algorithm for FIREMAP. In : *Proceedings of the International Conference on Forest Fire Research*, Coimbra, Portugal. B.14. pp. 1-15.

Philpot, C.W. 1968. *Mineral Content and Pyrolysis of Selected Plant Material.* USDA Forest Service Research Paper, INT-102.

Pompe, A. and Vines, R.G. 1966. The influence of moisture on the combustion of leaves. *Australian Forestry* **30** : 231-241.

Possingham, H.P., Comins, H.N. and Noble, I.R. 1995. The fire and flammability niches in plant communities. *Journal of Theoretical Biology* **174** : 97-108.

Potts, D.F. and Morris, G.A. 1989. Modelling diurnal fuel moisture behaviour. In : *Proceedings of the 10th Conference on Fire and Forest Meteorology*, 17-21 April,

1989. Ottawa, Canada. Forestry Canada. pp. 295-297.
Pyne, S.J. 1984. *Introduction to Wildland Fire : Fire Management in the United States.* John Wiley and Sons. New York.

Pyne, S.J. 1991. *Burning Bush : A Fire History of Australia.* Allen and Unwin, Sydney.

Pyne, S.J. 1992. Keeper of the flame : a survey of anthropogenic fire. In : Crutzen, P.J. and Goldammer, J.G. (eds) *Fire in the Environment : The Ecological, Atmospheric, and Climatic Importance of Vegetation Fires.* John Wiley and Sons, New York. pp. 245-267.

Reich, P.B., Uhl, C., Walters, M.B. and Ellsworth, D.S. 1991. Leaf life span as a determinant of leaf structure and function among 23 Amazonian tree species. *Oecologia* **86** : 16-24.

Romme, W.H. and Knight, D.H. 1981. Fire frequency and subalpine forest succession along a topographic gradient in Wyoming. *Ecology* **62** : 319-326.

Romme, W.H. and Despain. D.G. 1989. Historical perspectives on the Yellowstone fires of 1988. *BioScence* **39** : 695-699.

Rothermel, R.C. 1972. *A Mathematical Model for Predicting Fire Spread in Wildland Fuels.* USDA Forest Service Research Paper, INT-115.

Rothermel, R.C. 1983. *How to Predict the Spread and Intensity of Forest and Range Fires.* USDA Forest Service General Technical Report, INT-143.

Rothermel, R.C. 1991a. Predicting behaviour of the 1988 Yellowstone fires : projections vs. reality. *International Journal of Wildland Fire* **1** : 1-10.

Rothermel, R.C. 1991b. *Predicting the Behaviour and Size of Crown Fires in the North Rocky Mountains.* USDA Forest Service Research Paper, INT-438.

Rothermel, R.C. and Anderson, H.E. 1966. *Fire Spread Characteristics Determined in the Laboratory.* USDA Forest Service Research Paper, INT-30.

Rothermel, R.C. and Rinehart, G.C. 1983. *Field Procedures for Verification and Adjustment of Fire Behaviour Predictions.* USDA Forest Service General Technical Report, INT-142.

Salazar, L.A. and Bradshaw, L.S. 1986. Display and interpretation of fire behaviour probabilities for long-term planning. *Environmental Management* **10** : 393-402.

Salazar, L.A. and Palmer, K.E. 1987. Spatial analysis of fire behaviour for fuel management decision making. In : *Proceedings of the GIS/LIS '87 Symposium.* ASPRS, Falls Church, VA. Poster Paper.

Salazar, L.A. and Power, J. 1988. Three-dimensional representations for fire management planning. In : *Proceedings GIS/LIS Symposium, 1988*, November 30-December 2, San Antonio. Volume 2. pp. 948-960.

Sewell, T.G. 1969. Burning of montane tussock grassland. *Agriculture* **77** : 263-269.

Shafizadeh, F. 1968. Pyrolysis and combustion of cellulosic materials. *Advances in Carbohydrate Chemistry* **23** : 419 - 474.

Shanks, A., Glenny, D., Gibson, R., Rosser, K., Roozen, D., Phillipson, S., Steven, J. and Arand, J. 1990. *Coleridge, Cragieburn and Cass Ecological Districts : Survey Report for the Protected Natural Areas Programme.* Department of Conservation, Wellington.

Shasby, M.B., Burgan, R.E. and Johnson, R.R. 1981. Broad area forest fuels and topographic mapping using digitised Landsat and terrain data. In : *Proceedings of the 7th International Symposium on Machine Processing of Remotely Sensed Data.* West Lafayette, pp. 529-527.

Snyder, J.R. 1984. The role of fire: Mutch ado about nothing ? *Oikos* **43** : 404-405.

Sneeuwjagt, R.J. and Frandsen, W.H. 1977. Behaviour of experimental grass fires vs. predictions based on Rothermel's fire model. *Canadian Journal of Forest Research* **7** : 357-367.

Soma, S. and Saito, K. 1991. Reconstruction of fire whirls using scale models. *Combustion and Flame* **86** : 269-284.

Soons, J. 1977. The geomorphology of the Cass district. In : Burrows, C. (ed) *Cass : History and Science in the Cass District, Canterbury, New Zealand.* Department of Botany, University of Canterbury. pp. 79-93.

Southgate, R. and Possingham, H.P. 1995. Modelling the re-introduction of the greater bilby, *Macrotis lagotis*, using the metapopulation model analysis of the likelihood of extinction (ALEX). *Biological Conservation* **73** : 151-160.

Stauffer, D. 1985. *Introduction to Percolation Modelling*. Taylor and Francis, London.

Steward, F.R. 1974. Fire spread through a fuel bed. In : Blackshear, P.L. (ed) *Heat Transfer in Fires : Thermophysics, Social Aspects, Economic Importance*. Scripta Book Co. pp. 315-379.

Steyaert, L.T. 1992. A perspective on the state of environmental simulation modelling. In : Goodchild, M.F., Parks, B.O. and Steyaert, L.T. (eds). *Environmental Modelling With GIS*. Oxford University Press, New York and London. pp. 16-31.

Stocks, B.J., Lawson, B.D., Alexander, M.E., Van Wagner, C.E., McAlpine, R.S., Lynham, T.J. and Dube, D.E. 1989. The Canadian Forest Fire Danger Rating System : an overview. *Forestry Chronicle* **65** : 450-457.

Stokstad, E. 1996. Model wind helps build fire. *New Scientist* **151** (13 July, 1996) : 15

Strauss, D., Bednar, L. and Mees, R. 1989. Do one percent of forest fires cause ninety-nine percent of the damage ? *Forest Science* **35** : 319-328.

Sundgren, B. 1975. *Theory of Data Bases*. Petrocelli Information Series. Petrocelli/ Charter, New York.

Sun Soft, 1994. *Fortran 3.0.1: User's Guide*. Sun Soft, California.

Swetnam, T.W. 1993. Fire history and climate in Giant Sequoia groves. *Science* **262** : 885-889.

Swetman, T.W. and Betancourt, J.L. 1990. Fire-Southern Oscillation relationships in the southwestern United States. *Science* **249** : 1017-1020.

Tangren, C.D. 1976. The trouble with fire intensity. *Fire Technology* **12** : 261-265.

Thomas, P.H. 1967. Some aspects of the spread and growth of fire in the open. *Forestry* **20** : 139-164.

Thomas, P.H. 1971. Rates of spread of some wind-driven fires. *Forestry* **44** : 155-175.

Timmins, S. M. 1992. Wetland vegetation recovery after fire : Eweburn Bog, Te Anau, New Zealand. *New Zealand Journal of Botany* **30** : 383-399.

Tomlin, C.D. 1986. *The IBM Personal Computer Version of the Map Analysis Package.* GSD/IBM AcIS Project, Report Number LCGSA-85-16. Laboratory for Computer Graphics and Spatial Anlaysis. Graduate School of Design, Harvard University.

Travaud, L.V., Christensen, N.L. and Gill, A.M. 1993 Historical biogeography of fire in temperate and mediterranean ecosystems. In : Crutzen, P.J. and Goldammer, J.G. (eds) *Fire in the Environment : The Ecological, Atmospheric, and Climatic Importance of Vegetation Fires*. John Wiley and Sons, New York pp 277-297.

Trollope, W.S. 1984. Fire in savanna. In : Booysen, P. de V and Tainton, N.M. (eds). *Ecological Effects of Fire in South African Ecosystems*. Spreinger-Verlag, Berlin. pp. 151-175.

Troumbis, A.S. and Trabaud, L. 1989. Some questions about flammability in plant ecology. *Acta Oecologia Plant* **10** : 167-175.

Van Wagner, C.E. 1967. *Calculations on Forest Fire Spread by Flame Radiation.* Candian Department of Forestry, Report Number 1185.

Van Wagner, C.E. 1969. A simple fire-growth model. *The Forestry Chronicle* **45** : 103-104.

Van Wagner, C.E. 1977a. Conditions for the start and spread of crown fires. *Canadian Journal of Forest Research* **7** : 23-34.

Van Wagner, C.E. 1977b. Effect of slope on fire spread rate. *Canadian Forest Service Bimonthly Research Notes* **33** (1) : 7-8

Van Wagner, C.E. 1983. Fire behaviour in northern conifer forests and shrublands. In : Wein, R.W. and MacLean, D.A. (eds) *The Role of Northern Circumpolar Ecosystems.* John Wiley and Sons, New York. pp. 65-80.

Van Wagner, C.E. 1988. Effect of slope on fires spreading downhill. *Canadian Journal of Forest Research* **18** : 819-820.

Van Wilgen, B.J. 1984. Adaption of the United States Fire Danger Rating System to fynbos conditions. I : A fuel model for fire danger rating in the fynbos biome. *South African Forestry Journal* **129** : 61-65.

Van Wilgen, B.W., le Maitre, D.C., Kruger, F.J. 1985. Fire modelling in South African fynbos (macchia) vegetation and predictions from Rothermel's fire model. *Journal of Applied Ecology* **22** : 207-216.

Van Wilgen, B.W. and Wills, A.J. 1988. Fire behaviour prediction in savanna vegetation. *South African Wildlife Research* **18** : 41-46.

Van Wilgen, B.J., Higgins, K.B. and Bellstedt, D.U. 1990. The role of vegetation structure and fuel chemistry in excluding fire from forest patches in the fire-prone fynbos shrublands of South Africa. *Journal of Ecology* **78** : 210-222.

Vasconcelos, M.J. 1988. *Simulation of Fire Behaviour with a Geographic Information System*. Unpublished M.Sc Thesis, School of Renewable Natural Resources, University of Arizona. Tuscon, Arizona.

Vasconcelos, M.J., Guertin, D.P., and Zwolinski, M.J. 1990. FIREMAP - Simulation of fire behaviour - A GIS supported system. In : Krammes, J.S. (tech coord) *Proceedings of the Effects of Fire in Management of Southwestern Ecosystems.* USDA Forest Service General Technical Report, RM-191. pp. 217-221.

Vasconcelos, M.J. and Guertin, D.P. 1992. FIREMAP - Simulation of fire growth with a Geographic Information System. *International Journal of Wildland Fire* **2** : 87-96.

Vasconcelos, M.J. and Zeigler, B.P. 1993. Discrete-event simulation of forest landscape response to fire disturbances. *Ecological Modelling* **65** : 177-198.

Vasconcelos, M.J., Zeigler, B.P. and Graham, L.A. 1993. Modelling multi-scale ecological processes under the discrete-event systems paradigm. *Landscape Ecology* **8** : 273-286.

Veno, P.A. 1976. Successional relationships of five Florida plant communities. *Ecology* **57** : 498-508.

Vasconcelos, M.J., Pereira, J.M.C. and Zeigler, B.P. 1994. Simulation of fire growth in mountain environments. In : Price, M.F. and Heywood, D.I. (eds) *Mountain*

Environments and Geographical Information Systems. Taylor and Francis, Bristol. pp. 167-185.

Vines, R.G. 1981. Physics and chemistry of rural fires. In : Gill, A.M., Groves, R.H. and Noble, I.R. (eds) *Fire and the Australian Biota*. Australian Academy of Science, Canberra. pp. 129-151.

Viosca, P. Jr. 1931. Spontaneous combustion in the marshes of Southern Louisiana. *Ecology* **12** : 439-442.

Viruozo. 1996. *Virtuozo Soft Photogrammetry Package 1.2a for Irix*. Virtuozo Limited, Brisbane.

Vogl, R.J. 1974. Effects of fire on grasslands. In : Kozlowski, T.T. and Ahlgremn, C.E. (eds) *Fire and Ecosystems*. Academic Press, New York. pp. 139-194.

Von Niessen, W. and Blumen, A. 1988. Dynamic simulation of forest fires. *Canadian Journal of Forest Research* **18** : 805-812.

Walker, J. 1981. Physics and chemistry of rural fires. In : Gill, A.M., Groves, R.H. and Gill, I.R. (eds) *Fire and the Australian Biota*. Australian Academy of Sciences, Canberra. pp. 101-127.

Wallace, G. 1993. A numerical fire simulation model. *International Journal of Wildland Fire* **3** : 111-116.

Wade, D.D. and Ward, D.E. 1973. *An Analysis of the Air Force Bombing Range Fire*. USDA Forest Service Research Paper, SE-105.

Ward, D.E. and Radke, L.F. 1993. Emissions measurements from vegetation fires : a comparative evaluation of methods and results. In : Crutzen, P.J. and Goldammer, J.G. (eds) *Fire in the Environment : The Ecological, Atmospheric, and Climatic Importance of Vegetation Fires*. John Wiley and Sons, New York. pp. 53-77.

Wardle, J.A. 1984. *The New Zealand Beeches: Ecology, Utilisation and Management*. New Zealand Forest Service, 1984.

Weber, R.O. 1989a. Analytical models for fire spread due to radiation. *Combustion and Flame* **78** : 398-408.

Weber, R.O. 1989b. Thermal theory for determining the burning velocity of a laminar flame using the inflection point in the temperature profile. *Combustion Science Technology* **64** : 135-139.

Weber, R.O. 1990. A model for fire propagation in arrays. *Mathematical and Computer Modelling* **13** (12) : 95-102.

Weber, R.O. 1991a. Modelling fire spread through fuel beds. *Progress in Energy and Combustion Science* **17** : 67-82.

Weber, R.O. 1991b. Towards a comprehensive fire spread model. *International Journal of Wildland Fire* **1** : 245-8.

Wesseling, C.G., Kassenburg, D.J., Burrough, P.A. and Van Deursen, W.P.A. 1996. Integrating dynamic environmental models in GIS : the development of a Dynamic Modelling language. *Transactions in GIS* **1** : 1-9.

Whelan, R.J. 1995. *The Ecology of Fire.* Cambridge University Press, Cambridge.

Whitehouse, I.E. 1984. Erosion in the eastern South Island high country - a changing perspective. *Journal of the Tussock Grasslands and Mountain Lands Institute Review* **42** : 3-23.

Williams, F.A. 1977a. Mechanics of fire spread. *16th Symposium (International) on Combustion.* The Combustion Institute, Pittsburg. pp. 1281-1294.

Williams, F.A. 1985. Urban and wildland fire phenomenology. *Progress in Energy and Combustion Science* **8** : 317-354.

Williams, P.A. 1977b. Growth, biomass and net productivity of tall tussock (*Chionochloa*) grasslands, Canterbury, New Zealand. *New Zealand Journal of Botany* **15** : 399-442.

Williamson, G.B. and Black, E.M. 1981. High temperatures of forest fires under pines as a selective advantage over oaks. *Nature* **293** : 643-644.

Williamson, H.D. 1988. Fuel curing and fuel quantity from remotely sensed data. In : Cheney, N.P. and Gill, A.M. (eds) *Proceedings of the Conference on Bushfire Modelling and Fire Danger Rating Systems,* Canberra, 11-12 July, 1988. CSIRO,

Canberra. pp. 177-183.

Wilson, A.A.G. 1988. Width of a firebreak that is necessary to stop grass fires: some field experiments. *Canadian Journal of Forest Research* **18** : 682-688.

Wilson, C.W., Masters, R.E. and Bukenhofer, G.A. 1995. Breeding bird response to pine-grassland restoration for red-cockaded woodpeckers. *Journal of Wildlife Management* **59** : 56-67.

Wilson, H.D. 1994. Regeneration of native forest on Hinewai Reserve, Banks Peninsula. *New Zealand Journal of Botany* **32** : 373-383.

Wilson, R.A. 1980. *Reformulation of Forest Fire Spread Equations*. USDA Forest Service Research Note, INT-292.

Wilson, R.A. 1985. Observations of extinction and marginal burning states in free burning porous fuel beds. *Combustion Science and Technology* **44** : 179-193.

Wilson, R.A. 1990. *Reexamination of Rothermel's Fire Spread Equations in No-wind and No-slope Conditions*. USDA Forest Service Research Paper, INT-434.

Yool, S.R., Eckhardt, D., Estes, J.E. and Consentino, M.J. 1985. Describing the bushfire hazard in southern California. *Annals of the Association of American Geographers* **75** : 417-430.

Zack, J.A. and Minnich, R.A. Integration of Geographic Information Systems with a diagnostic wind field for fire management. *Forest Science* **37** : 560-574.

Appendix 1 - Summary of Basic (Metricised) Fire Spread Equations

Input Parameters for Basic Equations in Metric Form

w_o - Ovendry fuel loading, $kg.m^{-2}$

δ - Fuel bed depth, m.

σ - Surface-area to volume ratio, cm^{-1}

h - Fuel heat content $kJ.kg^{-1}$

ρ_p - Fuel particle density, $kg.m^{-3}$

m_f - Fuel moisture content, dimensionless fraction.

s_t - Fuel total mineral content, dimensionless fraction.

s_e - Fuel effective (silica-free) mineral content, dimensionless fraction.

U - Windspeed at mid-flame height, $m.min^{-1}$.

ϕ - Slope (vertical rise/vertical run), dimensionless fraction.

m_x - Fuel moisture content of extinction, dimensionless fraction.

Output Parameters for Basic Equations in Metric Form

R - Rate of spread, $m.min^{-1}$

I_R - Reaction intensity, $kJ.m^{-2}.m^{-1}$

I_B - Byram's fireline intensity, $kW.m^{-1}$.

L_f - Flame length, m.

Basic (Metricised) Fire Spread Equations

$$R = \frac{I_R \xi (1 + \phi_w + \phi_s)}{\rho_b \varepsilon Q_{ig}}$$ Rate of spread ($m.min^{-1}$)

$$I_R = \Gamma' w_n h \eta_m \eta_s$$ Reaction Intensity $kJ.min^{-1}.m^{-2}$

$$\Gamma' = \Gamma'_{max} \left(\frac{\beta}{\beta_{op}}\right)^A \exp\left[A\left(\frac{1 - \beta}{\beta_{op}}\right)\right]$$ ***Optimum reaction velocity (min^{-1})

$$\Gamma'_{max} = (0.0591 + 2.926\sigma^{-1.5})^{-1}$$ Maximum reaction velocity ($m.min^{-1}$)

$$\beta_{op} = 0.20395\sigma^{-0.8189}$$ Optimum packing ratio (dimensionless)

$$A = 1/(6.7229\sigma^{0.1} - 7.27)$$ ***

$$\eta_m = 1 - 2.59\left(\frac{m_f}{m_x}\right)^3 + 5.11\left(\frac{m_f}{m_x}\right)^2 - 3.52\left(\frac{m_f}{m_x}\right)$$ Mineral damping coefficient (dimensionless)

$\eta_s = 0.174 s_e^{-0.19}$ Mineral damping coefficient (dimensionless)

$\xi = (192 + 7.9095\sigma)^{-1} \exp[(0.792 + 3.7597\sigma^{0.5})(\beta + 0.1)]$ Propagating flux ratio (dimensionless)

$\phi_w = C(3.281U)^B (\frac{\beta}{\beta_{op}})^{-E}$ Wind coefficient (dimensionless)

$C = 7.47\exp(0.8711\sigma^{0.55})$

$B = 0.15988\sigma^{0.54}$

$E = 0.715\exp(-0.01094\sigma)$

$w_n = w_o(1 - s_t)$ Net fuel loading ($kg.m^{-2}$)

$\phi_s = 5.275\beta^{-0.3}(\tan\phi)^2$ Slope factor (dimensionless)

$\rho_b = \frac{w_o}{\delta}$ Ovendry bulk density ($kg.m^{-3}$)

$\varepsilon = \exp(\frac{-4.528}{\sigma})$ Effective heating number (dimensionless)

$Q_{ig} = 581 + 2549 m_f$ Heat of preignition ($kJ.kg^{-1}$)

$\beta = \frac{\rho_p}{\rho_b}$ Packing ratio (dimensionless)

$I_B = (\frac{1}{60}) I_R R(\frac{12.6}{\sigma})$ Byram's Fireline Intensity ($kW.m^{-1}$)

$L_f = 0.0775 I_B^{0.46}$ Flame Length (m)

The expressions for Byram's fireline intensity and for flame length are metric revisions of those of Albini (1976).

*** Denotes equations that were corrected from those of Wilson (1980) such that they conformed with the original formulations of Rothermel (1972).

Appendix 2 - Fortran Routines

Sensitivity Analysis Routine

The routine *sensan.f* was written to perform the various sensitivity analyses of the fire spread model of Rothermel (1972) performed in the thesis. These include analysis of the effect of individual variables on the outputs and also the analysis of different fuel models (both those of Rothermel, 1972 and those built for this thesis). The program uses the metric revisions of Wilson (1980).

```
c ---------------------------------------------------------------------------------------------------
                program sensan
c Designed to conduct sensitivity analysis on the model of Rothermel (1972)
c Writes out CSV files to a specified OP text file

c Initiate the variables used in the analysis.
                real mf,st,se,sv,ld,dp,h,pd,mx,bdens,pk,efht,nld,opk,qig,r
                real wf,sf,prop,c,b,e,scr,min,moist,gmax,gopt,a,ri,s,w

c Assign variables constants depending upon the fuel being used.
                data s,ld,h,se,st/0,0.1,18608,0.01,0.0555/
                data pd,sv,w,mx,dp,mf/512,49,431,0.3,0.762,0.1/
                data pi/3.1415927/

c Set up a loop to incrementally test the variable of interest
                do 1000, w=0,498,83

c Calculate the secondary fuel parameters for the ignited cell

                bdens=ld/dp
                pk=bdens/pd
                efht=exp(-4.528/sv)
                nld=ld/(1-st)
                opk=(sv**-0.8189)*0.20395
                qig=581+(2594*mf)

c Calculate the wind co-efficient (wf)

                c=7.47*exp(-0.8711*sv**0.55)
                b=0.15988*sv**0.54
                e=0.715*exp(-0.01094*sv)
                wf=(c*(3.281*w)**b)*((pk/opk)**-e)

c Calculate the slope coefficient (sf).
                scr=atan(s)
                sf=(5.275*pk**-0.3)*(tan(scr)**2)

c Calculate the propagating flux ratio (prop)
                prop=((192+7.9095*sv)**-1)*(exp((0.792+3.7597*sv**0.5)*(pk+0.1)))

c Calculate the mineral and moisture damping coefficients (min and moist)
```

```
                min=0.174*(se**-0.19)
                moist=1-(2.59*(mf/mx))+(5.11*((mf/mx)**2))-(3.52*((mf/mx)**3))

c Calculate the maximum & optimum reaction velocities (gmax and gopt)

                gmax=(0.0591+2.926*sv**-1.5)**-1
                a=1/(((sv**0.1)*6.7229)-7.27)
                interm=(1-pk/opk)
                gopt=(gmax*(pk/opk)**a)*exp(a*(1-pk/opk))

c Calculate the reaction intensity (ri)
                ri=gopt*nld*h*min*moist

c Finally calculate the rate of spread for cell(i,j) to cell(k,l)
                r=(ri*prop*(1+wf+sf))/(bdens*efht*qig)
                if(r.lt.0) r=0

c Write the results of the analysis out to an ASCII file in CSV format.
                open(10,status='unknown',file='grassland')
                write (10,2000) w/16.6,r
2000            format(f7.2,',',f7.2)

1000            continue

                end
c ---------------------------------------------------------------------------------------------------
```

Sørensen Analysis Routine

The routine similarity.f was used to calculate the Sorensen coefficient values presented in Chapters 5 and 6. The expression used was taken from Greig-Smith (1983).

```
c ---------------------------------------------------------------------------------------------------
                program similarity

c Define the arrays and variables to be used.
                integer,a,b,c
                real index
                integer model(43,124),cass(43,124),dirn(43,124)


c Define the size of the arrays
                xdim=43
                ydim=124

c Read in files containing information on the simulated and real fires.
                open(10,status='old',file='fire330.dat')
                open(20,status='old',file='burngrid.dat')

                do 130,i=1,ydim

                read(10,100) (model(j,ydim+1-i),j=1,xdim)
                read(20,110) (cass(j,ydim+1-i),j=1,xdim)

130             continue
```

```
100         format(100(100(i1,x),:,/) )
110         format(100(100(i1,x),:,/) )

            close (10)
            close (20)


            do 200,n=1,xdim,1
            do 210,o=1,ydim,1

            if(model(n,o).eq.1.and.cass(n,o).eq.1) a=a+1
            if(model(n,o).eq.1.and.cass(n,o).eq.0) b=b+1
            if(model(n,o).eq.0.and.cass(n,o).eq.1) c=c+1
210         continue
200         continue

            index=2*a/2*a+b+c
            print *,'a :',a
            print *,'b :',b
            print *,'c:',c
            print *,'index :',index

            end
c -------------------------------------------------------------------------------------------------
```

PYROCART Test Routine

The following routine (*hetero.f*) was that used to produce the fire shapes presented in Chapter 5. The specific routine below was used to create the fire shapes in spatially non-uniform fuels and terrain in a temporally non-uniform wind field. Included in the routine are the flanking/backing routines of Green *et al.* (1990) and the downslope corrections of Van Wagner (1988).

~ denotes where a complete line was divided into two text lines.

```
c -------------------------------------------------------------------------------------------------
            program hetero

c Designed to simulate fire spread in a spatially heterogenous environment
c using the fire spread model of Rothermel (1972). Included in the model
c are the downslope rate of spread corrections of Van Wagner (1988) and the
c flanking/backing rate of spread coreections of Green et al. (1990).

c Firstly initiate variables (fuel descriptors, wind & elevation).
            integer height(100,100)
            integer fuel(100,100), status(100,100), wind(100,100)

c Descriptors of array size for writing to Ascii files. xdim and ydim specify
c the x and y extent of the landscape (array) and fx and fy specify the ignition
c source.
            xdim=100
            ydim=100
            fx=50
            fy=25
```

```
c Read in Arc/InfoASCII grids (*.dat files - wind, elevation & fuel). Arrays are
c read in bottom to top, left to right to ensure that cells are referenced as in a
c Cartesian plane.
                open(10,status='old',file='wind.dat')
                open(20,status='old',file='height.dat')
                open(30,status='old',file='fuel.dat')

                do 125,i=1,ydim
                read(10,100) (wind (j,ydim+1-i),j=1,xdim)
                read(20,110) (height (j,ydim+1-i),j=1,xdim)
                read(30,120) (fuel (j,ydim+1-i),j=1,xdim)

100             format(100(100(i3,x),:,/) )
110             format(100(100(i3,x),:,/) )
120             format(100(100(i1,x),:,/) )

125             continue

                close(10)
                close(20)
                close(30)

c Ignite the first cell (fx,fy)
                status(fx,fy)=1

c Now into the main loop sequence of the program (i.e check for burning cells,
c calculate spread rate out of them into their neighbours, check for fire spread
c and update the appropriate grids, parameters).
                print *,'How many iterations is the routine to run for ?'
                read *,it
                do 500, m=1,it,1

                 do 450, n=1,100
                  do 400, o=1,100

                    if (status(n,o).gt.1) status(n,o) = status(n,o)-1

400              continue
450             continue

                call burnsearch(status,fuel,wind,height,m,it)

500             continue

                status(fx,fy)=4

c Finally write the <<status>> array to a format suitable for IP to Arc/Info. See
c the Arc commands <<asciigrid>> and <<gridascii>> for more information.
                open(50,status='unknown',file='fire.dat')
                write(50,600)xdim,ydim
                do 550,i=1,100
                write(50,650) (status(j,101-i),j=1,100)
550             continue
600             format('ncols',x,f4.0/'nrows',x,f4.0/'xllcorner 0'/'yllcorner 0'/'cellsize 50')
650             format(x,100(i1,x))

                end
```

```
c ------------------------------------------------------------------------------------------
c Subroutines are found below here in the order in which they are called.
c Subroutine <<burnsearch>> checks for burning cells.

                subroutine burnsearch(status,fuel,wind,height,m,it)

                integer status(100,100),fuel(100,100), wind (100,100)
                integer height(100,100)

                do 1000, i=1,100
                 do 1010, j=1,100
                  if (status(i,j).eq.1) call rosout(status,height,wind,fuel,i,j,m,it)
1010             continue
1000            continue

                return
                end

c ------------------------------------------------------------------------------------------
c Subroutine <<rosout>> initiates the calculation of rate of spread out of
c the burning cell into adjacent cells.

                subroutine rosout(status,hgt,wd,fl,i,j,m,it)

c Firstly initiate variables read in landscape parameters etc.
                real rosadj, e
                integer hgt(100,100), status(100,100), wd(100,100), fl(100,100), i, j, cell,
~               dlag

c Set up a loop to calculate ROS in the eight cardinal directions
c Ensure fire does not burn beyond the array boundaries.
                dirn=0
                dlag=0

                do 2000, k=i-1,i+1,1
                 do 2010, l=j-1,j+1,1

                    if (k.lt.1.or.k.gt.100) goto 2000
                    if (l.lt.1.or.l.gt.100) goto 2010

                   dirn=dirn+1
                   sd=sd+1


                  if (dirn.eq.2.or.dirn.eq.4.or.dirn.eq.6.or.dirn.eq.8) cell=1
                  if (dirn.eq.1.or.dirn.eq.3.or.dirn.eq.7.or.dirn.eq.9) cell=2
                  if (dirn.eq.5) goto 2010

c Now call <<roscalc>> to calculate the maximum rate of spread out of the focal cell.
                call roscalc(hgt,wd,fl,ros,rosz,i,j,k,l,cell,w)

c 'cw' is the wind speed in km/hr (converted from m/min)
                cw=w/16.6

c Calculate the parameter 'e' according to wind speed and fuel type
                if (cw.le.1) e=0
                if (cw.gt.1.and.fl(k,l).eq.1) e=(1-0.826*cw**-0.928)**0.5
                if(cw.gt.1.and.fl(k,l).gt.1) e=(1-exp(0.0058-0.0324*cw**1.2))**0.5
```

```
c Calculate the wind-direction based on the iteration number.
                if(m.le.it*0.667) winddir=180
                if(m.gt.it*0.667) winddir=225

c Adjust the forward rate of spread according to the wind speed and direction.
                if(dirn.eq.1) ang=225
                if (dirn.eq.2) ang=270
                if (dirn.eq.3) ang = 315
                if(dirn.eq.4) ang = 180
                if (dirn.eq.6) ang = 360
                if (dirn.eq.7) ang =135
                if (dirn.eq.8) ang = 90
                if (dirn.eq.9) ang = 45

c Calculate the adjusted rate of spread using the function(s) of Green et al. (1990)
                pmc=(ang-winddir+180)*(3.141/180)
                diff=winddir-ang
                rosadj = ros*(1-e)/(1-e*cos(pmc))

c Limit the flanking and backing spread rates at high(er) wind speeds.
                if (diff.eq.0.and.cw.ge.5.and.rosadj.gt.1.05) rosadj=1.05
                if(diff.eq.45.and.cw.ge.5.and.rosadj.gt.1.21) rosadj=1.21
                if (rosadj.lt.0) rosadj=0

c Test for diagonal lag.
                sd=sd+1
                if (rand(sd).le.0.707) dlag=1
                if (rand(sd).gt.0.707)  dlag=2

                if(rosadj*0.3/25.gt.test.and.status(k,l).eq.0.and.cell.eq.1) status(k,l) = 2
                if(rosadj*0.335.35.gt.test.and.status(k,l).eq.0.and.cell.eq.2.and.dlag.eq.1)
~               status(k,l) = 2
                if(rosadj*0.335.35.gt.test.and.status(k,l).eq.0.and.cell.eq.2.and.dlag.eq.2)
~               status(k,l)=3

2010            continue
2000            continue

                return
                end
c ---------------------------------------------------------------------------------------------
c Subroutine <<roscalc>> calculates the rate of spread out of the burning cell
c into adjacent cells.

                subroutine roscalc(hgt,wd,fl,r,rz,i,j,k,l,cell,w)
                real mf,st,se,sv,ld,dp,h,pd,mx,bdens,pk,efht,nld,opk,qig,r,rz
                real wf,sf,prop,c,b,e,scr,min,moist,gmax,gopt,a,ri,s,ns,negs,sang
                integer fl(100,100),wd(100,100),i,j,cell,hgt(100,100)

c Calculate the slope between the cells (rise/run) and correct for diagonals
                if (cell.eq.1) s=(hgt(k,l)-hgt(i,j))/25
                if (cell.eq.2) s=(hgt(k,l)-hgt(i,j))/35.35

                if (s.lt.0) ns=s*-1
                if (s.ge.0) ns=0
                negs=atan(ns)
                sang=negs*(180/3.1415927)
```

```
                if (s.lt.0) s=0

c Set the wind speed in m/min (as required by Wilson (1980)).
                w=0

c Now check the fuel class and read in the appropriate fuel data file.
                if (fl(k,l).eq.1) then
                open(40,status='old',file='grasst.dat')
                read(40,3010,end=3000) mf,st,se,sv,ld,dp,h,pd,mx

                else if (fl(k,l).eq.2) then
                open(40,status='old',file='unburn.dat')
                read(40,3010,end=3000) mf,st,se,sv,ld,dp,h,pd,mx

                else if (fl(k,l).eq.3) then
                open(40,status='old',file='lslash.dat')
                read(40,3010,end=3000) mf,st,se,sv,ld,dp,h,pd,mx

                else if (fl(k,l).eq.4) then
                open(40,status='old',file='chap2.dat')
                read(40,3010,end=3000) mf,st,se,sv,ld,dp,h,pd,mx

                else if (fl(k,l).eq.5) then
                open(40,status='old',file='chap.dat')
                read(40,3010,end=3000) mf,st,se,sv,ld,dp,h,pd,mx

                else if (fl(k,l).eq.6) then
                open(40,status='old',file='brush.dat')
                read(40,3010,end=3000) mf,st,se,sv,ld,dp,h,pd,mx

                else if (fl(k,l).eq.7) then
                open(40,status='old',file='lslash.dat')
                read(40,3010,end=3000) mf,st,se,sv,ld,dp,h,pd,mx

                else if (fl(k,l).eq.8) then
                open(40,status='old',file='brush2.dat')
                read(40,3010,end=3000) mf,st,se,sv,ld,dp,h,pd,mx

                else if (fl(k,l).eq.9) then
                open(40,status='old',file='timber.dat')
                read(40,3010,end=3000) mf,st,se,sv,ld,dp,h,pd,mx

                else if (fl(k,l).gt.9) then
                print *,'Error in fuel file loading - unable to run the simulation.'
                stop

                end if

                close (40)

3000            continue
3010            format(//,9(//,f12.0))

c Calculate the secondary fuel parameters for the ignited cell
                bdens=ld/dp
                pk=bdens/pd
                efht=exp(-4.528/sv)
```

```
                nld=ld/(1-st)
                opk=(sv**-0.8189)*0.20395
                qig=581+(2594*mf)
c Firstly calculate the wind co-efficient (wf)
                c=7.47*exp(-0.8711*sv**0.55)
                b=0.15988*sv**0.54
                e=0.715*exp(-0.01094*sv)
                wf=(c*(3.281*w)**b)*((pk/opk)**-e)

c Secondly calculate the slope coefficient (sf).
                scr=atan(s)
                sf=(5.275*pk**-0.3)*(tan(scr))

c Now calculate the propagating flux ratio (prop)
                prop=((192+7.9095*sv)**-1)*(exp((0.792+3.7597*sv**0.5)*(pk+0.1)))

c Calculate the mineral and moisture damping coefficients (min and moist)
                min=0.174*(se**-0.19)
                moist=1-(2.59*(mf/mx))+(5.11*((mf/mx)**2))-(3.52*((mf/mx)**3))

c Now calculate the maximum & optimum reaction velocities (gmax and gopt)
                gmax=(0.0591+2.926*sv**-1.5)**-1
                a=1/(((sv**0.1)*6.7229)-7.27)
                interm=(1-pk/opk)
                gopt=(gmax*(pk/opk)**a)*exp(a*(1-pk/opk))

c Calculate the reaction intensity (ri)
                ri=gopt*nld*h*min*moist

c Finally calculate the rate of spread from cell(i,j) to cell(k,l)
                r=(ri*prop*(1+wf+sf))/(bdens*efht*qig)

c Correct for down-slopes using the corrections of Van Wagner (1988).
                rz=(ri*prop*(1+wf+0))/(bdens*efht*qig)
                if(ns.ne.0) sf=1-(0.0330*sang)+(0.000749*sang**2)
                if(ns.ne.0) r=rz*sf
                if(r.lt.0) r=0

                return
                end
c ---------------------------------------------------------------------------------------------
```

PYROCART Cass Validation Routine

The version of PYROCART presented in this section is identical to that used for the validation of the PYROCART model presented in Chapter 6. In essence it is similar to that presented in Section 1.2 above. However there are several major revisions:

- fuel models are stored as linear arrays to minimise file swapping
- the model searches specifically for buring cells on the fire perimeter
- random variations in wind speed and wind direction are simulated.

The first two of these revisions were designed to minimise the time required to run the model.

~ denotes where a complete line was divided into two text lines.

```
c-----------------------------------------------------------------------------------------------
                program spread

c Designed to simulate fire spread in a spatially heterogenous environment
c using the fire spread model of Rothermel (1972). Included in the model
c are the downslope rate of spread corrections of Van Wagner (1988) and the
c flanking/backing rate of spread coreections of Green et al. (1990).
c Firstly initiate variables (fuels, wind speed & direction, and elevation).
c This version includes revised file swapping and array processing routines.

c Firstly initiate variables (fuel descriptors, wind & elevation).
                integer xdim,ydim
                integer height(43,124),fuel(43,124),status(43,124)
                integer speed(43,124),dirn(43,124),sstd(43,124),dstd(43,124)
                real mf(9),st(9),se(9),sv(9),ld(9),dp(9),h(9),pd(9),mx(9)

c Descriptors of array size for writing to ASCII files.
                xdim=43
                ydim=124
                fx=10
                fy=113

c Read in Arc/Info ASCII grids (*.dat files - wind, elevation & fuel).

                open(10,status='old',file='speed.dat')
                open(15,status='old',file='direction.dat')
                open(20,status='old',file='spdstd.dat')
                open(25,status='old',file='dirstd.dat')
                open(30,status='old',file='height.dat')
                open(35,status='old',file='fuel.dat')

                do 130,i=1,ydim

                read(10,100) (speed (j,ydim+1-i),j=1,xdim)
                read(15,105) (dirn (j,ydim+1-i),j=1,xdim)
                read(20,110) (sstd (j,ydim+1-i),j=1,xdim)
                read(25,115) (dstd (j,ydim+1-i),j=1,xdim)
                read(30,120) (height (j,ydim+1-i),j=1,xdim)
                read(35,125) (fuel (j,ydim+1-i),j=1,xdim)

100             format(100(100(i3,x),:,/) )
105             format(100(100(i3,x),:,/) )
110             format(100(100(i3,x),:,/) )
115             format(100(100(i2,x),:,/) )
120             format(100(100(i4,x),:,/) )
125             format(100(100(i1,x),:,/) )

130             continue

                close(10)
                close(15)
                close(20)
                close(25)
                close(30)
                close(35)
```

```
c Read in fuel data and assign to vector (i.e. uni-dimensional) arrays.
                f=1
                open(10,status='old',file='mixed.dat')
                read(10,250,end=200) mf(f),st(f),se(f),sv(f),ld(f),dp(f),h(f),pd(f),mx(f)
                close(10)

                f=2
                open(10,status='old',file='wetms.dat')
                read(10,250,end=200) mf(f),st(f),se(f),sv(f),ld(f),dp(f),h(f),pd(f),mx(f)
                close(10)

                f=3
                open(10,status='old',file='beech.dat')
                read(10,250,end=200) mf(f),st(f),se(f),sv(f),ld(f),dp(f),h(f),pd(f),mx(f)
                close(10)

                f=4
                open(10,status='old',file='bog.dat')
                read(10,250,end=200) mf(f),st(f),se(f),sv(f),ld(f),dp(f),h(f),pd(f),mx(f)
                close(10)

                f=5
                open(10,status='old',file='manuka.dat')
                read(10,250,end=200) mf(f),st(f),se(f),sv(f),ld(f),dp(f),h(f),pd(f),mx(f)
                close(10)

                f=6
                open(10,status='old',file='matagouri.dat')
                read(10,250,end=200) mf(f),st(f),se(f),sv(f),ld(f),dp(f),h(f),pd(f),mx(f)
                close(10)

                f=7
                open(10,status='old',file='lightms.dat')
                read(10,250,end=200) mf(f),st(f),se(f),sv(f),ld(f),dp(f),h(f),pd(f),mx(f)
                close(10)

                f=8
                open(10,status='old',file='grassld.dat')
                read(10,250,end=200) mf(f),st(f),se(f),sv(f),ld(f),dp(f),h(f),pd(f),mx(f)
                close(10)

                f=9
                open(10,status='old',file='wetland.dat')
                read(10,250,end=200) mf(f),st(f),se(f),sv(f),ld(f),dp(f),h(f),pd(f),mx(f)
                close(10)

200             continue
250             format(//,9(//,f12.0))

c Ignite the first cell (fx,fy)

                status(fx,fy)=1

c Now into the main loop sequence of the program (i.e check for burning cells,
c calculate spread rate out of them into their neighbours, check for fire spread
c and update the appropriate grids, parameters).

                do 500, m=1,330,1
```

```
                do 450, n=1,xdim
                do 400, o=1,ydim
                if (status(n,o).gt.1) status(n,o) = status(n,o)-1
400             continue
450             continue

                call
burnsearch(status,fuel,height,speed,sstd,dirn,dstd,mf,st,se,sv,ld,dp,h,pd,mx)
                print *,'Iteration : ',m

c Finally write the <<status>> array to a format suitable for input to Arc/Info.
c See the Arc commands <<asciigrid>> and <<gridascii>> for more info.

                if(m.eq.30) then
                open(50,status='unknown',file='fire30.dat')
                write(50,610)xdim,ydim
                do 550,i=1,ydim
                write(50,650) (status(j,ydim+1-i),j=1,xdim)
550             continue

                else if(m.eq.60) then
                open(50,status='unknown',file='fire60.dat')
                write(50,610)xdim,ydim
                do 555,i=1,ydim
                write(50,650) (status(j,ydim+1-i),j=1,xdim)
555             continue

                else if(m.eq.90) then
                open(50,status='unknown',file='fire90.dat')
                write(50,610)xdim,ydim
                do 560,i=1,ydim
                write(50,650) (status(j,ydim+1-i),j=1,xdim)
560             continue

                else if(m.eq.120) then
                open(50,status='unknown',file='fire120.dat')
                write(50,610)xdim,ydim
                do 565,i=1,ydim
                write(50,650) (status(j,ydim+1-i),j=1,xdim)
565             continue

                else if(m.eq.150) then
                open(50,status='unknown',file='fire150.dat')
                write(50,610)xdim,ydim
                do 570,i=1,ydim
                write(50,650) (status(j,ydim+1-i),j=1,xdim)
570             continue

                else if(m.eq.180) then
                open(50,status='unknown',file='fire180.dat')
                write(50,610)xdim,ydim
                do 575,i=1,ydim
                write(50,650) (status(j,ydim+1-i),j=1,xdim)
575             continue

                else if(m.eq.210) then
                open(50,status='unknown',file='fire210.dat')
                write(50,610)xdim,ydim
```

```
                do 580,i=1,ydim
                write(50,650) (status(j,ydim+1-i),j=1,xdim)
580             continue

                else if(m.eq.240) then
                open(50,status='unknown',file='fire240.dat')
                write(50,610)xdim,ydim
                do 585,i=1,ydim
                write(50,650) (status(j,ydim+1-i),j=1,xdim)
585             continue

                else if(m.eq.270) then
                open(50,status='unknown',file='fire270.dat')
                write(50,610)xdim,ydim
                do 590,i=1,ydim
                write(50,650) (status(j,ydim+1-i),j=1,xdim)
590             continue

                else if(m.eq.300) then
                open(50,status='unknown',file='fire300.dat')
                write(50,610)xdim,ydim
                do 595,i=1,ydim
                write(50,650) (status(j,ydim+1-i),j=1,xdim)
595             continue

                else if(m.eq.330) then
                open(50,status='unknown',file='fire330.dat')
                write(50,610)xdim,ydim
                do 600,i=1,ydim
                write(50,650) (status(j,ydim+1-i),j=1,xdim)
600             continue

                end if

610             format('ncols',x,i2/'nrows',x,i3/'xllcorner 2405756'/'yllcorner 5793418'/
'cellsize 50')
650             format(x,100(i1,x))

500             continue


c ---------------------------------------------------------------------------------------------
c Subroutines are found below here in the order in which they are called.

c Subroutine <<burnsearch>> checks for burning cells.

                subroutine burnsearch(status,fuel,height,speed,sstd,dirn,dstd,mf,st,se,sv,
~               ld,dp,h,pd,mx)

                integer status(43,124),fuel(43,124),height(43,124)
                integer speed(43,124),sstd(43,124),dirn(43,124),dstd(43,124)
                real mf(9),st(9),se(9),sv(9),ld(9),dp(9),h(9),pd(9),mx(9)

                do 1000, i=1,43
                do 1010, j=1,124
                if(status(i,j).eq.1) call rosout(status,fuel,height,speed,sstd,dirn,dstd,i,j,mf,
~               st,se,sv, ld,dp,h,
~               pd,mx)
```

```
1010        continue
1000        continue

            return
            end

c ---------------------------------------------------------------------------------------------
c Subroutine <<rosout>> initiates the calculation of rate of spread out of
c the burning cell into adjacent cells.

            subroutine
rosout(status,fl,hgt,spd,sstd,dirn,dstd,i,j,mf,st,se,sv,ld,dp,h,pd,mx)

c Firstly initiate variables read in landscape parameters etc.
            real rosadj,e,w
            integer hgt(43,124),status(43,124),fl(43,124),i,j,cell,dlag,cnhb,a,b
            integer spd(43,124),sstd(43,124),dirn(43,124),dstd(43,124)
            real mf(9),st(9),se(9),sv(9),ld(9),dp(9),h(9),pd(9),mx(9)

c Set up a loop to calculate ROS in the eight cardinal directions
c Routine for diagonal burning
            dir=0
            dlag=0
            cnhb=0

c Check whether the cell is located on the current fire perimeter.
c If cell (i,j) is surrounded by burning cells then skip the loop (fire spread not possible).
            do 1500,a=i-1,i+1,1
            do 1550,b=j-1,j+1,1
            if(status(a,b).ge.1) cnhb=cnhb+1
1550        continue
1500        continue
            if(cnhb.ge.9) goto 2500

c Ensure fire does not burn beyond the array boundaries
            do 2000, k=i-1,i+1,1
            do 2010, l=j-1,j+1,1

             if (k.lt.1.or.k.gt.43) then
             goto 2000
             else if (l.lt.1.or.l.gt.124) then
             goto 2010
             end if

             dir=dir+1
             sd=sd+1
             test=rand(sd)

             if (dir.eq.2.or.dir.eq.4.or.dir.eq.6.or.dir.eq.8) then
             cell=1
             else if (dir.eq.1.or.dir.eq.3.or.dir.eq.7.or.dir.eq.9) then
             cell=2
             else if (dir.eq.5) then
             goto 2010
             end if

c If the cell being into [cell(k,l)} is unburnt call <<roscalc>> to calculate the maximum
c rate of spread out of the focal cell.
```

```
                if(status(k,l).eq.0)call roscalc (hgt,spd,sstd,fl,ros,rosz,i,j,k,l,cell,mf,st,se,
~               sv,ld,dp,h,pd,mx,w)

c 'cw' is the wind speed in km/hr (converted from m/min)
                cw=w/16.6

c Calculate the parameter 'e' according to wind speed and fuel type.
                if (cw.le.1) e=0
                if (cw.gt.1.and.fl(k,l).eq.4.or.fl(k,l).eq.8) e=(1-0.826*cw**-0.928)**0.5
                if(cw.gt.1.and.fl(k,l).ne.4.and.fl(k,l).ne.8)e=(1-exp(0.0058-0.0324*cw**
~               1.2))**0.5

c Simulate variation in wind direction using the direction standard deviation array.
                sd=sd+1
                if(rand(sd).gt.0.5) winddirn=dirn(k,l)+(rand(sd)*(dstd(k,l)-10))
                if(rand(sd).lt.0.5) winddirn=dirn(k,l)-(rand(sd)*(dstd(k,l)-10))
                if(rand(sd).eq.0.5) winddirn=dirn(k,l)

c Adjust the forward rate of spread according to the wind speed and direction.
                if(dir.eq.1) ang=225
                if (dir.eq.2) ang=270
                if (dir.eq.3) ang = 315
                if (dir.eq.4) ang = 180
                if (dir.eq.6)ang = 360
                if (dir.eq.7) ang =135
                if (dir.eq.8)ang = 90
                if (dir.eq.9) ang = 45

c Calculate the adjusted rate of spread using the function(s) of Green et al. (1990)
                pmc=(ang-winddirn+180)*(3.141/180)
                diff=winddirn-ang
                rosadj = ros*(1-e)/(1-e*cos(pmc))

c Limit the flanking and backing rates of spread at high(er) wind speeds.
                if(diff.le.22.5.and.diff.ge.-22.5.and.cw.ge.5.and.rosadj.gt.1.05)
~               rosadj=1.05
                if(diff.le.67.5.and.diff.ge.-67.5.and.cw.ge.5.and.rosadj.gt.1.21)
~               rosadj=1.21
                if (rosadj.lt.0) rosadj=0

c Test for diagonal lag.
                sd=sd+1
                dtest=rand(sd)
                if (dtest.le.0.707) dlag=1
                if (dtest.gt.0.707) dlag=2

                if (rosadj*0.5/70.71.gt.test.and.status(k,l).eq.0.and.cell.eq.1)
~               status(k,l) = 2
                if(rosadj*0.5/70.71.gt.test.and.status(k,l).eq.0.and.cell.eq.2.and.
~               dlag.eq.1) status(k,l) = 2
                if (rosadj*0.5/70.71.gt.test.and.status(k,l).eq.0.and.cell.eq.2.and.
~               dlag.eq.2)  status(k,l)=3

2010            continue
2000            continue

2500            return
                end
```

```
c ------------------------------------------------------------------------------------------------
c Subroutine <<roscalc>> calculates the maximumrate of spread out of the
c burning cell into adjacent cells.
                subroutine
roscalc(hgt,spd,sstd,fl,r,rz,i,j,k,l,cell,mf,st,se,sv,ld,dp,h,pd,mx,w)

                real bdens,pk,efht,nld,opk,qig,r,rz
                real wf,sf,prop,c,b,e,scr,min,moist,gmax,gopt,a,ri,s,ns,negs,sang
                integer fl(43,124),spd(43,124),sstd(43,124),hgt(43,124),i,j,cell
                real mf(9),st(9),se(9),sv(9),ld(9),dp(9),h(9),pd(9),mx(9)


c Calculate the slope between the cells (rise/run) and correct for diagonals.
                if (cell.eq.1) s=(hgt(k,l)-hgt(i,j))/50
                if (cell.eq.2) s=(hgt(k,l)-hgt(i,j))/70.71

                if (s.lt.0) ns=s*-1
                if (s.ge.0) ns=0
                negs=atan(ns)
                sang=negs*(180/3.1415927)

c Allow for NODATA values (9999) to be read as flat slopes
                if(hgt(k,l).eq.9999.or.hgt(i,j).eq.9999) s=0
                if (s.lt.0) s=0
                sd=sd+1

c Estimate wind speed and simulate gusts using the wind speed standard deviation
c array.
                if(rand(sd).gt.0.5) w=spd(k,l)+(rand(sd)*(sstd(k,l)-100))
                if(rand(sd).lt.0.5) w=spd(k,l)-(rand(sd)*(sstd(k,l)-100))
                if(rand(sd).eq.0.5) w=spd(k,l)

c Calculate the secondary fuel parameters for the ignited cell
                bdens=ld(fl(k,l))/dp(fl(k,l))
                pk=bdens/pd(fl(k,l))
                efht=exp(-4.528/sv(fl(k,l)))
                nld=ld(fl(k,l))/(1-st(fl(k,l)))
                opk=(sv(fl(k,l))**-0.8189)*0.20395
                qig=581+(2594*mf(fl(k,l)))

c Firstly calculate the wind co-efficient (wf)
                c=7.47*exp(-0.8711*sv(fl(k,l))**0.55)
                b=0.15988*sv(fl(k,l))**0.54
                e=0.715*exp(-0.01094*sv(fl(k,l)))
                wf=(c*(3.281*w)**b)*((pk/opk)**-e)

c Secondly calculate the slope coefficient (sf).
                scr=atan(s)
                sf=(5.275*pk**-0.3)*(tan(scr))

c Now calculate the propagating flux ratio (prop)
                prop=((192+7.9095*sv(fl(k,l)))**-
1)*(exp((0.792+3.7597*sv(fl(k,l))**0.5)*(pk+0.1)))

c Calculate the mineral and moisture damping coefficients (min and moist)
                min=0.174*(se(fl(k,l))**-0.19)
                moist=1-(2.59*(mf(fl(k,l))/mx(fl(k,l))))+(5.11*((mf(fl(k,l))/mx(fl(k,l)))
~               **2))-(3.52*((mf(fl(k,l))/mx(fl(k,l))) **3))
```

```
c Now calculate the maximum & optimum reaction velocities (gmax,gopt)
                gmax=(0.0591+2.926*sv(fl(k,l))**-1.5)**-1
                a=1/(((sv(fl(k,l))**0.1)*6.7229)-7.27)
                interm=(1-pk/opk)
                gopt=(gmax*(pk/opk)**a)*exp(a*(1-pk/opk))

c Calculate the reaction intensity (ri)
                ri=gopt*nld*h(fl(k,l))*min*moist

c Finally calculate the rate of spread from cell(i,j) to cell(k,l)
                r=(ri*prop*(1+wf+sf))/(bdens*efht*qig)

c Correct for down-slopes using Van Wagner (1988) corrections.
                rz=(ri*prop*(1+wf+0))/(bdens*efht*qig)
                if(ns.ne.0) sf=1-(0.0330*sang)+(0.000749*sang**2)
                if(ns.ne.0) r=rz*sf
                if(r.lt.0) r=0
                if (fl(k,l).eq.0) r=0
                return
                end
c ---------------------------------------------------------------------------------------------------
```

Fuel Model Data Files

The fuel models used in the simulations described in Chpater 5 and 6 all used a standard fuel data file format. This is presented below:

```
Tall Grass Fuel Type
Fuel Class Data

Moisture (dimensionless fraction)
0.1
Total mineral content (dimensionless fraction)
0.0555
Effective mineral content (dimensionless fraction)
0.01
Surface-area to volume ratio (cm^-1)
50
Load (kg/m^3)
0.67
Depth (m)
0.762
Low heat content (kJ/kg^-1)
18608.0
Particle Density (kg/m^3)
512
Moisture content of extinction (dimensionless fraction)
0.3
```

Appendix 3 - Fuel Models

This Appendix presents the fuel model used in the course of the thesis. This includes both the fuel models parameterised for the validation of the PYROCART model and those of Rothermel (1972) used in its development.

Rothermels (1972) Fuel Models -

The fuel models of Rothermel (1972) are presented in the same manner as in his research report.

Fuel Types	Total Loading	Dead Fuel						Living Fuel		Fuel Depth
		Fine		Medium		Large				
		σ	w_o	σ	w_o	σ	w_o	σ	w_o	
	Tons/acre	*Ft.*$^{-1}$	*lb./ft.*^{2}	*Ft.*$^{-1}$	*lb./ft.*^{2}	*Ft.*$^{-1}$	*lb./ft.*^{2}	*Ft.*$^{-1}$	*lb./ft.*^{2}	*Ft.*
Grass (Short)	0.75	3500	0.034							1
Grass (Tall)	3	1500	0.138							2.5
Brsuh (not chaparral)	6	2000	0.046	109	0.023			1500	0.092	2
Chaparral	25	2000	0.23	109	0.184	30	0.092	1500	0.23	6
Timber (grass & understorey)	4	3000	0.092	109	0.046	30	0.023	1500	0.023	1.5
Timber (litter)	15	2000	0.069	109	0.046	30	0.115			0.2
Timber (litter and understorey)	30	2000	0.138	109	0.092	30	0.23	1500	0.092	1
Hardwood (litter)	15	2500	0.134	109	0.019	30	0.007			0.2
Logging slash (light)	40	1500	0.069	109	0.207	30	0.253			1
Logging slash (medium)	120	1500	0.184	109	0.644	30	0.759			2.3
Logging slash (heavy)	200	1500	0.322	109	1.058	30	1.288			3

For all fuel models $s_t = 0.0555$; $s_t = 0.010$; h = 8000 BTU/lb; $\rho_p = 32$lb/ft ; $m_x = 0.30$.

Fuel Models Used in the PYROCART Simulation

The fuel models below were those used for the validation of the PYROCART model on the Cass fire of May 1995. The load category includes all fuels for the fule cpmlex with a diamtere of less than 7.25 cm. Surface-area to volume ratio was calculated using the formulae of Brown (1970).

Fuel Type	Ovendry Load ($kg.m^{-2}$)	SAVR (cm^{-1})	Depth (m)	FMC	Extinction FMC
Mixed Shrub	0.34	95.2	0.41	0.3	0.5
Wet Mixed Shrub	0.41	78.63	0.5	0.35	0.4
Mountain beech	52	45.01	2	0.49	0.5
Bog	0.15	44.85	0.29	0.36	0.4
Manuka Shrubland	0.31	95.2	1.4	0.36	0.5
Matagouri Shrubland	0.54	35.14	0.83	0.37	0.5
Light Mixed Shrub	0.12	95.37	0.32	0.25	0.5
Tussockland	0.1	71.8	0.26	0.19	0.4
Wetland	0.22	54.69	0.34	0.36	0.4

Total Mineral Content = 0.0555; Effective (silica-free) Mineral Content = 0.01; Particle Density (kg/m^3) = 512.